ABSTRACT

Magnitudes of Cytotoxic T-Lymphocyte Infiltration and Secretion of Their Targeting Chemokines are Bimodally Distributed Among a Population of Colorectal Tumor Microenvironments

Timothy J. Zumwalt, Ph.D.

Mentor: C. Richard Boland, M.D.

T-cell infiltration varies among colorectal tumors and directly impacts patient survival. Chemoattraction and infiltration of $CD8^+$ T-cells are mediated by surface chemokine receptors CXCR3 and CCR5, and are associated with favorable prognosis. Transcriptional expression of these receptors' cognate chemokines, as well as other inflammation-associated chemokines, correlate with prolonged disease-free survival (DFS). These findings, however, were derived from paraffin embedded tissues, thus little is known about the pattern of secreted T-cell targeting chemokines from colorectal tumors. Therefore, this investigation aimed to determine the secretion pattern of chemokines associated with DFS from immediately excised live tumor tissues. Our results demonstrate the first real functional analysis of chemokine activity in colorectal tumors beyond immunohistochemistry and real-time PCR. Forty-four colorectal tumors were procured immediately after surgery and categorized by transcriptional expression of two T-cell marker genes that represent the magnitude of type-1 T-cell activity. Tumors that more highly co-expressed *IFNG* and *TBX21* consequently have a higher frequency of infiltrating $GzmB^+$ CTLs and IFN-γ^+ $CD4^+$ helper T-cells and transcribe a unique pattern of DFS-associated chemokines when

compared to normal mucosa. High co-expression of *IFNG* and *TBX21* was bimodally distributed across the tumors collected. Tumors with higher co-expression more strongly secreted two DFS-associated chemokines, CXCR3 ligand, CXCL10 and CCR5 ligand, CCL5. Additional results demonstrate that tumors with higher co-expression are proportionally skewed towards early TMN stages and with mismatch repair-deficiency, confirming that infiltration of $CD8^+$ T-cells are associated with early TNM stages and lack of metastasis. Secreted chemokines were detected using a novel immunoassay that may have implications for future development of immunopotentiating treatments in cancer.

Magnitudes of Cytotoxic T-Lymphocyte Infiltration and Secretion of Their Targeting Chemokines are Bimodally Distributed Among a Population of Colorectal Tumor Microenvironments

by

Timothy J. Zumwalt, B.Sc.

A Dissertation

Approved by the Institute of Biomedical Studies

_____

Robert R. Kane, Ph.D., Director

Submitted to the Graduate Faculty of
Baylor University in Partial Fulfillment of the
Requirements for the Degree
of

Doctor of Philosophy

Approved by the Dissertation Committee

_____

C. Richard Boland, M.D., Chairperson

_____

Christopher J. Kearney, Ph.D.

_____

Teodoro G. Bottiglieri, Ph.D.

_____

Erich J. Baker, Ph.D.

_____

Mark Taylor, Ph.D.

Accepted by the Graduate School

December 2014

_____

J. Larry Lyon, Ph.D., Dean

Page bearing signatures is kept on file in the Graduate School.

TABLE OF CONTENTS

LIST OF FIGURES

LIST OF TABLES

LIST OF ABBREVIATIONS

(m)RNA	(messenger) ribonucleic acid
5-FU	fluorouracil
AJCC/UICC	American Joint Committee on Cancer/Union for International Cancer Control
AGO	argonaute RISC catalytic component
AKT	Ak thymoma also known as protein kinase B (PKB)
APC	adenomatous polyposis coli
APC	antigen-presenting cell
APC	allophycocyanin
APC-Cy	allophycocyanin-cyanine
ATCC	American Type Culture Collection
BIIR	Baylor Institute for Immunology Research
BIO	biotinylated
BRI	Baylor Research Institute
BUMC	Baylor University Medical Center
CCL	chemokine (C-C motif) ligand
CCR	chemokine (C-C motif) chemokine receptor
CD	cluster of differentiation
CEACAM	carcinoembryonic antigen-related cell adhesion molecule
CHIDIST	(Excel function) one-tailed probability of the chi-squared distribution
CI	confidence interval
CIMP	CpG island methylator phenotype

CIN	chromosomal instability
CpG	cytosine-phosphate-guanine
CRC	colorectal cancer
CS	cancer (or disease)-specific survival
CT	center of the tumor
CTL	cytotoxic T-lymphocyte
CTLA	cytotoxic T-lymphocyte antigen
CX3CL	chemokine (C-X3-C motif) ligand
CXCL	chemokine (C-X-C motif) ligand
CXCR	chemokine (C-X-C motif) receptor
DC	dendritic cells
DCC	deleted in colorectal cancer
DcR	decoy receptor
df	degrees of freedom
DFS	disease-free survival
DNA	deoxyribonucleic acid
dNTP	deoxynucleotide triphosphate
DTT	dithiothreitol
EDTA	ethylenediaminetetraacetic acid
EGF(R)	epidermal growth factor (receptor)
ELISA	enzyme-linked immunosorbent assay
EMT	epithelial-mesenchymal transition
Est	effect size
Est_v	overall effect size adjusted by variance constant (v)
FCS	fetal calf serum

FGF	fibroblast growth factor
FGF2	basic fibroblast growth factor
FOXP	forkhead box protein
FS	forward scatter
GAPDH	glyceraldehyde 3-phosphate dehydrogenase
GATA	GATA binding protein
GNLY	granulysin
GTPase	guanosine triphosphate hydrolase enzyme
GZMB	granzyme B
HBSS	Hank's balanced salt solution
HER2/neu	receptor tyrosine-protein kinase erbB-2
HET	heterogeneous
HGF	hepatocyte growth factor
HiHi	high *IFNG* and high *TBX21*
HIPAA	Health Insurance Portability and Accountability Act
HIV	human immunodeficiency virus
HR	hazard ratio
I^2	heterogeneity
ICAM	intercellular adhesion molecule
IFNGR	interferon gamma receptor
IFN	interferon
IHC	immunohistochemistry
IL	interleukin
IM	invasive margin
IMDM	Iscove's modified dulbecco's media

IRB	institutional review board
IRF	interferon regulatory factor
KRAS	Kirsten rat sarcoma viral oncogene homolog
l	natural logarithm of lower confidence interval (CI)
LOH	loss of heterozygosity
LoLo	low *IFNG* and low *TBX21*
l_v	natural logarithm lower confidence interval (CI) adjusted by variance constant (v)
M	macrophage type (specific)
MADCAM	mucosal vascular addressin cell adhesion molecule
MAGE	melanoma-associated antigen
MDTH	molecular distance to health
MHC	major histocompatibility complex
MLH	mutL homolog
miRISCs	miRNA-induced silencing complexes
miRNA	microRNA
MMP	matrix metalloproteinase
MMR	DNA mismatch repair
MSH	mutS homolog
MSI	microsatellite instability
MSI-H	high degree of microsatellite instability
MSI-L	low degree of microsatellite instability
MSS	microsatellite stable
NCI	National Cancer Institute
NEUROG	neurogenin

NK	natural killer
NKT	natural killer T-cell
NS	not significant
OGT	O-linked β-N-acetylglucosamine transferase
oligo(dT)	deoxy-thymine nucleotides
OS	overall survival
P	*P* value
PCR	polymerase chain reaction
PDGF	platelet-derived growth factor
PE	phycoerythrin
PE-Cy	phycoerythrin-cyanine
PerCP-Cy	peridinin chlorophyll-cyanine
PF	platelet factor
PI_3K	phosphoinositide 3-kinase
PIK_3CA	phosphatidylinositol-4,5-bisphosphate 3-kinase, catalytic subunit alpha
PIP_3	phosphatidylinositol (3,4,5)-trisphosphate
PMA	phorbol 12-myristate 13-acetate
pRb	retinoblastoma protein
pri-RNA	primary-RNA
P_v	*P* value of variance constant (*v*) adjusted values
Q	Cochran's heterogeneity statistic
QMVR	quasi-monomorphic variation range
R^2	correlation coefficient
ras	rat sarcoma
Real-Time PCR	real-time polymerase chain reaction

RER	ribonucleotide excision repair
RISC	RNA-induced silencing complex
RNase	ribonuclease
ROR	RAR-related orphan receptor
RUNX	runt-related transcription factor
SC	side scatter
SE	standard error
SEM	standard error of the mean
SE_v	Overall standard error adjusted by variance constant (v)
SHIP	Src homology-2 domain-containing inositol 5-phosphatase
SMAD	SMAD family member
SOCS	suppressor of cytokine signaling
SQ	sequencing primer
SS	side scatter
STAT	signal transducer and activator of transcription
TAA	tumor-associated antigen
TAM	tumor-associated macrophage
TBX21	T-box transcription factor 21
TCGA	The Cancer Genome Atlas
TCR	T-cell receptor
T_{EM}	effector memory T-cell
TGF	transforming growth factor
T_H	helper T-cell type (specific)
TIL	tumor-infiltrating lymphocyte
TME	tumor microenvironment

TNF	tumor necrosis factor
TNM	tumor, lymph node, metastasis
TP53	tumor protein p53
T_{reg}	regulatory T-cell
u	natural logarithm of lower confidence interval (CI)
UCSC	University of California, Santa Cruz
u_v	natural logarithm of lower confidence interval (CI) adjusted by variance constant (v)
v	variance constant
Var	variance
VCAM	vascular cell adhesion molecule
VEGF	vascular endothelial growth factor
VELIPI	vascular emboli, lymphatic invasion, perineural invasion
w	weight
wEst	weighted effect size
w_v	weight (w) adjusted by variance constant (v)
z	z-score

ACKNOWLEDGMENTS

First, I thank Dr. Clement Richard Boland for believing in me. As a man with great insight and wisdom, he is a leader in the fight against cancer and is fully committed to teaching his craft to others. He happily extends his contagious passion to others in the hopes that they too will continue his important work. I also thank Dr. Boland for his advocacy and friendship. The focus of many of our meetings often deviated to non-research conversations, however we always found time discuss our work. The best advice he gave me was that although my hypotheses and ideas may not always be correct, as long as I design my experiments correctly I should learn something, and that is all we ever have to fear about science.

Baylor University deserves much of my gratitude for taking a chance on me. To Drs. Robert Kane, Chris Kearney, Bryan Gibbon, and Erich Baker, I am thankful for your guidance. These men are the first scientists to ever treat me as their equal and also showed me that they too believed in me. Special gratitude goes to Dr. Bryan Brooks who, on my first day in graduate school sat with me and the other freshly recruited students to make us understand that we are responsible for our own progress and that we must take the responsibility for completing the graduate school's requirements. Better advice cannot be given.

I did not always work for Dr. Boland during my time at Baylor. The story of how I joined his GI Cancer Research/Epigenetics and Cancer Prevention Laboratory is one that should be shared because if any freshly recruited graduate students happen to read this dissertation will learn a story about the benefits of perseverance, grim determination,

overcoming one's fear of making mistakes, and also understanding that the responsibility of finishing graduate school rests solely on us students. After finishing the bulk of my classroom work I began research at the Baylor Institute for Biomedical Studies (BIIR). I wanted my graduate work to focus towards immunology while being mentored by excellent and world renowned immunologists, however I slowly realized that this institute was not well equipped to train a naïve student like me. BIIR is only accommodating to those with previous immunology research experience. I thought my past jobs working in clinical pathology and biotech would be enough, however these positions were not 'research' and therefore did not prepare me for the rigors of scientific investigation. I quickly discovered how little I actually knew. I attempted to remedy my naiveté by rotating through four labs over eighteen weeks and participate in as many meetings and seminars as possible while speaking with as many knowledgeable scientists as I could.

My final rotation brought me to Dr. John Connolly, who was my first choice as mentor even before leaving Waco. He was brilliant and motivating, but when the time arrived for me to pick a laboratory he suddenly moved to Singapore. Upon leaving he suggested two options, either I stay in the institute and join another lab, or leave entirely and work with Dr. Boland, a revered gastrointestinal geneticist located just on the other side of the Baylor hospital campus. I spoke with Dr. Boland and was very impressed with his generosity to spend time discussing his research. However, after some thought I felt too afraid to leave BIIR because of the time and effort I had already invested, and also my lack of experience with genetic diseases. Basically, I didn't want to start over in a new discipline. So I took my chances with another mentor who brought me to the attention of Dr. Laia Alsina, a wonderful postdoc and mother of two. I am very thankful to have worked

with her. For one year we investigated childhood immune deficiencies and published in Blood and the New England Journal of Medicine. However, this valuable experience ended when my mentor decided to move to Seattle. Dr. Robert Kane quickly came to the rescue and assuaged my trepidation by provoking the head of the institute to mentor me. I am also very thankful for his effort.

Soon afterwards the head of the institute left to pursue a career in biotech, and I discovered that finding security in another lab was nearly impossible because the future of the institute was unknown. Multiple postdocs at BIIR pressured me to end my graduate studies. These individuals were very vocal about their opinions and very convincing towards my colleagues. In addition to this, some of my colleagues told me that I was not creative enough to earn a Ph.D., nor were my project ideas advanced enough for Baylor University. I was told that my best chances of a future in science was to become a technician at BIIR. However, these were not the opinions of all the postdocs and faculty at BIIR, but all were worried about me. I finally learned that to complete my degree I needed an environment that was encouraging for creating and developing projects, a laboratory where I can renew confidence in my abilities. I walked across Baylor campus again to discuss my situation with Dr. Boland and how I can be a part of a radically new idea that studied live tumor tissues and lymphocytes. I became incredibly enthusiastic and started work for him the very next Monday.

The work we completed over the next three years could not have been possible without the experience I gained at BIIR. That institute taught me to take control of my future and not give up when faced with adversity. I thank multiple postdocs at BIIR for forcing me to face my fears and to learn how to overcome them. When I stopped depending

on the opinions of others and learned to have faith in my own abilities, I was able to manage my fear of making mistakes and learned to turn that anxiety into hard work and determination.

I want to thank all of those at BIIR who provided encouragement and expert instruction. Those who taught me flow cytometry are Gerlinde Obermoser, Brandon Sells, Laia Alsina, and Simone Caielli. I also want to thank those in the Luminex core who helped me prepare samples and analyze data, Sandy Zurawski and Amy O'bar. A special thank you goes to Carson Harrod for allowing me to participate in BIIR journal club and for his continued support of Baylor graduate students. Also I thank Dr. John Connolly who taught me the importance of controlling one's own research funding.

My work could not be completed without the help of everybody at the GI Cancer Research/Epigenetics and Cancer Prevention Laboratory. Thank you to Ajay Goel for helping to refine my publication, and Jennifer Rhees, Melissa Garcia, Yoshinaga Okugawa, Keun Hur, and Thomas Jascur for helping me to operate machinery and teaching me how to perform the work.

My gratitude goes beyond the Baylor system. I thank my professors at my undergraduate university, Cal Poly, who provided letters of recommendation and encouragement to continue my education, Drs. Charles Knight, Larisa Vredevoe, and Michael Black. These individuals noticed my desire to never stop learning and provided the tools for doing so. Lastly, I am fortunate for my family, closest friends and loved ones, who never stopped encouraging me and kept me on the right track.

Somewhere, something incredible is waiting to be known.

--Carl Sagan

CHAPTER ONE

Introduction

Tumors harbor mutated genes that can encode immunogenic proteins (Vesely and Schreiber, 2013). Based on that, the immune system is expected to eradicate all tumors, however this does not always happen. Normally, activated anti-tumor lymphocytes[1] eradicate tumor cells (Quail and Joyce, 2013) and suppress disease progression (Pages et al., 2005; Galon et al., 2006; Galon et al., 2007; Pages et al., 2010; Fridman et al., 2011; Dahlin et al., 2011). However the opposite can occur when the tumor microenvironment (TME) undergoes a series of alterations that evade the immune response (Dunn et al., 2002; Dunn et al., 2006; Schreiber et al., 2011; Bindea et al., 2013). This suggests that anti-tumor immunity –or immunosurveillance– in the TME diminishes as the tumor progresses and metastasizes to distant sites (Bindea et al., 2013). The overarching goal of this investigation is to better understand the mechanisms that dictate lymphocyte infiltration into colorectal tumors by utilizing powerful investigational tools available in collaboration with investigators from other laboratories at Baylor University Medical Center (BUMC). Achievement of this goal will create avenues for developing more rational and personalized treatments for colorectal cancer (CRC) patients, as well as inspire further investigations inquiring about the mechanisms of lymphocyte infiltration into solid tumors.

Cancer is a complex and heterogeneous disease that needs to be treated differently for every patient. Solid tumors include both malignant and non-malignant cells that retain

[1] Lymphocytes represent one of the two major lineages hematopoietic stem cells give rise to, and consist of T-cells, B-cell, and natural killer (NK) cells.

the capacity to proliferate upon stimulation by both intrinsic and extrinsic signals (Zitvogel et al., 2006), therefore treating cancer is extremely complex and dangerous because of the difficultly to selectively killing cancer cells while sparing normal ones. The current paradigm for treating solid tumors of the colon and rectum is to initially excise the mass along with the immediate adjacent mucosa (Kordatou et al., 2014) then poison any remaining tumor cells that were not removed with a cocktail of chemicals matched to the tumor, however, these chemicals may or may not be effective for that particular tumor. This strategy is exceedingly inadequate especially once the tumor has metastasized to other organs. Prognosis is unfavorable at this stage due to the challenging tasks of detecting and removing metastases from multiple sites. However, the type and density of tumor infiltrating lymphocytes (TILs) varies among every colorectal tumor and directly impacts patient survival, *i.e.* infiltration of anti-tumor lymphocytes has shown to prevent metastasis and progression to advanced stage cancer (Pages et al., 2005; Galon et al., 2006; Galon et al., 2007; Pages et al., 2009; Pages et al., 2010). Therefore, the current paradigm of "one treatment for all CRCs" can no longer be accepted by practitioners because variation within this disease demands that more targeted approaches be tailored for each patient. Developing novel targeted approaches will require better evaluation and understanding of the current immunological status of each individual patient's tumor.

This chapter is a brief overview of the basic components of the investigation. Here is where the investigational niche will be introduced, the primary questions of the investigation will be presented, and the strategies, experiments, materials, and technologies used fill the niche will be described. Following in Chapter Two is a detailed review of the literature, as well as a thorough description of the main biological concepts pertinent to the

investigation. Chapter Three is reserved for technical descriptions of the material, methods and experimental designs, while Chapter Four contains the results of the investigation. Finally Chapter Five will end the investigation by discussing the relevance of the data to the body of knowledge pertaining to CRC immunology.

Gaps in the Knowledge and Theoretical Framework

The current body of knowledge pertaining to immunological infiltrates residing in colorectal tumors is limited to transcriptional data and low dimensional immunohistochemistry (IHC) obtained from paraffin embedded samples (Pages et al., 2008; Mlecnik et al., 2010; Anitei et al., 2014) in the form of tissue microarrays that limit the amount of tissues that can be sampled. Although these molecular and genetic studies have been vital to identify parameters that dictate patient disease (Anitei et al., 2014; Galon et al., 2014), they fail to correlate active secretion of immunological factors with functional and live TILs. Therefore studying only dead cells has created a gap in the knowledge, and therefore accurate assessment of secreted factors from live colorectal tumors still needs to be attempted. Also, the heterogeneity of lymphocyte infiltration has been deeply underestimated (Pages et al., 2005; Pages et al., 2010; Sadanandam et al., 2013); proper categorization of CRCs by magnitude of immunosurveillance will provide a necessary scheme for assessing actively secreted immune mediators. A second gap in the knowledge is the vague understanding of how genetic aberrations skew the lymphocyte composition of the TME. Genomic instability, or frequency of genetic aberrations (Lengauer et al., 1998), can generate novel phenotypes (Khong and Restifo, 2002), that may or may not elicit immunogenicity. Better categorization of the immunological activity in colorectal TMEs will provide practitioners with more precise treatment of individual cancers.

Justification for investigating these gaps in the knowledge was garnered from the theory that defective mismatch repair (MMR) contributes to genesis of mutated proteins and enhanced immunosurveillance (Kloor et al., 2007; Le Gouvello et al., 2008; Drescher et al., 2009). Tumor cells that present these proteins to lymphocytes are recognized as "non-self" and elicit an immune response (Palucka and Banchereau, 2012). Therefore the variety and degree of genomic instability adds to the magnitude of the immune response and shapes the TME (Banerjea et al., 2004; Sadanandam et al., 2013).

Purpose, Aims, and Significance of the Investigation

The purpose of this investigation was to assess the varying magnitudes of secreted immunological mediators that attract anti-tumor lymphocyte colorectal TMEs (also called chemokines), and to identify correlations between these secreted mediators and infiltrating anti-tumor immune cells. This investigation is superior to previous studies because earlier attempts to correlate chemokines with lymphocyte infiltration only collected paraffin embedded dead tissues. This investigation thoroughly examined live tumor tissues obtained immediately after surgery, and also aimed to demonstrate the heterogeneity of lymphocyte infiltration within a population of colorectal tumors by 1) identifying transcriptional biomarkers that represent strong immune activity, 2) phenotyping key lymphocytes that target and destroy tumor cells, 3) identifying key chemokines that are secreted and induce lymphocyte infiltration, and 4) investigate the degree of dysfunctional MMR in which contributes to the heterogeneity of anti-tumor activity among a population of colorectal tumors. In addition to the specific aims just mentioned, this investigation maintained an overall agenda that is important to mention: contribute to the general knowledge of the field of cancer immunology by reporting discoveries that directly benefit

future patients and practitioners. By keeping this agenda at the forefront of every experiment this investigation avoided losing focus by not pursuing data that does not contribute towards elucidating the mechanisms of this disease.

This investigation will significantly impact the cancer research field by providing important insights into tumor immunology that benefit cancer patients. Identifying which chemokines correlate with anti-tumor lymphocyte infiltration in CRC will clarify predictions for patient outcome. Identifying the magnitude of immune activity and composition of lymphocyte subsets within individual CRCs will equip medical practitioners with better means to manipulate the TME. Finally, this investigation advocates the restructuring of the current method involving the TNM stage classification systems to include an 'immunoscore' that represents the magnitude of immunosurveillance and better predicts patient outcome (Anitei et al., 2014; Galon et al., 2014). This restructuring will affirm the state of the immune system so that the medical community can understand and evaluate the disease across multiple disciplines from surgery to postoperative follow-ups.

Primary Research Questions and Hypothesis

The following questions and strategies were designed to focus the analysis of the data gathered. 1) How will colorectal tumors be categorized and separated into immunologically unique groups? Confronting this obstacle required a simple and logical transcription-based profiling system that accurately predicted and categorized colorectal tumors with strong anti-tumor activity, and then validated that accuracy by determining the average abundance of TILs in each profile. Also, the uniqueness of each profile was determined by measuring the transcriptional activity of other relevant genes involved in

anti-tumor lymphocyte infiltration and comparing to healthy normal mucosa. 2) Are these immunological profiles relevant to patient prognosis? This question required a comparison of these immunological profiles to patient clinicopathological data to validate the relevance to patient prognosis, such as tumor invasion into deeper tissue layers and metastasis to lymph nodes and distant organs. 3) Do secreted chemokines correlate with abundance of TILs? This question justified the collection of live tumor tissues because the secretion of these factors could only be assessed from live cells. Finally, 4) does the degree of dysfunctional MMR reflect the magnitude of anti-tumor activity? Tumors were isolated for DNA, screened for insertions/deletions and epigenetic alterations using previously established genetic markers (Goel et al., 2010a), and categorized based on the degree of MMR defect. These data were then compared to the magnitude of anti-tumor lymphocyte activity in each tumor.

The hypothesis of the investigation was designed to be a testable prediction within the previously defined gaps in the knowledge. The hypothesis states that colorectal tumors within the immunological profile with higher abundance of infiltrating anti-tumor lymphocytes will be the strongest secretors of anti-tumor lymphocyte attracting chemokines. This modular pattern of lymphocyte infiltration should be reflected by the pattern of secreted anti-tumor lymphocyte attracting chemokines.

Research Design, Scope and Limitations

To test the hypothesis, the following technologies were used. First, transcription of key anti-tumor immune genes were evaluated via Real-time PCR to evaluate the magnitude of anti-tumor activity in TMEs. Second, the abundance of TILs were determined via flow cytometry, a laser-based biomarker detection technology that allows for comprehensive

counting of TILs and their relevant secreted factors. Third, the secreted chemokine profiles of minced non-frozen tumor specimens were determined via a multiplex immunoassay that measures multiple protein analytes simultaneously. Fourth, the state of genomic instability of each tumor was determined via a highly sensitive pentaplex PCR and amplicon sequencing assay and pyrosequencing. And fifth, important findings was validated by comparing to a large publicly available gene transcription database clinicopathological, The Cancer Genome Atlas (TCGA).

Limitations to the investigation were few and only pertain to tumor sample availability and the capacity of the instruments to accurately record data: 1) the flow cytometer is limited to detecting 8 parameters (cellular biomarkers) and is further limited to which detection antibodies are available on the market, 2) reagent availability limits the immunoassay to analyze only specific chemokines, and 3) the sensitivity of the immunoassay is limited to a specific range of concentrations for each analyte.

The scope of the study was limited to no more than 50 CRC patients who received treatment at BUMC, and to those whose cancer was treatable, resectable, and large enough to provide materials for measuring the parameters of interest. Participants were excluded for the following reasons: receiving adjuvant chemotherapy for treatment of a previous tumor or any other factor that may alter the state of the tumor, not enough tissue to be spared for adequate diagnosis by the pathologists, severely advanced disease state where surgery was not performed, current infection and whether receiving antibiotics, steroid medications, blood thinner medications, antifolates, any current or previous history of tuberculosis, HIV, Hepatitis or any autoimmune disease, and/or the patient's decision not

to participate. These strict exclusion criteria ensured that the findings of the investigation represented CRC without medical intervention.

BUMC's institutional review board approved this investigation and allowed CRC tissues and healthy normal mucosa to be obtained in conjunction with the Department of Pathology. Patient protection was the highest priority; therefore contact with the patient was minimized and limited to trained medical professionals. Initial contact with each patient was made in person only by a trained nurse for the purpose of obtaining informed consent.

Summary

Understanding human cancer requires a close observations of the disease's native state. To the knowledge of the primary investigator, this investigation marks the first attempt to analyze secreted chemokines that are associated with anti-tumor activity from live colorectal tumors. The conclusions of the investigation will effectively provide a "snapshot" of the modularity of anti-tumor activity in a population of CRCs, and will connect this pattern to MMR dysfunction. The conclusions of the investigation will be reasonable and limited to the scope of materials collected and will be validated against a larger publicly available tumor database. The justification for the investigation is derived from a solid, well established, carefully reviewed body of literature, and endorsed by world renowned experts in the fields of tumor biology, tumor immunology, and cancer genetics.

CHAPTER TWO

Literature Review

The purpose of this literature review is to collect and summarize the most pertinent information available that connects tumor phenotype with cancer immunology. This is a methodological review that focuses on the techniques used by previous research and describes how these techniques shaped the current body of knowledge. Included is a historical perspective that provides an idea of how medical research has progressed towards solving the mysteries that have, and still are, plaguing cancer treatment. The remainder of the chapter will be partitioned into two major disciplines of cancer research: cancer genetics and tumor immunology, and then ending with a review of current research that combines both in the context of CRC. An exhaustive review is not attempted due to both length restraints and the increased risk of diverting the focus away from the two major research disciplines. To ensure the chapter is focused, accurate and well represented, only the strongest publications that are central or pivotal to each discipline will be discussed. Therefore, a strong attempt will be made to relieve the reader from the strains of reading through summaries of studies that are redundant and non-critical to the subject. This review will focus on human cancer; however mouse studies will be included when human data are not available.

Each section will start with a brief overview of the most relevant reviews then will later focus on the individual peer-reviewed publications that are repeatedly included among the reviews. This ensures that the literature discussed will represent the opinions that are

most commonly accepted by the key contributors of the research field and comprises only high quality studies pertaining to cancer genetics and immunology. Therefore the studies discussed will be important to the discussion and will be presented from the perspective of the authors. Data cited from reviewed studies will be evaluated in full for appropriateness of claims stated as reflected in the experimental design. Any inferences made about the literature as a whole outside a peer-reviewed article will only be stated as pertaining to the investigation's hypothesis. Definitions of important terms will be incorporated into the document as they are introduced. Liberty will be taken when referring to cell types mentioned between different studies. Depending on the study, a specific cell type may be identified by one of many identifying characteristics; therefore, the term used in this review to represent a specific cell type may never have been used in the article referenced. However such liberty will be taken with extreme caution and only to consolidate findings between studies.

Research Question of the Literature Review

The primary question of this review asks how the key contributors of tumor immunology research represent the current knowledge that describes the activation of immune system towards tumors, and if mismatch repair deficiency is a predictor of this immune activity in CRC. The focus of this review is to discuss which immune cells are believed to predict long term survival for CRC patients and the mechanisms that may be involved in protecting the patient.

This review will take a closer look at the key contributors who have shaped the current state of the CRC research field. Beginning with the seminal publication by Fearon and Vogelstein in 1990 that set the initial framework for CRC research, these two were the

first to propose a genetic model of multi-step carcinogenesis for CRC (Fearon and Vogelstein, 1990). Fearon and Vogelstein interpreted the prior decade's research pertaining to dysregulation of oncogenes and tumor suppressor genes to link the progressive step-wise changes in biological and phenotypic properties in cancer cells. Next to be discussed are the three independent laboratories led by Perucho, Thibodeau, and Vogelstein who discovered microsatellite instability (MSI) in CRC, and linked MSI to hereditary nonpolyposis colorectal cancer or Lynch syndrome. They found that MSI in CRC was associated with increased patient survival, and cemented the theory that tumor phenotype affects tumor biology (Aaltonen et al., 1993; Thibodeau et al., 1993; Peltomaki et al., 1993). Later, in 1998 C. Richard Boland was to act as foreman for the National Cancer Institute's (NCI) "International Workshop on Microsatellite Instability and RER Phenotypes in Cancer Detection and Familial Predisposition" workshop to solidify a strategy for classifying MSI tumors (Boland et al., 1998). Next, the concept of "tumor escape" from immunosurveillance will be discussed. Described by Dunn and Schreiber in 2004, the notion of tumor escape for immune detection began to be recognized as a major characteristic of cancer (Dunn et al., 2004). Discussed later will be the contributions by Kloor and von Knebel Doeberitz who clarified the paradoxical nature of MSI tumors having a low frequency of metastasis and proposed that enhanced immunosurveillance can be triggered by immunogenic tumor-associated antigens (TAAs) expressed in this tumor phenotype (Buckowitz et al., 2005). A major emphasis will be directed towards the progress made by Galon and Pagès who in 2006 showed that the abundance and nature of infiltrating anti-tumor lymphocytes predicts patient survival (Galon et al., 2006), and who proposed a paradigm shift in the current practice of cancer evaluation. The final topic that

will be discussed are the contributions by two pioneers, Palucka and Banchereau, who began proposing immunotherapy in the form of vaccinations that utilize master antigen-presenting cells to prime and activate lymphocytes that target tumors (Palucka et al., 2007). The aforementioned contributors each wedged their influence in the field of cancer immunology research to forge great progress towards more personalized care of cancer patients.

Multistep Genetic Model for Colorectal Carcinogenesis

Both inherited and somatic alterations to cellular pathways can interrupt homeostasis, therefore these pathways can become drivers for colorectal tumorigenesis when mutated (Vogelstein and Kinzler, 2004). The first genetic model of solid tumor progression, introduced by Fearon and Vogelstein, described the temporal progression of mutations commonly found in CRC from adenomas through carcinoma (Figure 1). Most mutations confer no effect on neoplastic progression; however, the model suggests that serial mutational events at specific genes trigger step-wise progression to advanced tumor stages (Fearon and Vogelstein, 1990). This is supported by the observation that colorectal neoplasms are monoclonal –having homogeneity in genetic alterations– which can be explained as an outgrowth of a cell with a mutation that grants growth or survival advantage over others (Fearon et al., 1987). This observation was made when 75% of carcinomas studied demonstrated loss of chromosome 17p sequences (Fearon et al., 1987), and verified by Boland et al, who demonstrated that the genetic loss occurred exactly at the adenoma-to-carcinoma transition (Boland et al., 1995). Below describes the temporal progression of mutation suggested by Fearon and Vogelstein.

Inactivation of the tumor suppressor gene *adenomatous polyposis coli* (*APC*) and subsequent unregulated activation of the Wnt signaling pathway contributes a particular growth advantage and marks the initiating event towards formation of aberrant crypt foci (Alberts et al., 2008). These foci are clusters of apoptosis resistant abnormal tube-like epithelial tissue of glandular origin (Takayama et al., 2005). *APC* derives its name from the observation that germline mutations in this gene are responsible for the disease adenomatous polyposis coli (more commonly called familial adenoma polyposis, or FAP) in which thousands of adenomatous polyps occur thoughout the colonic mucosal layer (Bodmer et al., 1987). In fact somatic *APC* mutations occur in 72% of sporadic tumors mainly between codons 1286 and 1513 (Luchtenborg et al., 2004), another 18% are hypermethylated at the promoter region of *APC* (Esteller et al., 2000). In either event, inactivation of APC prevents phosphorylation of β-catenin by casein kinase 3 and subsequent degradation of β-catenin by proteasomes. Unregulationof this pathway has been identified as responsible for the lack of control of cell proliferation in may cancers (Alberts et al., 2008).

As a GTPase, the *KRAS* protein affects many signal transduction pathways, and activating mutations of the proto-oncogene occurs in approximately 40% of CRCs (Alberts et al., 2008) and causes clonal expansion and progression into later stage adenomas. Evidence for this is observed when larger adenomas and carcinomas display much higher rates of ras gene mutation than smaller adenomas (Vogelstein et al., 1988). Only when *KRAS* is mutated after *APC* will it promote tumor progression (Haigis et al., 2008). Curiously, if the *KRAS* mutation occurs in the absence of inactivation of the *APC* gene, the

result is different, and the fate of the epithelial cell is directed to senescence (Bennecke et al., 2010).

Further mutation in tumor suppressor genes *TP53* and *SMAD4* (Alberts et al., 2008), and/or loss of heterozygosity (LOH)[1] at chromosome p18 can occur when the tumor advances to early carcinoma (Fearon and Vogelstein, 1990). Breakdown of the p53 cell cycle checkpoint, possible through the loss of the portion of chromosome p17 containing the p53 gene (Baker et al., 1989) accompanied by point mutations in *TP53*, will diminish the cell's ability to arrest at the G1/S phase in response to DNA damage. *TP53* is mutated in at least 61% of CRCs (Smith et al., 2002). An earlier study suggested that LOH at 18q removes *deleted in colorectal cancer* (*DCC*) gene, another known tumor suppressor gene that was speculated to be involved in cell adhesion and therefore may conduct growth-restraining signals (Baker et al., 1989), however this has been since debunked as a cause of colorectal carcinogenesis (Boland et al., 1995). The actual 18q tumor suppressor gene lost at this stage of carcinogenesis is recognized as the *SMAD4* gene, of which LOH occurs in approximately 54% of CRCs (Fleming et al., 2013). At this stage the tumor gains the ability to invade the basement membrane and metastasize to adjacent lymph nodes and distant organs, commonly the liver (Jones et al., 2008).

Activating mutations in *PIK3CA* occurs in a proportion of CRCs but occurs during the late adenoma-to-carcinoma transition (Pino and Chung, 2010). Mutations in the phosphatidylinositol 3-kinase (PI_3K) catalytic subunit affects apoptosis, cell growth, and other pathways regulating survival, mobility, and transformation (Karakas et al., 2006).

[1] Loss of heterozygosity occurs during the loss or gain of a segment of one chromosome due to unbalanced mitosis. Some investigators call this allelic imbalance to acknowledge the ambiguity of whether there has been a gain or a loss. In the case of tumor suppressor genes, allelic loss is assumed.

Activated PI_3K then proceeds to phosphorylate phosphatidylinositol 4,5 bisphosphate to phosphatidylinositol 3,4,5 bisphosphate (PIP_3), which drives pathways involved in cancer progression. Somatic mutations in *PIK3CA* are found in over 30% of solid tumors and 25% of colon cancers (Karakas et al., 2006) and increases kinase activity and stimulates AKT signaling; 40% of tumors have other mutations in the same pathway, marking *PIK3CA* an oncogene –or part of an oncogenic pathway (Samuels and Ericson, 2006).

This model may explain why tumors from elderly patients contain relatively twice as many mutations as a tumor from a middle-aged patient, and how pediatric cancers have relatively few mutations (Vogelstein et al., 2013). Therefore, the likelihood of accruing a mutation increases over time.

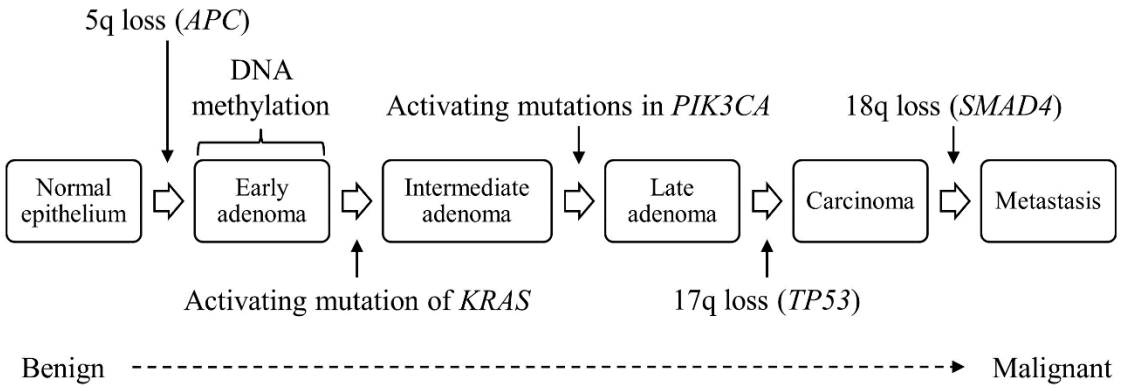

Figure 1. Multistep genetic model for colorectal carcinogenesis. Adapted from (Fearon and Vogelstein, 1990)

Hallmarks of Cancer

The complexity of the body of literature pertaining to cancer is boundless; however like most major areas of research, cancer specific discoveries are coalesced by the research community into legitimate categories that represent different traits of the disease. These traits are generalizations of existing postulates ranging from the loss of sensitivity to apoptotic stimuli to ability of tumor cells to gain growth advantages over normal cells

(Vogelstein et al., 1988; Fearon and Vogelstein, 1990). Hanahan in 2000 spearheaded this task by describing the six hallmarks of cancer (Hanahan and Weinberg, 2000), and later expanded this description of cancer to include the effects of inflammation (Hanahan and Weinberg, 2011).

"Self-sufficiency of growth signals" is the acquired ability of tumor cells to produce growth factors. Examples of growth factors are platelet-derived growth factor (PDGF) and tumor growth factor alpha (TGF-α). Also, neoplastic cells can express pro-growth extracellular matrix receptors, such as epidermal growth factor receptor (EGFR) and HER2/neu. This hallmark is not limited to extracellular signals, but can be derived from dysregulation of growth genes. Mentioned above, a mutated *KRAS* oncogene disrupts control of cell proliferation (Haigis et al., 2008).

Complementary to self-growth signals are "insensitivity to anti-growth signals", where cells move from a quiescent state to a growth phase even in the presence of anti-growth signals. Retinoblastoma protein (pRb) blocks progression into the S phase, however is non-functional in its phosphorylated state commonly found in neoplastic cells. Transforming growth factor beta (TGF-β) signals through the cytoplasmic Smad4 protein (mentioned above) to block phosphorylation of pRb (Schutte et al., 1996). Smad4 is mutated in 35% of primary invasive carcinomas and 31% of distant metastases (Miyaki et al., 1999b).

"Evading apoptosis" is the shutdown of programmed cell death pathways. These pathways involve intracellular receptors that detect abnormalities, such as DNA damage, to focus signals to the mitochondria that trigger the release of cytochrome C. Already mentioned above, p53 is a cell cycle regulator that functions in a transcription factor

cascade to halt cell cycle progression, and is inactivated in over 50% of colorectal tumors (Harris, 1996). Another mechanism for evasion of apoptosis common in CRC is the upregulation of the decoy receptors such as FAS death receptor (Pitti et al., 1998). The decoy receptor 3 (DcR3) gene is commonly activated and believed to divert apoptotic instructions received from apoptosis-inducing lymphocytes.

Overcoming senescence after a finite number of doublings is called "limitless replicative potential". Cells that lose the ability to enter senescence after erosion of telomeric DNA enter a state of extreme telomeric shortening called telomere[2] crisis. Shortened telomeres along with gene alterations in APC lead to chromosomal instability and subsequent CRC initiation (Roger et al., 2013). Increase in telomerase activity is associated with progression from benign tissue to carcinoma (Shay, 2013).

"Sustained angiogenesis" stems from the axiom that cancer is the wound that never heals (Motz and Coukos, 2011) due to constant induction of angiogenesis, inflammatory-cell infiltration, and cell proliferation (Dvorak, 1986). Characteristic of wound healing is inflammation and concomitant secretion of cytokines such as vascular endothelial growth factor (VEGF) and fibroblast growth factor (FGF). Cancer is a disease that affects the whole body therefore VEGF and other angiogenesis regulatory factors, platelet factor 4 (PF4) and PDGF, are elevated in platelets from CRC patients' peripheral blood (Peterson et al., 2012).

"Tissue invasion and metastasis" are characterized by outgrowth of the primary tumor into surrounding tissues and subsequent spread to distant organs. Tumor cells at the invasive margin (IM) undergo changes called epithelial-to-mesenchymal transition (EMT),

[2] Telomeres are located at the termini of chromosomes and consists of areas repeated DNA (TTAGGC repeats) and protein complexes.

which is characterized by expression of nuclear β-catenin, changes in cell-cell adhesion (down regulation of E-cadherin and upregulation of vimentin), loss of polarity, and gain of migratory properties (Kong et al., 2011). Cancer cells become dangerous when they migrate out of their origin, which is something ordinary epithelial cells cannot do.

"Tumor-promoting inflammation" is the main driver of evasion from immune detection (Hanahan and Weinberg, 2011). Tumor cells and infiltrating immune cells can contribute to other hallmarks by supplying the rest of the tumor with bioactive molecules that induce growth, proliferation, angiogenesis, and metastasis, as well as inhibiting tumor-targeting immune cells by secreting TGF-β (Shields et al., 2010). For example, necrotic tumor cells and colonic barrier defects plus microbial products can recruit and attract immunosuppressive and inflammatory immune cells (Grivennikov et al., 2010) that result in the inhibition of tumor eradication. One theory that explains this phenomenon suggests that inflammatory immune cells can secrete IL-17 and induce EMT in epithelial cells through TGF-beta-dependent pathways (Vittal et al., 2013) resulting in tissue invasion and metastasis (Figure 2).

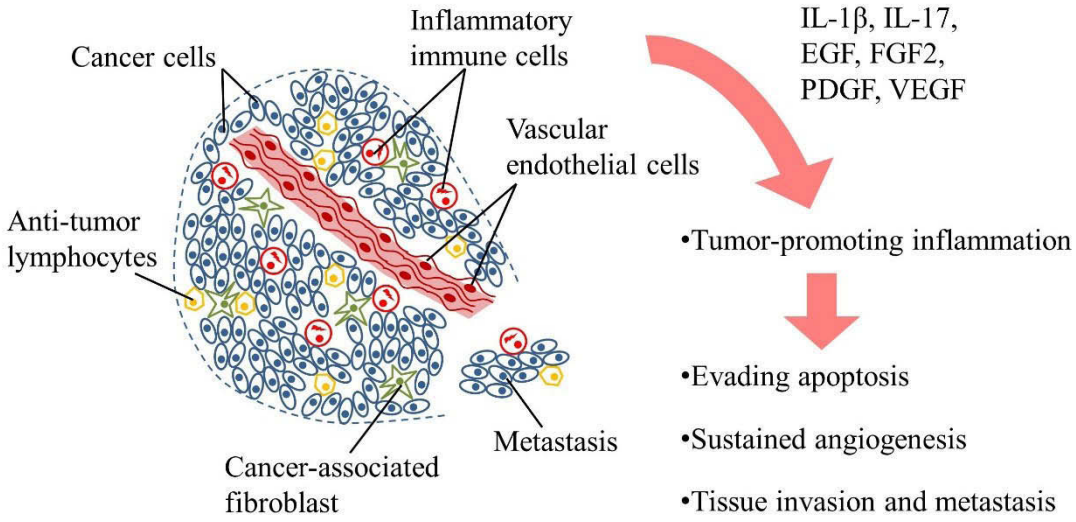

Figure 2. Hallmark of cancer: tumor-promoting inflammation

Genomic Instability: Causation of Cancer

Recent advances in gene sequencing technologies have confirmed that the initiation of cancer requires multiple mutations. Interestingly, different cancers originating from different parts of the body can harbor similarly mutated genes (Wood et al., 2007; Vogelstein et al., 2013). In that respect, recent efforts towards the comprehensive sequencing of genomes from multiple cancer types have concluded that only a relatively small number of select mutations actually contribute to neoplastic growth, while other mutations will provide no growth advantage at all. This next section will explore multiple forms of genomic instability that introduce further mutations into the cellular genome and contribute to tumorigenesis.

Tumors with mutations in genomic maintenance machinery are of particular interest to this investigation. Dysfunctional genome maintenance can induce a hypermutable phenotype or "mutator phenotype" (Loeb et al., 2003). This phenotype is speculated to generate tumor cells with genetic variability (Nowell, 1976). As a consequence, these cells can progressively accrue multiple driver mutations where an ensuing "multiple-hit" scenario can either activate and/or deactivate one or more genes that regulate cell proliferation (Nordling, 1953; Knudson, 1971). Many of these "driver gene" mutations are restricted to signaling pathways and dictate cell growth and survival, intracellular signaling, and genome maintenance (Leary et al., 2008; Vogelstein et al., 2013).

Genomic instability can range from subtle changes that are either restricted to gene sequences, such as point mutations and gene amplifications, to catastrophic changes involving chromosome number and translocations. Genomic instability in CRC is

classified into mainly three categories, chromosomal instability (CIN), microsatellite[3] instability (MSI) (Peltomaki et al., 1993; Aaltonen et al., 1993; Koi et al., 1994), and the CpG island[4] (Gardiner-Garden and Frommer, 1987) methylator phenotype (CIMP) (Pino and Chung, 2010). Each of which can generate a large number of "driver gene" mutations (Loeb, 1991). Of noteworthiness, tumor viruses can encode viral oncogenes that lead to genomic instability (Boland et al., 2005), however this review will not discuss virus-induced tumorigenesis. It can be predicted that genomic instability generates diverse changes in the cellular genome of which most are deleterious and lead to cell death, thereby having a self-correcting outcome. However, some of these changes will occasionally favor additional growth and survival and select specific cells for expansion.

CIN is defined as the accelerated generation of duplications, deletions, or rearrangements of parts or whole chromosomes, and is identified in 65%-85% of sporadic CRCs (Lengauer et al., 1998; Geigl et al., 2008; Pino and Chung, 2010). This particular pathway of tumorigenesis can begin with telomere breakage (Engelhardt et al., 1997). Telomeres function to maintain chromosome integrity by preventing fusion and breakage during anaphase (Friedberg et al., 2006). Telomeres progressively shorten during multiple rounds of cell duplication and eventually reach a critical length in an event called "telomere crisis" where the cell either enters senescence or initiates apoptosis (Shay, 2013). However, if this checkpoint is bypassed, chromosomes can undergo breaks and/or fusions that result in extensive genome rearrangements (O'Hagan et al., 2002). In contrast, some tumor cells

[3] A microsatellite is a highly repetitive nucleotide tract.

[4] CpG islands are genomic regions containing a high frequency of alternating cytosines (C) and guanines (G) on the same strand of DNA or RNA connected by a phosphodiester bond (p).

acquire increased telomerase activity that indefinitely maintains telomere integrity and effectively immortalizes tumor cells (Roger et al., 2013).

Mismatch Repair-Deficiency

MSI is a consequence of DNA mismatch repair (MMR)-deficiency where genetic mutations disrupt the expression of MMR machinery, creating a hypermutable phenotype that increases the probability of developing adenocarcinomas (Toyota et al., 1999; Kloor et al., 2007; Boland and Goel, 2010). The majority of mutations that cause MSI are found in two MMR genes, *MSH2* and *MLH1*, which are located on chromosome 2 (Fishel et al., 1993) and 3 (Koi et al., 1994), respectively, however other mutations are found in *MSH6* (Miyaki et al., 1997). Homologs of these genes were first identified in bacteria and yeast and classified as mutator genes because, when defective, they increase spontaneous mutation rates (Fishel, 2001) causing a hypermutable phenotype that generates frame-shift peptides (Boland and Goel, 2010; Kloor et al., 2010). Therefore, MSI is defined as a very large increase in either the rate or number of insertion/deletion mutations in DNA (Boland and Goel, 2010) when dysfunctional DNA MMR can no longer recognize or repair erroneous insertions, deletions, and mis-incorporations that arise with DNA polymerase activity and replication, recombination, and repairs (Iyer et al., 2006; Boland and Goel, 2010). The resulting MSI phenotype is likely to affect multiple molecular pathways rather than single genes (Kinzler and Vogelstein, 1996), and therefore has major implications in CRC. MSI will be at the center of this investigation because it has potential consequences at the interface between tumor phenotype and the anti-tumor immune responses, of which will be discussed later in this review.

MSI was first identified in cancer by Ionov and colleagues in 1993 who detected somatic deletions in highly repetitive DNA regions of poly-adenine repeats called microsatellites in 12% of colorectal tumors (Ionov et al., 1993). This finding marked this category of genomic instability as bimodally distributed (Ionov et al., 1993; Jass et al., 1998). Later other microsatellite regions, such as cytosine and adenine dinucleotide repeats, were also found to be mutated within MSI tumors (Fishel et al., 1993). Insertion and deletions are likely to accrue in microsatellites because highly repetitive sequences are prone to ineffective "proofreading" by DNA polymerases (Jascur and Boland, 2006) and are more likely to accumulate mutations when MMR machinery is ineffective. This can make microsatellite lengths variable among a population of tumor cells (Strauss, 1999). Screening for MSI can involve sequencing microsatellites, particularly mononucleotide and dinucleotide repeats, for length variations. Whether inherited or acquired, MSI phenotype occurs in approximately 15% of CRCs (Boland et al., 1998).

MMR deficiency can also be acquired through epigenetic silencing of *MLH1* (Weisenberger et al., 2006). This occurs as a consequence of hypermethylation of DNA (or CIMP) that causes changes in the expression of coding and non-coding RNAs (Esteller, 2008; Zlobec et al., 2011) in what is called CIMP-associated methylation of *MLH1* (Weisenberger et al., 2006). Therefore in many cases MSI is CIMP-driven (Issa, 2004; Esteller, 2008). Hypermethylation of promoter regions occurs at short nucleotide sequences containing high frequencies of CpG dinucleotides, or CpG islands (Bird, 1986). Methylation of cytosines is mediated by DNA methyltransferases and can persists through subsequent clonal lineages. Methylation at the *MLH1* promoter is often acquired during aging, but is not exclusive to that region. Approximately half of all human genes contain

CpG islands (Boland et al., 2009). Epigenetic silencing of *MLH1*, as well as other tumor-suppressor genes, is most severe when methylation occurs at the 3' promoter region (Kane et al., 1997; Toyota et al., 1999). Isolated methylation of the 5` promoter region does not silence gene expression (Kane et al., 1997). Tumors that are derived through hypermethylation of tumor-suppressor genes are considered sporadic (Toyota et al., 1999) and represent 12% of all CRCs (Kane et al., 1997).

Lynch syndrome was previously called the "cancer family syndrome" (Lynch et al., 1993) and involves inherited mutations in MMR genes (Boland and Goel, 2010). These patients bear approximately 3% of all CRCs (Boland, 2005) and develop multiple tumors in their gastrointestinal tracts between 20 and 50 years of age. They also have an increased frequency of tumors in the endometrium, urinary tract, stomach and other organs (Lynch et al., 1993).

CRCs with MSI have unique histopathological characteristics showing less aggressive clinical progression when compared to stage-matched microsatellite stable (MSS) tumors (Boland et al., 1998; Popat et al., 2005). In particular, a population based study including over 14,000 Finnish nationals concluded that patients with mutated *MLH1*-associated CRC have a significantly better chance of survival (Sankila et al., 1996) and improved prognosis (Gryfe et al., 2000; Popat et al., 2005; Laghi and Malesci, 2012) when compared to other CRCs. Activating mutations in β-catenin or inactivating mutations in APC can also contribute to progression of CRCs with MMR defects (Miyaki et al., 1999a). Interestingly however, as of 2010, eleven studies have reported no benefit from chemotherapeutic intervention for CRC patients with MSI tumors (Boland and Goel, 2010). Even more interesting, the use of 5-fluorouracil (5-FU)-based cytotoxic

chemotherapy was associated with increased cancer-related mortality in MSI patients (Ribic et al., 2003). One study recruited over 200 stage II and III CRC patients and concluded that although 5-FU-based therapy improved survival for non-MSI patients, while MSI patients did not demonstrate the same advantage (Carethers et al., 2004). An explanation for this paradox comes from multiple studies that demonstrate the mitigated effects of chemotherapy on MMR deficient cells. MMR is partly responsible for detecting DNA damage and initiating apoptosis, therefore defective MMR leaves cells resistant to alkylating agents, such as N-methyl-N-nitrosourea or N-methyl-N'-nitro-N-nitrosoguanidine (Branch et al., 1993; Branch et al., 1995) and the thymidylate synthase inhibitor, 5-FU, and leaving cells incapable of triggering apoptosis in response to excessive DNA damage (Meyers et al., 2001). Therefore testing for MSI should be incorporated into standard patient care for all patients with gastrointestinal tumors (Ribic et al., 2003).

MSI tumors are paradoxical because the same mechanism that increases an individual's chance of acquiring cancer will also contribute to their increased chance of surviving the disease. Perhaps this may be explained from an immunological stand point. MSI creates frame-shifted genes that translate into novel TAAs that may consistently vaccinate the host's body against TAA-presenting tumor cells (Reuschenbach et al., 2010; von Knebel Doeberitz and Kloor, 2013). However, this view does not completely explain why some CRCs are infiltrated more abundantly by tumor-infiltrating lymphocytes (TILs) (Smyrk et al., 2001; Drescher et al., 2009). Other factors such as tumor-inducing viruses, tumor stage, inflammatory bowel disease, etc. can also affect the TIL population. The remainder of this review will deeply explore the mechanisms involving the immune response against neoplastic growth in the context of genomic instability and MSI.

Cancer Immunoediting

Neoplastic cells undergoing phenotypic changes are predicted to be eliminated through immunosurveillance (Burnet, 1957; Mittal et al., 2014). This mechanism prevents tumorigenesis by triggering immune cells to mount anti-tumor activity against these cells (Burnet, 1957). However, the existence of cancer itself suggests that neoplastic cells are capable of evading immune detection, therefore immunosurveillance is not always successful. These observations suggest that tumor cells either only possess 'self' antigens that are tolerated by the immune system, or that TAAs are somehow becoming tolerated by the immune system (Burnet, 1957). One theory, which explains this in very broad terms, suggests that genomic instability generates a high frequency of new mutations that catalyzes the generation of novel phenotypes (Khong and Restifo, 2002). It is likely that most of these mutations will have a deleterious impact on cell survival, but by random chance, some variants can acquire the ability to evade immune detection and elimination, and clonally proliferate into a growing mass of malignant cells. Therefore, over time uncontrolled proliferation of a hypermutable cell population under the selective pressure of the immune system will eventually create a variant that evolves to evade the immune system (Khong and Restifo, 2002; Schreiber et al., 2011), and changes that are derived from genomic instability can randomly generated mutations that occasionally provide a growth or survival advantage over neighboring tumor cell populations (Wood et al., 2007; Vogelstein et al., 2013). This requires either silencing of tumor suppressor genes or activation of oncogenes.

Cell variants generated from genomic instability are believed to be naturally selected for escape over time in a process called immunoediting (Khong and Restifo, 2002)

(Figure 3). This process takes place in three stages, elimination, equilibrium, and escape (Dunn et al., 2002; Dunn et al., 2004; Dunn et al., 2006) all between the contending forces of tumor promotion and host protection, and results from a combination of prolonged anti-tumor immunity and outgrowth of non-immunogenic tumor cells (Zitvogel et al., 2006; Mittal et al., 2014).

Elimination involves proficient immunosurveillance that targets and eradicates cells identified as 'non-self'. These cells can also take the form of invading pathogens or any cell displaying unusual proteins that can be subsequently attacked by cytotoxic lymphocytes. Normally, lymphocytes that potentially recognize self-antigens are removed at the immature stage in the thymus before they can mature and enter the periphery; or once in the periphery, they can be suppressed by regulatory immune cells that aim to resolve inflammation through suppressive cytokines and induce tolerance to self-antigens. However lymphocytes that recognize only non-self-antigens are allowed to enter the periphery and potentially eliminate tumor cells as well as foreign cells (Murphy et al., 2008). If a portion of tumor cells are not directly eliminated by the immune system then the next stage of immunoediting begins (Dunn et al., 2006).

The equilibrium stage features a balance between rates of tumor cell elimination and generation of tumor cell variants through the accumulation of mutations in the setting of a mutator phenotype. Here, the immune system ignores and therefore selects for variants that are increasingly tolerated (Dunn et al., 2002). For example, tumor cells from immunodeficient mice are more immunogenic than tumor cells from immunocompetent mice, and are then less tolerated when transplanted into immunocompetent hosts (Schreiber et al., 2011). In other words, immunogenic tumor cell variants in the presence of

immunosurveillance are removed where non-immunogenic cells are allowed to proliferate. In this stage the immune system is still capable of controlling tumor expansion and halting metastasis, however, eventually tumor cell populations evolve the ability escape immune detection. Finally, this is followed by an escape from immune detection, which is highlighted by the uninhibited outgrowth of non-immunogenic tumor cells. Here, tumor cells are no longer targeted and eliminated by the immune system, and contain the capacity to metastasize to distant organs and lymph nodes. At this stage, advanced tumors have evolved into a phenotype that is no longer identified as non-self and no longer targeted by the immune system (Dunn et al., 2006).

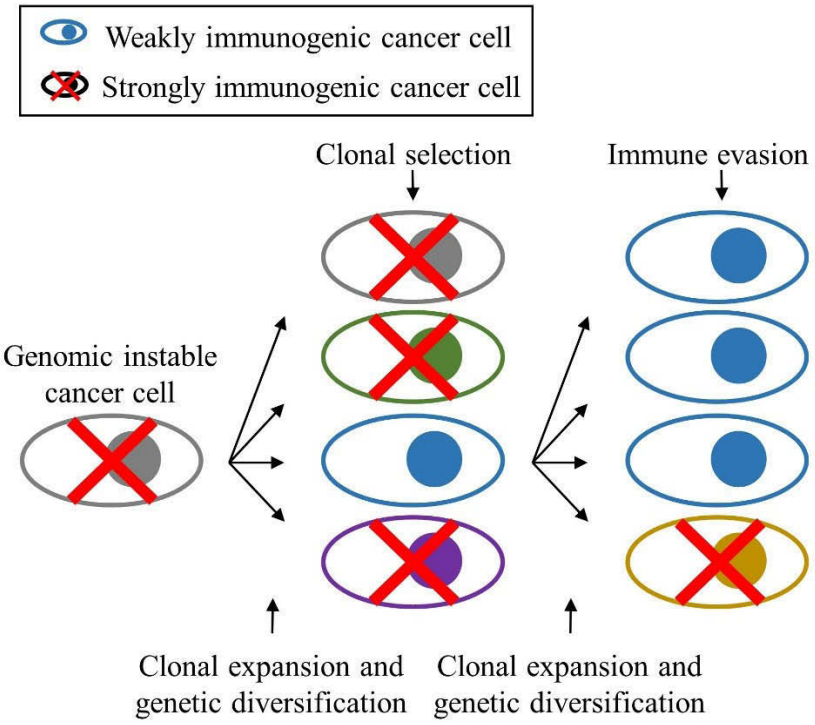

Figure 3. Mechanism of immunoediting and clonal selection

An exception to the theory that genomic instability contributes to immune evasion is MSI. Thoroughly described before, this form of genomic instability generates a very

large number of insertion-deletion mutations that create frameshifts in microsatellite regions and theoretically result in the generation of neo-antigens, or TAAs, and is hypothesized to contribute to enhanced immunosurveillance. Tumor cells expressing TAAs are less likely to escape immunosurveillance (Ajioka et al., 1996; Linnebacher et al., 2001; Ripberger et al., 2003; Koesters et al., 2004; Schwitalle et al., 2004; Reuschenbach et al., 2010), therefore patients with MSI tumors are believed to have a more favorable prognosis (Popat et al., 2005; Chang et al., 2009; Boland and Goel, 2010; Kloor et al., 2010). However researchers and practitioners still only have a vague understanding of the complex immune activities harboring in this subset of CRCs.

It has become clear that continued development of novel strategies that combat cancer should focus towards improving early detection before immune escape can occur. Developing better screening strategies that detect tumors at the earliest stages, and developing measures that stop the progression towards immune escape should be at the forefront of current and future cancer research.

The Tumor Microenvironment

The tumor microenvironment (TME) consists of a heterogeneous cell population that includes both malignant and non-malignant cells, connective tissue, fibroblasts, resident immune cells, other stromal cells, extracellular signaling molecules, and blood vessels that permeate and nourish the tumor (Bindea et al., 2013; Quail and Joyce, 2013). This review will now focus on the complexity of the TME as represented by the diverse milieu of immune cells that inhabit the tumor (Galon et al., 2007). Comparing two tumors will yield radically different immune cell compositions and signaling activity, ranging from

different magnitudes and proportions of immune cells and their subsets, all of which may affect tumor growth and invasion.

The variety of tumor infiltrating immune cells is complimented by secreted signaling molecules, called 'cytokines'. This classification of soluble proteins regulate cellular functions during normal and pathological conditions (Murphy et al., 2008; Grivennikov and Karin, 2011). These molecules target cell that express their cognate receptors and trigger a number of autocrine and paracrine functions. Of interest to this investigation, these functions induce differentiation of unprogrammed (or naïve) immune cells into anti-tumor effector cells, proliferation and angiogenesis (Motz and Coukos, 2011; Quail and Joyce, 2013) in stromal tissue, or senescence and apoptosis in tumor cells (Murphy et al., 2008). Cytokines are also responsible for initiating the wound healing response by triggering inflammation, proliferation and movement of endothelial cells. Another function of cytokines, which is the focus of this investigation, involves chemoattraction of anti-tumor lymphocytes to sites of inflammation (Murphy et al., 2008). These extracellular signals can either promote anti-tumor responses by promoting chemoattraction of cytotoxic lymphocytes (Pages et al., 2010; Fridman et al., 2011; Quail and Joyce, 2013) or induce immune tolerance by promoting chemoattraction of suppressor cells that inhibit anti-tumor responses (Mantovani et al., 2008; Forster et al., 2008; Motz and Coukos, 2011). Similar to genomic instability, the TME can also "edit" the tumor cell population through the conflicting pressures of anti-tumor activity and immune suppression; the variety of tumor cell phenotypes generated from genomic instability can naturally select for immune suppressing malignant cells (Dunn et al., 2006). Therefore, the

wide variety of cytokines secreted into the TME can further complicate the landscape of the disease by both aiding or controlling growth and progression.

Lymphocytes: Helping or Hindering Survival?

The variety and number of TILs that infiltrate colorectal tumors has attracted considerable attention over the past few decades because of their perceived effect on patient survival. In 1986 Jass and colleagues were one of the first to demonstrate improved survival rates of rectal cancer patients with high infiltration of lymphocytes (Jass, 1986). This study generated the hypothesis that an increased number of TILs provides a favorable prognosis. However, the relationship between TILs and clinical outcome is not obvious since multiple types of lymphocytes may infiltrate a tumor, of which only some may be beneficial.

Infiltration of T-cells. The immune system reacts to TAAs that are presented by tumor cells and "educating" other immune cells to clonally proliferate and attack other cells that present similar polypeptides as the TAA. This education against TAAs was first demonstrated when melanoma-associated antigen 1 (MAGE-1) was found to be expressed on multiple melanoma cell lines and encodes the antigen, MZ2-E. This antigen associates with class I major histocompatibility-complex (MHC) and is recognized by cytotoxic lymphocytes (van der Bruggen et al., 1991; Novellino et al., 2005). Later, this cytotoxic anti-tumor activity was demonstrated in CRC patients when lymphocytes that were isolated from patient blood elicited strong immune reactivity to the antigen mucin-1 (Koch et al., 2006), which is commonly expressed in colorectal tumors (Ajioka et al., 1996).

Cytotoxic activity is a highly coordinated attack involving a battery of specifically educated lymphocyte subsets that target a specific group of cells. This activity first requires TAAs to be proteasome-degraded into 7-11 amino acids length polypeptides and presented

by the class I MHC molecules on the extracellular surface of tumor cells. T-cells, a specific subset of lymphocytes, will then recognize a specific TAA via their T-cell receptor (TCR) and trigger individual tumor cells to undergo apoptosis.

A particular subset of T-cells that the focus of this investigation are effector cytotoxic T lymphocytes (CTLs)[5] that express the cell surface markers cluster of differentiation (CD) 3 and CD8. CD3 is a pan marker for all T-cells, while CD8 is a co-receptor for the TCR that specifically ligates to class I MHC (Murphy et al., 2008). CD8 is a transmembrane glycoprotein that can be expressed as a disulfide-liked heterodimer. Its two proteins are encoded by genes *CD8A* and *CD8B*, however it can be expressed as homodimer consisting of two alpha-chains on other T-cells as well as natural killer (NK) cells. Once the CTLs recognize TAAs that are presented by class I MHC, and co-receptors have ligated, CTLs will clonally proliferate and trigger apoptosis in target cells by releasing granules containing cytotoxic mediators. These cytotoxic mediators consist of a variety of proteins: perforin, which aids in delivering mediators to the cytosol of the target cell by inserting into the plasma membrane and forming a pore; granulysin (Gnly), which also forms pores in the target cell membrane; and granzymes, which are serine proteases that target and cleave caspase-3 to initiate downstream apoptotic pathways that affect mitochondrial membrane permeability and release cytochrome c (Murphy et al., 2008). Granzyme B (GzmB), encoded by the *GZMB* gene, is one of the more thoroughly studied granzymes and recognized as the most abundant cytotoxic mediator in CTLs during the elimination of tumor cells (Rousalova and Krepela, 2010). Important to their function,

[5] Cytotoxic lymphocytes (CTLs) are MHC class I-restricted $CD8^+$ T effector cells, and are important in host defense against cytosolic pathogens and tumor cells (Finn, 2008).

CTLs also secrete the cytokine interferon-gamma (IFN-γ) (Schoenborn and Wilson, 2007), which functions to further recruit and activate other CTLs and immune cells through upregulation of adhesion molecules, and transcription of interferon regulatory factor 1 (IRF-1). It is encoded by the *IFNG* gene, which is more highly expressed in CRC tissues when compared to normal colon (Csiszar et al., 2004).

CTLs are not the only T-cells involved in the eradication of tumor cells. Helper T-cells, which express CD4 and not CD8, interact with class II MHC to activate a variety of downstream signaling cascades of immune responses. Naïve $CD4^+$ T-cells differentiate into a variety of identifiable effector helper T-cell subsets. These subsets are identified by their repertoire of cytokines secreted upon recognition by their cognate antigen (Murphy et al., 2008). Important for protection against cancer, a particular subset of helper T-cells, 'type-1' Helper T-cells (T_H1 cells), polarize from naïve T-cells in the peripheral lymph nodes upon stimulation by the cytokine, interleukin-12 (IL-12) and expression of the transcription factor T-bet encoded by *T-box 21* (*TBX21*). *TBX21* is considered a 'master' transcription factor that defines the T_H1 cell subset (Baumjohann and Ansel, 2013). These T-cells send signals to other cells, including CTLs, to trigger cytotoxic activity. T_H1 cell activity is characterized by the secretion of cytokines IL-2, IFN-γ, tumor necrosis factor (TNF) (Mosmann et al., 1986), all of which trigger activation of acute inflammatory CTLs in a TAA-specific response. In other words, T_H1 cells are the main mediators of CTL proliferation and activation, tumor-rejecting immunity, cellular immune response, and acute inflammation (Szabo et al., 2003).

Interestingly, the transition from healthy normal mucosa to colorectal adenomas is marked by an increase in *IFNG*, *TNF*, and *IL12A*, which indicates a host reaction against

TAAs in adenomas, however this expression is strongly down-regulated in colorectal tumors (Cui et al., 2007). Studies on tumorigenesis in mice deficient in IFN-γ (Street et al., 2001), IFN-γ receptor 1 (IFNGR1), or downstream transcription factor signal transducer and activator of transcription 1 (STAT1), determined that IFN-γ is directly involved in tumor control (Kaplan et al., 1998). Also, tumor cells will upregulate class I MHC upon IFN-γ stimulation in a mechanism that enhances tumor cell recognition and apoptosis by CTLs (Bui et al., 2006). Altogether, these studies identified decreased T_H1 cell activity during tumorigenesis and suggest an overall defect in anti-tumor immunity in advanced CRC.

Of particular importance to TIL biology and this current investigation are the chemokines that control lymphocyte migration into inflamed tissues. Chemokines are part of a complex network of inflammatory mediators that dictate the type and density of the TIL population (Balkwill, 2004). CXCR3 is expressed on the majority of CTLs and a large portion of active T_H1 cells, and is the receptor for a trio of chemokines: CXCL9, CXCL10, CXCL11 (Bonecchi et al., 1998; Sallusto et al., 1998; Loetscher et al., 1998; Kim et al., 2003; Guarda et al., 2007). However, assuming immunosurveillance is mediated by only three chemokines would be short sighted. Other research suggests CCL5 is also critical to T-cell chemotaxis and infiltration into inflamed tissue (Erreni et al., 2009) as suggested by its receptor CCR5 (Samson et al., 1996) being co-expressed on CXCR3 expressing T_H1 cells and CTLs in the IM of colorectal tumors (Musha et al., 2005) and also being associated with CTL infiltration and absence of metastasis (Zimmermann et al., 2010). A flow cytometry and real-time PCR study of colorectal tumors identified stronger expression of CCR5 on surfaces of CTLs and stronger transcriptional activity of *CCL5* and *CXCL9*

and *CXCL10*, as well as *CCL3* and *CCL4*, when compared to non-neoplastic colonic mucosa (Musha et al., 2005). Interestingly, the same study showed using IHC, that one tumor was positive for CCL5 along the IM, indicating that this chemokine is differentially expressed across a population of tumors (Musha et al., 2005). The expression of all three CXCR3 ligands is induced by IFN-γ (Cole et al., 1998; Groom and Luster, 2011). This pattern of chemokine activity supports the arguments by Dunn and Schreiber who emphasize that IFN-γ has a pivotal role in cancer immunosurveillance (Dunn et al., 2006). Altogether these findings suggest that CXCR3 and CCR5 ligands are involved in IFN-γ-activated anti-tumor activity.

T-cell infiltration and patient prognosis. Currently, the traditional TNM[6] tumor staging protocol is recommended by the American Joint Committee on Cancer/Union Internationale Contre le Cancer (AJCC/UICC) to characterize CRC and evaluate patient prognosis, making it the most widely used guideline for this disease. This protocol instructs a trained pathologists to evaluate the tumor on mainly three criteria: tumor burden or invasion into the submucosa, muscularis propria, and/or into the subserosa, nonperitonealized pericolic or perirectal tissues (T); presence of tumor cells in one or many pericolic or perirectal lymph nodes (N); and distant organ metastasis, such as to the liver and/or lungs (M) (Beahrs et al., 1993). Higher scoring in any of these criteria reflects a higher degree of tumor progression and poorer prognosis. Stage I and II tumors are localized to colonic tissues and display no metastasis to regional lymph nodes or distant

[6] TNM stages are designed to classify tumors by size and invasiveness. These characteristics are directly correlated with patient survival; patients with advanced staged tumors have the lowest rate of survival. T stands for tumor size, N stands for lymph node involvement, and M for the presence of distant metastasis.

organs, while stage III and IV tumors demonstrate metastasis to lymph nodes and distant organs, respectively. However, this classification staging system ignores one major (and increasingly popular) variable within solid tumors, degree of anti-tumor lymphocyte infiltration, and is therefore antiquated and fails to incorporate a newly accepted variable that profoundly affects patient outcome. As a consequence its survival predictions vary significantly among patients with tumors of similar TNM stage (Nagtegaal et al., 2011). For example, patients with advanced stage cancer have reported spontaneous, partial, or full regression, yet others with early stage cancer have relapsed after surgery (Mlecnik et al., 2011a). Improvements to the TMN staging protocol should consider the inherent imbalance between invading tumors and the host's anti-tumor immune response.

A series of studies by Pagès and Galon addressed this issue and awakened the CRC research field by underscoring the important role of T-cells in protecting against advanced stage cancer. Previous studies only focused towards quantitatively assessing lymphocytes rather than exploring the behavior and activity of TILs in the TME, while the two agreed that the presence of TILs alone in the TME is not fully reliable for prognosis (Pages et al., 2010) and that the evaluation of the "nature, functional orientation, density, and location" (Galon et al., 2006) of specifically T-cells will provide a better tool for evaluating prognosis (Pages et al., 2008).

Their first major study collected hundreds of colorectal tumors with well-documented histological and molecular data, and utilized tissue microarrays along with flow cytometry, real-time PCR, and transcriptional microarray data to characterize the primary immune response in colorectal TMEs. In particular, they compared clinicopathological data, such as tumor relapse and early metastatic invasion (vascular

emboli, lymphatic invasion, and perineural invasion, collectively VELIPI) with the expression of the type-1-associated genes *CD8A*, *GZMB*, *TBX21*, *IRF1*, and *IFNG*. They found that colorectal tumors are infiltrated by variable densities of T-cells, and those patients with tumors that harbored higher densities of type-1 T-cells, such as T_H1 cells and CTLs, demonstrated better clinical outcome (Pages et al., 2005). In particular, the presence of effector memory T (T_{EM}) cells[7], which are essential immunological memory and CTL function, in the TME correlated with the absence of VELIPI and tumor reoccurrence.

Later Pagès and Galon published another major finding demonstrating that evaluating TILs by their "type, density, and location" in TMEs is a strong prognostic tool. Their 2006 Science publication relied again on gene expression data, and also *in situ* IHC, tissue microarrays, and flow cytometry to characterize the lymphocyte population in the TME. Their analysis expanded to a larger group of genes, all of which represent type-1 activity (*IL12RB1*, *IL12RB2*, *CCR5*, *IFNG*, and *TBX21*) and CTL activity (*IRF1*, *CCL5*, *CD8A*, and *STAT1*). The two found that tumors contained variable lymphocyte densities that consisted of a variety of subtypes, and the density of particular subtype strongly predicted patient survival (Galon et al., 2006). These findings allowed the two to make bold claims that immunological data, such as characterization of CTLs in colorectal tumors is more predictive of overall outcome than traditional AJCC/UICC TNM staging protocol (Galon et al., 2007; Pages et al., 2008; Galon et al., 2014; Anitei et al., 2014). Therefore the two determined that the "type, density, and location" of TILs in colorectal tissues directly dictate tumor progression (Galon et al., 2006).

[7] Effector memory T cells are $CD8^+$, $CD45RO^+$, $CCR7^-$ (negative for CC chemokine receptor), $CD62L^-$ (negative for CD62 ligand), $CD28^-$, $CD27^-$, $perforin^+$, $granulysin^+$, and $granzyme^+$ T-cells.

Their next study demonstrated that comprehensive TIL evaluation was powerful enough to accurately predict survival of patients with early (I and II) stage cancer. This study is particularly important because it demonstrates that the degree of anti-tumor immune activity can dictate DFS before a tumor has metastasized. Pagès and Galon determined that the presence of both T_{EM} cells and CTLs were associated with better outcomes in stage I and II CRCs, whereas tumors with low numbers of T_{EM} cells and low density of CTLs were associated with rapid recurrence (Pages et al., 2009). Once again the distribution of $CD3^+$ T-cells was an important factor in predicting prolonged survival; patients with high densities of T-cells in both the center of the tumor (CT) and the IM had a higher rate of disease-free survival (DFS)[8] (Pages et al., 2009).

To fully appreciate the immune response within colorectal TMEs, the complexity of the immune networks involved need to be further explored. Pagès and Galon's previous observations prompted them to explore the biomolecular networks that represent lymphocyte chemoattraction and infiltration. Their study pertained to the transcriptional activity of chemokines and adhesion molecules that are most associated with survival. They analyzed gene expression and tissue microarrays from a cohort of colorectal tumors then compared these data to patient DFS. Their findings revealed that chemokines *CX3CL1*, *CXCL9*, *CXCL10*, *CCL2*, *CCL5*, and *CCL11*, and adhesion molecules *ICAM1*, *VCAM1* and *MADCAM1*, as well as T_H1 cell-associated genes *IFNG*, *TBX21*, *IRF1*, and *STAT1* were closely associated with T-cell densities and DFS (Mlecnik et al., 2010). In particular, patient groups with higher transcriptional activity of both *CX3CL1* and *ICAM1*, or *CXCL10*

[8] DFS is the amount of time a cohort of cancer patients survives without reoccurrence of the disease after receiving primary treatment.

and *ICAM1* demonstrated prolonged DFS than groups with lower or heterogeneous expression of any of these genes (Mlecnik et al., 2010). This is supported by previous evidence that describes the initial events of T-cell activation and differentiation as involving downregulation of chemokine receptors that direct immune cells to lymph nodes and subsequent upregulation of receptors CCR5 and CXCR3 that direct T-cells to target tissues (Moser et al., 1998; Moser and Loetscher, 2001). Interestingly, genes associated with tumor invasion (*CEACAM1*), metastasis (*MMP7*), genes that oppose type-1 response (*GATA Binding Protein 3*, *GATA3*), and genes involved with immunosuppression (*IL10* and *FOXP3*) and angiogenesis (*VEGF*) did not correlate with improved DFS (Mlecnik et al., 2010). These data show that multiple lymphocyte homing factors function to promote patient survival, and this phenomenon is dependent on a complex network of immune related genes (Figure 4). This was an important study that demonstrates the deep complexity of the immune response in CRC. However, it fails to provide concrete results in two regards. First, the data are limited to transcriptional activity of immune mediators that do not answer the question of whether these are truly secreted from the TME. Secondly, it does not correlate any data with functional anti-tumor cells, such as IFN-γ-secreting T_H1 cells or cytotoxic mediator secreting CTLs that are expected to be found in the tumors of patients who will survive longer than average. And thirdly, this study does not explain why chemokine that are not known to attract anti-tumor immune cells are also upregulated along with CXCR3 and CCR5 ligands in patients with prolonged DFS. In other words, the biomolecular networks represented by *CX3CL1*, *CCL2*, and *CCL11* are not expected to contribute to the anti-tumor response. These are the topics of which this investigation is most interested.

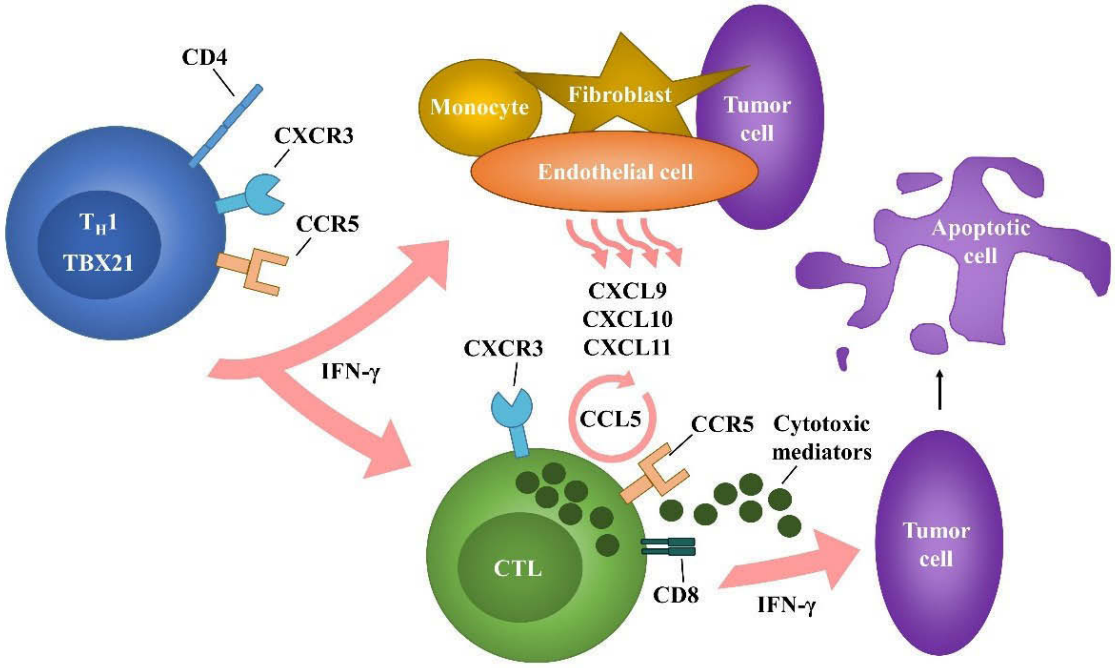

Figure 4. T-cell infiltration and anti-tumor activity

Their aforementioned work provided impetus for Galon and Pagès in 2014 to initiate an international consortium that promotes an "immunoscore" to compliment the antiquated TNM staging. In summary, their scoring system utilizes IHC to determine the density of both $CD3^+$ and $CD8^+$ cells in both CT and the IM (Galon et al., 2014). These variables are then used to assign a score for each of the four criteria: "0" for low density and "1" for high; for example an immunoscore of "0" represents low densities of $CD3^+$ and $CD8^+$ cells in both the CT and IM, and total score of "4" indicates high density of both markers in both tumor compartments (Galon et al., 2014; Anitei et al., 2014). The immunoscore approach has proven effective at predicating clinical outcome in a large cohort of cancer patients; less than 5% of patients with a high immunoscore relapsed and over 86% survived over 5 years. This system was further validated in a cohort of rectal

cancer patients (Anitei et al., 2014). It is not yet known how the immunoscore correlates with the use of cytotoxic chemotherapy, which could be the focus of further studies.

Other lymphocyte subsets. Other immune cell subsets share similar functions and responsibilities as CTLs are at the center of an ongoing debate over whether they influence clinical outcome (Fruci et al., 2013). CD56/CD57$^+$ NK-cells and NK T-cells (NKTs) migrate to sites of inflammation and target cells for elimination through mechanisms discussed earlier involving cytotoxic mediators. NK-cells are capable of directly targeting and killing cells without being sensitized to antigens (Lodoen and Lanier, 2006). Since these subsets of lymphocytes share similar functions with CTLs, they may be involved in the anti-tumor response (Pietra et al., 2012). However, Sconocchia and colleagues report that several types of human cancer demonstrate poor infiltration by NK-cells while detecting almost no CD56 in melanomas, hepatocellular carcinomas, breast cancers, renal cell carcinomas, and colorectal tumors (Sconocchia et al., 2012). This group also reports that CD56$^+$ and CD57$^+$ cell infiltration does not provide any prognostic significance in these cancer types (Sconocchia et al., 2011). Pugh and colleagues performed flow cytometry to analyze NK-cells and T-cells in colorectal liver metastases and concluded that T-cells, but and not NK-cells, are recruited to tumor sites and are positively associated with survival (Pugh et al., 2014). Benevolo and colleagues also reported that very few CD56$^+$ cells can be detected in colorectal tumors (Benevolo et al., 2011; Halama et al., 2011b; Fruci et al., 2013). Halama and colleagues concluded that infiltration of NK-cells is impaired, while infiltration of T-cells remains unabated and correlates with chemokine expression in some tumors (Halama et al., 2011a; Halama et al., 2011b). Halama and colleagues also suggest that escape from NK-cells may be a requirement for colorectal

tumorigenesis (Halama et al., 2011a). Therefore, based on the evidence from these studies, this investigation will not include NK-cells in its analysis.

In contrast to the type-1 response, other T-cell subsets have mutually exclusive roles that are different from tumor eradication. Naïve $CD4^+$ T-cells can differentiate into distinct T-cell subsets of specific polarity. Among these are T follicular helper, which are located in close proximity to B cells and located in secondary lymphoid organs that include tonsils, and organized into germinal centers that facilitate the antibody response (Breitfeld et al., 2000); T_H9 cells, which are characterized as strong IL-9 secretors, are thought to promote ulcerative colitis by stimulating IL-9 receptor expressing intestinal epithelial cells leading to intestinal barrier function disruption (Gerlach et al., 2014); T_H22 cells, named similarly as T_H9 but secrete IL-22 instead, have been demonstrated in a colon cancer mouse model to promote cancer cell stemness by upregulating STAT3 (Kryczek et al., 2014); T_H2 cells, which express a completely different set of cytokines (IL-4, IL-5, IL-6, IL-10 and IL-13) (Mosmann et al., 1986) than other subsets and favorably express receptors CCR3 and CCR4 (Sallusto et al., 1998), modulate the humoral response by up-regulating IgE production (Bonecchi et al., 1998) and cross-inhibit T_H1 cells (Mosmann et al., 1986; Street and Mosmann, 1991); and T_H17 cells, which secrete high amounts of IL-17A and -F, and IL-22 to provide anti-microbial defense at mucosal barriers especially in the gut and have gained notoriety in inflammatory autoimmune diseases (Harrington et al., 2005).

The discovery of a variety of T-cell subsets that can contribute to tumorigenesis and/or inflammatory colonic disease complicates any attempt to analyze genes and secreted factors that may affect tumor progression. T-cell cytokines, IFN-γ, IL-4, IL-5, and IL-12, are increased in serum during progression from healthy normal mucosa to adenoma and

cancer (Contasta et al., 2003). A contrasting study concluded that colorectal tumors more commonly express IL-6 when compared to normal adjacent mucosa, however IL-6 and IL-4 were not detected in cancer patient serum (Piancatelli et al., 1999). Included in the afore mentioned Pagès and Galon study (2011) involving type-1 activity and survival rates, an analysis of 'type-2' genes representing T_H2 cell activity, did not reveal an association with any particular outcome (Tosolini et al., 2011). However, their exploration into the T_H17 response (*RORC* and *IL17A*) (Dong, 2008) revealed that tumors with high expression of these genes had lower rates of DFS (Tosolini et al., 2011). These studies suggest the T_H2 or the T_H17 cell immune responses contribute to carcinogenesis by suppressing T_H1 cell activity and inhibiting the immune system from mounting an acute inflammatory response towards tumor rejection (Grivennikov et al., 2010; Grivennikov and Karin, 2011; Grivennikov et al., 2012). Altogether, these studies still do not elucidate which factors alter the helper T-cell responses among different CRC patients. Therefore, the preceding studies are incomplete because they do not consider the heterogeneity of tumors across a population of patients, and do not consider the possibility that each tumor may follow a different path towards tumorigenesis while under the influence of a unique combination of T-cell subsets, and despite the numerous causes and outcomes of cancer these studies assume that tumorigenesis follows a consistent and uniform path regardless of which combination of mutations cause genomic instability and cancer.

The final T-cell subset that will be discussed in this review merits its own section due to its confusing and counter-intuitive role in CRC prognosis. T_{regs} maintain tolerance to self-antigens by suppressing immune responses. FoxP3[9] is a transcription factor that

[9] FoxP3 or forkhead box P3 is the transcription factor that polarizes T-cell to develop immunosuppression functions.

controls the differentiation of T_{regs} from naïve T-cells (Murphy et al., 2008). These cells can play a role in immunosuppression during tumor immune evasion and escape (Mittal et al., 2014) by suppressing CTL responses and IFN-γ production in T_H1 cells (Murakami et al., 2002) through secretion of anti-inflammatory cytokines, such as IL-10 and TGF-β and expression of cytotoxic T-lymphocyte antigen 4 (CTLA-4). A high density of $FoxP3^+$ cells in most types of human cancers is associated with a poor prognosis (Ladoire et al., 2011). An *in vitro* study demonstrated the suppressive capacity of isolated colorectal tumor-infiltrating $Foxp3^+$ T-cells on autologous T-cell proliferation and IFN-γ production (Kryczek et al., 2009). *Ex vivo* experiments show that removal of T_{regs} freed T-cells from CRC patients to mount antigen specific immune responses (Clarke et al., 2006). Work done with mouse melanoma models report that some tumors secrete CCL21, which creates an immunotolerant environment (Shields et al., 2010) by recruiting naïve T cells and promoting their differentiation into $FoxP3^+$ immune suppressing T-cells, furthering the induction of helper T-cell senescence (Forster et al., 2008). Mouse studies show that removal of T_{regs} enhances immunosurveillance after cancer vaccination (Golgher et al., 2002). In contradiction to the immunosuppressive effects, a large body of data proposes that T_{regs} are associated with favorable prognosis in CRC (deLeeuw et al., 2012). IHC data from a large cohort of patients with either stage II and III CRC revealed that high density of $FoxP3^+$ cells in adjacent normal mucosa is associated with poor prognosis –hazard ratio[10] (HR) = 1.51– while high densities in tumor tissue was associated with better prognosis (HR = 0.54) (Salama et al., 2009; Frey et al., 2010). Another group reported that

[10] HR or hazard ratio is often used to present survival data and reflect the analyzed time the patients survived cancer. An HR < 1 indicates a population died at a slower rate than the control group, and an HR > 1 indicates a higher rate of 'hazard'.

high T_{reg} infiltration was found in tumors without metastasis, while those with low infiltration had higher rates of metastasis (Loddenkemper et al., 2006). These contradictory data raise the question of whether suppressor T cells are important for CRC prognosis. The perceived association of T_{regs} with survival be blurred for several reasons: T_{regs} associate with CTLs in tissues to regulate the immune response, therefore infiltration of CTLs promotes infiltration of these cells (Correale et al., 2010), and alternatively, these cells may actually benefit the patient by suppressing tumor-promoting inflammation that normally facilitates carcinogenesis (Haas et al., 2009). Either way more work is needed to identify under which circumstances T_{regs} are either hindering, helping, or not affecting tumor eradication.

Tumor-associated macrophages. The infiltrating immune milieu is not limited to lymphocytes. Tumor-associated macrophages (TAMs) are capable of supplying type-1-polarizing signals and shaping the TME. Macrophages represents a heterogeneous population which have not been fully evaluated, however they follow a similar pattern of polarization as helper T-cell subsets. Classically activated macrophages (M1s) are associated with T-cell immunity by producing the T_H1 cell stimulating cytokine IL-12 and phagocytizing targeted cells, while immune suppressive macrophages (M2) are associated with tumorigenesis and produce IL-10 and VEGF (Heusinkveld and van der Burg, 2011). TAMs isolated from colorectal tumors are shown to proliferate and activate T_H1 cells *in vivo* (Ong et al., 2012), retaining a high degree of plasticity; stimulation with IFN-γ and cognate interaction with T_H1 cells can encourage M2s to secrete more IL-12, less IL-10 (Heusinkveld et al., 2011), and express TNF and class II MHC (Qian and Pollard, 2010). In theory, IFN-γ and cognate interactions from stimulated T-cells can repolarize TAMs

into M1s (Heusinkveld et al., 2011). This cell type was included in this review because, like T_H1 cells and CTLs, M1s are found in higher abundance in tumors with certain types of genomic instability, such as MSI (Bauer et al., 2011), and are associated with better prognosis and survival rates (Funada et al., 2003; Zhou et al., 2010). Also, their relationship with the T_H1 cell response provides the possibility of contributing to improved DFS with MSI CRC patients.

The need for evaluating the immune contexture of the TME is becoming abundantly clear. The non-tumor cell composition of solid tumors can exceed 50% (Galon et al., 2014), and many of these cells are suspected to be hematopoietic in origin. To date, dozens of studies have shown that the abundance of TILs in solid tumors is directly associated with a better prognosis (Nosho et al., 2010). Infiltrating immune cell density has been correlated with improved tumor immunosurveillance (Mlecnik et al., 2011a), while a concurrent expression of an adaptive immune signal is associated with a more favorable prognosis (Mlecnik et al., 2010). The whole slew of studies elucidating the function and characteristics of TILs in CRC have centered on two concrete findings: the composition of these cell types is highly diverse among many tumors as shown in the reports from Pagès and Galon, and substantial evidence demonstrated by the same group, as well as others, suggest that the composition and abundance of T-cell subsets strongly dictates patient survival. Therefore, depending on the compositional makeup, TILs will either help or hinder patient survival. These data combined with the understanding of the variety of mutations that lead to tumorigenesis, raise the question of whether the "type, density, and location" of immune infiltrates follows any pattern within groups of tumors with similar

genomic instability. The next sections exercise the freedom to interpret the large body of literature to provide reasoning for this supposition.

MicroRNA Regulation of Lymphocyte Immune Function

The $CD4^+$ helper T-cell population is represented by range of different subsets that each express a unique biomolecular network of genes. A degree of plasticity exists between subset (Baumjohann and Ansel, 2013), which suggests in the context of cancer, the TME may influence which biomolecular network is active and which is not. These networks of genes can be regulated by many mechanisms. Of interest to this investigation and any future investigations by this investigator, is post-transcriptional modification of mRNAs facilitated by microRNAs (miRNAs). These are short nucleotides approximately 21 to 22 bases long, that function by partially binding to regions of mRNAs, called 'seed regions', in the 3′-untranslated region to silence mRNA translation (Bartel, 2009).

MiRNA biogenesis is an evolutionarily conserved process that occurs in both the nucleus and the cytoplasm. This next discussion will be limited to the human homologs that are required for this process. After transcription, the primary miRNA (pri-RNA is exported to the cytoplasm from the nucleus by exportin-5, where it can be cleaved and removed from the hairpin loop by the RNase III enzyme Dicer, producing a miRNA/miRNA duplex approximately 22 nucleotides long. The duplex dissociates yielding a mature miRNA that combines with the RNA-induced silencing complex (RISC), which also binds to the target mRNA and has catalytic regions called argonaute RISC catalytic component 1-4 (AGO1-4). In animals, the base paring is not perfectly complementary whereby only small seed regions, approximately 2 to 7 nucleotides in

length, are required for binding (Figure 5). Interestingly, however, in plants this matching is believed to be perfect (van Rooij and Olson, 2012).

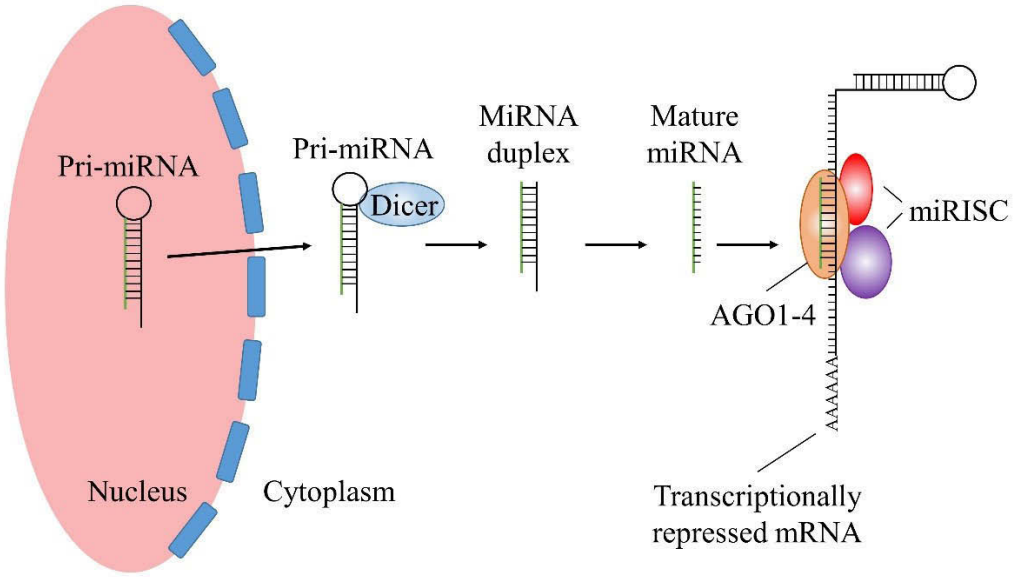

Figure 5. MicroRNA biogenesis

These short RNAs function through several mechanisms that are facilitated by RISCs, which repress mRNA translation and facilitate degradation of mRNA targets by: 1) guiding the cleavage of mRNA strands into separate pieces (Guo et al., 2005), 2) accelerating deadenylation or decay of the poly(A) tail (Wu et al., 2006), 3) recruiting factors mRNA-decapping enzyme 2 (van Dijk et al., 2002), trinucleotide repeat containing 6A (Rehwinkel et al., 2005), and other proteins that facilitate 5′ decapping (Nishihara et al., 2013) –both deadenylation and de-capping irreversibly destabilize the mRNA–, and 4) directly inhibiting ribosomal activity by recruiting eukaryotic translation initiation factor 6, which inhibits the association of the 40S and 60S ribosomal subunits (Chendrimada et al., 2007) (Figure 6). All mechanisms function to lower the efficiency of mRNA translation into proteins.

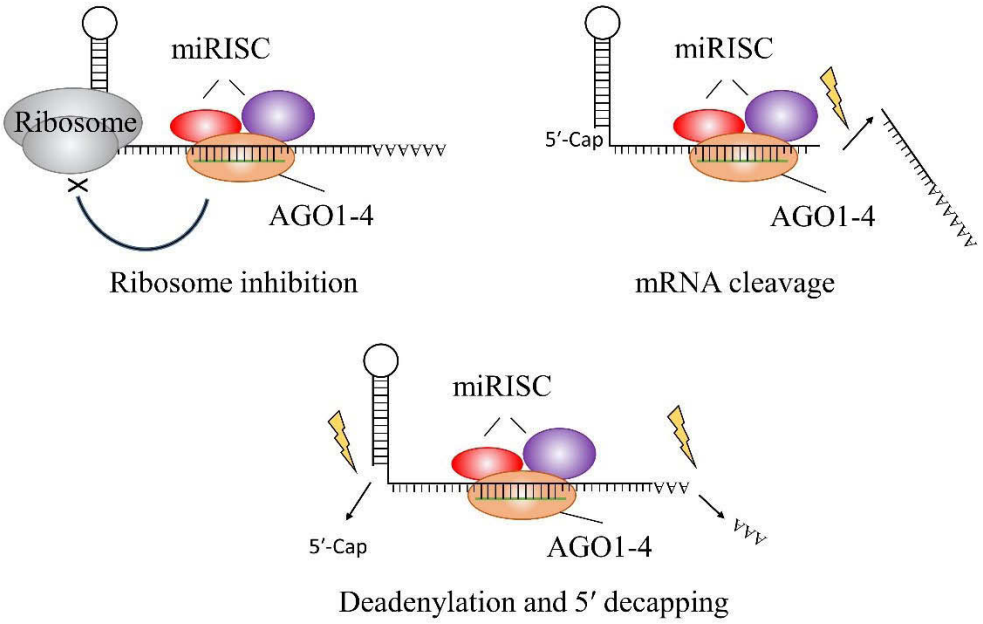

Figure 6. MiRISC-driven inhibition of mRNA translation

MicroRNAs can be designated into families that represent specific cell functions. For example, the *miR-16* family is thought to be a modulator of the cell cycle. Accelerated upregulation of miR-16 family members, *miR-16*, *miR-15*, *miR-195* and *miR-457*, reinforces cell-cycle arrest in the Gap 0 state and can lead to senescence. During cell-cycle re-entry, or the Gap 1 to synthesis transition, several members of this family are rapidly decayed and downregulated, and interestingly are deleted in some types of cancers (Rissland et al., 2011). Other microRNAs that control anti-tumor immune activities may include *miR-155*, *miR-21, miR-17*, *miR-19a* and *miR-92a* (Baumjohann and Ansel, 2013).

Of particular interest to this study are miRNAs that control the development and function of the immune system, such as $CD4^+$ T-cell activation and clonal expansion. *MiR-155* has been recognized as an important regulator of immune cell differentiation and function (Baumjohann and Ansel, 2013). Changes in miRNA expression are strong during naïve T-cell differentiation into cytokine-producing effector T-cells. Upon T-cell

activation (stimulation through CD3 and CD28) miRNAs become globally downregulated (Bronevetsky et al., 2013). Transcriptome-wide profiling performed on *miR-155* knockout mouse T-cells suggested that this microRNA is strongly involved in lymphocyte homeostasis, because *miR-155* targets multiple mRNAs that are involved in lymphocyte maintenance (Loeb et al., 2012). More specifically, *miR-155* is involved with mammalian immune functions and development of helper T-cells in germinal centers of secondary lymphoid organs, such as gut-associated lymphoid tissue and Peyer's patches. *Mir-155* knockout mice demonstrated a reduced number of lymphocytes in their germinal centers, and a reduction in antibody (immunoglobulin G1) titers after antigen challenge when compared to wild-type mice. This suggests that *miR-155* is also critical for T-cell dependent antibody responses (Thai et al., 2007). Although transcriptome-wide analysis suggested that *miR-155* targets many mRNAs, only a few have been confirmed. These include *Src homology-2 domain-containing inositol 5-phosphatase 1* (*SHIP1*), which when repressed disrupts myelogenous cells development (O'Connell et al., 2009), and IFN-γRα mRNA in which *miR-155* $^{-/-}$ $CD4^{+}$ T-cells are likely to differentiate towards type-2 upon stimulation. However, overexpression of *miR-155* leads to higher production of IFN-γ from T-cells, which is supported by the fact that *miR-155* is one of the most highly upregulated microRNAs during T_H1 cell stimulation and activation (Banerjee et al., 2010). Expanding towards cancer, *mir-155* is involved in anti-tumor immunity by promoting IFN-γ production. A mouse study involving *miR-155* knockout demonstrated increased tumor growth, and suggests that *miR-155* targets *SHIP1* mRNA to affect T-cell responses (Huffaker et al., 2012). All these studies suggest that microRNAs, specifically *miR-155* is involved in the type-1 response as a modulator of T-cell differentiation and/or IFN-γ

production from T-cells. Therefore its downregulation may be involved with tumorigenesis and cancer progression.

The effects of *miR-155* may not be limited to $CD4^+$ T-cell differentiation and cytokine secretion. *MiR-155* is also upregulated in $CD8^+$ T-cells upon CD3 and CD28 stimulation. Mice deficient in *miR-155* demonstrated severe impairment of anti-viral $CD8^+$ T-cell activity; alternatively, overexpression of *miR-155* increased anti-viral responses. These mice either demonstrated a decrease or increase of $CD8^+$ T-cell infiltration into the lungs after influenza infection depending on whether *miR-155* was deficient or overexpressed (Gracias et al., 2013). Another group confirmed these findings by reporting that *miR-155* also targets *suppressor of cytokine signaling 1* (*SOCS1*), a critical regulator of effector $CD8^+$ T-cells. This was done using a melanoma mouse model that demonstrated that *miR-155* deficient $CD8^+$ T-cells were ineffective at controlling tumor growth when compared to wild-type T-cells. *MiR-155* deficiency also resulted in the overproduction of SOCS1 and, combined with the fact that silencing of SOCS1 enhances the anti-tumor response, suggests that during $CD8^+$ T-cell activation, *miR-155* suppresses SOCS1 accumulation (Dudda et al., 2013). However, most of the studies mentioned above where done in mice, therefore the question of whether *miR-155* and related microRNAs are involved in human cancer, specifically CRC, still remains. More work needs to be done to assess the role *miR-155* plays in this disease or if it can be used as a biomarker for better prediction of disease outcome.

Future immunotherapies. Colorectal tumors can be infiltrated by dendritic cells (DCs) (Bauer et al., 2011). These cells are viewed as important for the immune response against malignant diseases (Nagorsen et al., 2007) and may be useful targets for the

development of novel treatments. Current studies in immunotherapy utilizing DC-based vaccines have the potential to activate the anti-tumor cascade (Palucka et al., 2007; Palucka and Banchereau, 2012). In brief, DCs were first identified as critical to the adaptive immune response by Steinman and Cohn in 1973 (Steinman and Cohn, 1973) and are believed to be central in the immune response against cancer, as well as other pathologies (Palucka et al., 2007). DCs are 'professional' antigen-presenting cells (APCs) that can strongly activate T-cells and initiate the adaptive immune response. Mature DCs reside in tissues and secrete CXCL9 (Rosenblum et al., 2010) and IL-12 upon interaction with polarizing IFN-γ-secreting T-cells and CTLs (Palucka et al., 2007). Palucka and Banchereau (while at the Baylor Institute for Immunology Research) made great progress towards developing immunotherapeutic options for melanoma patients using DC-based vaccines designed to mobilize the immune system to combat TAA-presenting tumor cells (Palucka et al., 2007).

DC-based vaccines seem plausible for treating CRC because DCs strongly infiltrate certain types of colorectal tumors (Bauer et al., 2011; von Knebel Doeberitz and Kloor, 2013) and inflamed breast tumors (Bell et al., 1999). $CD1A^+$ DCs have been reported as prominent at the advancing tumor margin, while mature ($CD208^+$) DCs are prominent in the stroma (Sandel et al., 2005) and IMs (Yuan et al., 2008) of CRCs. This is the basis of the arguments from von Knebel Doeberitz and Kloor who wish to use frameshift peptides to vaccinate Lynch syndrome patients. The treatment would require TAA-pulsed and activated DCs to be administered to patients. DCs would then activate TAA-specific T_H1 cells and CTLs inducing infiltration into tumor sites (von Knebel Doeberitz and Kloor, 2013).

Abundance of T-cells in MSI-Tumors

Mentioned above, the MSI population consists of Lynch syndrome patients with familial mutations in MMR genes (approximately 3%, mostly younger patients) and patients with silencing hypermethylation at their *MHL1* promoter (12%, mostly older patients with the CIMP) (Boland and Goel, 2010). MSI tumors are densely infiltrated by lymphocytes (Smyrk et al., 2001; Popat et al., 2005; de Miranda et al., 2012) and are associated with low frequencies of distant metastasis (Buckowitz et al., 2005), therefore, patients with MSI tumors tend to live longer than those with MSS tumor. These data point to an interesting contradiction involving a hypermutable tumor cell population that is less likely to evade immune surveillance and metastasize. The next section of this review explores the possible role the immune system plays with granting MSI CRC patients prolonged DFS, discusses studies that suggest mechanisms that may explain the robust, yet contradictory, type-1 response in MSI TMEs, and introduces the theoretical framework from which the experiments performed in this investigation are justified.

A variety of studies have consistently shown that MSI tumors are more strongly infiltrated by lymphocytes. IHC- based studies have revealed that MSI colorectal tumors and have higher expression of granzyme B than MSS tumors (Dolcetti et al., 1999; Lee et al., 2012). This phenomenon may be explained by higher influx of programmed tumor-fighting CTLs (Prall et al., 2004; Drescher et al., 2009), and suggests that immune cells overall have a propensity for infiltrating MSI tumors. It is important to note that T_{regs} are reported to abundantly infiltrate MSI tumors. IHC determined that high densities of $FoxP3^{+}$ T-cells in MSI tumors and indicate a better prognosis (Michel et al., 2008). This again can be explained by T_{regs} merely being associated with CTL activity, and not actively

contributing to tumor control. In summary, most of these findings are based on IHC, which only describes higher densities of lymphocytes; however, these studies do not describe the immune signals that favor T_H1 cell polarization and infiltration that encourages differentiation and activation of CTLs.

The leading theories that explain improved prognosis with MSI cancer patients involves how the immune system distinguishes MSI tumors from normal mucosa. Insertions and deletions within microsatellite regions contained within the coding regions of genes can create frameshift neo-peptides. Quite distinct from point mutations caused by chemical carcinogenesis (or inflammation and other factors), these frameshifts tend to occur at the same DNA sequences, exposing the host repeatedly to the same neo-antigen (von Knebel Doeberitz and Kloor, 2013). In turn, these TAAs are identified by lymphocytes as immunogenic and trigger an anti-tumor response. This immune response requires stable neo-peptides to be presented to T-cells, however critics of this theory suggest that insertions and deletions are likely to initiate nonsense-mediated decay of mutated mRNA and restrict the expression of potential TAAs (El-Bchiri et al., 2008; Williams et al., 2010), and that T-cells may be educated to tolerate TAAs while in a non-inflamed environment (Kammertoens and Blankenstein, 2009). However, these arguments are countered when patients with MSI colorectal tumors were shown to possess antibodies against neo-peptides that are derived from microsatellite-coding genes (Reuschenbach et al., 2010). Another counter to this argument includes an experiment where autologous APCs were pulsed with frameshift peptides which were derived from predicted frameshift sequences; these pulsed APCs were capable of generating peptide specific CTLs capable of lysing a MSI cell line (Linnebacher et al., 2001). This study suggests that MSI neo-

peptides are immunogenic and are indeed expressed by tumor cells (Figure 7). Approximately 40% of MSI colorectal tumors have a frameshift mutation in the coding thymine (10) microsatellite of the *O-linked N-acetylglucosamine transferase* gene (*OGT*), which results in a carboxy-terminal truncated protein. Another study identified specific CTL clones in human colorectal tumors that were capable of killing tumor cell lines expressing mutant OGT proteins via class I MHC molecules (Ripberger et al., 2003). In 2008, von Knebel Doeberitz performed a landmark study using 14 synthesized frameshift neo-peptides, known to be generated in MSI tumor, including OGT. His group found that CTLs isolated from the peripheral blood of MSI patients more strongly activated and secreted IFN-γ in response to the synthetic peptides presented by APCs than blood CTLs from MSS patients (Schwitalle et al., 2008).

Other groups used transcriptional profiling to show the increased immune activity in MSI colorectal TMEs. Transcriptional microarray is a high-throughput multiplex assaying technology that qualitatively measures the activity of a large number of genes by determining the abundance of specific messenger RNAs. This powerful tool was used to assess the transcriptional profile of MSI colorectal tumors. Two studies found that many inflammatory cytokines were upregulated in MSI tumors, indicating an upregulation of genes involved in lymphocyte regulation, T-cell maturation and cytotoxic immune responses (Banerjea et al., 2004; Bernal et al., 2012). The other group analyzed expression data from over 1,200 colorectal tumors, and performed unsupervised hierarchical clustering to identify groups of tumors that have similar expression patters. Of the five major clusters identified, one was marked with higher expression of chemokines and interferon-related genes and deemed “inflammatory”, where 94% of these tumors were

MSI (Sadanandam et al., 2013). These studies suggest that colorectal tumors are stratified bimodally with respect to T_H1 cell and CTL activity, and MMR fidelity could be a driving factor of this stratification.

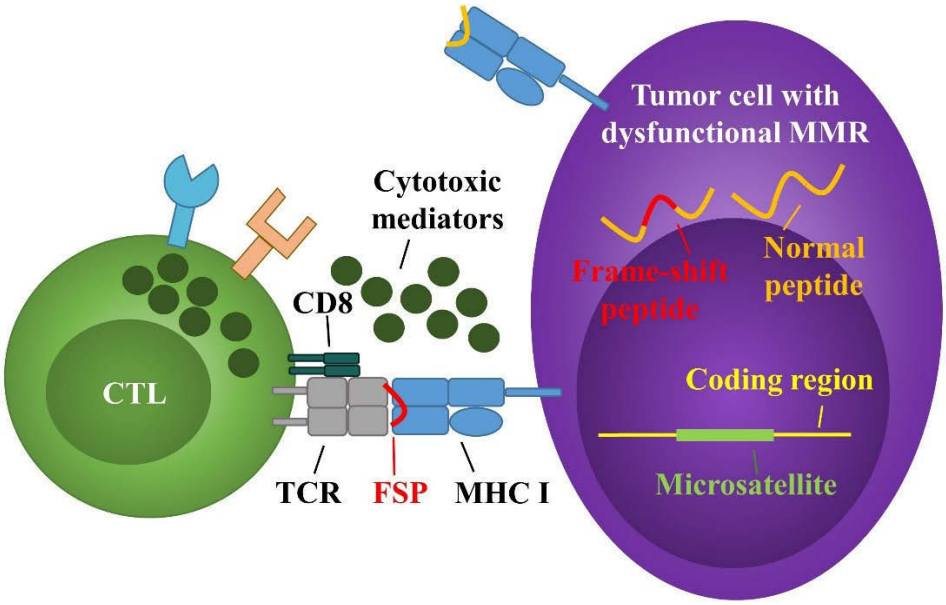

Figure 7. Frame-shift peptide presentation by MSI tumor cell

These data suggest that MSI patients are naturally –and repeatedly– immunized against their own tumors, while MSS patients are not immunized to the same degree. All these studies argue that the immune system is mounting cellular immune responses against TAAs generated from MSI tumor cells and protecting patients from metastatic disease. These studies also suggest that nonsense mediated decay does not completely block translation of mutated proteins.

Concluding Remarks

The ability of the immune system to kill tumor cells and the mechanisms by which tumor cells escape immunosurveillance represent the dynamic balance between tumor and

host. This field of research has captured the interest of thousands of researchers who share one goal: to better understand the disease and find ways to tip the balance in favor of the patient. The balance may be tipped by a number of factors, however many believe that no one treatment will ever eradicate the disease. Chemotherapy has improved survival for many, but it imposes severe side-effects, and benefits are limited to a subset of patients whose tumors do not eventually escape treatment. The uniqueness of each tumor requires the disease to be treated in a different way; not just as one disease, but as many, which all need better characterization and categorized in a way that makes treatment(s) more precise, personalized, and implemented in a way that offers the best chance of survival with improved quality of life. These treatments could be in the form of DC-based vaccinations as proposed by Palucka and Banchereau, which target the activity of T_H1 cells and CTLs (Palucka and Banchereau, 2012), as well as the use of compounds that potentiate the immune response. As proposed by Galon and Pagès, better diagnostic practices could identify patients at lower risk (Galon et al., 2014), and therefore identify those who may not require potentially toxic treatments, which may only result in lower quality of life. Also, the work done by Kloor and von Knebel Doeberitz has launched efforts to identify immunogenic TAAs that may serve as possible candidates for vaccination (von Knebel Doeberitz and Kloor, 2013).

A better understanding of the processes involved in tumor escape from immunosurveillance and how the immune systems counters tumor progression will allow the development of novel therapeutic strategies. Perhaps novel uses of compounds that enhance the production of IFN-γ will sensitize tumors to preventative therapy as proposed by Dunn and Schreiber (Dunn et al., 2006). Or perhaps obligatory phenotype screening

championed by Boland and Thibodeau can identity which tumors have defective MMR and may not benefit from traditional cytotoxic chemotherapy (Boland et al., 1998). These patients may be better candidates for immunotherapy because their tumors already contain key immune cells needed for such activity. All of these potential strategies were derived from the framework suggested by Fearon and Vogelstein who suggest that tumorigenesis is caused by the sequential accumulation of tissue-specific mutations. Their work is important because it sets the stage for conceptualizing the changes that take place during tumorigenesis and how those changes can be exploited for rational treatment of cancer.

All this past work commonly suggests that the immune system either recognizes the tumor as self and cannot react against it, allowing local outgrowth and generalized spread to distant organs, or recognizes it as non-self and initiates activities to counter progression and invasion. A major limitation of the work detailed in this review is that analysis of low-dimensional IHC and gene transcription data from dead and preserved tissues draws weak conclusions about the immune activity within the TME. These techniques cannot study live cells in the TME and thereby cannot detect secreted functional immune signals that may attract immune cells to tumor cells. By studying chemokines secreted from colorectal tumors this investigation will provide better insights into the mechanisms in which the immune system responds the tumors. Also, this investigation will challenge previous opinions that narrowly assume that all colorectal tumors share similar characteristics, when in fact different types of genomic instability may at least partially induce a bimodular distribution of strong anti-tumor immune responses across a population of tumors.

CHAPTER THREE

Methods and Materials

This chapter is divided into sections that detail the experimental designs and techniques used in this investigation. Each section includes a rationale for using each technique as it applies to the primary questions of the investigation. The technology behind each technique will be described in brief so that the reader will have a better understanding of how quantifiable results were obtained. When appropriate, provided will be summaries of the peer-reviewed articles from which inspiration for the experimental designs were gathered.

As a quantitative investigation, all experiments were designed to generate ordinal or measurable data. However, cancer is a disease characterized by multi-step selective pressures that gradually change genomic structure, gene expression, cell phenotype, and cellular composition. Therefore, the challenge of this investigation was profiling these gradual changes. In other words, the experimental results produced a spectrum of data across multiple tumors, and therefore further analysis required a non-biased method for profiling each tumor. This investigation tested the hypothesis that relatively high type-1 activity and prolific chemokine secretion are bimodally distributed across a population of colorectal tumors, and then compare this distribution to occurrence of MSI. Therefore an unbiased profiling system was created and validated by measuring the transcriptional activity of key immunological makers.

To evaluate the magnitude of immune activity in colorectal TMEs a healthy baseline was first established. Whenever appropriate, all tumor tissues were compared to healthy normal mucosa from either the colon of the rectum of CRC patients. This put into perspective the differences of immunological activity between healthy normal mucosa and each colorectal TME. Healthy normal tissue was not collected from other parts of the body because the immunological milieu between organs is expected to differ. Therefore, a multi-organ baseline would probably contain inherent variation and mislead data interpretation.

Patient Enrollment

To study CRC in its most native state, tumor specimens were obtained immediately after surgery in conjunction with the Department of Pathology at BUMC. Before enrolling a single patient, a strict standard operating procedure was designed by a certified research nurse (Millie Arnold RN BS OCN CCRC) to protect the identity of all potential candidates and ensure that patient care and quality of treatment was maintained to the highest degree, and then was approved by the Baylor Research Institute (BRI). All potential patients required an initial diagnosis of any stage CRC prior to surgery. To determine interest to participate in the study, each patient was initially contacted via telephone by the research nurse only after being referred by a participating North Texas Colon and Rectal Surgeon at BUMC. Informed consent was then acquired in person by the research nurse and a HIPAA-approved record release authorization was obtained in order to access each patient's protected health information. This meeting took place before surgery during the AM-admit visit at BUMC in Dallas located on the 2nd floor of Hoblitzelle in a private examination room located in the referring physician's office, or in the patient's hospital room prior to surgery also located on the campus of BUMC Dallas. All patients' identifying

information was protected in a locked cabinet located in the research nurse's office located on the BUMC campus Barnett Tower, 8th floor, Suite 805.

Immunohistochemistry

IHC was performed to detect CD3 and CD8 expressing cells in the colorectal tissues. This procedure is named in this way because it requires antigen detection via antibodies, hence "immuno-", and takes place in tissues, hence "histo-". Specific primary antibodies were used to detect specific molecular markers expressed by cells of interest. Secondary antibody were ligated to an enzyme, such as peroxidase, which catalyzes a reaction that produces color. The detection of color indicates that the antibody:antigen complex has formed in close proximity to the cell of interest.

Microtome Sectioning

Presence of $CD3^+$ and $CD8^+$ infiltrating cells in colorectal tumors was confirmed using IHC. The procedure is a followed. One paraffin embedded tumor was obtained from Pathology. The identity of the patient was kept hidden, and no clinicopathological data was acquired. The paraffin embedded tumor tissue was first sliced at 2 µm using a Leitz 1512 microtome. This instrument performs high cutting precision for the preparation of paraffin-embedded tissues. The 2 µm slices was melted to 3 x 1 inch glass microscope slides (VWR, Radnor, PA) then deparffinized in an oven (Isotemp 500 Series, Fisher Thermo Scientific, Waltham, MA) at 60 °C for 40 minutes. Slides were placed horizontal and upright in a staining rack to allow paraffin to gently drip off. Slides were allowed to cool at room temperature (RT) for 20 minutes. Slides were then submerged sequentially in xylene (VWR) 3 times for 30 minutes, then in 100% ethanol (VWR) 2 times for 4 minutes each,

then 95% ethanol 2 times for 4 minutes, than 70% ethanol 2 times for 4 minutes, and finally deionized water for 10 minutes.

Antigen Retrieval

Antigen retrieval was next performed because protein cross-linkages form during formalin fixation, and the hydrophobic environment of paraffin will cause hydrophilic epitopes to invert and become obscured. Therefore these linkages needed to be broken in a hydrophilic environment to allow all potential antigenic epitopes to revert back to their native state. Slides were rinsed 3 times for 5 minutes at RT Tris-Buffered Saline and Tween 20 (TBST), 0.5 molar Tris-HCl (Sigma, St Louis, MO), 3 molar NaCl (Sigma), and 0.1% Tween 20 (Sigma). Slides were then soaked in 10 mM citric acid (Sigma) pH 6.0 in a white staining tube and covered. The pH was measured using the Accument Basic AB15 pH meter (Thermo Fisher Scientific). The slides and staining tube were autoclaved using the AccuSterilizer AS12 (VWR) at 100 °C for 15 minutes, then allowed to cool for 20 minutes. Slides were then rinsed again in TBST 3 times for 5 minutes.

Endogenous Enzyme Blocking

Endogenous peroxidases are produced by a variety of cells and permeate tissues. Major peroxidase producers include neurons, granulocytes, and erythrocytes. Some of these enzymes are removed during fixation and embedding, however residual amounts remain. Therefore these enzymes need to be blocked in order to reduce background catalysis of added substrate. Slides were removed from the staining tube and rinsed with deionized water, and excess water was removed using a kimwipe. Each tissue was circled with a PAP pen so that the reagents applied will be confined to a specific area. Approximately 100 µL of Duel Endogenous Enzyme Block (Dako, Glostrup, Denmark)

was used to cover each tissue and allowed to incubate at RT for 10 minutes. Slides were then rinsed with deionized water and returned to fresh TBST.

Primary Antibody Stain

Primary monoclonal antibodies will bind to their specific antigens if the antigens are present, however their efficacy must be validated. To determine whether primary antibodies bind specifically to their target epitopes, and not to any non-specific epitopes, an isotype control was included. An isotype control is described as a non-immune reactive immunoglobulin of identical isotype as the primary antibody, and diluted in antibody diluent (BSA/TBST, 5% bovine serum albumin (Sigma) heated at 37 °C for 10 minutes) to the same concentration as the primary antibody.

Approximately 50 to 100 μL of primary antibody or isotype control diluted in antibody diluent was applied to each slide and incubated overnight in the dark and covered with parafilm at 4 °C. Each slide was rinsed 3 times with TBST and placed into a fresh TBST bath. Excess TBST was carefully removed from each tissue using a kimwipe. Primary antibodies used were rabbit polyclonal anti-CD3 (A0452; Dako; 1:400 dilution) and monoclonal IgG1 mouse anti-CD8 (clone C8/144B; Dako; 1:200 dilution), and the isotype control was mouse IgG1. The rabbit anti-CD3 was polyclonal therefore no isotype control was used, however it was compared to a non-stained control.

Labelling Polymer-HRP (Secondary Antibody)

The secondary antibody is conjugated to the enzyme horseradish peroxidase (HRP). The presence of HRP is made visible using an oxidized substrate. Hydrogen peroxide is used as the oxidizing agent, and creates a characteristic color change to brown-purple.

EnVision+ Dual Link System-HRP (Dako) was used as the secondary antibody. Approximately 50 µL were applied to each tissue. Tissues were covered with parafilm and incubated at RT for 30 minutes, then rinsed 3 times with TBST. Substrate-chromogen (DAB^+ chromogen, Dako, diluted 1 to 50 in Substrate Buffer (Dako)) was added to tissues at 50 to 100 µL and allowed to incubate at RT for 10 minutes. Tissues were rinsed with deionized water.

Hematoxylin Counter Stain

Counter staining is useful for contrasting principle colors of tissues and allows tissue structures to be more easily discerned. This was done using hemotoxylin (VWR), which when oxidized forms colored complexes with metal ions, Fe(III) and Al(III) salts. This staining is very useful for staining nuclei for microscopic examination.

Approximately 200 µL of hemotoxylin was added to cover each tissue and then incubated at RT for 3 minutes. Unbound hemotoxylin was rinsed off using deionized water before bluing reagent was added. Approximately 200 µL of diluted ammonium hydroxide (NH_4OH) was applied to cover the tissue, then quickly rinsed off in a deionized water bath for 5 minutes.

Dehydrate Tissues and Microscopy

In order for tissues to be observed by microscopy and preserved for later use, they first needed to be dehydrated. The slides were first soaked in 70% ethanol 2 times for 3 minutes, then placed in 95% ethanol 2 times for 3 minutes, then 100% ethanol 2 times for 3 minutes, and finally xylene 3 times for 3 minutes. The tissues were allowed to air dry and excess xylene was wiped off carefully using a kimwipe. A cover slip was fixed to the slide using Fisher Chemical Permount™ Mounting Medium (Fisher Thermo Scientific). The

tissues were then observed using the Axioskop 2 plus upright microscope (Carl Zeiss, Oberkochen, Germany) with the AxioCam HRc (Carl Zeiss). This system captures natural color reproductions of tissues with a dynamic range of up to 2500X. These observations were later complimented using flow cytometry.

Meta-Analysis

A meta-analysis was performed with the goal to compile peer-reviewed studies that pertain to the ramifications of a particular subset of infiltrating T-cells on patient survival, and also to provide an overview of the overall findings from the research field as a whole. This meta-analysis focused to summarize the impact of $CD8^+$ T-cells on survival rates of a larger number of CRC patients by collecting, considering, and combining all reliable primary research data. In other words, this meta-analysis increased the statistical power of many small studies pertaining to TILs and CRC patient survival rates by and focusing all the data into a perceptible summary.

This paragraph reviews the lexicon and structure of the meta-analysis. The studies included needed to report survival rates as a (log) hazard ratio (HR). This statistic measures the magnitude difference between two Kaplan-Myers curves, which depicts the survival rates between two patient groups over a specified post-surgery follow-up period (Parmar et al., 1998). A $HR < 1$ indicates improved survival of one particular group over the other, whereas a $HR > 1$ indicates poorer survival. Acceptable survival rate definitions were limited to DFS (or recurrence-free survival), overall survival (OS), and cancer (or disease)-specific survival (CS). Relevant studies often provided results from two major regions of the tumor; the epithelium is the compartment that contains the cancer cells, and the stroma is the compartment in close proximity to the epithelium but does not contain tumor cells.

Shinto et al in 2014 determined that TILs located in the epithelium are stronger predictors of tumor regression after chemotherapy (Shinto et al., 2014); therefore epithelial data are more pertinent to the meta-analysis and were selected over stroma whenever a study provided both.

The analysis was performed using a strict inclusion criteria that selected only relevant studies. The criteria specified that each study focused on primary colon and/or rectal cancers, that data were gathered only from IHC studies that included HR and 95% confidence intervals (CI), immune infiltrates were identified by markers that normally represent lymphocytes with cytotoxic activity, and that HRs represented patients with high densities of infiltrating $CD8^+$ T-cells compared against low. However results given as low compared to high were simply converted to the reciprocal. Only multivariate analysis data that used the Cox proportional hazard model were included in the meta-analysis, where all studies must have been adjusted for (at least) age and TNM staging.

PubMed (http://www.ncbi.nlm.nih.gov/pubmed) was used to retrieve all relevant studies. The goal was to identify studies that screened colorectal tumors for markers that detected $CD8^+$ T-cells. Terms used in the search represented the names of the subset's common cell markers and activities. The following Boolean search was performed: (T-cell* OR T cell* OR granzyme* OR GZM* OR CD45* OR CD3* OR CD8* OR CTL* OR cytotoxic* OR cytolytic* OR killer* OR lymphocyte* OR helper*) AND (colon OR rectal OR colorectal OR CRC*) AND (hazard OR HR*). The relevancy of each retrieved study was evaluated by first inspecting the title and abstract. Studies representing redundant patient populations were removed from the analysis. Lastly, each relevant study was

thoroughly scrutinized to ensure that it properly represented CRC patient survival rates as functions of anti-tumor lymphocyte infiltration.

A separate meta-analysis of each survival rate definition was calculated following the method detailed by Neyeloff (2012) (Neyeloff et al., 2012). First, this method outlined a procedure that assessed heterogeneity between studies. Any observed interstudy heterogeneity was most likely due to differences between study designs and follow-up procedures. Heterogeneity was quantified using the I^2 statistic and arbitrarily assigned as low, moderate, and high ($I^2 < 25$, $25 \geq I^2 < 50$, and $\geq 50\%$, respectively) (Higgins et al., 2003), then tested for a chi-square (X^2) distribution. A P value < 0.10 was the cutoff for significant heterogeneity (Higgins et al., 2003). This test has been criticized as being poor at detecting true heterogeneity, therefore a cut-off of 10% for significance relieved the risk of interpreting a low P value as non-significant (Higgins et al., 2003). Second, this method outlined the calculations for overall HRs following the random-effects model if interstudy heterogeneity was detected. This model assisted in controlling for unobserved heterogeneity by favoring larger and more reliable studies and weighting each by their inverse variance. The null hypothesis of the meta-analysis was that the overall effect of infiltrating $CD8^+$ T-cells on patient survival rate is zero (overall HR = 1) in all studies.

Calculating the Weighted Effect Size

The effect size (*Est*) represents the study's estimated magnitude (or strength) of the phenomenon in question. The effect size in this meta-analysis represented each study's estimated HR and was weighted relative to each study's variance (*Var*). The variance was calculated from the lower and upper confidence intervals (CI) l and u, respectively. The size of the CI indicated the study's precision, therefore the variance was appropriate for

calculating each study's weight (*w*). Microsoft Excel (Microsoft Corporation, Redmond, Washington), was used for all calculations unless otherwise specified.

HR is a ratio measurement, therefore *l* and *u* were natural log transformed before the variance was calculated (Altman and Bland, 2011) (Equation 1). The standard error (*SE*) of the effect size was calculated from the log transformed Cis (Equation 2). The variance of each study was calculated as the square of the standard error (Equation 3). The weight of each study was calculated as the inverse of the variance (or standard error squared) (Equation 4). The effect size was the natural logarithm of each study's estimated HR (Equation 5). The weighted effect size (*wEst*) of each study was calculated by multiplying each study's effect size by its weight (Equation 6).

$$l = \ln(\text{lower CI}) \text{ and } u = \ln(\text{upper CI}) \quad \text{(Equation 1)}$$

$$SE = {}^{(u-l)}\!/_{(2 \times 1.96)} \quad \text{(Equation 2)}$$

$$Var = SE^2 \quad \text{(Equation 3)}$$

$$w = {}^{1}\!/_{SE^2} \quad \text{(Equation 4)}$$

$$Est = \ln(\text{HR}) \quad \text{(Equation 5)}$$

$$wEst = w \times Est \quad \text{(Equation 6)}$$

Testing for Heterogeneity

Heterogeneity in meta-analysis is a measurement of inconsistency between the effect sizes of all the studies. It is denoted as I^2 and represents the percentage of the total variation among the studies not due to random error. Heterogeneity is calculated from Cochran's heterogeneity statistic (*Q*) and the degrees of freedom (*df*) of the meta-analysis.

Cochran's Q was calculated as the weighted sum of the squared differences between each study's weighted effect size and fixed-effects-derived overall estimate (Equation 7). The degrees of freedom was simply calculated as 1 minus the number of studies (k) (Equation 8). Heterogeneity was calculated using Cochran's Q and represented as a percentage (Equation 9).

$$Q = \sum(w \text{ x } Est^{\,2}) - {[\sum(w \text{ x } Est)]^2}\Big/{\sum w} \qquad \text{(Equation 7)}$$

$$df = k - 1 \qquad \text{(Equation 8)}$$

$$I^2 = {(Q - df)}\Big/{Q} \text{ x } 100 \qquad \text{(Equation 9)}$$

A P value was calculated by assuming Cochran's Q followed a X^2 distribution with $df = k - 1$ under the null hypothesis of homogeneity. This was calculated using the Microsoft Excel function "CHIDIST". A P value < 0.10 is indicative of significant heterogeneity and variation within and between each study should be adjusted for.

Selecting the Random-Effects Model

It is unlikely that all the accumulated data from multiple studies performed by different groups are functionally equivalent. The effect size cannot be assumed to be similar among the studies due to variability among the patient populations and the means in which those populations were studied, also these inconsistencies cannot be from sampling error only; therefore a common or fixed effect size cannot be assumed (Borenstein and Higgins, 2013) as determined above. The random-effects model requires a reversal of the inverse variance weighting by applying a random-effects variance constant (v), which is derived from the variance within a study plus the variance between studies.

In other words, heterogeneity is controlled for by adjusting the weight of each study by its variance constant to calculate an adjusted weight (w_v) for each study.

The v was calculated from Cochran's Q, the weight of each study, and number of degrees of freedom (Equation 10). The adjusted weight for each study was calculated by inversing the sum of the variance constant and the standard error squared (variance) (Equation 11).

$$v = {Q - df}/{\sum w - \left(\sum w^2 / \sum w\right)} \quad \text{(Equation 10)}$$

$$w_v = {1}/{(SE^2 + v)} \quad \text{(Equation 11)}$$

Testing for Overall Effect

The goal of the meta-analysis was to combine a large number of studies to determine whether the overall effect of infiltrating $CD8^+$ T-cells improves survival rates (CS, DFS, and/or OS) for CRC patients. To determine if this was true the null hypothesis needed to be rejected. A P value (P_v) for the overall effect size (Est_v) was calculated from the z-score (z) for each survival rate definition, and significance was determined as $P < 0.05$.

The overall effect size was calculated using each study's effect size and adjusted weight (Equation 12). The overall standard error (SE_v) of the overall effect size was calculated by taking the square root of the inversed sum of each study's adjusted weight (Equation 13). Finally, the overall CIs of the overall effect size, l_v and u_v were calculated using the overall effect size and the overall standard error (Equation 14).

$$Est_v = {\sum(w_v \text{ x } Est)}/{\sum w_v} \quad \text{(Equation 12)}$$

$$SE_v = \sqrt{1/\sum w_v} \quad \text{(Equation 13)}$$

$$l_v = Est_v - (1.96 \text{ x } SE_v) \text{ and } u_v = Est_v + (1.96 \text{ x } SE_v) \quad \text{(Equation 14)}$$

The overall effect size and CIs were in the natural logarithm and therefore needed to be undone by the natural exponent (Equation 15). A separate *z*-score was calculated from the overall standard error and the overall effect size for each survival definition (Altman and Bland, 2011; Borenstein and Higgins, 2013) (Equation 16). Finally, a two-tailed overall *P* value (P_v) was calculated from the *z*-score (Altman and Bland, 2011) (Equation 17).

$$\text{HR} = e^{Est_v} \text{; lower CI} = e^{l_v} \text{; and upper CI} = e^{u_v} \quad \text{(Equation 15)}$$

$$z = \left| Est_v / SE_v \right| \quad \text{(Equation 16)}$$

$$P_v = e^{(-0.717 \text{ x } z - 0.416 \text{ x } z^2)} \quad \text{(Equation 17)}$$

Specimen Procurement

The BUMC Department of Surgery in Dallas reported that after pathological analysis and complete TNM staging of excised colorectal tumors, the majority of tissues were eventually discarded, and therefore excess tumor tissues were available for research purposes. This investigation took advantage of these tissues before they could be stored in formalin. After tissues were excised and thoroughly examined by a staff Pathologist, one 0.5 - 1.0 gram (approximately dime to quarter size) specimen was obtained for research. The remaining tissue was then taken for fixation, sectioning, and staging by a trained staff pathologist. This investigation was careful to only collect specimens from the portion of tumor tissues that would have otherwise been discarded after complete pathological

assessment. If all tumor tissue was needed for assessment then none was obtained for research.

Healthy normal mucosa was also collected from excised colons no more than 5 centimeters from the edge of the tumor lesion. All tissues were stored on ice or at 4 °C in a sterile covered Petri dish and delivered to the GI Cancer Research/Epigenetics and Cancer Prevention Laboratory on the 2nd floor of Hoblitzelle Hospital, the Baylor Institute for Immunology Research (BIIR) Laboratory located on the 1st and 2nd floors of the Lieberman Building, and the 6th floor of the Baylor Charles A Sammons Cancer Center, all of which were located in Dallas. Tissues were prepared for experiments no more than 30 minutes after completion of surgery. At no time was any tissue used ever placed in formalin or frozen before analysis. Masses initially diagnosed as adenomatous polyps were not normally collected.

Clinicopathological data, including full TNM staging of each tumor, along with the location and patient gender and age, were recorded for later analysis. The identity of the each participant remained hidden from the investigation's primary researcher. Due to the small number of participants, a larger cohort was included to validate any findings pertaining to the clinicopathological data. The TCGA (http://cancergenome.nih.gov/) was utilized to validate these findings (Cancer Genome Atlas Research Network et al., 2013). TCGA's mission is to provide publicly available expression data from microarray studies performed by multiple laboratories around the world, along with corresponding clinicopathological data such as age tumor stage, location, MMR status, and other data, pertaining to primary CRCs and other cancers. The identity of TCGA patients were also kept hidden from the primary researcher.

Ex-vivo *Tissue Cultures and Multiplex Cytokine Analysis (Luminex)*

A novel approach was developed to measure cytokine and chemokine secretions from live tissues, and to determine whether immune mediators were secreted from tumor cells into the extracellular environment, thereby relieving the investigation of the limitation of measuring only transcriptional activity of these mediators. Observations were validated using multiparametric flow cytometric analysis of infiltrating T-cells.

Dr. Karolina Palucka, formerly at the BIIR, developed a successful model for studying secreted immune mediators from breast cancer tissues. Fragments of breast tumors were cultured in media and stimulated for 16 hours with phorbol 12-myristate 13-acetate (PMA)[1] and ionomycin[2] (Pedroza-Gonzalez et al., 2011). PMA/ionomycin induces transport of calcium into the intracellular compartment and activates protein kinase C to induce the production of interferons and other cytokines through the NF-κB-dependent signaling pathway (Baier and Wagner, 2009). The supernatants were then collected and analyzed by multiplex cytokine analysis (Luminex, Merck KGaA, Darmstadt, Germany) (Aspord et al., 2007) to identify secreted type-2 immune mediators from artificially stimulated tumor tissues. Importantly, this system was able to differentiated type-2 responses from type-1 and allowed Palucka's group to characterize TIL activity and profile immune response within the TME of breast tumors (Aspord et al., 2007; Pedroza-Gonzalez et al., 2011).

[1] Phorbol 12-myristate 13-acetate (PMA) is a diester of phorbol that mimics diacylglyceride, which activates signal transduction of enzyme protein kinase C.

[2] Ionomycin is an ionophore that raises the intracellular levels of calcium to stimulate the production of perforin, cytokines, and interferons.

The current investigation adapted Palucka's method to study immune mediators secreted from colorectal tumors and healthy normal mucosa. Colonic and rectal tissues necessitated the removal of mucous layers by rinsing with 1.0 mM DL-dithiothreitol (DTT) (Sigma) in Hank's Balanced Salt Solution (HBSS) without calcium, magnesium or phenol red (Life Technologies, Carlsbad, CA) for 15 minutes with mild agitation at 4 °C. Residual DTT was removed by rinsing 2 more times with plain ice cold HBSS. 0.20 grams of colorectal tumor tissue and healthy normal mucosa were minced (80 cuts) into smaller pieces (approximately 1 mm^3) with a sterile blade and placed into tissue culture flasks with 4 mL Iscove's Modified Dulbecco's Medium (IMDM) (Life Technologies) plus 10% fetal calf serum (FCS) (Life Technologies), and 1X penicillin, streptomycin (Life Technologies), 1X gentamicin and amphotericin (Life Technologies), and incubated at 37 °C in 5% CO_2. Supernatants were collected after 16 hours and stored at -80 °C until further use. Supernatants were then thawed and centrifuged at 1500 rpm for 5 minutes to remove debris. Finally, cleared supernatants were immunoassayed for secreted cytokines and chemokines using the EMD Millipore's MILLIPLEX MAP Human Cytokine/Chemokine Luminex kit system located on the 6^{th} floor of the Baylor Charles A. Sammons Cancer Center.

The Luminex technology utilizes a mixture of microspheres conjugated to analyte-specific capture antibodies and fluorescent dye-conjugated reporter antibodies. The microspheres capture analytes through their conjugated antibodies, then the fluorescent dye-conjugated reporter antibodies, which are also specific to a specific analyte, bind to the analyte:microsphere complexes. The different microspheres and the fluorescent dye-conjugated reporter antibodies can be distinguished and quantified when passed through a

laser. The combination of dyes and the excitation intensity of the microspheres are used to determine the concentration of each analyte and allows for a variety of analytes to be measured in the same reaction mixture. The following cytokines and chemokines were included in the immunoassay, CCL2 (MCP-1), CCL5 (RANTES), CCL11 (Eotaxin), CX3CL1 (Fractalkine), CXCL1 (GRO), CXCL10 (IP-10), IFN-γ, IL-4, IL-5, and IL-13. Data were analyzed using Bio-Plex Manager 6.0 (Bio-Rad, Hercules, CA).

Flow Cytometry

The Luminex data were validated by measuring the abundance of immune cells that are associated with the immune mediators of interest. The abundance and contexture of infiltrating immune cells in the TME were determined quantitatively using flow cytometric analysis. Flow cytometry is a powerful technology that allows for the instigation of many facets of cell biology, and generates data representing the quantities of individual cells with specific characteristics of interest. The technology can be customized to detect characteristics of a cell's surface, intracellular composition, and size, and allows for multiple cell types to be simultaneously counted (Alvarez et al., 2010). Many of these cellular characteristics are detected by fluorescence when a signal surpasses a set threshold determined by the operator; a cell is deemed "positive" or "negative" for markers if the signal is strong enough. The flow cytometer used in this investigation is the FACSCanto II (BD Biosciences), which is equipped with 3 lasers (488 nm, 633 nm, and 405 nm) and can detect up to 8 parameters. Specimens are stained with marker specific antibodies conjugated to fluorophores after being disaggregated into single-cell suspensions. If an antibody ligates to a cell, the laser will excite the conjugated fluorophore and indicate positive detection of a cell possessing that specific characteristic (Figure 8). Cell sorters

can be utilized to isolate cells with specific characteristics by briefly adjusting the voltage as specific cells of interest pass through the cytometer, however this technology was not used in this current investigation, but may be used for future investigations.

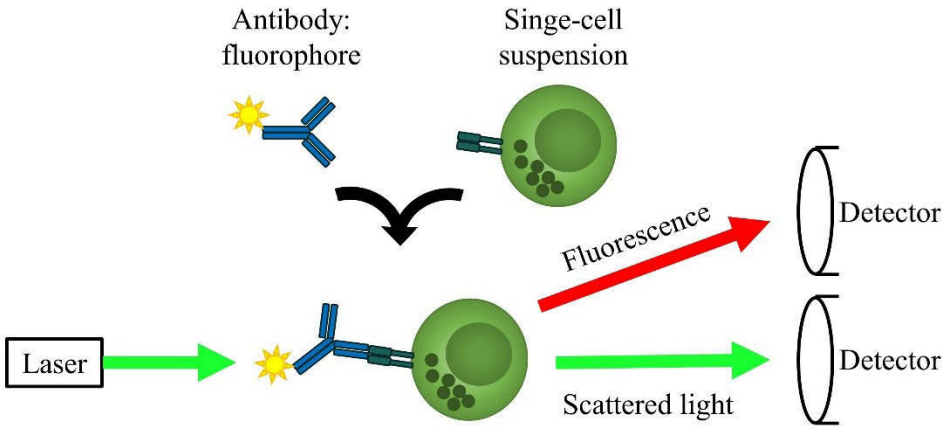

Figure 8. Diagram of flow cytometric analysis

In this investigation approximately 0.5 grams of each excised colorectal tumor and healthy normal mucosa were disaggregated into single-cell suspensions using 2.5 mg/mL of collagenase D (Roche, Basel, Switzerland), 1 mg/mL of hyaluronidase (Sigma), and 20 units/mL of DNase I (Sigma) in phosphate-buffered saline (PBS) (Life Technologies) and incubated for 2 hours at 37 °C with mild agitation and vortexing every 15 minutes. Each single-cell suspension was then passed through a 70 µM nylon cell strainer (BD Biosciences, San Jose, CA) to remove any large aggregates. The cells were then stimulated with 50 ng/mL of PMA and 1 µg/mL of ionomycin and treated with 1 µL/mL of GolgiPlug (BD Biosciences) for 12 hours at 37 °C in 5% CO_2. PMA/ionomycin treatment induced expression of intracellular markers while GolgiPlug inhibits protein transport and prevents intracellular markers from being secreted from the cell. This was done to amplify the accumulation of intracellular markers for the antibody:fluorophores to ligate. Suspensions

were washed in ice cold PBS 3 times and centrifuged as 1200 rpm for 3 minutes to remove cell debris.

The viability of the cells was evaluated using LIVE/DEAD® Fixable Dead Cell Stain (aqua) (Life Technologies) to distinguish between live cells and debris. Suspensions of colorectal tumors and healthy normal mucosa were prepared at 1 million cells per 1 mL in ice cold PBS and treated with 1 µL of fluorescent reactive dye for 30 minutes in the dark at RT. This dye reacts with free amines that become exposed when membranes become compromised during cell necrosis. Cells were then centrifuged and resuspended at 10^5 cells in 50 µL of ice cold FACS Staining Buffer (PBS, 5% FCS, 0.05% NaAzide (Sigma), and 2 mM ethylenediaminetetraacetic acid (EDTA) (Sigma), then stained with 2.5 µL of Humans TruStain FcX™ (BioLegend, San Diego, CA) for 5 minutes at RT to block non-specific binding of antibodies to Fc receptors.

Flow Cytometry for T_H1 Cells and CTLs

The cell suspensions were then stained with a panel of T-cell specific antibody-fluorophore conjugates that targeted IFN-γ positive (IFN-γ^+) Helper T cells and Granzyme B positive (GzmB$^+$) CTLs. CD45 is also known as leukocyte common antigen and is expressed on all human leukocytes including lymphocytes; it was detected by staining with 2.5 µL of PE-Cy™7 mouse anti-human CD45 conjugated antibody (BD Biosciences, clone HI30). CD3 is a TCR co-receptor and a pan T-cell marker that was detected using 5 µL of APC-Cy™7 mouse anti-human CD3 conjugated antibody (BD Biosciences, clone SK7). Helper T-cells are identified as expressing the CD4 antigen, which interacts with class II MHC. It was detected using 5 µL Pacific Blue™ mouse anti-human CD4 conjugated antibody (BD Biosciences, clone RPA-T4). CTLs express CD8 antigen, which interacts

with class I MHC. It was detected using 4 µL PerCP-Cy™5.5 mouse anti-human CD8 conjugated antibody (BD Biosciences, clone RPA-T8). Extracellular staining was done on ice in the dark for 30 minutes and unligated antibodies were washed away by centrifuging 3 times at 1200 rpm for 3 minutes with ice cold FACS staining buffer. Helper T-cells and CTLs are mutually exclusive for CD4 and CD8.

Intracellular markers were stained for to confirm the functionality of T-cell subtypes. Intracellular staining required permeabilization of cellular membranes. This was achieved using BD Cytofix/Cytoperm™ Plus Fixation/Permeabilization Kit (BD Biosciences). Cells were resuspended in 250 µL of Fixation/Permeabilization solution and incubated on ice for 20 minutes then centrifuged and washed 2 times with 250 µL of 1X Perm/Wash™ buffer and resuspended in 50 µL of buffer. T_H1 cells were identified by staining with 5 µL PE mouse anti-human IFN-γ (BD Biosciences, clone 4S.B3). Functionally active CTLs were identified by staining for GzmB using 2.5 µL of conjugated antibody (Invitrogen, Carlsbad, CA, clone GB12). See Table 1 for details pertaining to excitation/emission wavelengths and fluorophore descriptions.

Table 1. T-cell flow cytometry study design for FACSCanto II

Excitation wavelength (nm)	Fluorophore	Detector	Emission wavelength (nm)	Antigen
488	SC	F	x	x
488	PE	D	578	IFN-γ
488	PerCP-Cy™5.5	B	695	CD8
488	PE-Cy™7	A	767	CD45
633	APC	C	660	GzmB
633	APC-Cy™7	A	755	CD3
405	Pacific Blue™	B	455	CD4
405	LIVE/DEAD® (Aqua)	A	525	free amines

SC, side scatter; PE, phycoerythrin; PerCP-Cy5.5, peridinin chlorophyll-cyanine5.5; PE-Cy7, phycoerythrin-cyanine7; APC, allophycocyanin; APC-Cy7; allophycocyanin-cyanine7

Cells were incubated on ice for 30 minutes in the dark, then washed 2 times with Perm/Wash™ buffer and resuspended in 100 µL FACS Staining Buffer. Analysis was performed using a FACSCanto II cytometer at the BIIR at BUMC and the data were analyzed using FlowJo software. All antibodies were tested against isotype controls (clone MOPC-21) (BD Biosciences). Markers were gated similarly between each tumor and corresponding healthy normal mucosa using the tumor's isotype control stained lymphocyte population.

Flow Cytometry for IL-12-Expressing Immune Cells

The detection of IL-12-expressing immune cells was performed similarly as T-cells. Colorectal tumor and healthy normal mucosa were disaggregated into single-cell suspensions using a cocktail of collagenase D, hyaluronidase, and DNase I as before. The viability of the cells was evaluated using LIVE/DEAD® Fixable Dead Cell Stain and Fc receptors were blocked as before. Cell suspensions were extracellularly stained with PE-Cy™7 mouse anti-human CD45 conjugated antibody as before. However, the extracellular surfaces were also stained with 5 µL of Pacific Blue™ mouse anti-human CD14. Immune cells double positive for CD45 and CD14 are components of the innate immune system. These cells are not 'educated' nor adapted to novel antigens, however have an innate ability to internalize 'non-self' antigens and trigger the adaptive immune response, which involves educating and priming antigen-specific T-cells. These double positive immune cells can be represented by monocytes, macrophages, DCs, and in some cases granulocytes (Mantovani and Sica, 2010). Permeabilization of cellular membranes was done using BD Cytofix/Cytoperm™ Plus Fixation/Permeabilization Kit as described before. Cells were then stained with 5 µL of PE mouse anti-human IL-12. See Table 2 for details pertaining

to excitation/emission wavelengths and fluorophore descriptions. All antibodies were tested against isotype controls (clone MOPC-21) (BD Biosciences). Markers were gated similarly between each tumor and corresponding healthy normal mucosa using the tumor's isotype control stained non-lymphocyte population.

Table 2. IL-12-expressing non-lymphoid cell flow cytometry study design for FACSCanto II

Excitation wavelength (nm)	Fluorophore	Detector	Emission wavelength (nm)	Antigen
488	SC	F	x	x
488	PE	D	578	IL-12
488	PE-Cy™7	A	767	CD45
405	Pacific Blue™	B	455	CD14
405	LIVE/DEAD® (Aqua)	A	525	free amines

SC, side scatter; PE, phycoerythrin; PE-Cy7, phycoerythrin-cyanine7; APC-Cy7; allophycocyanin-cyanine7

Real-Time PCR

All immune markers that were relevant to this investigation were further analyzed using SYBR Green-based real-time PCR. Luminex and flow cytometry data were confirmed by studying the magnitude of transcriptional activity representing T_H1 cell polarizing transcription factors, relevant chemokines, and CTL activity associated markers. *TBX21* and *IFNG* represented T_H1 cell activity, relevant chemokines associated with prolonged DFS in CRC patient were *CXCL9*, *CXCL10*, *CCL5*, *CCL2*, *CX3CL1*, and *CCL11* (Mlecnik et al., 2010), while *CD8A*, *IRF1*, *GNLY*, and *GZMB* represented CTL activity (Pages et al., 2005; Pages et al., 2010), and *ICAM1* represented immune cell adhesion and migration into inflamed tissues. All cT values were normalized to *glyceraldehyde 3-phosphate dehydrogenase* (*GAPDH*). Primers were purchased from Integrated DNA Technologies (Coralville, IA). Primers sequences were obtained from the RTPrimerDB

(http://www.rtprimerdb.org/index.php) (Pattyn et al., 2003; Pattyn et al., 2006), the PrimerBank database (http://pga.mgh.harvard.edu/primerbank/) (Wang and Seed, 2003; Spandidos et al., 2008; Spandidos et al., 2010) and the Quantitative PCR Primer Database (QDDP) (http://www.rt-pcr.info/qppd-quantitative-pcr-primer-database/). The primer sequences are indicated in Table 3.

Table 3. Real-time PCR Primer Sequences

Gene	Sequence (5′ – 3′)	Size (bp)	Database ID
CCL2	F-GATCTCAGTGCAGAGGCTCG (20 bp) R-TGCTTGTCCAGGTGGTCCAT (20 bp)	153	RTPrimerDB 1642
CCL5	F-TACCATGAAGGTCTCCGC (18 bp) R-GACAAAGACGACTGCTGG (18 bp)	199	RTPrimerDB 1650
CCL11	F-ATACCCCTTCAGCGACTAGAG (21 bp) R-GCTTTGGAGTTGGAGATTTTTGG (23 bp)	169	PrimerBank 4506827A1
CD8A	F-ATGGCCTTACCAGTGACCG (19 bp) R-AGGTTCCAGGTCCGATCCAG (20 bp)	104	PrimerBank 225007533C1
CXCL9	F-GACCTTAAACAATTTGCCCCAAG (23 bp) R-CACATCTGCTGAATCTGGGTTTA (23 bp)	105	QPPD 3055
CXCL10	F-TTCAAGGAGTACCTCTCTCTAG (22 bp) R-CTGGATTCAGACATCTCTTCTC (22 bp)	177	RTPrimerDB 3537
CX3CL1	F-ACCACGGTGTGACGAAATG (19 bp) R-CTCCAAGATGATTGCGCGTTT (21 bp)	122	PrimerBank 4506857A1
GAPDH	F-TGAACGGGAAGCTCACTGG (19 bp) R-TCCACCACCCTGTTGCTGTA (20 bp)	307	QPPD 96
GATA3	F-CAGACCACCACAACCACAC (19 bp) R-TGCCTTCCTTCTTCATAGTCAG (22 bp)	121	RTPrimerDB 7757
GNLY	F-CCTGTCTGACGATAGTCCAAAAA (23 bp) R-GACCTCCCCGTCCTACACA (19 bp)	100	PrimerBank 7108346A1
GZMB	F-TACCATTGAGTTGTGCGTGGG (21 bp) R-GCCATTGTTTCGTCCATAGGAGA (23 bp)	124	PrimerBank 221625527C2
ICAM	F-CTGCAGACAGTGACCATC (18 bp) R-GTCCAGTTTCCCGGACAA (18 bp)	320	RTPrimerDB 3020
IFNG	F-CTCTTGGCTGTTACTGCCAGG (21 bp) R-CTCCACACTCTTTTGGATGCT (21 bp)	230	PrimerBank 10835171A1
IRF1	F-CTCTGAAGCTACAACAGATGAG (22 bp) R-GTAGACTCAGCCCAATATCCC (21 bp)	215	RTPrimerDB 3571
TBX21	F-CAGAATGCCGAGATTACTCAG (21 bp) R-GGTTGGGTAGGAGAGGAGAG (20 bp	169	RTPrimerDB 7752

bp, base pair

Each primer was evaluated *in silico* using the University of California at Santa Cruz Genome Browser (http://genome.ucsc.edu/) (Kent et al., 2002) to ensure each amplicon straddled multiple exons and that binding sites avoided single-nucleotide polymorphisms. These strategies reduced the chance of contaminating DNA obscuring transcription and ensured optimal primer binding throughout all specimens.

Multiple portions of both tumor and healthy normal mucosa were preserved in RNAlater® (Qiagen, Valencia, CA) per manufacture's specifications to maintain nucleic acid integrity, and stored at -80 °C. Prior to RNA isolation, tissues were removed from RNAlater® and mechanically disrupted using the TissueLyser LT (Qiagen) loaded with 5 mm stainless steel beads (Qiagen) for 5 minutes at 50 oscillations per second in ice cold RLT Plus buffer (Qiagen) with 1% beta-mercaptoethanol (Sigma). Tissues were further disrupted by passing though QIAshredder columns (Qiagen), then RNA was isolated using RNeasy® Plus Mini Kit (Qiagen) and eluted in RNase-free H_2O. RNA concentration and quality were determined using the NanoDrop 2000 spectrophotometer (Thermo Fisher Scientific).

Real-Time PCR for MRNA Expression

The Advantage RT-for-PCR Kit (Clonetech Laboratories, Mountain View, CA) was used for cDNA conversion following manufacture's specifications. 200 ng of RNA was normalized to 12.5 µL with molecular grade UltraPure™ DNase/RNase-Free Distilled Water (Invitrogen) in a MicroAmp® Fast Optical 96-Well Reaction Plate with Barcode (Applied Biosystems). 1 µL of oligo$(dT)_{18}$ was added to each well, then the primer was annealed to RNA by heating to 70 °C for 2 minutes using a PTC-100 Programmable Thermal Controller (Bio-Rad) and rapidly quenched on ice. A master mix was prepared as

detailed in Table 4 with 5% overage added (volumes are for a single reaction), then added to normalized RNA and oligo$(dT)_{18}$ primer and mixed. The mixture was incubated at 42 °C for 60 minutes, then heated to 94 °C for 5 minutes to stop the cDNA synthesis reaction and stop any DNase activity. The cDNA was diluted to a final volume of 100 µL by adding diethylpyrocarbonate-treated H_2O.

Table 4. Master mix for mRNA cDNA synthesis

Reagent	Volume (µL)
5x reaction buffer	4.0
dNTP mix (10 mM each)	1.0
Recombinant RNase inhibitor	0.5
MMLV reverse transcriptase	1.0
Total volume	6.5

Gene expression was analyzed using quantitative real-time QuantiTect SYBR Green PCR kit (Qiagen) following manufacture's specifications with the StepOnePlus Real-Time PCR System (Applied Biosystems, Carlsbad, CA). The SYBR Green I dye binds to double-stranded DNA generated during PCR and generates a fluorescent signal that represents the amount of double-stranded PCR product at each cycle. A master mix was prepared with 5 µL of pre-prepared 2x SYBR Green master mix, 3.9 µL of UltraPure™ DNase/RNase-Free Distilled Water, 0.05 µL of forward and reverse primers, plus 5% overage. The master mix was added to a MicroAmp® Fast Optical 96-Well Reaction Plate with Barcode with 1 µL of cDNA. Forward and reverse primers were used at a final concentration of 0.5 µM. Two-Step Real-time PCR was done with an initial activation step at 95 °C for 10 minutes, then 40 cycles at 95 °C for 15 seconds, 60 °C for 1 minute, and final extension for 95 °C for 15 seconds. Data was analyzed using StepOne™ Software (Life Technologies) and Microsoft Excel.

Calculating Molecular Distance to Health

This calculation combines and quantifies transcriptional changes relative to a pre-determined baseline value in a selected group of genes (Berry et al., 2010). First the healthy baseline value for each gene was calculated as the mean expression ($\bar{x}_{healthy}$) and standard deviation ($SD_{healthy}$) of all healthy normal mucosa. Next, for each gene, the number of standard deviations from the $\bar{x}_{healthy}$ was calculated by first determining the absolute difference between gene expression and the $\bar{x}_{healthy}$, and then dividing that difference by the $SD_{healthy}$ (Equation 18). Finally, the absolute summations of the number of *SDs* from $\bar{x}_{healthy}$ of all genes were calculated to determine a single value for each tissue (Pankla et al., 2009; Berry et al., 2010) (Equation 19).

$$\text{Number of } SDs \text{ from } \bar{x}_{healthy} = \left| \bar{x}_{healthy} - \text{gene expression}_{tissue} \right| \Big/ SD_{healthy} \qquad \text{(Equation 18)}$$

$$\text{MDTH} = \sum \text{Number of } SDs \text{ from healthy baseline} \qquad \text{(Equation 19)}$$

Real-Time PCR for MicroRNAs

Little work has been done to determine whether microRNAs are involved in the human anti-tumor responses. Most work, to this date has been limited to mice, therefore this investigator asked whether *miR-155* and related microRNAs could be involved in the immune response against CRCs, or whether *miR-155* could be used as a biomarker for evaluating the immune response in colorectal TMEs. Further exploration into the literature yielded several other miRNAs that could possibly be important for T-cell activities in cancer tissues and therefore were included in this Real-time PCR screen (Baumjohann and Ansel, 2013).

The Ambion® TaqMan® Small RNA Assay was used to measure miRNA expression. It was selected because it was specifically preformulated to detect miRNAs, as well as other small RNAs. Isolated RNA was normalized to 5 ng/µL the converted to cDNA using the TaqMan® Reverse Transcription Kit (Applied Biosystems). Reverse transcription primers and probes were ordered from Ambion® Life Technologies (Applied Biosystems). See Table 5 for miRNA number and Ambion® assay identifier. A master mix was prepared as detailed in Table 6 plus 5% overage (volumes are for one reaction).

Table 5. Ambion® TaqMan Small RNA Assay name and assay identification number

Assay Name	Assay ID
hsa-miR-155	002623
hsa-miR-21	000397
hsa-miR-17	002308
hsa-miR-19a	000395
hsa-miR-92a	000431
hsa-miR-16*	000391

*Included as a normalizing control

Table 6. Master mix volumes for microRNA cDNAs

Reagent	Volume (µL)
100mM dNTPs	0.15
MultiScribe™ Reverse Transcriptase	1.0
10x Reverse Transcription Buffer	1.5
RNase Inhibitor	0.19
Nuclease Free Water	9.16
5x Reverse Transcription primer*	1.0
Total volume	13.0

*See Table 7 for specific miRNA assay

A MicroAmp® Fast Optical 96-Well Reaction Plate with Barcode was loaded with 13 µL of master mix, which included primers specific to each miRNA. Next, 2 µL of normalized RNA was added to each well and covered with MicroAmp® Optical 8-Cap

Strips (Applied Biosystems). Master mix and RNA were allowed to incubate for 5 minutes at RT then mixed and centrifuged of 1000 rpms for 1 minute. Primers were annealed at 15 °C for 30 minutes, extension occurred at 42 °C for 30 seconds, and the reaction was stopped by raising to 85 °C for 5 minutes.

The TaqMan® Universal PCR Master Mix (Applied Biosystems) was used to amplify cDNA converted miRNA. A PCR master mix was prepared as detailed in Table 7 plus 5% overage (volumes are for one reaction). 14 µL of master mix and 6 µL of cDNA were added to each designated well in a MicroAmp® Fast Optical 96-Well Reaction Plate and capped with MicroAmp® Optical 8-Cap Strips. Each sample was amplified in duplicate in the same plate as the control (miR-16 assay). Real-time PCR was done using either the StepOnePlus Real-Time PCR System or the QuantStudio™ 6 Flex Real-Time PCR System (Applied Biosystems) with an initial activation step at 95 °C for 10 minutes, then 45 cycles at 95 °C for 15 seconds and 60 °C for 1 minute.

Table 7. TaqMan® PCR master mix for StepOnePlus Real-Time PCR System (96-well plates)

Reagent	Volume (µL)
TaqMan® Small RNA Assay (20x) probe*	0.5
TaqMan® Universal PCR Master Mix (2x)	10
Nuclease Free Water	3.5
Total Volume	14

*See Table 7 for specific miRNA assay

Assays performed using the QuantStudio™ 6 Flex Real-Time PCR System required MicroAmp® EnduraPlate™ Optical 384-Well Clear Reaction Plates with Barcode (Applied Biosystems) and half the volumes (including cDNA, 3 µL), see Table 8. Data was analyzed using StepOne™ Software (Life Technologies) and Microsoft Excel.

Table 8. TaqMan® PCR master mix for QuantStudio™ 6 Flex Real-Time PCR System (384-well plates)

Reagent	Volume (µL)
TaqMan® Small RNA Assay (20x) probe*	0.2
TaqMan® Universal PCR Master Mix (2x)	5
Nuclease Free Water	1.75
Total Volume	7

*See Table 7 for specific miRNA assay

PCR Phenotyping for MSI

MSI tumors are strongly infiltrated by CTLs (Dolcetti et al., 1999; Phillips et al., 2004; Drescher et al., 2009; Lee et al., 2012), therefore this investigation questioned whether defects in MMR activity correlate with relatively higher type-1 activity. IHC can detect defective MMR through the absence of MMR proteins, however this method has limited sensitivity because the immunodetection of defective or mutated MMR proteins will lead to false negative results for MSI. This investigation evaluated microsatellite markers using a pentaplex PCR-based assay optimized by Goel and colleagues in 2010 (Goel et al., 2010a). This method utilizes a highly sensitive panel of five microsatellite markers (Boland and Goel, 2010) designed to assess MSI in DNA. Due to the quasi-monomorphic nature of the microsatellite sequences that were selected for this panel, the lengths of each marker are consistent throughout the human population and can therefore be compared to previously established size standards or variation range (QMVR) previously determined from a pool of healthy normal mucosal DNA samples. While other microsatellites are polymorphic across the human population, this panel of markers eliminated the need for comparison against matched healthy normal mucosa (Goel et al., 2010a). The recommended panel of markers consists of five mononucleotide repeats (BAT25, BAT26, NR-21, NR-24, and NR-27). This assay also detects MSI in tumors with

a hypermethylated *MLH1* promoter and therefore is not limited to detecting tumors with mutated MMR genes. This method is superior to IHC because it tests for MMR function instead of presence. MSI-high (MSI-H) status is identified when two or more marker lengths fall outside the QMVR. MSI-low (MSI-L) is identified when one marker is outside of the variable range, and microsatellite stable (MSS) has zero (Figure 9).

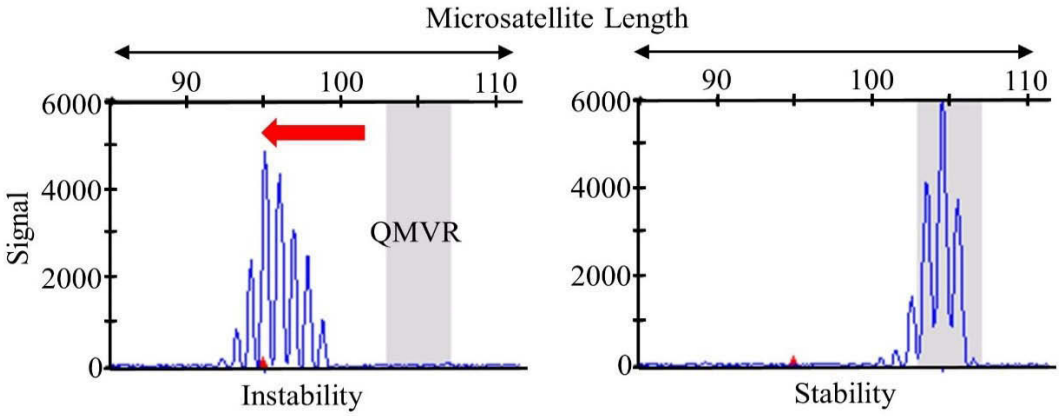

Figure 9. Example of variable microsatellite marker lengths (number of nucleotides)

Mononucleotide repeats provide a more precise determination of high-degree MSI, while dinucleotide repeats are optimal for determining MSI-L tumors (Perucho, 1999). As a point of historical fact, the panel recommended by the 1998 NCI workshop mentioned in Chapter Two of this investigation recommended the use of 3 dinucleotide markers (Boland et al., 1998), and is not optimal for detecting tumors with the highest degree of MSI (Umar et al., 2004). The 1998 panel is outmoded for this reason, and has been replaced by the more robust panel introduced by Goel and colleagues (2010) (Goel et al., 2010a). This investigation has utilized the latter because highly microsatellite instable tumors are of interest. Primer sequences that target the markers are in Table 9.

Table 9. MSI Primer Sequences and Reaction Dyes

Marker	Reaction Dye-Sequence (5′ – 3′)	QMVR (bp)
NR-27	HEX-F-CGATAATACTAGCAATGACC R- AACCATGCTTGCAAACCACT	82-87
NR-21	FAM-F-CTGGTCACTCGCGTTTACAA R- GAGTCGCTGGCACAGTTCTA	102-106
NR-24	NED-F-ATTGTGCCATTGCATTCCAA R- GCTGAATTTTACCTCCTGAC	120-125
BAT-25	HEX-F-TCTGCATTTTAACTATGGCTC R-TACCAGGTGGCAAAGGGCA	142-148
BAT-26	FAM-F-AACCATTCAACATTTTTAACCC R-CTGCGGTAATCAAGTTTTTAG	174-179

bp, base pair; QMVR, quasi-monomorphic variation range

Approximately 15 mg of each tumor tissue was preserved in RNAlater® (Qiagen) to maintain nucleic acid integrity following manufacture's specifications, and then stored at -80 °C. Tissues were removed from RNAlater® and digested using proteinase K (Qiagen) at 56 °C for 18 hours with mild agitation. Genomic DNA was isolated using QIAamp DNA Mini Kit (Qiagen) following manufacture's specifications. Concentration and quality of DNA was determined using the NanoDrop 2000 spectrophotometer (Thermo Scientific). 2x Type-it Multiplex PCR Master Mix (Qiagen) was used to amplify microsatellite markers via PCR because it is optimized for fluorescent primers and fragment analysis. Primers were added at a final concentration of 0.2 μM to 100 ng of DNA. PCR was performed by activating DNA polymerase at 95 °C for 5 minutes, then proceeding through 28 cycles (denaturation at 95 °C for 30 seconds, annealing at 55 °C for 90 seconds, and extension at 72 °C for 30 seconds) and finishing with a final extension at 60 °C for 30 minutes.

Fragment analysis was performed using the 3130 XL Genetic Analyzer (Applied Biosystems). GeneScan® 400HD ROX size standard dye (Applied Biosystems) was diluted 1:45 in Hi-Di™ formamide (Applied Biosystems) and added to 1 μL of amplified DNA.

HCT116 and SW480 cell lines (ATCC) were included with tissues as positive and negative controls for MSI, respectively. Before sequencing, DNA and formamide mix were melted at 95 °C for 3 minutes then quickly cooled on ice. TCGA data were used to supplement and validate the finding of the main investigation. Clinicopathological and expression data were extracted from the database and compiled similarly as before.

Pyrosequencing for CpG Island Methylator Phenotype

In addition to inherited mutation in MMR genes, MSI can result from biallelic hypermethylation of the *MLH1* promoter as a consequence of the CpG island methylator phenotype (CIMP) (Fishel, 1999; Ogino et al., 2006; Weisenberger et al., 2006). Hypermethylation of the promoter disrupts transcriptional activation of this critical MMR gene (Goel et al., 2007). Therefore, DNA from colorectal tumors were also screened for CIMP following the procedure in Goel and colleagues (2010) (Goel et al., 2010b). The recommended panel consisted of five markers located in CpG rich segments of promoter regions (*CACNAG1*, *SOCS1*, *RUNX3*, *NEUROG1*, and *MLH1*). 500 ng of DNA from 43 colorectal tumor tissues were modified with sodium bisulfite using the EZ Methylation Gold Kit (Zymo Research, Irvine, CA) to convert cytosines into uracils. The bisulfite converted markers were then amplified by PCR containing 2x HotStart Taq DNA polymerase (Qiagen), forward primers, biotinylated (BIO) reverse primers, and water. Each marker has a unique primer set as well as a sequencing primer (SQ) (Table 10). Primers were added at a final concentration of 0.5 μM to 2 μL of bisulfite DNA. PCR was performed by first activating DNA polymerase at 95 °C for 15 minutes, then proceeded through cycles of denaturation at 94 °C for 30 seconds, annealing, extension at 72 °C for 45 seconds, and finishing with a final extension at 60 °C for 30 minutes (see Table 10 for

annealing temperatures, extension times, and number of cycles). Single stranded biotinylated templates were isolated using the PyroMark Vacuum Prep Workstation (Biotage) following the manufacture's specifications. The Pyro-Mark MD (Qiagen) was used to perform pyrosequencing reactions and the Q-CpG Software (Biotage, Uppsala, Sweden) was used to analyze the results. The minimum cutoff for methylation was set at 5% for the following markers: *CACNAG1*, *SOCS1*, *RUNX3*, and *MLH1*; and 10% for *NEUROG1*. Four or more markers exceeding minimum cutoffs were the requirement for CIMP positivity ($CIMP^+$) (Goel et al., 2010b).

Table 10. CIMP PCR Primer Sequences, Pyrosequencing primers, and PCR conditions

Marker	PCR primer Sequences and Pyrosequencing primers (5′ – 3′)	Anneal (°C)	Extension (seconds)	Cycles
CACNAG1	F-GAAGGATATGGGTTATAGAT BIO-R- CTACTTAAACCAAAACAACC (SQ) GAAGGATATGGGTTATAGAT	53	45	55
SOCS1	F-GTGGGTATTTTTTTGGTG BIO-R-ACTACCATCCAAATAAAAAC (SQ) TGGGTATTTTTTTGGTG	50	45	55
RUNX3	F-GGGTAGTAYGGAGTAGAGGAAGTTGG BIO-R-ACCTCCCTCCCCRACCTTCC (SQ) GTGGTTAGTTAGTAAGTTTATTAT	63	45	55
NEUROG1	F-TGTAGTTYGGATTGAGGGTAGAG BIO-R-CCCCTACACCCTTCCAAA (SQ) TAGTTAGGATTGAGGGTAGA	53	60	50
MLH1	F-GGTATTTTTGTTTTTATTGGTT BIO-R-ACTCTATAAATTACTAAATCTCTT (SQ) AAAAAAGAATTAATAGGAA	46	45	50

Statistical Analysis

Graphpad Prism 6.0 software (Graphpad Software, San Diego, CA) was used to generate all correlation coefficients (R^2) and *P* values. Transcriptional data, cytokine secretion, abundance of lymphocytes, and all other tumor groupings were analyzed using two-tailed Student's *t*-test unless otherwise stated or by one-way ANOVA test for linear trend. Transcription data were $\log_2$ transformed before determining significance.

Contingency tables were analyzed using Fisher's exact test or the Cochran–Armitage test for linear trend in proportion.

CHAPTER FOUR

Results and Conclusions

This results section contains the summary of the data obtained while following the methodologies described in Chapter Three. Data from outside sources will not be presented here. This section will make no attempt to interpret the biological meaning of these data, but will simply state the findings and list pithy conclusions about the efficacy of the experiment and the value of the data. The data are presented in a logical sequence to provide the reader a sense of how and why the investigator tested the hypothesis. This section will not speculate beyond the meaning of the data nor will it provide any alternative hypotheses to explain unexpected data, but will only confirm or reject the questions that pertain to the gaps in the knowledge highlighted in Chapter One and expanded upon in Chapter Two. Any speculations about how the data represents infiltrating T_H1 cells and CTLs in colorectal tumors, how these data may affect patient survival, and how these findings are connected to genomic instability, will be reserved for the discussion in Chapter Five.

Infiltrating $CD8^+$ T-cells Can Be Detected via Immunohistochemistry

The only goal for performing IHC on one paraffin embedded tumor was to demonstrate the existence of infiltrating cytotoxic lymphocytes in colorectal tumors. These findings were later expanded upon using flow cytometry, which more thoroughly scrutinized the infiltrating lymphocyte population by measuring multiple parameters and characteristics such as production of cytotoxic mediators and type-1 mediating cytokines.

$CD3^+$ T-cells

$CD3^+$ T-cells were detected in colorectal tumors (Figure 10). However this experiment cannot fully confirm that the polyclonal antibody did not non-specifically bind to non-$CD3^+$ cells because no isotype control could be used. However, a non-stained negative control showed no positive staining for $CD3^+$ cells. For the duration of the investigation all other antibodies were compared to an appropriate isotype control.

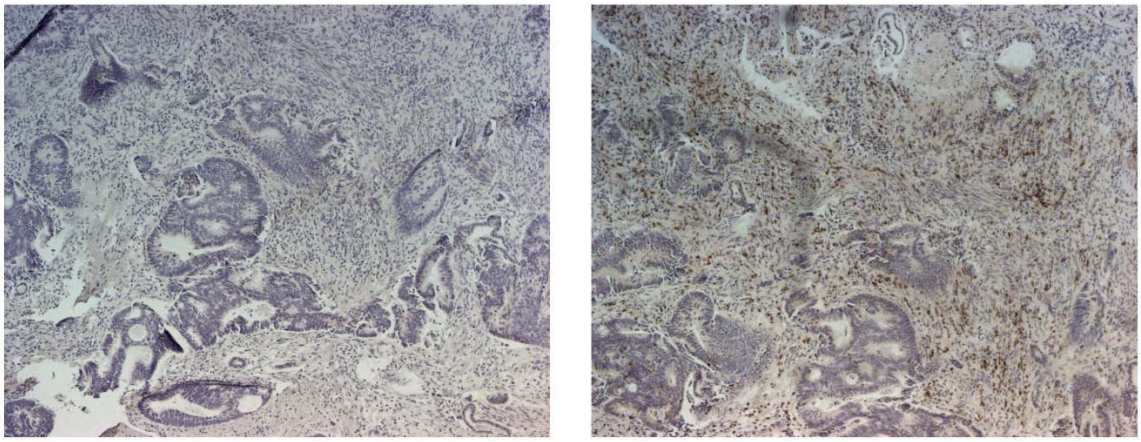

Negative control 10X Anti-CD3 10X

Figure 10. IHC of paraffin-embedded colorectal tumor stained for $CD3^+$ T-cells

$CD8^+$ Lymphocytes

$CD8^+$ lymphocytes were detected in colorectal tumors (Figure 11). However this experiment cannot conclude that these cells are specifically CTLs since some NK-cells can express a similar extracellular receptor. However, as mentioned earlier in Chapter Two infiltration of NK-cells into colorectal tumors is rare. The isotype control detected no $CD8^+$ lymphocytes and demonstrate no observable non-specific binding, therefore the primary antibody can be assumed to truly stain for cytotoxic lymphocytes.

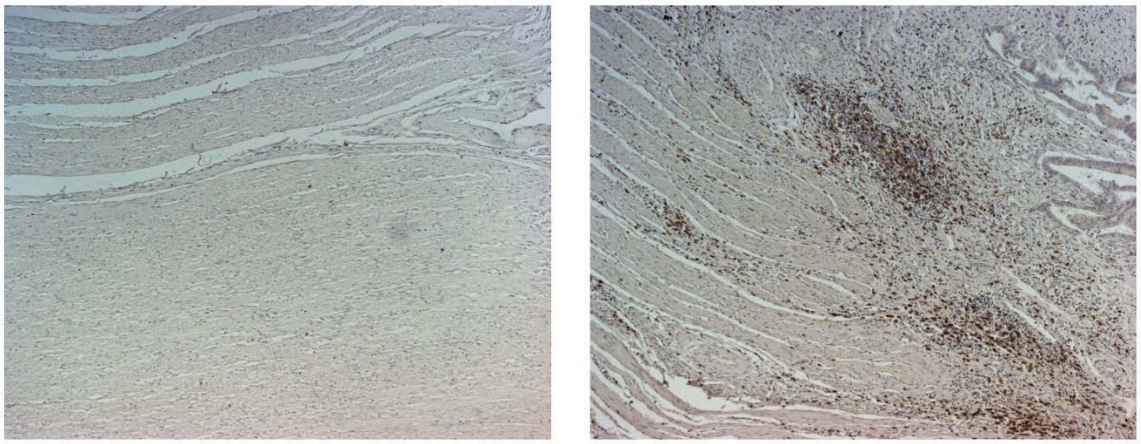

Isotype control IgG1 10X Anti-CD8 10X

Figure 11. IHC of paraffin-embedded colorectal tumor stained for $CD8^+$ lymphocytes

In conclusion, IHC staining for $CD8^+$ lymphocytes successfully demonstrated that cytotoxic lymphocytes can infiltrate colorectal tumors. Although the presence of $CD3^+$ and $CD8^+$ infiltrating lymphocytes was confirmed, this experiment made no attempt to observe the functionality of infiltrating $CD8^+$ T-cells nor $CD4^+$ Helper T-cells, therefore cytotoxic mediators such as GzmB and type-1 cytokines such as IFN-γ were not stained for in this experiment. This staining not done because the primary aim of the investigation was to study CRC using live tissues and cells to generate unique data that more closely describes the disease in its most native state, and not to perform another investigation that generates data from dead fixed tissues.

Infiltrating CTLs Contribute to Favorable Prognosis in CRC: A Meta-Analysis

The goal of the meta-analysis was to compile all previously published peer-reviewed data to calculate an overall summary of the impact of CTLs on survival rates in a large cohort of CRC patients. To maximize the number of patient populations analyzed, all studies that fit the criteria mentioned in Chapter Three were included. As of May 2014

a comprehensive PubMed search containing keywords that appropriately distinguish CTLs returned 486 studies. After all inappropriate studies were eliminated by title and abstract, the remaining were read in entirety for appropriateness, and studies with similar authors were excluded if their patient populations were duplicated. The remaining 9 studies, plus an additional 6 studies identified through manual reference search, provided sufficient data to perform the meta-analysis. The studies included were Anitei, 2014 (Anitei et al., 2014); Chiba, 2004 (Chiba et al., 2004); Correale, 2012 (Correale et al., 2012); Guidoboni, 2001 (Guidoboni et al., 2001); Koelzer, 2014 (Koelzer et al., 2014); Lugli, 2009 (Lugli et al., 2009); Menon, 2004 (Menon et al., 2004); Mlecnik, 2011 (Mlecnik et al., 2011b); Naito, 1998 (Naito et al., 1998); Nosho, 2001 (Nosho et al., 2010); Pagès, 2009 (Pages et al., 2009); Simpson, 2010 (Simpson et al., 2010); Suzuki, 2010 (Suzuki et al., 2010); Yoon, 2012 (Yoon et al., 2012); and Zlobec, 2010 (Zlobec et al., 2010). A large portion of these studies provided multiple survival rate definitions represented as CS, DFS, and OS. Therefore these subgroups were distributed into separate meta-analyses. Some studies reported multiple cohorts of patients, therefore each cohort was considered a separate study.

Each survival rate definition consisted of a large population of CRC patients (CS, n = 3160; DFS, n = 1493; and OS, n = 2727). Heterogeneity was calculated for each definition to determine whether the random-effects model will be appropriate for adjusting the weight of each study. The CS meta-analysis demonstrated high heterogeneity (I^2 = 67.06%; P = 0.006) (Table 11 and Figure 12), DFS demonstrated moderate heterogeneity (I^2 = 48.18%; P = 0.061) (Table 12 and Figure 13), while OS demonstrated low heterogeneity (I^2 = 19.50%; P = 0.247) (Table 13 and Figure 14).

Table 11. Details of studies included in the random-effects meta-analysis to determine the impact of infiltrating $CD8^+$ T-cells on cancer-specific survival

Study	HR (95% CI)	Cancer Cohort	Cell Type	% Weight
Pagès F (2009)	0.35 (0.24, 0.52)	Stage I/II CRC	$CD45RO^+CD8^+$	13.5
Mlecnik B (2011)	0.42 (0.27, 0.65)	CRC Cohort 2	$CD45RO^+CD8^+$	11.8
Chiba T (2004)	0.43 (0.23, 0.82)	CRC	$CD8^+$	7.2
Simpson JAD (2010)	0.48 (0.28, 0.82)	CRC	Nuclear STAT1	9.3
Mlecnik B (2011)	0.63 (0.50, 0.79)	CRC Cohort 1	$CD45RO^+CD8^+$	20.0
Zlobec I (2010)	0.66 (0.64, 0.68)	MSS CRC	$CD8^+$	26.8
Nosho K (2010)	0.81 (0.52, 1.27)	CRC	$CD8^+$	11.5
Overall	0.55 (0.45, 0.67)			100.0
	Heterogeneity	$I^2 = 67.06\%$	$P = 0.006$	
	Test for overall effect	$z = 5.87$	$P < 0.001$	

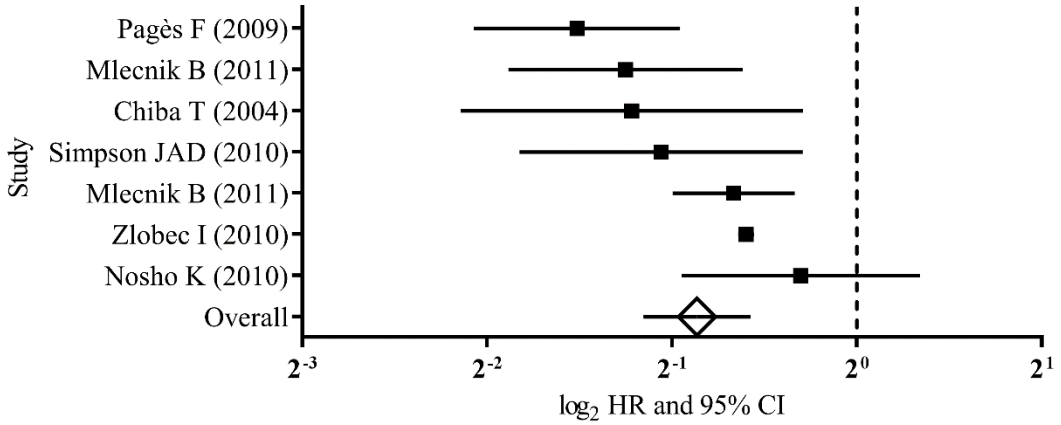

Figure 12. Forest plot of the random-effects meta-analysis to determine the impact of infiltrating $CD8^+$ T-cells on cancer-specific survival (CS)

Application of the random-effects model was considered appropriate because two of the three survival rate definitions demonstrated significant heterogeneity. After weighing each study by its inverse adjusted variance, the overall impact (effect size) of high abundance of infiltrating cytotoxic lymphocytes was estimated to be favorable for CRC patients in all three definitions [CS: HR = 0.55 (95% CI: 0.45 – 0.67); $P < 0.001$] (Table 11), [DFS: HR = 0.47 (95% CI: 0.38 – 0.58); $P < 0.001$] (Table 12), and [OS: HR

= 0.63 (95% CI: 0.57 – 0.70; $P < 0.001$] (Table 13). Interestingly, data from these studies varied greatly, however the overall findings provided a comprehensive view of the correlation between CTL infiltration and survival rates of CRC patients from multiple locations including different hospitals and countries. Presumably these data were acquired across many ethnic backgrounds.

Table 12. Details of studies included in the random-effects meta-analysis to determine the impact of infiltrating $CD8^+$ T-cells on disease-free survival (DFS)

Study	HR (95% CI)	Cancer Cohort	Cell Type	% Weight
Pagès F (2009)	0.34 (0.24, 0.48)	Stage I/II CRC	$CD45RO^+CD8^+$	16.5
Guidoboni M (2001)	0.35 (0.16, 0.77)	CRC	$CD8^+$	5.7
Mlecnik B (2011)	0.39 (0.28, 0.54)	CRC Cohort 2	$CD45RO^+CD8^+$	17.6
Correale P (2012)	0.54 (0.28, 1.03)	metastatic CRC	$CD8^+CCR7^+$	7.9
Anitei MG (2014)	0.55 (0.38, 0.78)	Rectal	$CD3^+CD8^+$	16.2
Menon AG (2004)	0.56 (0.32, 0.98)	CRC	$CD8^+$	9.5
Suzuki H (2010)	0.60 (0.22, 1.61)	CRC	$CD8^+$	4.0
Mlecnik B (2011)	0.64 (0.52, 0.79)	CRC Cohort 1	$CD45RO^+CD8^+$	22.6
Overall	0.47 (0.38, 0.58)			100.0
	Heterogeneity	$I^2 = 48.18\%$	$P = 0.061$	
	Test for overall effect	$z = 6.73$	$P < 0.001$	

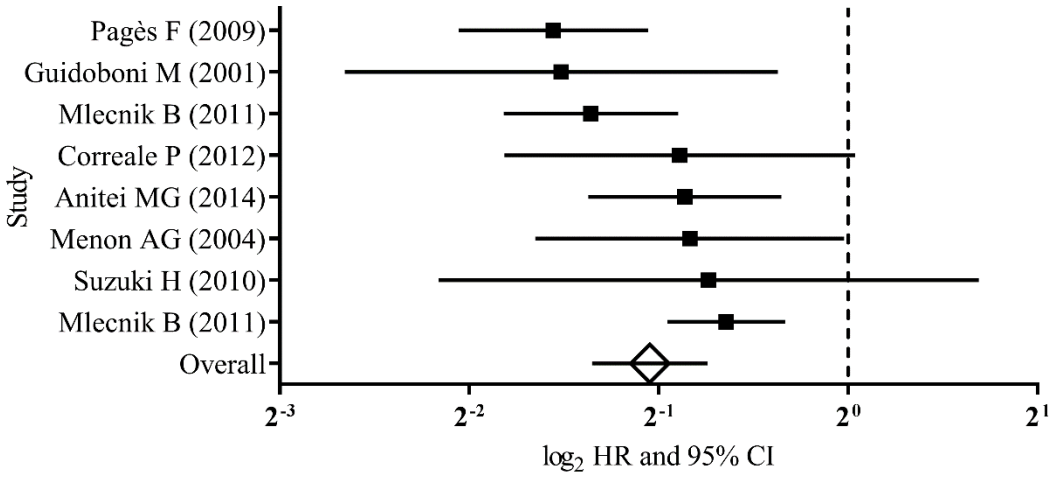

Figure 13. Forest plot of the random-effects meta-analysis to determine the impact of infiltrating $CD8^+$ T-cells on disease-free survival

Table 13. Details of studies included in the random-effects meta-analysis to determine the impact of infiltrating $CD8^+$ T-cells on overall survival (OS)

Study	HR (95% CI)	Cancer Cohort	Cell Type	% Weight
Guidoboni M (2001)	0.33 (0.15, 0.73)	CRC	$CD8^+$	1.7
Lugli A (2009)	0.45 (0.29, 0.69)	CRC Cohort 1	$CD8^+$	5.4
Correale P (2012)	0.48 (0.24, 0.96)	metastatic CRC	$CD8^+CCR7^+$	2.2
Pagès F (2009)	0.52 (0.41, 0.66)	Stage I/II CRC	$CD45RO^+CD8^+$	13.6
Suzuki H (2010)	0.53 (0.24, 1.15)	CRC	$CD8^+$	1.8
Yoon H (2012)	0.56 (0.34, 0.93)	Colon	$CD8^+$	4.0
Naito Y (1998)	0.61 (0.41, 0.89)	CRC	$CD8^+$	6.3
Anitei MG (2014)	0.62 (0.47, 0.81)	Rectal	$CD3^+CD8^+$	11.1
Mlecnik B (2011)	0.64 (0.48, 0.86)	CRC Cohort 2	$CD45RO^+CD8^+$	10.0
Mlecnik B (2011)	0.71 (0.60, 0.85)	CRC Cohort 1	$CD45RO^+CD8^+$	19.4
Koelzer VH (2014)	0.72 (0.55, 0.95)	CRC	$CD8^+$	14.2
Lugli A (2009)	0.79 (0.41, 1.53)	CRC Cohort 2	$CD8^+$	2.4
Nosho K (2010)	0.85 (0.60, 1.20)	CRC	$CD8^+$	7.6
Overall	0.63 (0.57, 0.70)			100.0
	Heterogeneity	$I^2 = 19.50\%$	$P = 0.247$	
	Test for overall effect	$z = 8.58$	$P < 0.001$	

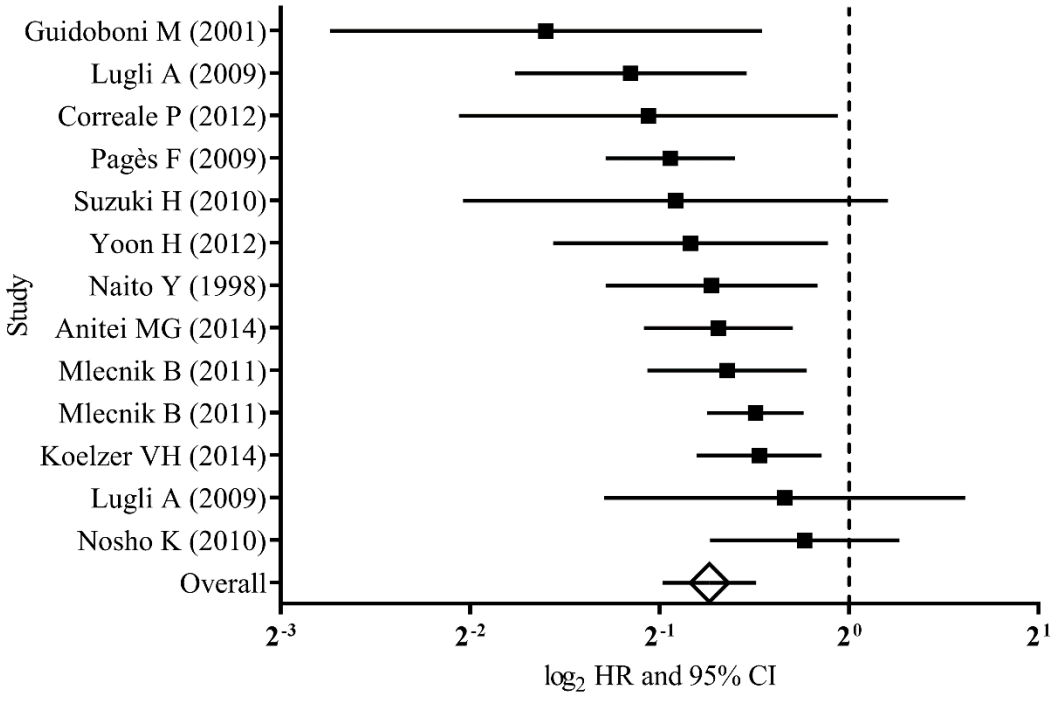

Figure 14. Forest plot of the random-effects meta-analysis to determine the impact of infiltrating $CD8^+$ T-cells on overall survival

In conclusion, CTL infiltration is a significant prognostic factor for patients with CRC. This meta-analysis evaluated a large number of patients to demonstrate the overall benefit of anti-tumor lymphocyte infiltration for patient survival. Performing a meta-analysis allowed concrete findings to be determined from repeated studies, and created solidarity between findings even when individual studies may not have derived the same conclusions. However, the limitations of this analysis need to be addressed. Lymphocyte infiltration was determined solely from IHC in which methodologies between studies can differ significantly. The first major difference could pertain to the different primary and secondary antibodies that were selected for each study. Each antibody may differ slightly in epitope recognition, and be used at different concentrations. Another major difference between studies is the lack of a consistent cut-off criterion used to define high and low degrees of infiltration. Finally, studies that report positive results are more likely to be published while those with negative results are often rejected by journals and are rarely published. Nevertheless, the results of this meta-analysis make a resounding case that a population of colorectal tumors is heterogeneously infiltrated by anti-tumor lymphocytes, and patients with highly infiltrated tumors are associated with improved survival rates. Therefore the mechanisms involving cytotoxic lymphocyte infiltration need to be further explored.

Magnitude of Helper T-Cell Activity Across TNM Stages

Immune activity is altered during the transition from normal mucosa to adenoma and cancer (Contasta et al., 2003; Evans et al., 2006; Cui et al., 2007; Cui and Florholmen, 2008). To investigate more clearly the changes in immune contexture of the TME as cancer progresses, the expression of transcription factor genes that polarize T-cells into

determinate lineages were measured via real-time PCR. A preliminary study determined 30 mg is the optimal amount of tissue needed to extract sufficient RNA (data not shown). The magnitude of gene activity was also evaluated in healthy normal mucosa.

The expression of transcription factor genes that polarize T-cells to either type-1 or type-2, *TBX21* and *GATA3*, respectively, were measured via Real-time PCR to evaluate more clearly the changes in the TME's immune contexture as cancer progresses from healthy normal mucosa through TNM stages. The efficacy of RNA isolation and cDNA synthesis were evaluated by comparing the expression of the housekeeping *GAPDH*. No difference was observed was observed between healthy normal mucosa and tumor tissue (normal, n = 22; tumor n = 43) (Figure 15).

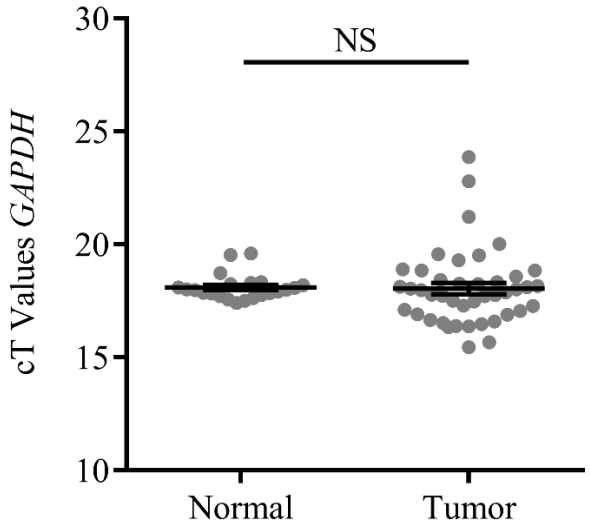

Figure 15. *GAPDH* mRNA expression between recently excised healthy normal mucosa and tumor tissue

Host protection requires anti-tumor immunity (Dunn et al., 2002; Dunn et al., 2004; Mittal et al., 2014) against TAAs identified as "non-self" followed by elimination of tumor cells through the activation of CTLs. The elimination stage gives way to equilibrium and

escape as tumor cells evolve to evade immunosurveillance, grow uninhibited, and develop the capacity to metastasize. Therefore, the magnitude of type-1 activity in CRC is expected to decrease as tumors either invade locally or spread into regional lymph nodes and distant organs. TNM stages 0, I, and II are associated with a comparably more favorable prognosis while stages III and IV represent tumor progression into regional lymph nodes and distant organs. *TBX21* expression decreased relative to healthy normal mucosa as CRCs progressed through TNM stages; stages III and IV both demonstrated decreased *TBX21* expression when compared to healthy normal mucosa. One-way ANOVA test for trend revealed that *TBX21* decreases with disease progression ($P = 0.020$) normal, n = 22; stage 0/I, n = 12; stage II, n = 15; stage III, n = 12; and stage IV, n = 4 (Figure 16).

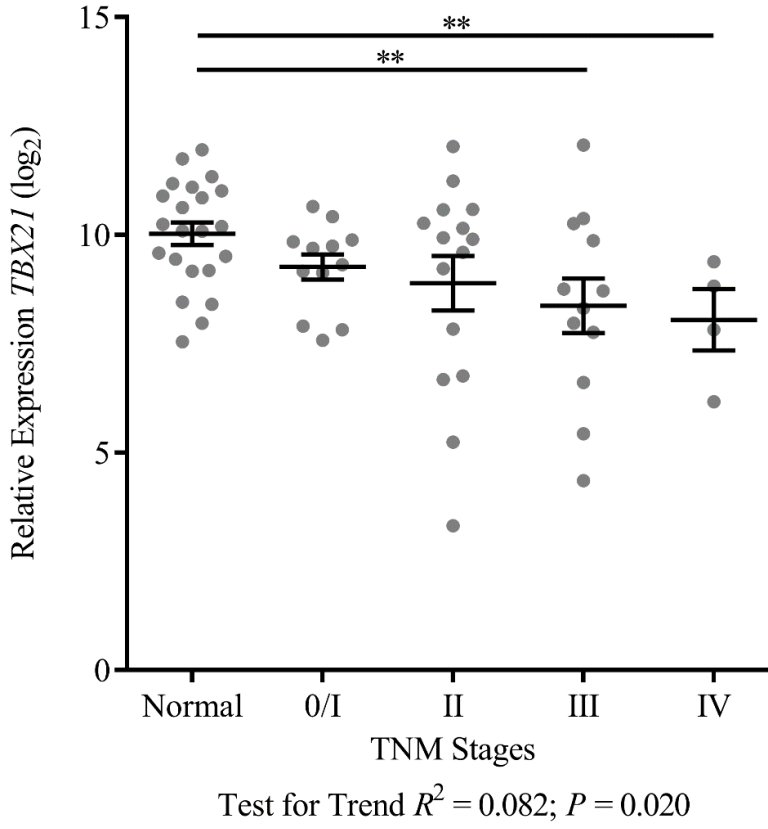

Figure 16. *TBX21* mRNA expression across healthy normal mucosa and TNM stages

A previous study used the expression ratio between *TBX21* and *GATA3* to determine the polarity of T-cells isolated from the lamina propria of colonic tissues from inflammatory bowel disease patients (Kikuchi et al., 2008). Therefore, this investigation measured *GATA3* to determine whether a decrease in type-2 T-cell activity could be evaluated similarly as type-1 T-cell activity. No difference in *GATA3* expression was detected at any stage when compared to healthy normal mucosa (Figure 17). This may be because a variety of tissue types express *GATA3*, such as urothelial tumors, breast cancers, and epithelial cells (Chou et al., 2010) and *GATA3* transcription from T_H2 cells may have been obscured by background expression. Therefore, no further analysis of this transcription factor was pursued.

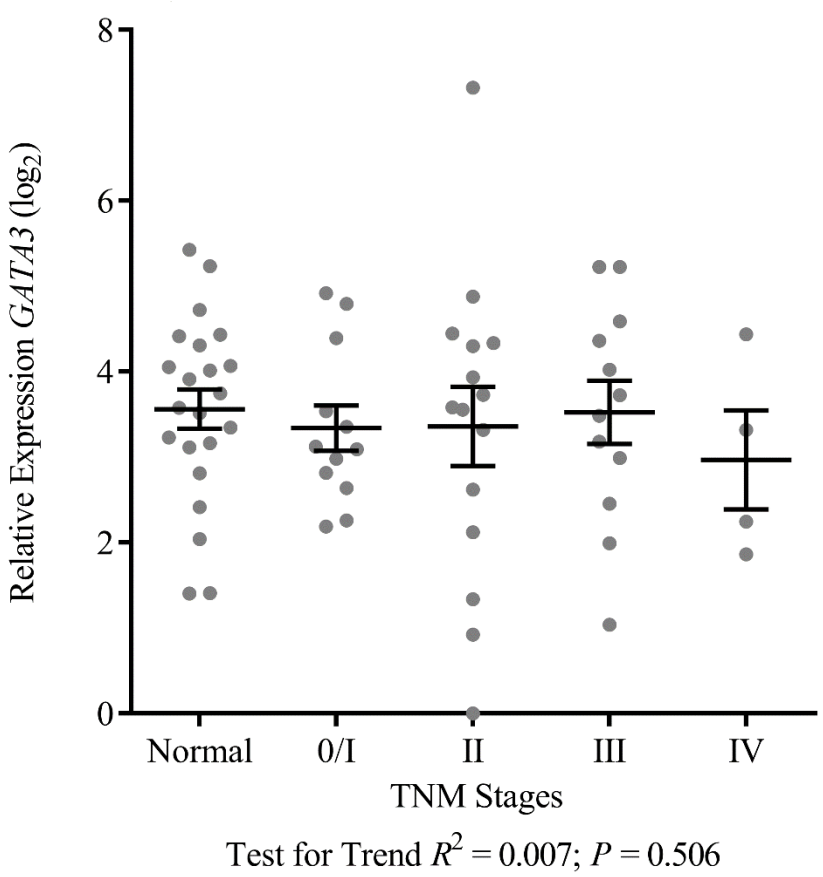

Figure 17. *GATA3* mRNA expression across healthy normal mucosa and TNM stages

Two-tailed Student's t-test was performed using cT values of *GAPDH* and $\log_2$ transformed values of *TBX21* and *GATA3* relative transcription. Error bars represent SEM of grouped tissues. *, $P < 0.05$ and **, $P < 0.01$. One-way ANOVA test for linear trend was performed on *TBX21* and *GATA3* expression across healthy normal mucosa and TNM stages with $P < 0.05$ significant for trend.

These results impelled the investigation to examine the secretion of cytokines known to be produced by T_H1 and T_H2 cells. Concentrations of secreted cytokines were determined from recently resected tissues minced into < 3 millimeter pieces and placed into culture media for 16 hours (normal, n = 22; stage 0/I/II, n = 18; and stage III/IV, n = 15). Culturing was limited to 16 hours because longer incubations lead to degradation of analyte signal (data not shown) and also increased the chance of bacterial overgrowth and contamination into other culturing flasks. Enough tissue was collected to detect cytokines concentrations within the optimal ranges of the assay (data not shown), therefore stimulatory agents were not used. Due to the small size of the study, data were consolidated by non-metastatic or metastatic stages to reinforce findings. TNM stages 0, I, and II are similar with respect to metastasis, and all three represent a more favorable prognosis when compared to stages III and IV (both include metastasis). As expected, IFN-γ was secreted more strongly in stage 0/I/II tumors when compare to stages III/IV confirming the decline of type-1 activity in the TMEs of late stages CRCs (Figure 18). Evidence for any changes in type-2 activity was further investigated, however no difference was determined for IL-4, IL-5, nor IL-13 secretion (Figure 18). No conclusions can be reached about type-2 activity among CRCs in this investigation. One-tailed Student's t-test was performed on cytokine concentrations.

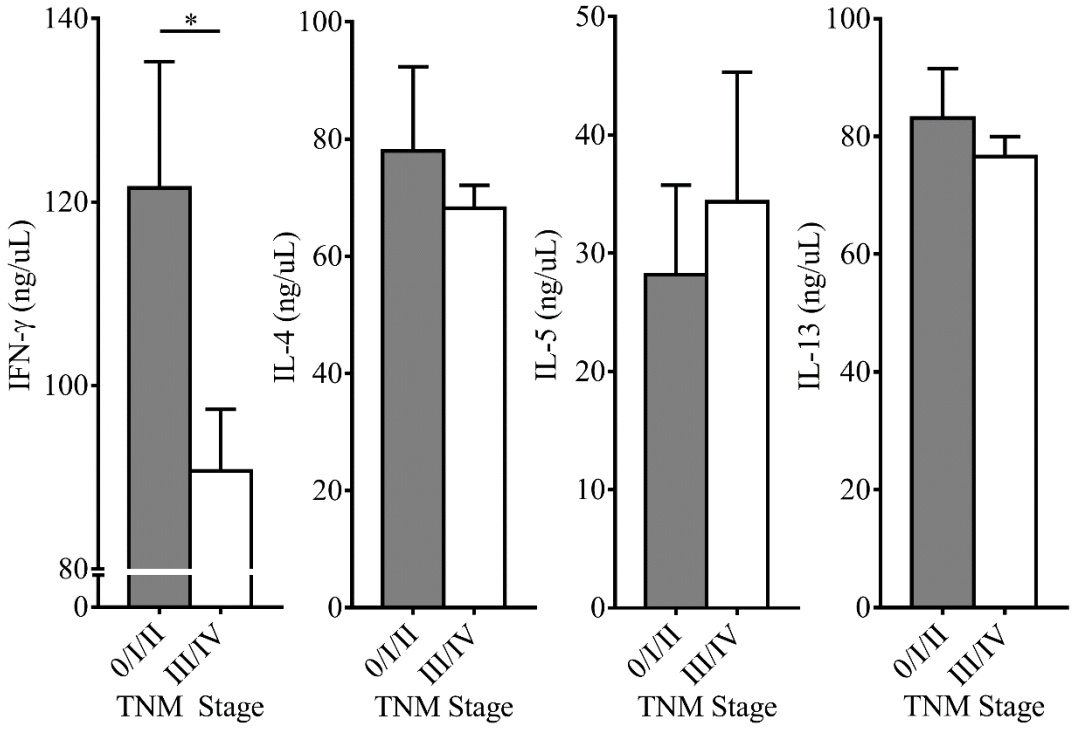

Figure 18. Secreted IFN-γ, IL-4, IL-5, and IL-13 concentrations from recently resected tissues (CRC and healthy normal mucosa) minced and cultured (16 hours)

The data above mainly addresses the immune activity during metastasis, however ignores the any association between T-cell activity and tumor invasion into adjacent tissues. Interestingly, type-1 activity did not decrease with depth of invasion (T) (Figure 19), supporting that it is largely altered during metastatic disease, which is relevant because direct invasion into deep tissues layers is biologically distinct from regional (III) or distant (IV) metastasis (T0/1/2, n = 15; T3, n = 20; and T4, n = 8). Tissue invasion requires extracellular matrix degradation, tissue remodeling, and outgrowth into surrounding tissues. Error bars represent SEM of grouped tissues. A one-tailed Student's t-test was performed on cytokine concentrations because IFN-γ secretion from stage 0/I/II colorectal tumors was expected to be increased per results in Figure 16.

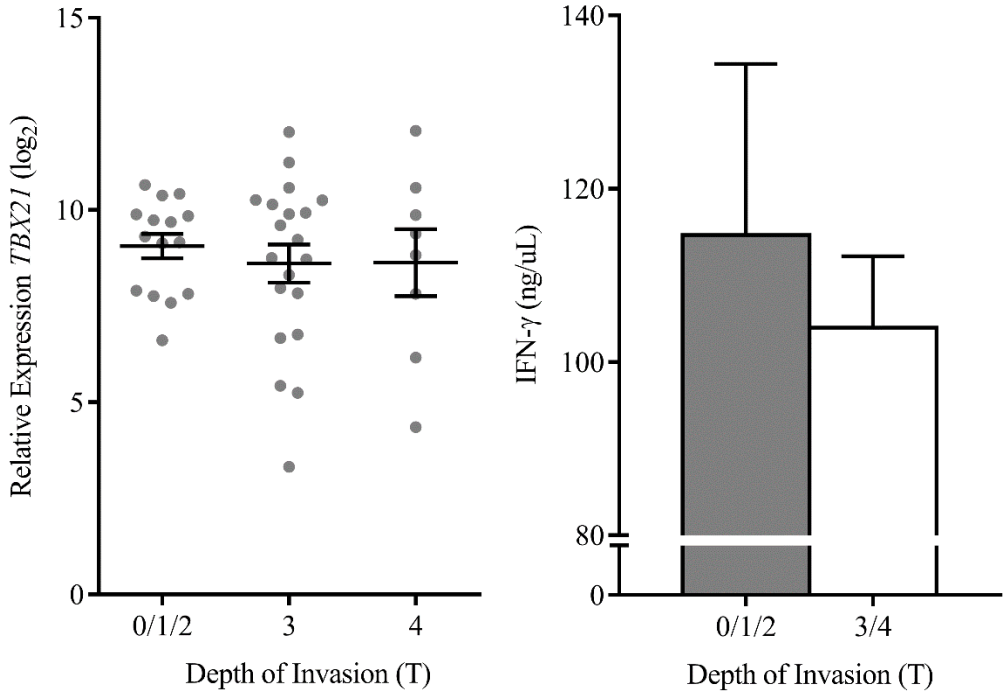

Figure 19. *TBX21* mRNA expression and secreted IFN-γ concentration among degree of invasion depth (T)

In conclusion, as determined by Real-time PCR for *TBX21* expression and Luminex immunoassaying for IFN-γ secretion, type-1 activity decreased as colorectal tumors progressed towards lymph node and distant organ metastasis. However, this type-1 activity was not shown to be altered as the depth of invasion advanced into deeper layers of tissues. *GATA3* expression, IL-4, IL-5, and IL-13 secretion were not altered at any stage of the disease. These data in this section, however, do not demonstrate whether the colorectal tumors with stronger type-1 activity have a higher potential for chemoattracting IFN-γ secreting T-cells and other anti-tumor T-cells. The next sections of this investigation will now focus on the expression of chemokines from the TME and the frequency of TILs and resident T-cells in both tumor and normal tissues.

High Type-1 Activity is Bimodally Distributed in CRC TMEs

The decreasing expression of *TBX21* across healthy normal mucosa and TNM stages suggests that a portion of CRCs have relatively high type-1 activity. This pattern may suggest that a population of tumors is heterogeneous in respect to type-1 activity. To further explore this idea, *IFNG* and *TBX21* mRNA expression from 43 tumors were plotted together to demonstrate an apparent bimodal distribution of type-1 marker expression among TMEs. A dashed line represents an apparent separation between TMEs with relatively high and low type-1 activity (Figure 20). To test for whether bimodality of chemotactic potential while maintaining unbiased analysis, tumors were profiled into 3 groups according to their expression of type-1 marker genes: tumors were ranked by expression of *IFNG* and *TBX21* then separated at the medians and profiled as either high ('Hi') or low ('Lo'). Tumors with high expression of both markers were profiled as 'HiHi' (n = 16), tumors with low expression of both were profiled as 'LoLo' (n = 16), and those that heterogeneously expressed *IFNG* and *TBX21* were profiled as 'Het' (n = 11) (Figure 21). To test whether each profile more strongly expressed chemokine genes that are associated with DFS, as reported by Mlecnik and colleagues (2010), *CXCL9*, *CXCL10*, *CCL5*, *CCL11*, *CX3CL1*, and *CCL2* were measured and compared to healthy normal mucosa (Figure 22). The chemokines and their cognate receptors are listed in Table 14. For all chemokines except for *CCL5* the HiHi profile showed increased expression compared to heathy normal mucosa. Interestingly, *CCL5* expression was decreased in both the Het and LoLo profiles, and *CCL11* was decreased in the LoLo profile when compared to heathy normal mucosa.

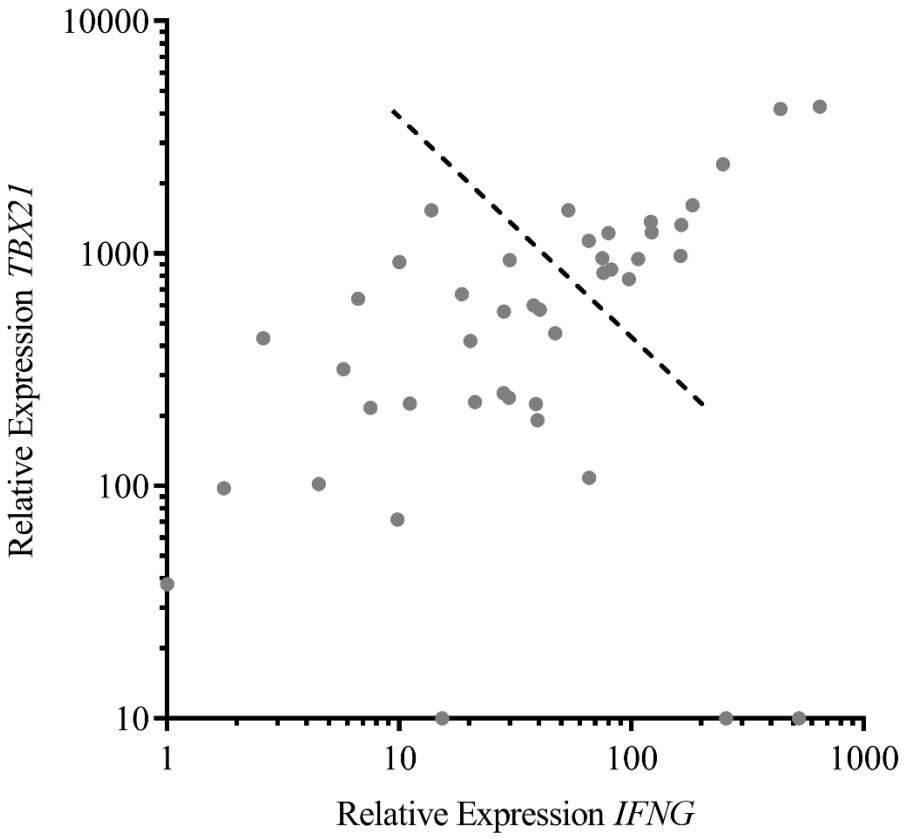

Figure 20. Dot plot of *IFNG* and *TBX21* mRNA expression from TMEs of CRCs

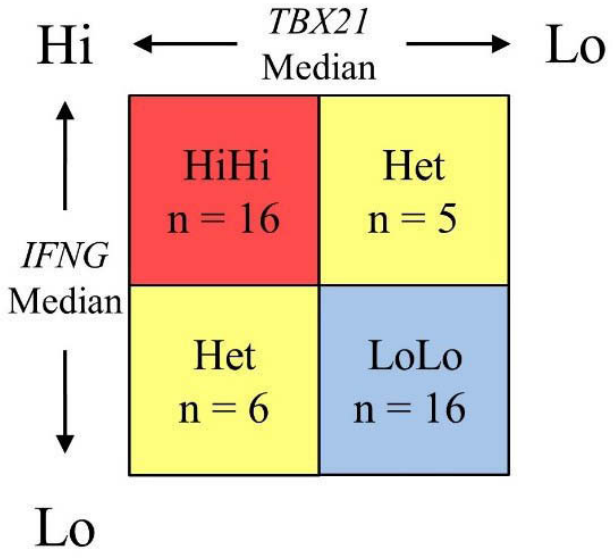

Figure 21. Diagram of unbiased profiling of TMEs into groups representing relatively high (HiHi), heterogeneous (HiLo and LoHi), and low (LoLo) type-1 activity

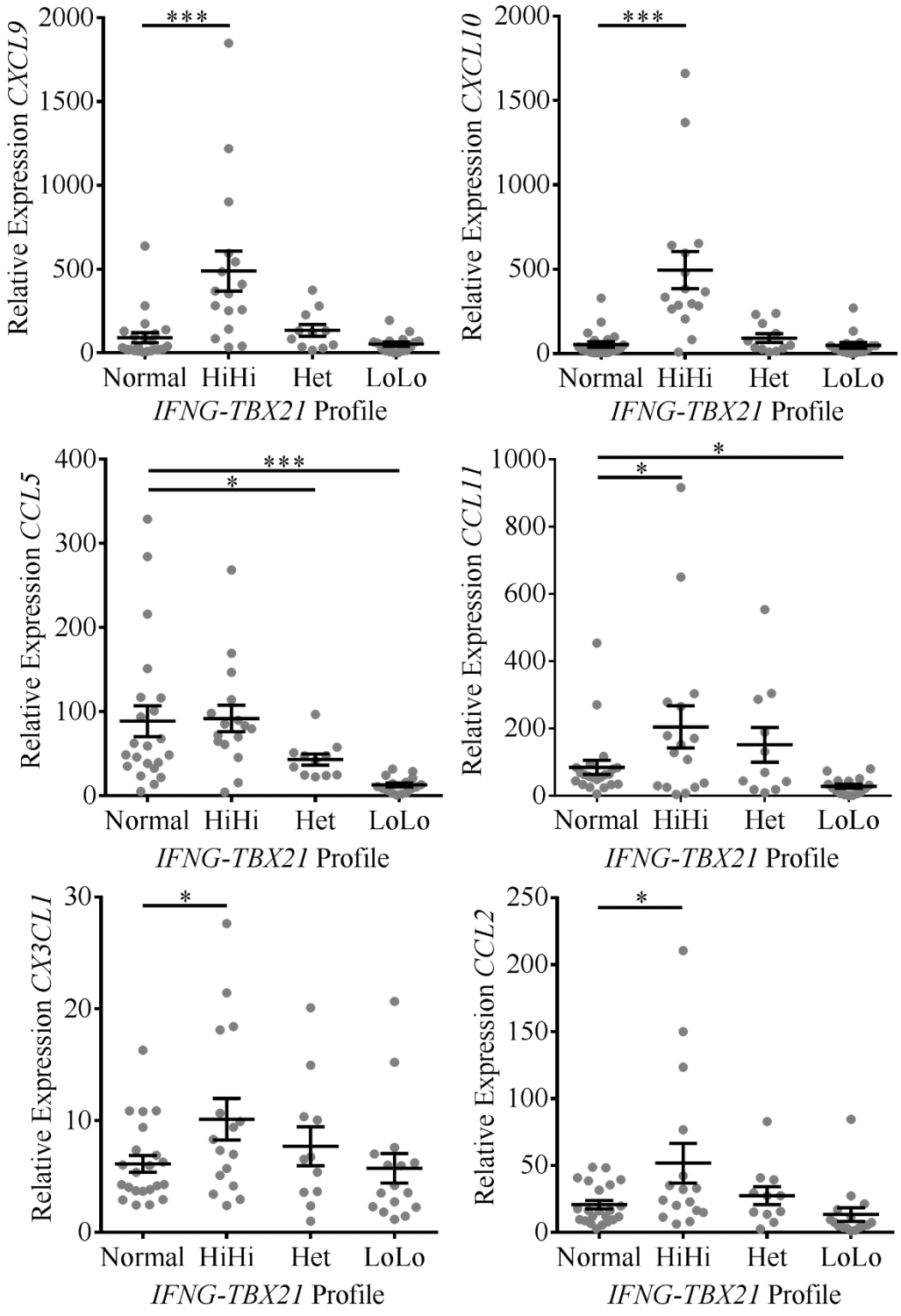

Figure 22. Expression of, *CXCL9*, *CXCL10*, *CCL5*, *CCL11*, *CX3CL1*, and *CCL2* among type-1 profiles and healthy normal mucosa

To test whether each profile truly possessed unique chemotactic potential, the chemokine transcription data was combined to calculate the molecular distance to health (MDTH). This calculation was used to test whether lymphocytes are attracted to certain tumors differently than normal mucosa; a MDTH value closer to that of normal mucosa is indicative of a minimal immune response and homeostasis. The MDTH for anti-tumor T-cell attracting chemokines was increased in the HiHi profile relative to the other profiles as well as healthy normal mucosa. However, the Het and LoLo profiles were not different from each other, nor were they different from healthy normal mucosa (Figure 23). All data for this section was calculated using the two-tailed Student's t-test for significance. Error bars represent SEM of profiles. * $P < 0.05$, ** $P < 0.01$, and *** $P < 0.001$.

Table 14. List of chemokines and cognate receptors correlated with improved DFS and anti-tumor T-cell chemotaxis

Chemokine	Receptors
CCL2	CCR2 and 4
CCL5	CCR5
CCL11	CCR2, 3 and 5
CXCL9	CXCR3
CXCL10	CXCR3
CX3CL1	CX3CR1

These data confirm the bimodal distribution of anti-tumor T-cell attracting chemokine gene activity in colorectal TMEs, and suggest that colorectal tumors with relatively high type-1 activity may not be evading the immune system and are currently the focus of an immunological response. Since the Het and LoLo profiles could not be separated statistically they were combined into a 'non-HiHi' profile. For the remainder of the investigation, each colorectal tumors will be profiled into either group to simplify and consolidate the findings and conclusions.

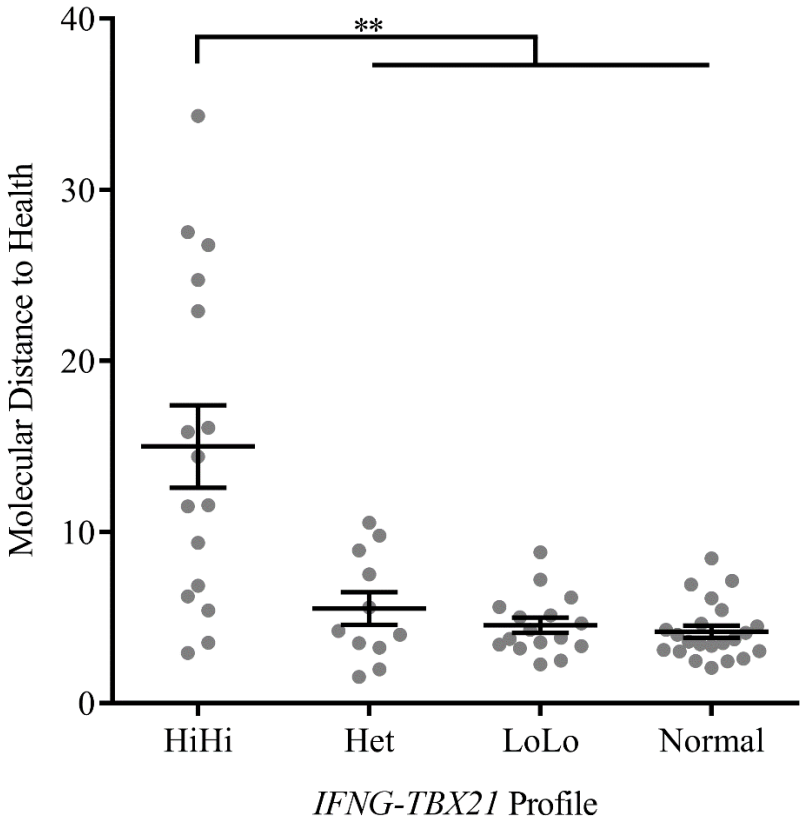

Figure 23. Molecular distance to health (MDTH) of TMEs and healthy normal mucosa

In conclusion, the population of colorectal tumors is heterogeneous for type-1 activity. When this population was divided into 3 distinct profiles defined by magnitudes of type-1 gene expression, only the HiHi profile demonstrated a unique pattern of chemokine gene expression when compared to healthy normal mucosa. These data, however, do not determine whether HiHi colorectal tumors are up or down regulating chemokines genes or if chemokines are secreted differently than non-tumor tissues.

TMEs With Relatively High Type-1 Activity Upregulate CTL Marker Genes

Previous studies have shown that TMEs of colorectal tumors with suppressed expression of *CD8A*, *GZMB*, *TBX21*, *IRF1*, and *IFNG* demonstrate higher rates of tumor

relapse and early metastatic invasion. However, tumors that highly express these type-1 response genes strongly display more CTL activity as demonstrated with higher expression of *IRF1*, *GZMB*, *CCL5*, *CD8A*, and *STAT1* (Pages et al., 2005), show upregulation of adhesion molecules (*ICAM1*, *VCAM1* and *MADCAM1*), and are associated with prolonged DFS (Mlecnik et al., 2010). The type-1 response is characterized by presence of CTLs, tumor-rejecting immunity, cellular immune response, and acute inflammation (Szabo et al., 2003). Therefore, it can be proposed that HiHi colorectal tumors will also demonstrate stronger cytotoxic activity through the expression of CTL related genes. As expected, the HiHi tumors expressed two genes encoding cytotoxic mediators, *GZMB* and *GNLY*, more highly than the non-HiHi tumors (normal, n = 23; HiHi, n = 16; Het, n = 11; LoLo, n = 16; and non-HiHi, n = 27) (Figure 24). These findings were confirmed by also analyzing the expression of *CD8A* and *IRF1*, both of which code for major CTL markers, and also *ICAM1*, of which codes for a molecule involved in lymphocyte transmigration into inflamed tissues (Figure 25). Interestingly, the non-HiHi tumors expressed *GNLY* (Figure 24), *CD8A*, and *IRF1* lower than healthy normal mucosa (Figure 25). These data suggest that the CTL response is upregulated in CRC TMEs that have relatively high type-1 activity (HiHi) when compared to healthy normal mucosa and the non-HiHi tumors. Two-tailed student's t-test was performed using $\log_2$ scale of relative transcription for all genes. Error bars represent SEM of grouped tissues. *, $P < 0.05$; **, $P < 0.01$; and ***, $P < 0.001$.

MicroRNA-155 is Bimodally Expressed Among colorectal TMEs

The investigation questioned whether miRNAs that are potentially involved in T-cell activities follow a similar bimodal expression pattern as other genes. Therefore, expression of microRNAs suspected to be expressed during the type-1 response were

measured. Due to the limited number of wells on each PCR plate (96 wells), and the necessary requirement that all samples are to be screened in duplicate on the same plate as the control miRNA, not all tissues could be used. Therefore, only 12 tumors and matching healthy normal mucosa were screened for miRNA expression as described in Chapter Three. Six colorectal tumors profiled as HiHi and 6 profiled as non-HiHi were selected at random.

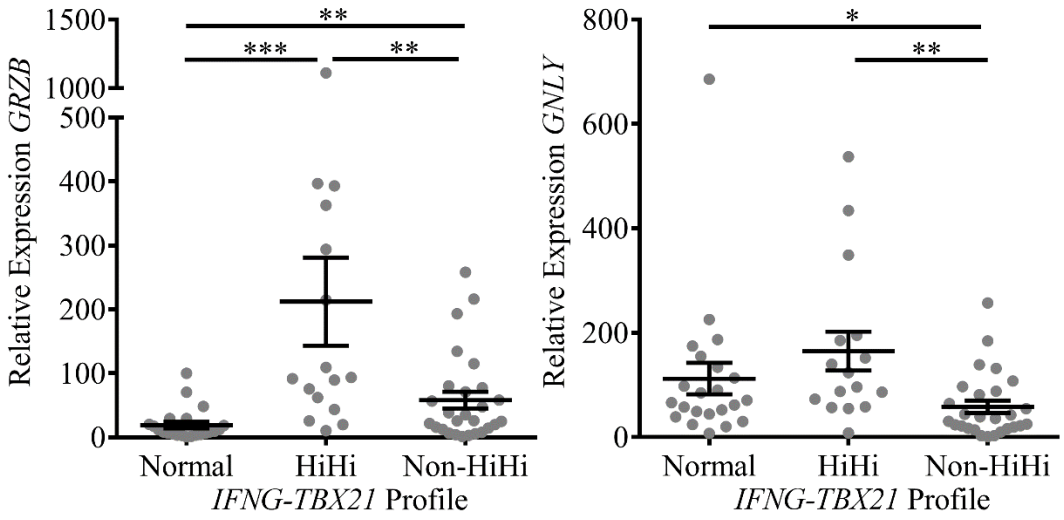

Figure 24. Cytotoxic mediator (*GZMB*, *GNLY*) mRNA expression of healthy normal mucosa and CRC profiles HiHi and non-HiHi type-1 activity

MiR-155 expression was decreased in non-HiHi tumors when compared to HiHi tumors and matching healthy normal mucosa; however the HiHi colorectal tumors were not decreased when compared to matched healthy normal mucosa. *MiR-21* was increased when compared to both groups of healthy normal mucosa; however, no difference could be detected between type-1 profiles. Therefore, further investigation into *miR-21* expression in colorectal tumors was not pursued at this time. This biomarker may be further explored in future studies. No other miRNAs demonstrated any difference in expression

between type-1 profiles or healthy normal mucosa (Figure 26) and were also not investigated any further. Two-tailed student's t-test was performed using $\log_2$ scale of relative transcription for all miRNAs. Error bars represent SEM of grouped tissues. *, $P < 0.05$ and **, $P < 0.01$.

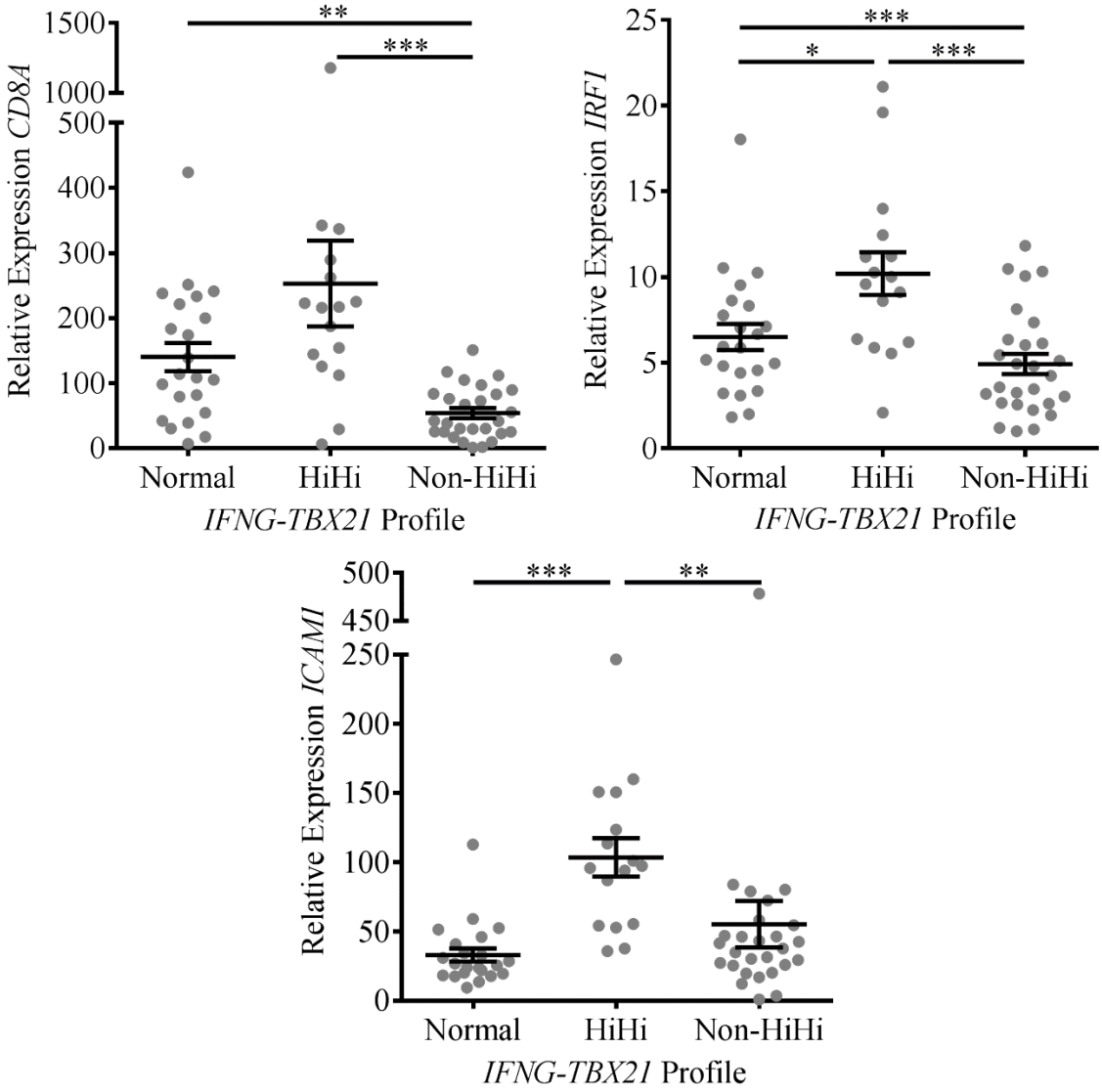

Figure 25. Other CTL markers (*CD8A*, *IRF1*) and *ICAM1* mRNA expression of healthy normal mucosa and CRC profiles HiHi and non-HiHi type-1 activity

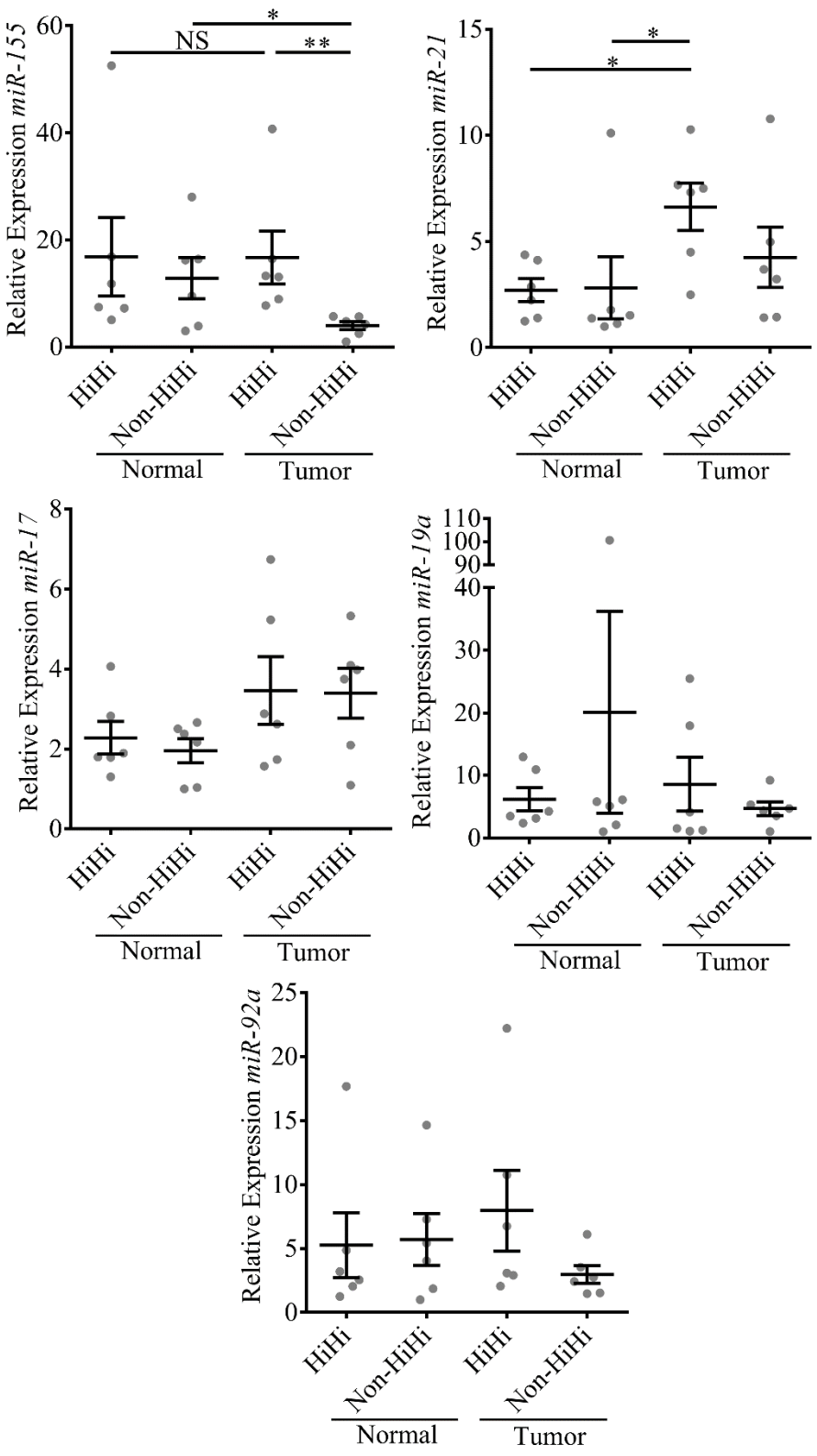

Figure 26. T-cell-associated microRNA expression in 6 CRCs profiled as HiHi and non-HiHi and 12 matched healthy normal mucosa

Mir-155 was the only microRNA was expressed differently between both profiles, therefore it was measured in all samples. To accommodate all tissues in duplicate, both healthy normal (n = 22) and tumor (n = 41), and assay for both *miR-155* and *miR-16* the QuantStudio™ 6 Flex Real-Time PCR System was used. Two tumors no longer had sufficient RNA, and were therefore excluded from the microRNA screen. This machine is capable of performing real-time PCR in 384-well plates. These data confirm that *miR-155* is expressed higher in TMEs with relatively high type-1 activity, however no difference was determined between non-metastatic (0/I/II) and metastatic (III/IV) tumors (Figure 27). Also, these data do not confirm that TMEs with relatively high type-1 activity express *miR-155* higher that healthy normal mucosa, nor determine whether anti-tumor T-cells, or other stromal cells or tumor cells, are the source of *miR-155*. This question may be interesting to investigate in the future, however this investigation is mostly concerned with immune activity that can be correlated to lack of metastasis. Therefore assays for *miR-155* expression were not pursued further. Two-tailed student's t-test was performed using $\log_2$ scale of relative transcription for all miRNAs. Error bars represent SEM of grouped tissues. *, $P < 0.05$.

In conclusion, the preceding transcriptional studies demonstrate that HiHi colorectal tumors have increased activity of genes that relate to T-cell directed anti-tumor activities. These genes include chemokines genes that target CXCR3 expressing T-cells, and genes that represent cytotoxic activity. However, for the most part the non-HiHi profile demonstrated both similar and decreased transcriptional activity of these genes when compared to healthy normal mucosa. When measuring microRNA expression, the bimodular nature of type-1 activity in colorectal tumors could only be expanded to include

miR-155 and *miR-21*. Since no conclusion can be derived pertaining to whether *miR-155* is connected to patient survival and prognosis, investigation into these microRNAs were not pursued at this time. These data, however, do not determine whether patients with increased type-1 activity in the microenvironments of their tumors have less advanced disease (stage 0/I/II) than those without (stage III/IV). This is the topic that will be investigated in the next section.

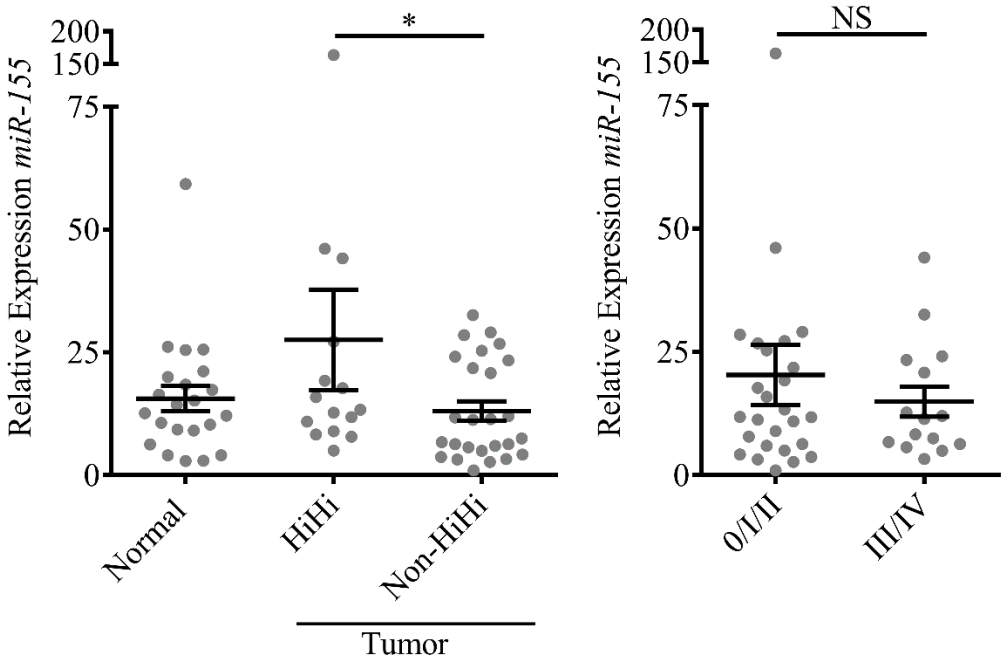

Figure 27. *MiR-155* expression of healthy normal mucosa, CRC profiles HiHi and non-HiHi type-1 activity, and tumor stages

Discrimination of Relatively High Type-1 Activity in TMEs Across Clinicopathological Characteristics of Two Study Cohorts

The evaluation of the anti-tumor immune response within the TME is important for CRC patient prognosis (Pages et al., 2005; Mlecnik et al., 2010; Pages et al., 2010; Fridman et al., 2011; Galon et al., 2014). The type-1 signature in colorectal TMEs has been identified as a valuable prognostic tool (Pages et al., 2005) and is more accurate than

conventional AJCC/UICC TNM staging at predicting disease outcome (Anitei et al., 2014; Galon et al., 2014). Therefore, determining the significance of type-1 activity on disease progression in terms of TNM staging was addressed in this investigation using two cohorts of CRC patients.

The small size of the cohort of tumors collected (IRB#011-030) lacked statistical power; therefore the analysis also included a second cohort (n = 221) extracted from TCGA. Both cohorts were distributed into contingency tables and analyzed using Fisher's exact test to determine whether the HiHi and non-HiHi profiles had a propensity to distribute by certain clinicopathological characteristics. Fisher's exact test can be used to analyze categorical data when sample sizes are small. Here, one variable was separated by categories of relative type-1 activity (HiHi and non-HiHi) and the other variables were separated into profiles listed in Table 15.

No differences were detected between the mean ages of the HiHi and non-HiHi profiles in either the IRB#011-030 nor the TCGA cohort of patients (Table 15). The magnitude of type-1 activity was earlier determined to be independent from the depth of invasion (T) (Figure 19), therefore patients were also separated into T0/T1/T2 and T3/T4 groups. Neither cohort demonstrated a difference in proportional distribution by gender, location of primary tumor or depth of tumor invasion, however the HiHi profile of the TCGA cohort demonstrated to proportionally skew towards absence of lymph node (N) and distant organ metastasis (M) ($P = 0.011$ and $P = 0.022$, respectively). 72% of colorectal tumors profiled as HiHi did not metastasize to the lymph nodes, while 54% of the non-HiHi tumors did metastasize to either locations (Table 15). The IRB#011-030 cohort could not be confirmed to follow a similar distribution for distant organ metastasis ($P = 0.131$),

however none of the tumor that showed distant organ metastasis were profiled as HiHi, and did suggest a trend for similar distribution with lymph node metastasis (N) (P = 0.050). 81% (or 13 out of 16) of the HiHi profiled colorectal tumors had no lymph node metastasis (N0) while 19% (or 3 out of 16) did have lymph node metastasis (N1-3), and 45% (or 12 out of 27) of the colorectal tumors profiled as non-HiHi had lymph node metastasis, while 48% (or 13 out of 27) did not (Table 15). These data suggest that profiling tumors using *IFNG* and *TBX21* transcriptional patterns may predict tumor progression.

The Cochran–Armitage test for linear trend in proportions was used to determine whether the proportion of either profile favored early or late TNM stages. This test analyses categorical data to determine whether an association exists between two separate variables. In this investigation, one variable had two categories (HiHi and non-HiHi profiles) and the other having three (TNM stages 0/I/II, III, and IV). The HiHi profile in both cohorts was skewed towards earlier TNM stages (0/I/II), while the non-HiHi tumors were skewed towards later stages (III and IV) (IRB#011-030, P = 0.034 and TCGA, P = 0.002; Table 16). This trend is illustrated in Figure 28. These data demonstrate that colorectal tumors with relatively high type-1 activity mainly lack invasion into lymph nodes and metastasis to distant organs.

Table 16. Cochran–Armitage test for linear trend in proportions performed on *IFNG-TBX21* profiles among TNM stages

Cohort	IRB#011-030			TCGA		
TNM stage	HiHi	Non-HiHi	Test	HiHi	Non-HiHi	Test
0/I/II	13 (48%)	14 (52%)	0.034	61 (47%)	70 (53%)	0.002
III	3 (25%)	9 (75%)		17 (31%)	38 (69%)	
IV	0 (0%)	4 (100%)		7 (20%)	28 (80%)	
						$P < 0.05$ is significant

Table 15. Clinicopathological characteristics of two study cohorts and discrimination of type-1 activity profiles

	Cohort IRB#011-030				Cohort TCGA			
Characteristics	Total	HiHi	Non-HiHi	Test	Total	HiHi	Non-HiHi	Test
Tumors (n)	43 (100%)	16 (100%)	27 (100%)		221 (100%)	85 (100%)	136 (100%)	
Age (y; $\bar{x} \pm SD$)	61.51 ± 14.02	57.44 ± 13.29	63.93 ± 14.12	NS	69.42 ± 11.49	69.72 ± 11.28	69.23 ± 11.67	NS
Gender								
Male	29 (67%)	10 (63%)	18 (67%)	NS	116 (52%)	45 (53%)	71 (52%)	NS
Female	14 (33%)	6 (37%)	9 (33%)		105 (48%)	40 (47%)	65 (48%)	
Primary tumor								
Colon	24 (56%)	9 (56%)	15 (56%)	NS	156 (71%)	65 (76%)	91 (67%)	NS
Rectum	19 (44%)	7 (44%)	12 (44%)		65 (29%)	20 (24%)	45 (33%)	
Depth of invasion								
pT0/pT1/pT2	15 (35%)	6 (37%)	9 (33%)	NS	54 (24%)	22 (26%)	32 (24%)	NS
pT3/pT4	28 (65%)	10 (63%)	18 (67%)		167 (76%)	63 (74%)	104 (76%)	
LN metastasis								
NX	3 (7%)	0 (0%)	2 (7%)		0 (0%)	0 (0%)	0 (0%)	
N0	24 (56%)	13 (81%)	12 (45%)	0.050	134 (61%)	61 (72%)	73 (54%)	0.011
N1-3	16 (37%)	3 (19%)	13 (48%)		87 (39%)	24 (28%)	63 (46%)	
Organ Metastasis								
MX	6 (14%)	1 (6%)	5 (18%)		1 (< 1%)	1 (1%)	0 (0%)	
M0	33 (77%)	15 (94%)	18 (67%)	0.131	185 (84%)	77 (91%)	108 (79%)	0.022
M1-2	4 (9%)	0 (0%)	4 (15%)		35 (16%)	7 (8%)	28 (21%)	
								$P < 0.05$ is significant

T, depth of invasion; N, lymph node metastasis; M, distant organ metastasis; NS, not significant; $\bar{x}$, mean; *SD*, standard deviation

Contingency table was analyzed using Fisher's exact test

In conclusion, clinicopathological data from two separate cohorts of CRC patients determined that patients with increased type-1 activity in the TMEs of their tumors have less advanced disease than those without. These data also determined that depth of invasion is not correlated with relatively high type-1 activity, nor is the location of the tumor, or age and gender of the patient. These data, however, cannot determine whether patients with tumors with relatively high type-1 activity have any survival advantage over patients without. These data will be interesting to analyze at the 5-year follow-up period sometime after October 2018.

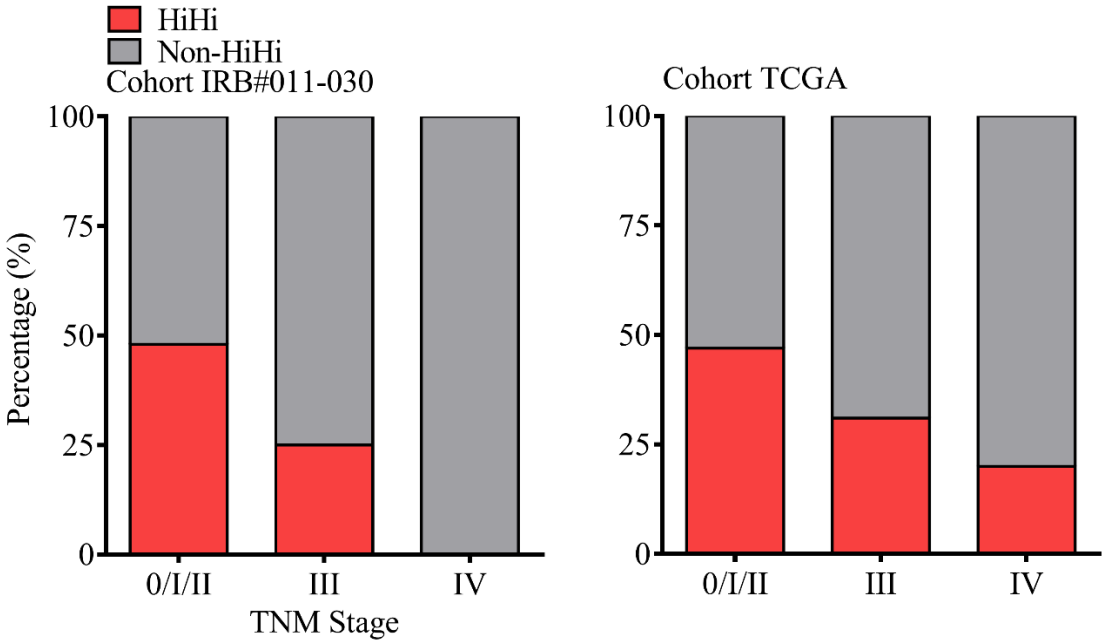

Figure 28. Illustration of linear trend in proportions of *IFNG-TBX21* profiles among TNM stages

Frequency of Type-1-Associated Immune cell Infiltration and Secretion of CTL Targeting Chemokines Are Bimodally Distributed Among CRCs

Flow cytometry was performed to confirm the increased abundance of CTLs and T_H1 cells in HiHi tumors and confirm that CTLs are engaged in cytotoxic activity. Also

investigated was a similar increase of IL-12 expressing immune cells in colorectal TMEs. To strengthen and expand the findings of this investigation, the detection of T-cells that are involved with the type-1 response, as well as immune cells that polarize those T-cells towards the type-1 response, were performed simultaneously. Immune cell populations were identified as described in Chapter Three.

Identifying and Counting T-cells

The gating strategy that identifying functionally active CTLs and T_H1 cells is described here. Positive gates for fluorescent populations were determined using isotype controls. Only live singlet cells were counted for analysis, and foreword scatter (FS) and side scatter (SS) were used to identify lymphocytes, which are smaller and non-granulated cells (Figure 29). T-cells were identified from the lymphocyte population as the $CD45^+$ and $CD3^+$ cells (Figure 30). From the $CD45^+CD3^+$ double positive T-cell population, Helper T-cells were identified as $CD4^+$ and $CD8^-$, and effector T-cells were identified as $CD4^-$ $CD8^+$ (Figure 31).

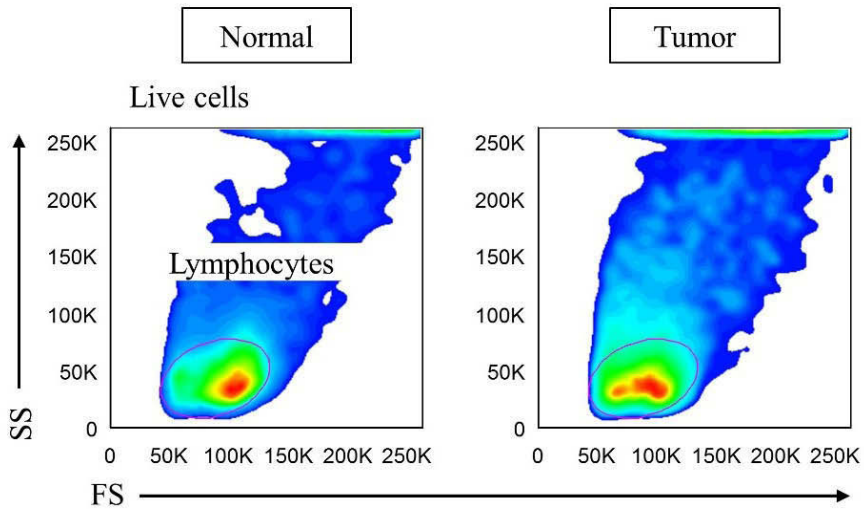

Figure 29. Gating strategy used to identify from healthy normal mucosa and tumor tissue

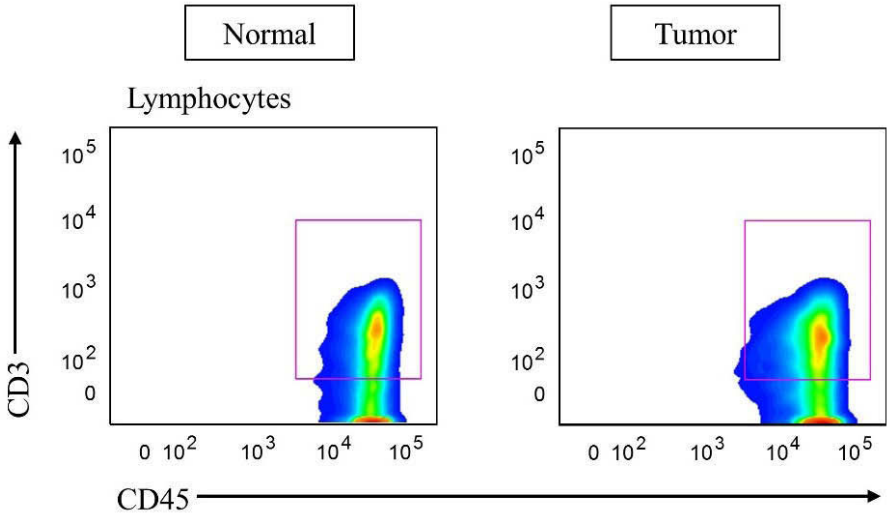

Figure 30. Gating strategy used to identify T-cells from healthy normal mucosa and tumor tissue

Finally, type-1 polarized helper T-cells were identified by gating for IFN-γ positivity; these cells represented the IFN-γ^+ T_H1 cell population (Figure 32), and the cytotoxic mediator producing $CD4^-CD8^+$ T-cells were identified by gating for GzmB positivity, these cells represented the $GzmB^+$ CTL population (Figure 32). Isotype controls were used to set the positive threshold. The frequency of $CD45^+CD3^+$ double T-cells was increased in the HiHi tumors, however no difference was detected between healthy normal mucosa and the non-HiHi tumors. As expected IFN-γ^+ T_H1 cells and $GzmB^+$ CTLs were increased in HiHi tumors, and no difference was detected between healthy normal mucosa and non-HiHi tumors (normal, n = 15; HiHi, n = 5; and non-HiHi, n = 11) (Figure 33). These data concluded that colorectal tumors with relatively high type-1 activity are more infiltrated by anti-tumor T-cells than colorectal tumors without relatively high type-1 activity. Two-tailed Student's t-test was performed using the total number of cell per 1000 cells. Error bars represent SEM of grouped tissues. *, $P < 0.05$.

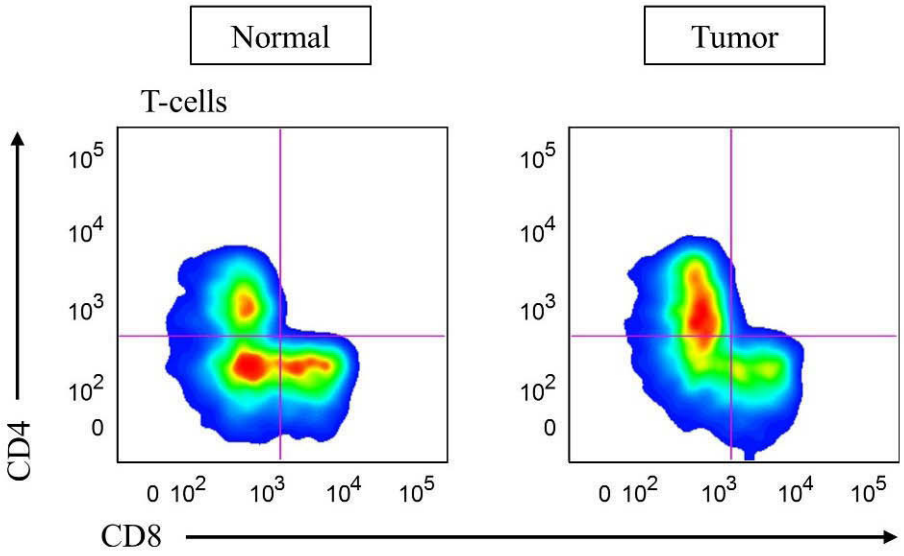

Figure 31. Gating strategy used to identify $CD4^+CD8^-$ T-cells and $CD4^-CD8^+$ T-cells from healthy normal mucosa and tumor tissue

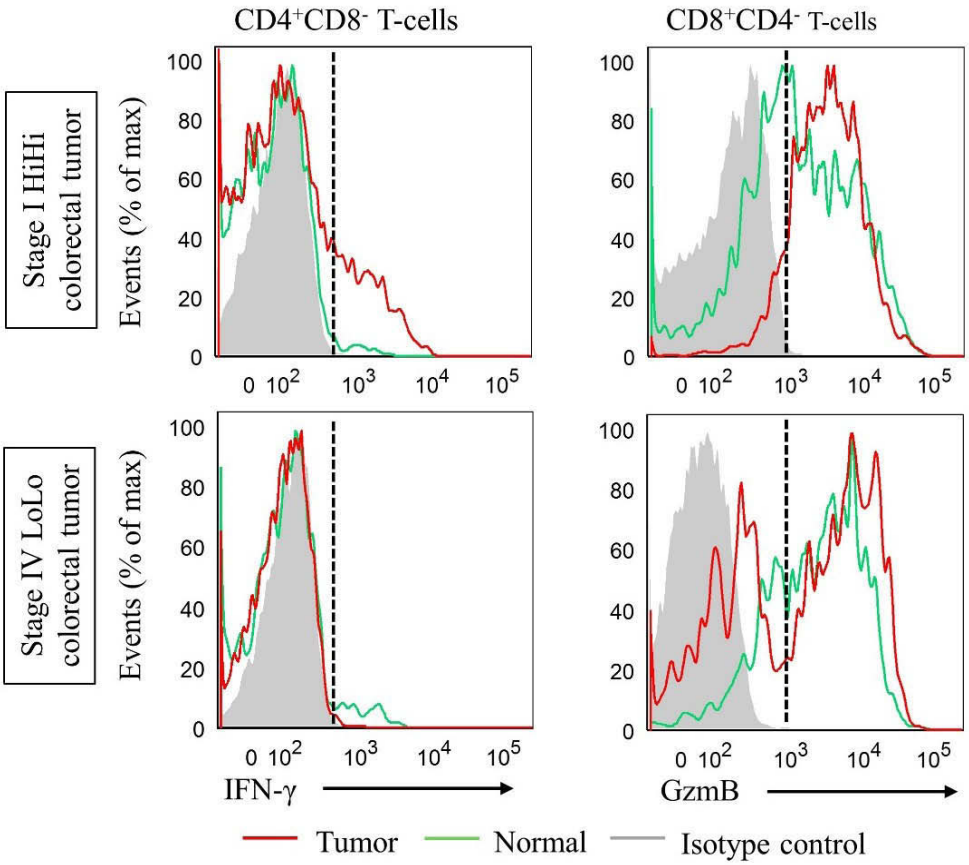

Figure 32. Comparison of proportions of IFN-γ^+ helper T-cells cells and $GzmB^+$ CTLs between a stage I HiHi profiled tumor and a stage IV LoLo profiled tumor

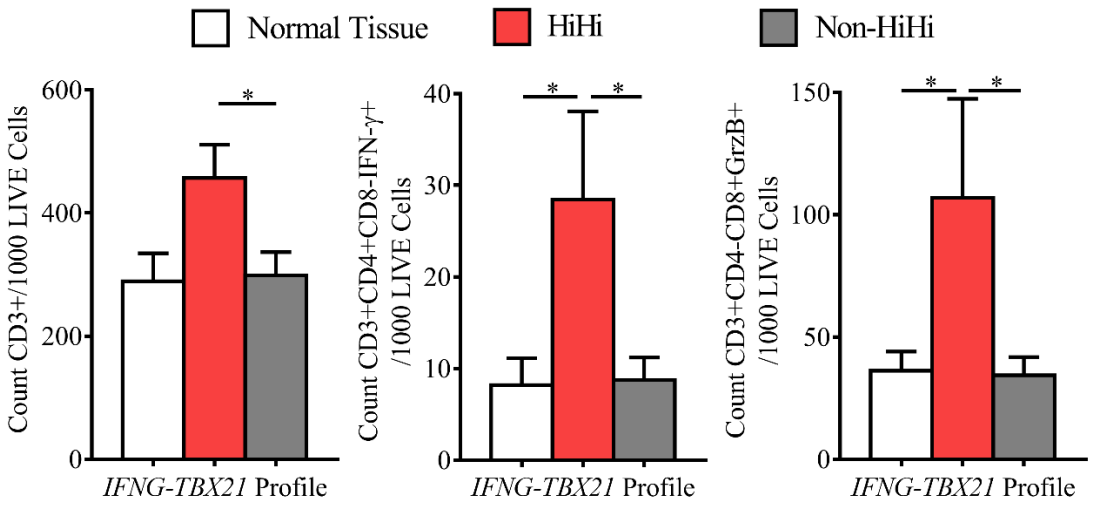

Figure 33. Average counts of T-cells, IFN-γ^+ T_H1 cells, and $GzmB^+$ CTLs determined via flow cytometry

Identifying and Counting Non-Lymphoid IL-12 Expressing $CD14^+$ Immune Cells

T-cells directed towards anti-tumor activity were previously shown to be more frequent in colorectal TMEs with relatively high type-1 activity. This led the investigation to question whether other immune cells that secrete type-1 polarizing IL-12 were also infiltrating colorectal TMEs with relatively high type-1 activity. Disaggregated single-cell suspensions of live cells from colorectal tumors were treated similarly as those for T-cell detection, but stained only for LIVE/DEAD® viability marker, CD45, CD14, and IL-12 immune cell makers.

The gating strategy for identifying IL-12 expressing $CD45^+CD14^+$ double positive cells is described here. Positive gates for fluorescent populations were determined using isotype controls; only live singlet cells were counted for analysis and foreword scatter (FS) and side scatter (SS) were used to identify immune cells. Lymphocytes were excluded while larger granulated cells were included (Figure 34). $CD45^+CD14^+$ double positive cells were identified form the non-lymphocyte population (Figure 35).

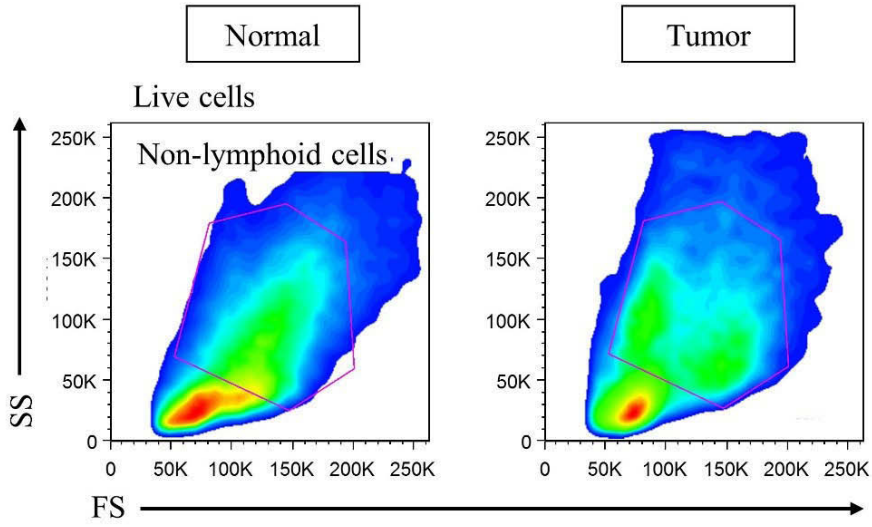

Figure 34. Gating strategy used to identify non-lymphoid cells from healthy normal mucosa and tumor tissue

Finally, from this double positive population of IL-12^{+} immune cells was detected by setting the threshold at the extreme right end of the isotype control peak (Figure 36). CD45^{+}CD14^{+} non-lymphoid cells were not increased in HiHi tumors, and no difference was detected between healthy normal mucosa and non-HiHi tumors.

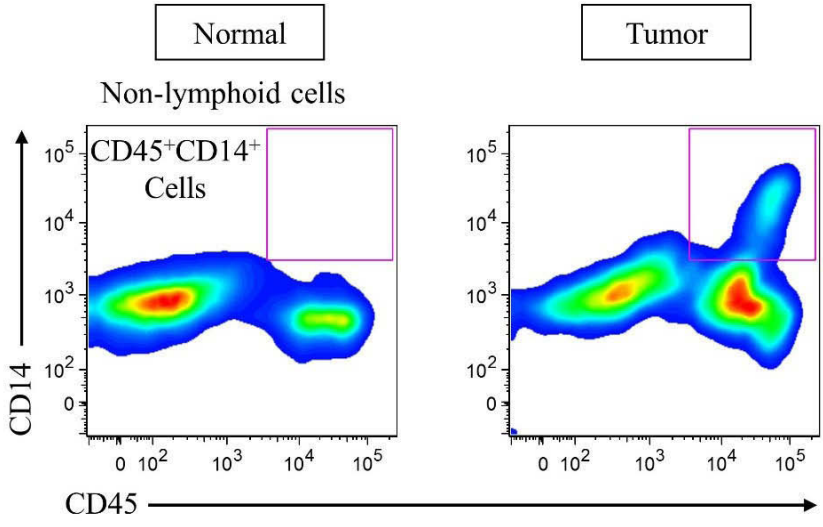

Figure 35. Gating strategy used to identify CD45^{+}CD14^{+} double positive cells from healthy normal mucosa and tumor tissue

As expected frequency of IL-12$^+$ CD45$^+$CD14$^+$ non-lymphoid cells were increased in HiHi colorectal tumors when compared to both healthy normal mucosa and non-HiHi tumors (normal, n = 15; HiHi, n = 5; and non-HiHi, n = 11) (Figure 37). These data concluded that colorectal TMEs with relatively high type-1 activity are more infiltrated by immune cells that express the type-1 polarizing cytokine IL-12 than colorectal tumors without relatively high type-1 activity. Two-tailed Student's t-test was performed using the total number of cell per 1000 cells. Error bars represent SEM of grouped tissues. *, $P < 0.05$ and ***, $P < 0.001$.

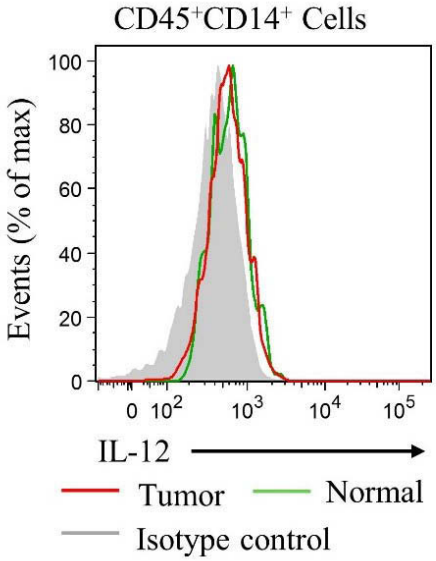

Figure 36. Gating strategy used to identify IL-12$^+$ non-lymphoid cells from healthy normal mucosa and tumor tissue

Secretion of CTL Targeting Chemokines

To determine whether the chemokines most associated with DFS in CRC (Mlecnik et al., 2010) are increasingly secreted from TMEs with relatively high type-1 activity and CTL infiltration, supernatants from CRC and healthy normal mucosa were assayed for

secreted chemokines using the EMD Millipore's MILLIPLEX Human Cytokine/Chemokine Luminex immunoassay.

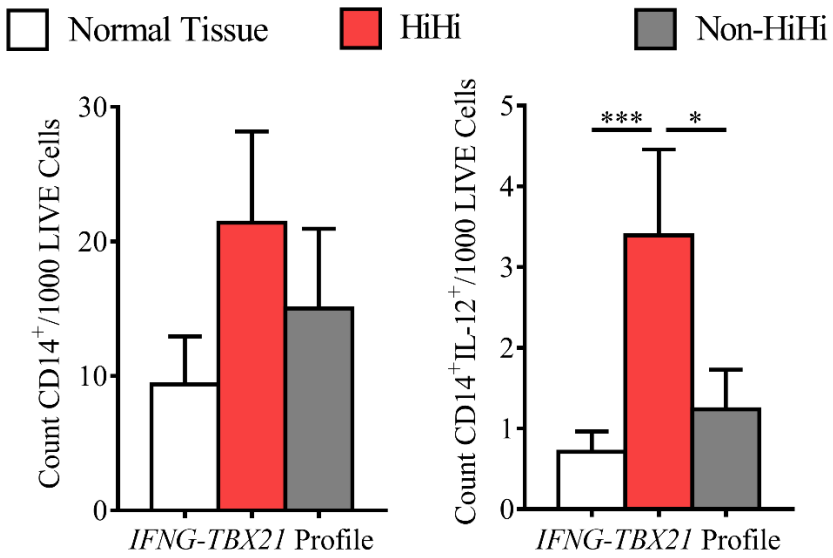

Figure 37. Average counts of $CD45^+CD14^+$ immune cells and IL-12^+ $CD45^+CD14^+$ immune cells determined via flow cytometry

Chemokine data were separated into either the HiHi or the non-HiHi profiles and compared to healthy normal mucosa. Fold changes (FCs) and *P* values were calculated between healthy normal mucosa and tumor tissue. A FC of > 2 and *P* value ≤ 0.05 was set as the threshold for increased secretion. CXCL1 was included as a negative control because, to the knowledge of the investigator, no literature has suggested that it is strongly expressed during the type-1 response in colorectal tumors. As expected both CCL5 and CXCL10 were increasingly secreted from HiHi tumors when compared to healthy normal mucosa, however were not strongly secreted from non-HiHi tumors (normal, n = 24; HiHi, n = 13; and non-HiHi, n = 20) (Figure 38). CXCL1 secretion was not increased from either group, and interestingly, CCL2, CX3CL1, and CCL11 were not strongly secreted from the HiHi CRCs (Figure 38). Two-tailed student's t-test was performed using concentrations of

chemokines. Dashed lines represent thresholds for increased secretion ($P < 0.05$, and FC > 2). These data suggest that secretion of two chemokines identified as main contributors to T_H1 cell and CTL chemoattraction is increased from TMEs with relatively high type-1 activity while not from TMEs without relatively high type-1 activity. Next, it was reasoned that if CCL5 and CXCL10 secretion is increased in CRCs with relatively high type-1 activity, then abundance of anti-tumor T-cells should correlate with secretion of both chemokines. Abundance of T-cells in CRCs was determined earlier via flow cytometry and compared to chemokine secretion. As expected, a positive correlation was detected between CTL abundance and CCL5 and CXCL10 (Figure 39 and Table 17). CX3CL1 was included as a negative control, and healthy normal mucosa was included as a comparison. CCL5 and CXCL10 demonstrated a strong correlation with $GzmB^+$ CTLs in CRCs only (normal, n = 15 and tumor, n = 16) ($R^2 = 0.703$ and 0.879, respectively (Figure 39 and Table 17). $P < 0.05$ is significant for trend. However, IFN-γ^+ T_H1 cells did not appear to follow the same pattern for any cytokine (Figure 40 and Table 18).

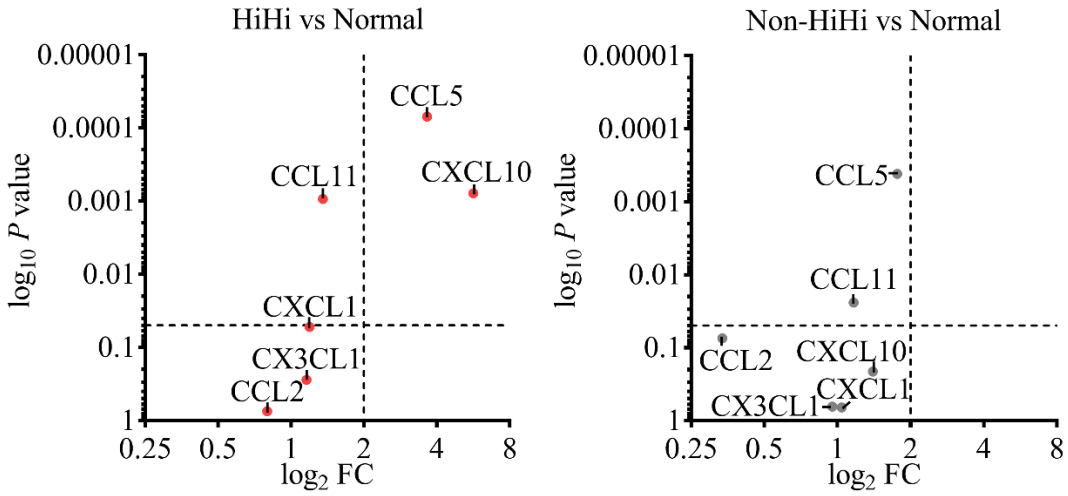

Figure 38. Dot plots of *P* values and fold changes (FCs) of six chemokines secreted from freshly resected CRCs and healthy normal mucosa

Table 17. R^2 and P values chemokines versus frequency of GzmB$^+$ CTLs

R^2 (P)	CXCL10	CCL5	CX3CL1
Tumor	0.879 (< 0.001)	0.703 (< 0.001)	0.057 (0.372)
Normal	0.004 (0.820)	0.023 (0.592)	0.052 (0.414)
			$P < 0.05$ is significant

Table 18. R^2 and P values chemokines versus frequency of IFN-γ T_H1 cells

R^2 (P)	CXCL10	CCL5	CX3CL1
Tumor	0.035 (0.488)	0.010 (0.711)	0.018 (0.689)
Normal	0.046 (0.445)	0.038 (0.488)	0.0469 (0.438)
			$P < 0.05$ is significant

These data suggest that as the frequency of CTL infiltration increases, the secretion of CCL5 and CXCL10 increases as well. This trend was not repeated in healthy normal mucosa which were used as a comparison. These data suggest that this pattern of T-cell infiltration is not repeated in all tissues, but may be a feature of most solid tumors from other parts of the body or other tissues under inflammatory conditions and at the center of an immunological attack.

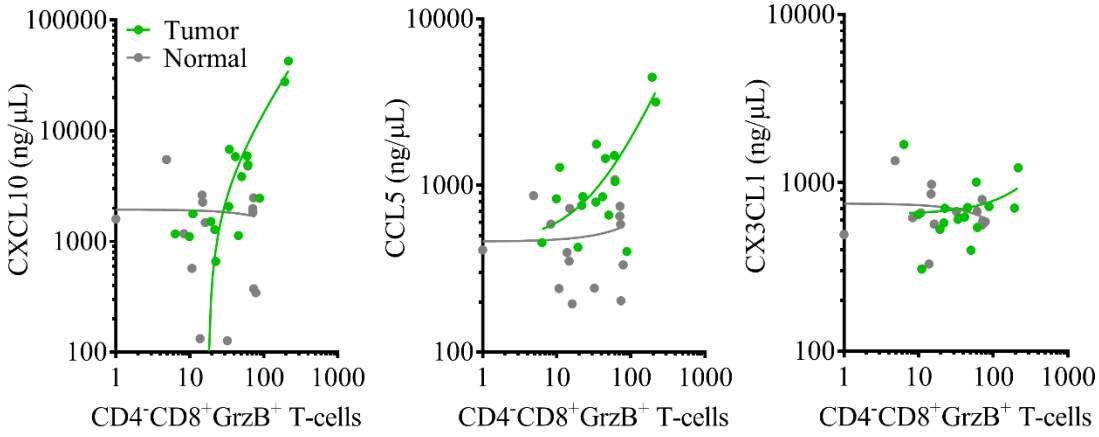

Figure 39. Dot plots of chemokine concentrations versus frequency of GzmB$^+$ CTL

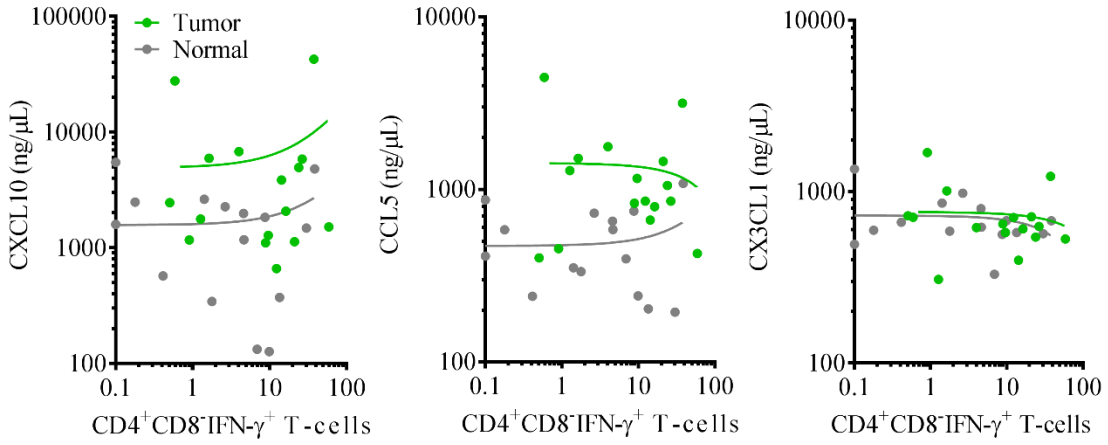

Figure 40. Dot plots of chemokine concentrations versus frequency of IFN-γ^+ T_H1 cells

In conclusion, these data demonstrated that colorectal tumors with relatively high type-1 activity have a higher frequency of infiltrating immune cells that are involved in the T-cell directed anti-tumor response, and these tumors more strongly secreted chemokines that target anti-tumor T-cells when compared to tumor with relatively lower type-1 activity. These data, however, do not prove whether CXCL10 and CCL5 are actively attracting these cells, nor provide any possible mechanism for the bimodality of the tumor population.

Type-1 T-cell-Targeting Chemokines Are Expressed in MSI colorectal tumors

Patients with MSI tumors have a more favorable prognosis when compared to those with MSS tumors (Popat et al., 2005; Laghi and Malesci, 2012) as suggested by low occurrence of lymph node and distant organ metastasis (Buckowitz et al., 2005; de Miranda et al., 2012) and significant increase of lymphocyte infiltration (Dolcetti et al., 1999; Michel et al., 2008; Drescher et al., 2009; Tougeron et al., 2013). Since MSI tumors have a propensity to be highly infiltrated by immune cells, MSI may be a mechanism for increased type-1 activity in a portion of colorectal TMEs and may explain the bimodality

of the type-1 response. Forty-three colorectal tumors from the IRB#011-030 cohort yielded sufficient high quality DNA for MSI screening. Seven tumors (16.3%) were identified as having one or more markers fall outside the QMVR. This percentage was consistent with a previously study (Boland et al., 1998). Fold changes of *IFNG* and *TBX21* and all six chemokines that were previously identified by Mlecnik and colleagues (2010) as associated with DFS were calculated between MSI and MSS tumors. As expected, MSI tumors showed a trend for increased expression of *IFNG*, *TBX21*, *CXCL10*, and *CCL5*. However, these changes were not significant (Figure 41). Interestingly *CXCL9* did not follow the same trend. These data suggested that type-1 activity, and the potential to chemoattract type-1 T-cells, is increased in MSI tumors when compared to MSS tumors.

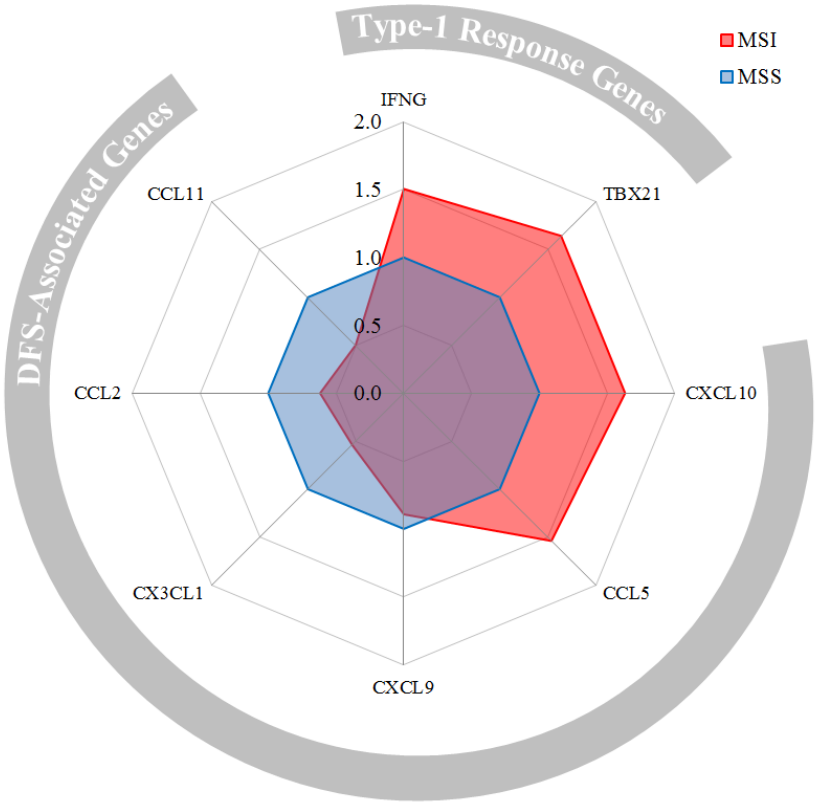

Figure 41. Radar plot of transcription FC of *IFNG*, *TBX21* and DFS-associated chemokines between MSI and MSS tumors

Next, this investigation hypothesized that tumors with different degrees of MMR-deficiency expressed *IFNG*, *TBX21*, *CXCL10*, and *CCL5* differently. If correct, this finding would suggest that tumors with high degree of microsatellite instability –those having two or more marker lengths fall outside the QMVR (MSI-H)– may be more immunogenic that tumors with low (MSI-L) or no microsatellite instability (MSS). Due to the small size of the IRB#011-030 cohort, only three tumors were identified as MSI-H and therefore were too few to pool and analyze. However, the TCGA cohort contained enough MSI-H tumors (n = 27) to test this hypothesis. MSI-H tumors from the TCGA cohort did express *IFNG* and *TBX21* higher than both MSI-L and MSS tumors, while MSI-L tumors were downregulated when compared to MSS (Figure 42). Both *CXCL10* and *TBX21* were also expressed higher than both MSI-L and MSS tumors (Figure 43). Two-tailed student's t-test was performed using $\log_2$ scale of relative transcription of all four genes. Error bars represent SEM of grouped tissues. *, $P < 0.05$ and ***, $P < 0.001$.

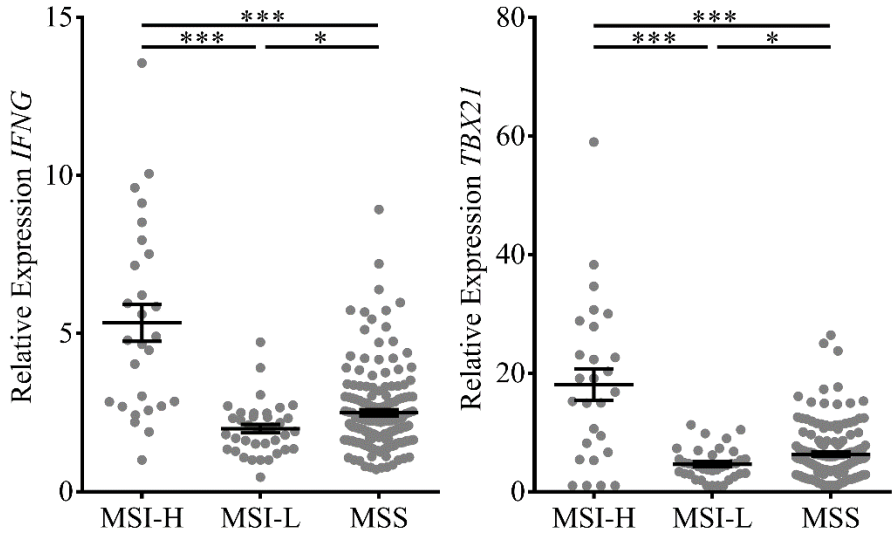

Figure 42. *IFNG* and *TBX21* mRNA expression in colorectal tumors among varying categories of MMR proficiency

These data suggest that MSI-H colorectal TMEs are skewed more towards the type-1 response when compared to MSI-L and MSS tumors. To confirm the connection between the type-1 response and MSI, tumors from both cohorts were sorted into contingency tables to determine whether the distribution of HiHi and non-HiHi profiled tumors were skewed towards any degree of MMR proficiency. Fisher's exact test revealed that HiHi profiled tumors were skewed more towards MSI-H when compared to the non-HiHi profile (Table 19). These data confirmed that MSI-H tumors are eliciting a stronger type-1 response that MSI-L and MSS tumors. *, $P < 0.05$ and ***, $P < 0.001$.

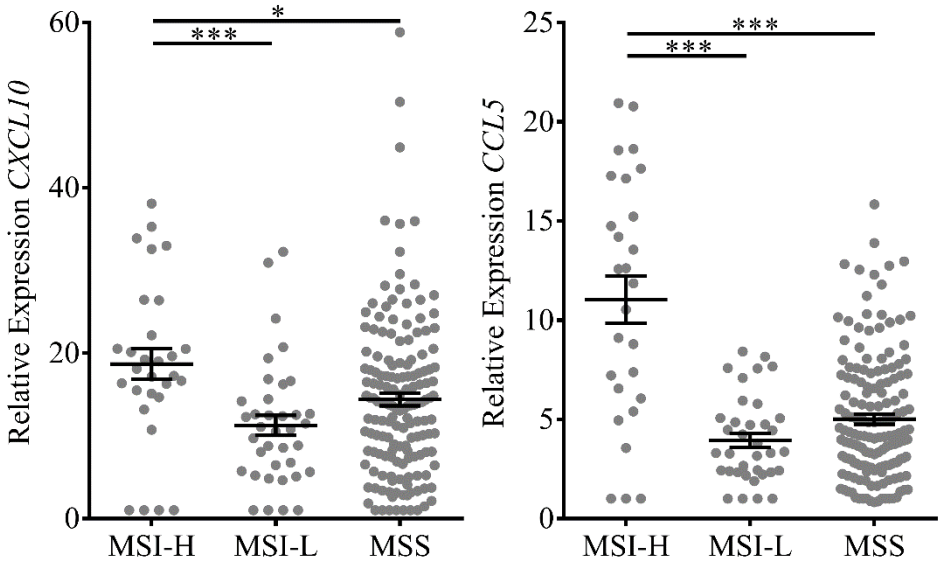

Figure 43. *CXCL10* and *CCL5* mRNA expression in colorectal tumors among varying categories of MMR proficiency

Microsatellite instability and the CpG methylator phenotype often coincide within same tumor genome. The connection between these phenotypes is explained by the ability of the *MLH1* promoter to become hypermethylated in what is called CIMP-associated methylation of *MLH1* (Weisenberger et al., 2006). Therefore this investigation made the

effort to screen the IRB#011-030 cohort for CIMP. Unfortunately due to the small sample size, only four CIMP tumors were identified, and only one was identified as MSI. Also, TCGA did not provide methylation data. Therefore, no further analysis could be performed to correlate immune activity with this variety of epigenetic alteration.

Table 19. MMR fidelity and discrimination of *IFNG-TBX21* profiles

MMR Proficiency	Total	HiHi	Non-HiHi	Test
	Cohort IRB# 011-030			
Tumors (n)	43 (100%)	16 (100%)	27 (100%)	
Indeterminate	0 (0%)	0 (0%)	0 (0%)	
MSI-H	3 (7%)	1 (6%)	2 (7%)	NS
MSI-L/MSS	40 (93%)	15 (94%)	25 (93%)	
	Cohort TCGA			
Tumors (n)	221 (100%)	85 (100%)	136 (100%)	
Indeterminate	2 (1%)	1 (1%)	1 (< 1%)	
MSI-H	27 (12%)	22 (26%)	5 (4%)	< 0.001
MSI-L/MSS	192 (87%)	62 (73%)	130 (96%)	
				$P < 0.05$ is significant

Abbreviation: NS, not significant

Enhanced secretion of IFN-γ, CCL5, and CXCL10 from MSI-H tumors was not tested due to the low number of MSI-H tumor collected in this investigation. In conclusion however, colorectal tumors with the dysfunctional MMR phenotype are skewed towards type-1 T-cell activity as shown with both cohorts. The TCGA cohort identified that tumors with a high degree of microsatellite instability transcribed chemokines that target CXCR3 and CCR5 expressing T-cells more highly than those that were MSI-L or MMR proficient tumors. However, this investigation failed to determine whether the MSI-H associated increase of type-1 activity was directed by the hypermethylation of the *MLH1* promoter.

CHAPTER FIVE

Discussion

This investigation applied an integrated approach to gain a better understanding of the immune responses within colorectal tumors. An array of techniques were utilized to investigate the expression patterns of immune-related biomarkers at the cellular and molecular level with the goal of correlating frequencies of immunological infiltrates, chemokine secretion, genomic instability, and clinical prognosis. The difficulty of deriving concrete conclusions from the data generated in this investigation dwelled in the heterogeneity among the population of human tumors collected. However, in respect to the wide range of type-1 activity observed across TMEs, and considering all the data collected, this investigation was able to conclude that CRC is a disease that is bimodally distributed in respect to varying degrees of immunosurveillance.

The pattern of T-cell activity in colorectal tumors has been the focus of much research. Type-1 T-cell activity has been identified as important for prolonged patient survival (Pages et al., 2005; Pages et al., 2010; Ong et al., 2012) where CTLs are one of the main effector cells of the anti-tumor response that may provide protection (Pages et al., 2010). The first experiment in this investigation utilized IHC to demonstrate the existence of $CD8^+$ T-cells in colorectal tumors, demonstrate how IHC studies are normally performed, and served as a prelude to the meta-analysis, which collected peer-reviewed studies that utilized a similar procedure. The IHC experiment was limited to one tumor, so no statistics or cell counts were recorded.

The meta-analysis collected and combined peer-reviewed studies to fortify the correlation between survival trends and $CD8^+$ T-cells infiltration. In summary, the meta-analysis confirmed that higher $CD8^+$ T-cell infiltration is predictive of prolonged cancer-specific, disease-free, and overall survival in CRC by combining many studies into a single cohort. These findings may be extrapolated to other diseases. The impact of $CD8^+$ T-cell infiltration on survival may also be reflected by cancers from other parts of the body (Palucka et al., 2007; Pages et al., 2010; Palucka and Banchereau, 2012). However, this meta-analysis did not determine whether infiltrating CTLs were inhibiting tumor progression, or if these cells were simply bystanders in the early stages of cancer where their impact is quickly diminished by either becoming outnumbered by suppressor cells or becoming unresponsive as tumor cells grow out and overwhelm surrounding tissues. Questions still remains: Why does the TME demonstrate a relative decrease in type-1 activity as the cancer spreads to other parts of the body? Why are NK-cells not infiltrating colorectal tumors? What is unique about CRC that makes the tumors deprived of NK-cells? And, why is infiltration of NK-cells an indicator of prolonged DFS for other cancers and not CRC (Marcus et al., 2014)? The answers to these questions will have profound impact on the way practitioners attempt to counter the progression of this disease in the future.

The next section of this investigation sought to survey anti-tumor immune activity within the context of TNM tumor stages as a means to underpin the existing perception of altered immunosurveillance in advanced stages of CRC. Drawing inspiration from the meta-analysis, this investigation observed a decrease in the anti-tumor activity as the disease progressed. Being impossible and highly unethical to observe CRC progression in

patients without first treating them, this investigation required a consortium that included the department of Pathology and gastrointestinal surgeons at BUMC in Dallas to collect TNM staged tumor and colonic samples from a cohort of patients. Interestingly, magnitude of type-1 activity –measured by transcriptional expression of *TBX21* and secretion of IFN-γ– in CRC TMEs decreased as prognosis became more negative. These results are consistent with those of Pagès and colleagues (2005) who reported that patients whose tumors more strongly expressed CTL and type-1 genes demonstrated lower rates of relapse and VELIPI (Pages et al., 2005). Of noteworthiness, type-1 activity was not altered as tumor invasiveness (T) advanced through the muscularis propria or other organs (T3 - T4). No explanation for this can be given at this time, other than that invasiveness and metastasis are regulated by unrelated mechanisms. Also, no change in type-2 activity could be determined by measuring *GATA3* transcription and secretion of IL-4, IL-5, and IL-13. The data from this aim were consistent with other studies that suggest anti-tumor T-cell activity prolongs patient survival by inhibiting metastasis (Pages et al., 2005; Galon et al., 2007; Pages et al., 2008; Pages et al., 2009; Pages et al., 2010; Galon et al., 2014).

The inspiration to profile the type-1 response to two biomarkers, *IFNG* and *TBX21*, was derived from the work done by Galon and Pagès who advocate for a similar assessment of the immunological state of colorectal tumors. Galon and Pagès champion a growing movement within the gastrointestinal cancer research community to incorporate an 'immunoscore' that compliments current practices of assessing disease prognosis (Galon et al., 2014; Anitei et al., 2014). Their novel strategy shows that anti-tumor T-cell activity can be evaluated through IHC by determining the density of $CD8^+$ and $CD3^+$ cells in both the CT and the IM of colorectal tumors (Anitei et al., 2014; Galon et al., 2014). The

objectives of these two researcher is consistent with that of the GI Cancer Research/Epigenetics and Cancer Prevention Laboratory at BUMC, Dallas: to identify biomarkers that either predict cancer onset or represent the current status of the disease in terms of lethality to the patient. This was done in this investigation unbiasedly by assessing tumors by the expression of *IFNG* and *TBX21*. This investigation concluded that colorectal tumors with relatively high expedition of type-1 response gene correlated with lower occurrence of metastasis in mesenteric lymph nodes and/or distant organs. These findings do not counter those of Galon and Pagès, but reinforces their ideas by assessing type-1 activity by measuring two genes that reflect the same immune response. The bimodal pattern identified by this investigation demonstrated that high co-expression of *TBX21* and *IFNG* is predictive of a more favorable outcome. Colorectal tumors that were profiled as high expressers of these genes shared similar expression of multiple CTL related genes, and where demonstrated to more strongly express a biomolecular network of chemokine genes that were associated with prolonged DFS.

The next question logically progressed to the expression of microRNAs that may be involved with $CD8^+$ T-cell activities and differentiation. Both *miR-155* and *miR-21* were found to be expressed higher in HiHi tumors when compared to non-HiHi tumors. This pattern of *miR-21* expression is consistent with earlier discoveries made by the GI Cancer Research/Epigenetic and Cancer Prevention Laboratory, which demonstrated that preoperative serum levels of this microRNA were elevated in patients with adenomas and colorectal tumors, and serum *miR-21* expression dropped in these patients after curative surgery. These findings suggest that the tumor itself is releasing microRNAs into the extratumoral environment and therefore makes this microRNA a potential biomarkers for

predicting prognosis (Toiyama et al., 2013). The expression pattern of *miR-155* reported in this investigation gives promise to future investigations that screen other microRNAs in patients' serum for biomarker that predict prognosis and whether a patient's tumor is the center of an anti-tumor immune response. These observations bring about other questions: Are colorectal tumors with relatively low type-1 activity expressing other chemokines that attract immune cells that either suppress CTL activity or facilitate neoplastic growth and angiogenesis? Are tumors with relatively high type-1 activity expressing chemokines that attract T_H17 cells and contribute to inflammation? And, can this strategy be adapted to identify other modes of bimodality that pertain to other arms of the immune system?

Colorectal tumors with relatively high co-expression of *TBX21* and *IFNG* were confirmed to be more infiltrated by IFN-γ^+ T_H1 and $GzmB^+$ CTLs than tumors with relatively low type-1 response and healthy normal mucosa. This was confirmed using flow cytometric analysis which counted the number of T-cells that potentially supplied IFN-γ to the tumor microenvironment and T-cell that were functionally capable of targeting tumors cells for apoptosis. These data also reflect the major findings of Galon and Pagès pertaining to T-cell infiltration and prolonged patient survival (Pages et al., 2005; Galon et al., 2006). Flow cytometry is a powerful tool, yet is limited to the number of parameters that can be assessed. Its customizability allows it to superbly assess a few selected cell types by a finite number of parameters, however fails when used to assess many cell types at once. Therefore this investigation focused towards only assessing T_H1 cells and CTLs, and to a smaller degree non-lymphoid immune cells. Its conclusions could have been stronger if other immune cells that facilitate the activation and programming of anti-tumor T-cells were fully assessed.

Non-lymphoid immune cells were investigated for IL-12 expression. IL-12 expressing $CD14^+$ immune cells were found to be increased in TMEs that have relatively high type-1 activity. These data are supported by several studies. Ong and colleagues recognized that inflammatory macrophages can infiltrate colorectal tumors and encourage type-1 T-cell activity by secreting T-cell-attracting chemokines into the TME. By isolating and culturing $CD68^+$ and $CD14^+$ macrophages this group found that when coupled with T-cells, macrophages exert tumor suppression (Ong et al., 2012). Bauer and colleagues used IHC to report and increase of $CD163^+$ macrophages and $CD208^+$ mature DCs in MSI colorectal tumors (Bauer et al., 2011). Heusinkveld and colleagues generated M2 polarized $CD14^+$ macrophages *in vitro* using IL-6 and granulocyte macrophage colony-stimulating factor and used IFN-γ to switch these cells to activated M1-like macrophages that expressed high levels IL-12 and low amounts of IL-10 (Heusinkveld and van der Burg, 2011; Heusinkveld et al., 2011). Sconocchia and colleagues reported that high infiltration of $CD16^+$ myeloid cells in colorectal tumors, determined by IHC, was correlated with prolonged survival (Sconocchia et al., 2011). However, these studies are contradicted by strong evidence that suggests solid tumors can be infiltrated by M2 (inflammatory-inducing macrophages) which contribute to tumorigenesis and inhibit anti-tumor activity by promoting immune tolerance (Mantovani and Sica, 2010). This current investigation would have been strengthened by detecting infiltrating macrophages and DCs to determine whether these cells were secreting type-1 polarizing cytokines, such as IL-12 and TNF as tumor progress through TNM stages (Palucka et al., 2007; Palucka and Banchereau, 2012). This would suggest that T-cell programming does occur in the TME and that it can be manipulated for therapeutic use. Future investigations could use TAM-associated markers

such as CD16, CD14, CD163, IL-12, IL-10 to further discover therapeutic strategies in which exploit the T_H1–macrophage axis in antitumor immunity.

To complete the primary aim of the investigation, the secretion of immune mediators that control T-cell infiltration needed to be studied. This was done by introducing a novel multiplex immunoassay that quantified the secretion of these cytokines and elucidated the dynamic range of immunological activity in colorectal tumors beyond transcriptional profiling and low dimensional IHC. Also, completion of this aim was only possible by studying a unique set of samples, which contained live cells immediately excised from patients' colons and rectums. This study, to the knowledge of the investigator, is the first to demonstrate the enhanced secretion of CXCL10 and CCL5 from colorectal TMEs with relatively high type-1 activity. Tumors with the highest co-expression of *IFNG* and *TBX21* secreted these two type-1 effector T-cell attracting chemokines more strongly than healthy normal mucosa, and were not secreted differently between tumors that were not highly expressing both *IFNG* and *TBX21* genes and healthy normal mucosa. As expected concentrations of these two chemokines were positively correlated with the frequency of infiltrating $GzmB^+$ CTLs. These data are essentially consistent with those of Mlecnik and colleagues (Mlecnik et al., 2010) where these two chemokines are associated with anti-tumor activity; however CCL2, CCL11, and CX3CL1 were not strongly secreted from TMEs with relatively high type-1 activity. Interestingly, no correlation was detected between CXCL10 and CCL5 secretion and IFN-γ^+ T_H1 cell frequency. This may be due to the low number of IFN-γ^+ cells detected that is beyond the capacity of the flow cytometer to produce reliable data. The low numbers could be explained as a physiological fact of CRC TMEs, or low affinity of the antibody used to detect IFN-γ. These findings, however,

only partial highlight the mechanisms behind CTL infiltration in CRC. Questions still remain pertaining to the source of these chemokines. These data fail to demonstrate whether these two chemokines are solely responsible for CTL infiltration, or if other chemokines can also facilitate this process. Also, these data fail to identify which cells (immune, epithelia, or both) are the main source of these chemokines. Better foresight would have allowed the investigator to incorporate other customized flow cytometric experiments that could have assessed chemokine production in different cell types.

One cannot assume that the bimodal distribution of type-1 activity among colorectal tumors is random, therefore a possible catalyst for this activity was investigated. The leading theory that explains why some tumors are more infiltrated by CTLs when compared to others, as described in detail in Chapter Two, is through the presentation of neo-antigens generated from frameshifts in coding regions containing microsatellites (Schwitalle et al., 2004). MMR-deficient cells, in theory, can catalyze the type-1 response through the programming of anti-tumor cells by APCs either in the TME or draining lymph nodes. Therefore, this investigation focused to compare different states of microsatellite instability across colorectal tumors with different type-1 biomarker profiles. Considering the type-1 response as part of an inflammatory cascade, these results are consistent with those of a large microarray study, which identified an 'inflammatory' subset of CRCs "marked by comparatively high expression of chemokines and interferon-related genes" and consisting of 94% MSI tumors (Sadanandam et al., 2013). Reinforcing these findings, the expression of *IFNG* and *TBX21* were increased in MSI-H colorectal tumors of the TCGA cohort. This pattern was repeated with the expression of two chemokines that target CXCR3 and CCR5 expressing T-cells. However, this investigation primarily focused on chemokine secretion.

Although both chemokines, *TBX21*, and *IFNG* were more highly expressed in MSI-H tumors when compared to MSI-L and MSS, no pattern of secreted proteins could be correlated with MMR-fidelity. The limited number of colorectal tumors collected only yielded a small number of MSI-H and CIMP specimens, and due to the standard deviation of results (a signature of all human tissues) this investigation could not determine any pattern of chemokine secretion that is attributed to genomic instability.

This investigation was a comprehensive and ambitious survey of the immunological activity in CRC; however while addressing certain questions about the disease, many oversights pertaining to the study design became apparent only after the data was analyzed. Firstly, it should be recognized that these data do not determine whether anti-tumor T-cells during tumor progression are decreasing in abundance, repolarizing to either T_H2 or T_H17 cell responses, or both. Although type-2 activity did not change while type-1 activity decreased with advanced stage disease, this may be because the *GATA3* signal may not have been exclusively from T-cells. Therefore, the investigation focused to evaluating the magnitude of only type-1 activity in CRC. Other studies suggest that strong inflammatory T_H17 cell activity drives tumorigenesis and angiogenesis and interferes with type-1 activity (Langowski et al., 2006; Grivennikov et al., 2010; Grivennikov and Karin, 2011; Grivennikov et al., 2012; Straus, 2013). This investigation can neither confirm nor counter these studies. Therefore, the interplay between T-cell subsets and other infiltrating immune cells needs to be further explored in the next investigation. The possibility of investigating how inflammatory cytokines influence the invasiveness of the disease is highly likely due to the means by which this investigation collected data. Further Luminex or ELISA analysis can be performed on frozen supernatants and will only be limited to

antibodies available on the market. Secondly, four stage IV tumors is not a large number of data to draw concrete conclusions from, therefore this investigation was careful not overstate conclusions about this group. Analysis of these stage IV tumors was limited to determining trends within the whole tumor population collected. Thirdly, this investigation anticipated that heterogeneity existed within each tissue collected, therefore samples were obtained from multiple tissue sites to represent each tissue as a whole and to mitigate the chance of randomly selecting a unique compartment within each tissue that may be misrepresentative. However, it cannot be known whether the assembly of samples truly represented each tissue. That acknowledged however, the techniques employed in this investigation more broadly sampled the TME than can be normally achieved by tissue microarrays, IHC, and real-time PCR alone.

For the conclusions of this investigation to be accurate, two assumptions need to be true. Firstly, CRC progress linearly from healthy colonic cells to neoplasms to metastases and can be sequentially staged into definitive steps. Pathologists as a whole predict that tumors invade local tissues first before metastasizing, although tumors from different patients can progress at different rates. And secondly, forty-four collected tumors represented an accurate "snapshot" of untreated CRCs. Enough tumors were collected to generate powerful data that achieved significance and satisfied many of the investigation's aims.

The final word of this dissertation is to reflect the impression the investigation exerted on the primary investigator. Cancer is an impressively complex disease in which internal immunological patterns become increasingly complicated to identify when studying a human population. However, only when the investigator began to understand

the value of establishing a concrete, yet simple and limited, criterion for evaluating a particular phenomenon such as immunosurveillance, could he generalize his findings into subgroups that truly represent the differing magnitudes of anti-tumor activity among tumors. Therefore, this investigator cannot claim that the *IFNG-TBX21* profile is the only means in which to measure anti-tumor activity. However, many other criteria could have been used to identify the same phenomenon. For that matter, this investigation cannot conclude without admitting to the reader that CRC, and most probably other cancers, are bimodal for immunological signatures other that the type-1 response, such as regulator T-cell and/or inflammatory immune cell signatures. This investigation also admits that other immunological responses that may dictate patient survival have yet to be identified. In summary, the novel ideas and findings introduced in this investigation for evaluating CRC will provide practitioners a better idea of how to predict a patient's odds for survival, and in turn will clarify which treatment strategy, if any, will be most appropriate. Therefore, this investigation fully embraced the mission of the GI Cancer Research/Epigenetic and Cancer Prevention Laboratory. And in a final note, this investigation did not gain impetus from one student's ambition to change the practice of oncology, but gained from his inexorable drive to study, understand, and improve everything around him.

APPENDICES

APPENDIX A

Table A.1 Sample Types Collected for Each Patient, IRB#011-030 Cohort

	Tissue Culture		RNA		DNA	
Patient #	Normal	Tumor	Normal	Tumor	Normal	Tumor
1	x	x	x	x	x	x
2	x	x	x	Y	x	x
3	x	x	x	Y	x	x
4	x	x	x	Y	x	x
5	x	x	x	Y	x	x
6	x	x	x	Y	x	x
7	x	x	x	Y	x	x
8	x	x	x	Y	x	x
9	x	Y	x	Y	x	x
10	x	x	x	x	x	x
11	x	Y	x	Y	x	x
12	x	Y	x	Y	x	x
13	x	x	x	x	x	x
14	x	Y	x	Y	x	x
15	x	x	x	Y	x	x
16	x	Y	x	Y	x	x
17	x	Y	x	Y	x	x
18	x	x	x	Y	x	x
19	x	Y	x	x	x	x
20	x	Y	x	Y	x	x
21	x	Y	x	Y	x	x
22	x	Y	x	Y	x	x
23	x	x	x	Y	x	x
24	Y	Y	x	Y	x	x
25	Y	Y	Y	Y	x	x
26	Y	Y	Y	Y	x	x
27a	Y	Y	Y	Y	x	x
27b	Y	Y	Y	Y	x	x
28	x	x	x	x	x	x
29	Y	Y	Y	Y	x	x
30	x	x	x	x	x	x
31	Y	Y	Y	Y	Y	Y
32	Y	Y	Y	Y	Y	Y
33	Y	Y	Y	Y	Y	Y
34	Y	Y	Y	Y	Y	Y
35	Y	Y	Y	Y	Y	Y
36	Y	Y	Y	Y	Y	Y

Table A.1 Sample Types Collected for Each Patient, IRB#011-030 Cohort --continued

	Tissue Culture		RNA		DNA	
Patient #	Normal	Tumor	Normal	Tumor	Normal	Tumor
37	Y	Y	Y	Y	Y	Y
38	Y	Y	Y	Y	Y	Y
39	Y	Y	Y	Y	Y	Y
40	Y	Y	Y	Y	Y	Y
41a	Y	Y	Y	Y	x	x
41b	Y	Y	Y	Y	Y	Y
42	Y	Y	x	Y	x	Y
43	Y	Y	Y	Y	Y	Y
44	Y	Y	Y	Y	Y	Y
45	Y	Y	Y	Y	Y	Y
46	Y	Y	Y	Y	Y	Y
47	Y	x	Y	Y	x	x
48	x	x	x	x	x	x
49	x	x	x	x	x	x

Y, sample collected; x, sample not collected

APPENDIX B

Table B.1 Clinicopathological Data of Enrolled Patients, IRB#011-030 Cohort

Patient #	Date collected	Primary Tumor	Stage	Age	Sex
1	8-Mar-11	x	x	65	F
2	25-May-11	Rectum	IVB	57	F
3	2-Jun-11	Colon	IIA	62	M
4	9-Jun-11	Rectum	I	45	M
5	15-Jun-11	Rectum	IIA	52	F
6	22-Jun-11	Rectum	IIA	40	M
7	22-Jun-11	Colon	IIA	61	M
8	24-Aug-11	Colon	I	59	M
9	7-Sep-11	Colon	I	69	M
10	Not Collected	x	x	65	M
11	31-Jan-12	Colon	IIIC	33	M
12	3-Feb-12	Rectum	IIIA	82	M
13	Not Collected	x	x	46	F
14	15-Feb-12	Rectum	I	51	M
15	1-Mar-12	Colon	I	55	M
16	2-Mar-12	Rectum	IIA	61	M
17	12-Mar-12	Colon	IIA	50	M
18	28-Mar-12	x	x	52	F
19	29-Mar-12	Colon	IIIB	59	M
20	29-Mar-12	Colon	IIIA	57	F
21	4-Apr-12	Colon	IIIB	46	F
22	9-Apr-13	Colon	I	49	M
23	23-Apr-12	Rectum	IIIB	63	M
24	17-May-12	Rectum	I	79	M
25	25-May-12	Rectum	IIIB	78	M
26	30-May-12	Rectum	IIB	72	M
27a	6-Jun-12	Rectum	IIIC	65	F
27b	6-Jun-12	Rectum	IIIC	65	F
28	Not Collected	x	x	49	M
29	22-Aug-12	Colon	IIIB	88	F
30	Not Collected	x	x	61	F
31	20-Sep-12	Colon	IVB	66	M
32	8-Oct-12	Rectum	I	61	F
33	11-Oct-12	Colon	IVA	31	M
34	7-Dec-12	Rectum	I	51	F
35	17-Jan-13	Colon	IIA	63	F
36	6-Feb-13	Colon	0	64	M

Table B.1 Clinicopathological Data of Enrolled Patients, IRB#011-030 Cohort --continued

Patient #	Date collected	Primary Tumor	Stage	Age	Sex
37	4-Mar-13	Rectum	I	90	F
38	10-Mar-13	Colon	IV	58	M
39	24-Apr-13	Colon	IIIC	79	F
40	24-Apr-13	Rectum	IIIA	61	M
41a	1-May-13	Colon	IIA	74	M
41b	1-May-13	Colon	IIA	74	M
42	1-Jul-13	Colon	IIA	66	F
43	16-Aug-13	Colon	IIA	55	M
44	21-Aug-13	Rectum	IIA	45	M
45	3-Sep-13	Colon	IIA	84	M
46	19-Sep-13	Colon	IIA	82	M
47	16-Oct-13	Rectum	I	50	F
48	Not Collected	x	x	68	F
49	Not Collected	x	x	53	F

APPENDIX C

Table C.1 Clinicopathological Data of TCGA Cohort

Patient #	Primary Tumor	Stage	Age	Sex
TCGA-A6-2670	Sigmoid Colon	II	45	M
TCGA-A6-2672	Transverse Colon	III	82	F
TCGA-A6-2674	Sigmoid Colon	IV	71	M
TCGA-A6-2676	Cecum	II	75	F
TCGA-A6-2677	Cecum	III	68	F
TCGA-A6-2678	Transverse Colon	III	43	F
TCGA-A6-2683	Ascending Colon	IV	57	F
TCGA-A6-3807	Sigmoid Colon	III	53	F
TCGA-A6-3808	Cecum	II	73	M
TCGA-A6-3809	Transverse Colon	II	71	F
TCGA-A6-3810	Sigmoid Colon	II	62	M
TCGA-AA-3514	Ascending Colon	I	81	F
TCGA-AA-3516	Ascending Colon	III	74	F
TCGA-AA-3517	Splenic Flexure	II	60	M
TCGA-AA-3518	Cecum	II	81	F
TCGA-AA-3519	Sigmoid Colon	III	63	M
TCGA-AA-3520	Ascending Colon	II	86	F
TCGA-AA-3521	Sigmoid Colon	II	87	M
TCGA-AA-3522	Ascending Colon	II	67	M
TCGA-AA-3524	Sigmoid Colon	II	85	M
TCGA-AA-3525	Hepatic Flexure	III	90	M
TCGA-AA-3526	Sigmoid Colon	I	57	M
TCGA-AA-3527	Cecum	II	90	F
TCGA-AA-3529	Sigmoid Colon	III	78	F
TCGA-AA-3530	Cecum	I	80	M
TCGA-AA-3531	Sigmoid Colon	II	75	F
TCGA-AA-3532	Sigmoid Colon	II	63	M
TCGA-AA-3534	Ascending Colon	II	78	F
TCGA-AA-3538	Descending Colon	I	54	F
TCGA-AA-3542	Sigmoid Colon	III	69	M
TCGA-AA-3543	Cecum	I	84	M
TCGA-AA-3544	Sigmoid Colon	I	68	M
TCGA-AA-3548	Cecum	III	71	F
TCGA-AA-3549	Cecum	I	69	M
TCGA-AA-3552	Cecum	III	85	M
TCGA-AA-3553	Sigmoid Colon	I	61	F
TCGA-AA-3554	Ascending Colon	II	62	F
TCGA-AA-3555	Hepatic Flexure	II	81	F

Table C.1 Clinicopathological Data of TCGA Cohort --continued

Patient #	Primary Tumor	Stage	Age	Sex
TCGA-AA-3558	Sigmoid Colon	I	70	M
TCGA-AA-3556	Sigmoid Colon	I	78	M
TCGA-AA-3560	Sigmoid Colon	III	72	F
TCGA-AA-3561	Ascending Colon	II	72	M
TCGA-AA-3562	Descending Colon	III	82	M
TCGA-AA-3664	Cecum	II	74	F
TCGA-AA-3666	Cecum	III	68	M
TCGA-AA-3667	Sigmoid Colon	I	36	F
TCGA-AA-3672	Transverse Colon	III	90	F
TCGA-AA-3673	Transverse Colon	II	53	F
TCGA-AA-3675	Hepatic Flexure	II	84	M
TCGA-AA-3678	Sigmoid Colon	III	60	F
TCGA-AA-3679	Descending Colon	IV	59	M
TCGA-AA-3680	Cecum	IV	67	F
TCGA-AA-3681	Cecum	III	77	F
TCGA-AA-3684	Cecum	IV	65	F
TCGA-AA-3685	Sigmoid Colon	II	69	M
TCGA-AA-3688	Sigmoid Colon	IV	80	M
TCGA-AA-3692	Splenic Flexure	IV	47	F
TCGA-AA-3693	Sigmoid Colon	IV	77	F
TCGA-AA-3695	Cecum	IV	63	F
TCGA-AA-3696	Sigmoid Colon	IV	75	F
TCGA-AA-3710	Hepatic Flexure	II	80	F
TCGA-AA-3715	Ascending Colon	II	77	M
TCGA-AA-3811	Hepatic Flexure	III	84	F
TCGA-AA-3812	Sigmoid Colon	II	82	F
TCGA-AA-3814	Ascending Colon	II	85	F
TCGA-AA-3815	Cecum	II	65	F
TCGA-AA-3818	Hepatic Flexure	II	78	F
TCGA-AA-3819	Sigmoid Colon	II	41	F
TCGA-AA-3821	Hepatic Flexure	I	81	F
TCGA-AA-3831	Sigmoid Colon	II	66	M
TCGA-AA-3833	Ascending Colon	II	63	F
TCGA-AA-3837	Hepatic Flexure	II	67	M
TCGA-AA-3841	Sigmoid Colon	II	66	M
TCGA-AA-3842	Sigmoid Colon	III	51	M
TCGA-AA-3844	Sigmoid Colon	III	78	F
TCGA-AA-3845	Ascending Colon	II	86	F
TCGA-AA-3846	Sigmoid Colon	II	74	F
TCGA-AA-3848	Sigmoid Colon	III	82	F
TCGA-AA-3850	Transverse Colon	I	74	M
TCGA-AA-3851	Ascending Colon	II	74	M
TCGA-AA-3852	Transverse Colon	II	88	M

Table C.1 Clinicopathological Data of TCGA Cohort --continued

Patient #	Primary Tumor	Stage	Age	Sex
TCGA-AA-3855	Sigmoid Colon	I	72	M
TCGA-AA-3854	Sigmoid Colon	I	71	F
TCGA-AA-3856	Sigmoid Colon	II	59	M
TCGA-AA-3858	Sigmoid Colon	I	67	M
TCGA-AA-3860	Sigmoid Colon	III	53	F
TCGA-AA-3861	Cecum	II	72	M
TCGA-AA-3862	Transverse Colon	II	82	M
TCGA-AA-3864	Cecum	II	71	M
TCGA-AA-3866	Cecum	I	78	F
TCGA-AA-3867	Sigmoid Colon	IV	74	M
TCGA-AA-3869	Cecum	IV	76	M
TCGA-AA-3870	Ascending Colon	IV	71	F
TCGA-AA-3872	Sigmoid Colon	IV	45	M
TCGA-AA-3875	Ascending Colon	I	78	F
TCGA-AA-3877	Transverse Colon	I	83	F
TCGA-AA-3930	Ascending Colon	IV	66	M
TCGA-AA-3939	Ascending Colon	II	83	M
TCGA-AA-3941	Ascending Colon	IV	84	F
TCGA-AA-3947	Ascending Colon	II	60	F
TCGA-AA-3949	Ascending Colon	III	87	F
TCGA-AA-3950	Ascending Colon	II	79	F
TCGA-AA-3952	Descending Colon	III	68	M
TCGA-AA-3955	Descending Colon	III	38	M
TCGA-AA-3956	Cecum	II	65	M
TCGA-AA-3966	Hepatic Flexure	II	89	F
TCGA-AA-3968	Sigmoid Colon	I	55	F
TCGA-AA-3970	Sigmoid Colon	II	65	M
TCGA-AA-3971	Sigmoid Colon	III	58	M
TCGA-AA-3972	Sigmoid Colon	IV	72	M
TCGA-AA-3973	Sigmoid Colon	IV	69	M
TCGA-AA-3975	Sigmoid Colon	I	80	M
TCGA-AA-3976	Sigmoid Colon	III	70	M
TCGA-AA-3977	Sigmoid Colon	II	65	M
TCGA-AA-3979	Sigmoid Colon	II	84	M
TCGA-AA-3980	Sigmoid Colon	I	89	F
TCGA-AA-3982	Sigmoid Colon	III	75	M
TCGA-AA-3984	Sigmoid Colon	II	61	F
TCGA-AA-3986	Transverse Colon	I	73	M
TCGA-AA-3989	Transverse Colon	IV	84	M
TCGA-AA-3994	Transverse Colon	III	69	M
TCGA-AA-A004	Sigmoid Colon	II	76	M
TCGA-AA-A00D	Ascending Colon	I	70	M
TCGA-AA-A00E	Ascending Colon	II	65	M

Table C.1 Clinicopathological Data of TCGA Cohort --continued

Patient #	Primary Tumor	Stage	Age	Sex
TCGA-AA-A00F	Sigmoid Colon	III	66	M
TCGA-AA-A00J	Ascending Colon	III	80	M
TCGA-AA-A00K	Sigmoid Colon	II	79	M
TCGA-AA-A00L	Transverse Colon	II	66	M
TCGA-AA-A00N	Cecum	II	75	M
TCGA-AA-A00O	Sigmoid Colon	III	83	F
TCGA-AA-A00Q	Sigmoid Colon	III	66	F
TCGA-AA-A00R	Cecum	I	64	F
TCGA-AA-A00U	Ascending Colon	III	50	M
TCGA-AA-A00W	Sigmoid Colon	I	80	M
TCGA-AA-A00Z	Sigmoid Colon	II	70	M
TCGA-AA-A010	Transverse Colon	II	46	F
TCGA-AA-A017	Sigmoid Colon	II	57	F
TCGA-AA-A01C	Ascending Colon	III	75	M
TCGA-AA-A01D	Sigmoid Colon	III	47	F
TCGA-AA-A01F	Sigmoid Colon	III	72	M
TCGA-AA-A01G	Cecum	II	63	M
TCGA-AA-A01I	Sigmoid Colon	I	76	M
TCGA-AA-A01K	Sigmoid Colon	III	74	F
TCGA-AA-A01Q	Ascending Colon	II	48	F
TCGA-AA-A024	Descending Colon	II	81	M
TCGA-AA-A029	Cecum	II	67	M
TCGA-AA-A02E	Cecum	IV	82	F
TCGA-AA-A02F	Sigmoid Colon	IV	68	F
TCGA-AA-A02H	Sigmoid Colon	IV	74	F
TCGA-AA-A02J	Sigmoid Colon	IV	70	F
TCGA-AA-A02R	Cecum	II	84	F
TCGA-AA-A02W	Sigmoid Colon	I	73	F
TCGA-AF-2689	Rectosigmoid Junction	IV	41	F
TCGA-AF-2691	Rectum	I	48	F
TCGA-AF-3400	Rectosigmoid Junction	II	54	M
TCGA-AF-3913	Rectosigmoid Junction	IV	60	M
TCGA-AG-3574	Rectum	II	89	F
TCGA-AG-3575	Rectum	II	51	M
TCGA-AG-3578	Rectum	II	76	F
TCGA-AG-3580	Rectum	I	67	M
TCGA-AG-3581	Rectum	I	63	M
TCGA-AG-3582	Rectum	IV	75	M
TCGA-AG-3583	Rectum	IV	66	M
TCGA-AG-3584	Rectum	IV	60	M
TCGA-AG-3586	Rectum	III	72	F
TCGA-AG-3587	Rectum	I	65	M
TCGA-AG-3593	Rectum	II	72	F

Table C.1 Clinicopathological Data of TCGA Cohort --continued

Patient #	Primary Tumor	Stage	Age	Sex
TCGA-AG-3594	Rectum	II	77	M
TCGA-AG-3598	Rectum	II	69	M
TCGA-AG-3599	Rectum	I	70	M
TCGA-AG-3600	Rectum	III	62	M
TCGA-AG-3601	Rectum	III	68	M
TCGA-AG-3602	Rectum	III	66	F
TCGA-AG-3605	Rectum	IV	85	F
TCGA-AG-3608	Rectum	II	79	F
TCGA-AG-3609	Rectum	III	65	F
TCGA-AG-3611	Rectum	II	72	M
TCGA-AG-3612	Rectum	III	55	F
TCGA-AG-3726	Rectum	I	63	F
TCGA-AG-3727	Rectum	III	78	F
TCGA-AG-3728	Rectum	III	73	M
TCGA-AG-3878	Rectum	I	64	M
TCGA-AG-3881	Rectum	II	83	F
TCGA-AG-3882	Rectum	I	66	F
TCGA-AG-3883	Rectum	I	69	M
TCGA-AG-3885	Rectum	III	71	F
TCGA-AG-3887	Rectum	II	68	M
TCGA-AG-3890	Rectum	I	62	M
TCGA-AG-3892	Rectum	I	57	F
TCGA-AG-3893	Rectum	III	74	M
TCGA-AG-3894	Rectum	II	65	M
TCGA-AG-3896	Rectum	I	85	F
TCGA-AG-3898	Rectum	II	61	M
TCGA-AG-3901	Rectum	III	67	F
TCGA-AG-3902	Rectum	II	61	M
TCGA-AG-3909	Rectum	III	69	F
TCGA-AG-3999	Rectum	III	61	F
TCGA-AG-4001	Rectum	II	74	F
TCGA-AG-4005	Rectum	IV	64	M
TCGA-AG-4007	Rectum	IV	87	M
TCGA-AG-4008	Rectum	II	63	M
TCGA-AG-4015	Rectum	II	85	F
TCGA-AG-A002	Rectum	I	35	M
TCGA-AG-A008	Rectum	I	50	F
TCGA-AG-A00C	Rectum	III	49	F
TCGA-AG-A00H	Rectum	II	75	M
TCGA-AG-A00Y	Rectum	II	68	M
TCGA-AG-A011	Rectum	II	80	M
TCGA-AG-A014	Rectum	I	86	M
TCGA-AG-A015	Rectum	I	64	F

Table C.1 Clinicopathological Data of TCGA Cohort --continued

Patient #	Primary Tumor	Stage	Age	Sex
TCGA-AG-A016	Rectum	IV	55	M
TCGA-AG-A01J	Rectum	II	59	F
TCGA-AG-A01L	Rectum	III	58	M
TCGA-AG-A01N	Rectum	IV	68	F
TCGA-AG-A023	Rectum	IV	62	F
TCGA-AG-A025	Rectum	I	62	F
TCGA-AG-A026	Rectum	II	66	M
TCGA-AG-A02G	Rectum	IV	66	M
TCGA-AG-A02X	Rectum	I	77	M
TCGA-AG-A032	Rectum	III	68	M
TCGA-AY-4070	Cecum	III	50	F

APPENDIX D

Table D.1 Summary of Microsatellite Instability Markers Outside QMVR, IRB#011-030 Cohort

Patient #	NR-27	NR-21	NR-24	BAT-25	BAT-26	MSI-H/L?
1	NA	NA	NA	NA	NA	
2						
3						
4						
5						
6						
7	Y					MSI-L
8						
9						
10	NA	NA	NA	NA	NA	NA
11						
12						
13	NA	NA	NA	NA	NA	NA
14						
15						
16						
17						
18						
19						
20				Y		MSI-L
21						
22						
23						
24						
25						
26		Y		Y		MSI-H
27a						
27b						
28	NA	NA	NA	NA	NA	NA
29						
30	NA	NA	NA	NA	NA	NA
31						
32						
33	Y	Y	Y	Y	Y	MSI-H
34						
35						
36				Y		MSI-L

Table D.1 Summary of Microsatellite Instability Markers Outside QMVR, IRB#011-030 Cohort --continued

Patient #	NR-27	NR-21	NR-24	BAT-25	BAT-26	MSI-H/L?
37						
38						
39	Y	Y	Y	Y	Y	MSI-H
40						
41a						
41b						
42						
43						
44						
45						
46						
47		Y				MSI-L
48	NA	NA	NA	NA	NA	NA
49	NA	NA	NA	NA	NA	NA

Y, marker outside QMVR

APPENDIX E

Table E.1 Summary of Microsatellite Instability Data for TCGA Cohort

Patient #	MMR Fidelity	Patient #	MMR Fidelity
TCGA-A6-2670	x	TCGA-AA-3555	MSS
TCGA-A6-2672	MSI-H	TCGA-AA-3556	MSS
TCGA-A6-2674	MSS	TCGA-AA-3558	MSS
TCGA-A6-2676	MSI-H	TCGA-AA-3560	MSS
TCGA-A6-2677	MSS	TCGA-AA-3561	MSS
TCGA-A6-2678	MSS	TCGA-AA-3562	MSS
TCGA-A6-2683	MSI-L	TCGA-AA-3664	MSS
TCGA-A6-3807	MSS	TCGA-AA-3666	MSS
TCGA-A6-3808	MSI-L	TCGA-AA-3667	MSI-L
TCGA-A6-3809	MSI-H	TCGA-AA-3672	MSI-H
TCGA-A6-3810	MSS	TCGA-AA-3673	MSS
TCGA-AA-3514	MSS	TCGA-AA-3675	MSS
TCGA-AA-3516	MSI-H	TCGA-AA-3678	MSS
TCGA-AA-3517	MSI-L	TCGA-AA-3679	MSS
TCGA-AA-3518	MSI-H	TCGA-AA-3680	MSI-L
TCGA-AA-3519	MSS	TCGA-AA-3681	MSS
TCGA-AA-3520	MSI-L	TCGA-AA-3684	MSS
TCGA-AA-3521	MSS	TCGA-AA-3685	MSS
TCGA-AA-3522	MSS	TCGA-AA-3688	MSI-L
TCGA-AA-3524	MSS	TCGA-AA-3692	MSI-L
TCGA-AA-3525	MSI-H	TCGA-AA-3693	MSS
TCGA-AA-3526	MSI-L	TCGA-AA-3695	MSS
TCGA-AA-3527	MSS	TCGA-AA-3696	MSS
TCGA-AA-3529	MSI-L	TCGA-AA-3710	MSI-H
TCGA-AA-3530	MSS	TCGA-AA-3715	MSI-H
TCGA-AA-3531	MSI-L	TCGA-AA-3811	MSI-H
TCGA-AA-3532	MSS	TCGA-AA-3812	MSS
TCGA-AA-3534	MSS	TCGA-AA-3814	MSS
TCGA-AA-3538	MSS	TCGA-AA-3815	MSI-H
TCGA-AA-3542	MSS	TCGA-AA-3818	MSS
TCGA-AA-3543	MSI-H	TCGA-AA-3819	MSI-L
TCGA-AA-3544	MSS	TCGA-AA-3821	MSI-H
TCGA-AA-3548	MSS	TCGA-AA-3831	MSS
TCGA-AA-3549	MSS	TCGA-AA-3833	MSI-H
TCGA-AA-3552	MSS	TCGA-AA-3837	MSS
TCGA-AA-3553	MSI-L	TCGA-AA-3841	MSS
TCGA-AA-3554	MSI-H	TCGA-AA-3842	MSS
TCGA-AA-3844	MSS	TCGA-AA-3989	MSS

Table E.1 Summary of Microsatellite Instability Data for TCGA Cohort --continued

Patient #	MMR Fidelity	Patient #	MMR Fidelity
TCGA-AA-3845	MSI-H	TCGA-AA-3994	MSS
TCGA-AA-3846	MSS	TCGA-AA-A004	MSI-L
TCGA-AA-3848	MSS	TCGA-AA-A00D	MSS
TCGA-AA-3850	MSS	TCGA-AA-A00E	MSI-H
TCGA-AA-3851	MSS	TCGA-AA-A00F	MSS
TCGA-AA-3852	MSI-L	TCGA-AA-A00J	MSI-H
TCGA-AA-3854	MSI-L	TCGA-AA-A00K	MSI-L
TCGA-AA-3855	MSI-L	TCGA-AA-A00L	MSS
TCGA-AA-3856	MSS	TCGA-AA-A00N	MSI-L
TCGA-AA-3858	MSS	TCGA-AA-A00O	MSI-L
TCGA-AA-3860	MSS	TCGA-AA-A00Q	MSS
TCGA-AA-3861	MSI-L	TCGA-AA-A00R	MSI-H
TCGA-AA-3862	MSS	TCGA-AA-A00U	MSS
TCGA-AA-3864	MSI-H	TCGA-AA-A00W	MSS
TCGA-AA-3866	MSI-L	TCGA-AA-A00Z	MSS
TCGA-AA-3867	MSS	TCGA-AA-A010	MSI-L
TCGA-AA-3869	MSS	TCGA-AA-A017	MSS
TCGA-AA-3870	MSS	TCGA-AA-A01C	MSS
TCGA-AA-3872	MSS	TCGA-AA-A01D	MSS
TCGA-AA-3875	MSS	TCGA-AA-A01F	MSS
TCGA-AA-3877	MSI-H	TCGA-AA-A01G	MSI-L
TCGA-AA-3930	MSI-L	TCGA-AA-A01I	MSS
TCGA-AA-3939	MSS	TCGA-AA-A01K	MSS
TCGA-AA-3941	MSI-L	TCGA-AA-A01Q	MSI-H
TCGA-AA-3947	MSI-H	TCGA-AA-A024	MSI-L
TCGA-AA-3949	MSI-H	TCGA-AA-A029	MSI-L
TCGA-AA-3950	MSI-H	TCGA-AA-A02E	MSI-L
TCGA-AA-3952	MSS	TCGA-AA-A02F	MSS
TCGA-AA-3955	MSS	TCGA-AA-A02H	MSS
TCGA-AA-3956	MSS	TCGA-AA-A02J	MSS
TCGA-AA-3966	MSI-H	TCGA-AA-A02R	MSI-H
TCGA-AA-3968	MSS	TCGA-AA-A02W	MSI-L
TCGA-AA-3970	MSS	TCGA-AF-2689	MSS
TCGA-AA-3971	MSS	TCGA-AF-2691	MSS
TCGA-AA-3972	MSI-L	TCGA-AF-3400	MSS
TCGA-AA-3973	MSI-L	TCGA-AF-3913	MSS
TCGA-AA-3975	MSS	TCGA-AG-3574	MSS
TCGA-AA-3976	MSS	TCGA-AG-3575	MSS
TCGA-AA-3977	MSS	TCGA-AG-3578	MSS
TCGA-AA-3979	MSS	TCGA-AG-4007	MSI-L
TCGA-AA-3980	MSS	TCGA-AG-4008	MSS
TCGA-AA-3982	MSI-L	TCGA-AG-3580	MSS
TCGA-AA-3984	MSS	TCGA-AG-3581	MSS

Table E.1 Summary of Microsatellite Instability Data for TCGA Cohort --continued

Patient #	MMR Fidelity	Patient #	MMR Fidelity
TCGA-AA-3986	MSS	TCGA-AG-3582	MSS
TCGA-AG-3586	MSS	TCGA-AG-3583	MSI-L
TCGA-AG-3587	MSS	TCGA-AG-3584	MSS
TCGA-AG-3593	MSS	TCGA-AG-A002	MSS
TCGA-AG-3594	MSS	TCGA-AG-A008	MSS
TCGA-AG-3598	MSS	TCGA-AG-A00C	MSS
TCGA-AG-3599	MSS	TCGA-AG-A00H	MSS
TCGA-AG-3600	MSS	TCGA-AG-A00Y	MSS
TCGA-AG-3601	MSI-L	TCGA-AG-A011	MSS
TCGA-AG-3602	MSS	TCGA-AG-A014	MSS
TCGA-AG-3605	MSS	TCGA-AG-A015	MSS
TCGA-AG-3608	Indeterminate	TCGA-AG-A016	MSS
TCGA-AG-3609	MSS	TCGA-AG-A01J	MSS
TCGA-AG-3611	MSS	TCGA-AG-A01L	MSS
TCGA-AG-3612	MSS	TCGA-AG-A01N	MSS
TCGA-AG-3726	MSS	TCGA-AG-A023	MSS
TCGA-AG-3727	MSS	TCGA-AG-A025	MSS
TCGA-AG-3728	MSS	TCGA-AG-A026	MSS
TCGA-AG-3878	MSS	TCGA-AG-A02G	MSS
TCGA-AG-3881	MSS	TCGA-AG-A02X	MSS
TCGA-AG-3882	MSS	TCGA-AG-A032	MSS
TCGA-AG-3883	MSS	TCGA-AY-4070	MSS
TCGA-AG-3885	MSS		
TCGA-AG-3887	MSS		
TCGA-AG-3890	MSS		
TCGA-AG-3892	MSS		
TCGA-AG-3893	MSS		
TCGA-AG-3894	MSS		
TCGA-AG-3896	MSS		
TCGA-AG-3898	MSS		
TCGA-AG-3901	MSS		
TCGA-AG-3902	MSS		
TCGA-AG-3909	MSS		
TCGA-AG-3999	MSS		
TCGA-AG-4001	MSI-L		
TCGA-AG-4005	MSS		
TCGA-AG-4015	MSS		

APPENDIX F

Table F.1 Primary Tumor (T), Regional Lymph Node (N), and Metastasis (M) Scores for, IRB#011-030 Cohort

Patient #	Tumor (T)	Lymph Node (N)	Metastasis (M)
1	x	x	x
2	T4	N1-3	M1
3	T3	N0	M0
4	T2	N0	M0
5	T3	N0	M0
6	T3	N0	M0
7	T3	N0	M0
8	T1	N0	x
9	T2	N0	M0
11	T4	N2	M0
12	T4	N1	M0
14	T2	N0	M0
15	T2	N0	M0
16	T3	N0	M0
17	T3	N0	M0
19	T2	N2	M0
20	T2	N1	M0
21	T3	N2	M0
22	T2	N0	M0
23	T3	N1	M0
24	T1	N0	M0
25	T3	N1	M0
26	T4	x	x
27a	T3	N2	M0
27b	T3	N2	M0
29	T3	N1	M0
31	T4	N2	M1
32	T2	N0	x
33	T4	N2	M1
34	T2	N0	M0
35	T3	N0	M0
36	T0	N0	M0
37	T2	x	M0
38	T4	N2	M1
39	T4	N1	M0
40	T2	N1	M0
41a	T3	N0	x

Table F.1 Primary Tumor (T), Regional Lymph Node (N), and Metastasis (M) Scores for, IRB#011-030 Cohort --continued

Patient #	Tumor (T)	Lymph Node (N)	Metastasis (M)
41b	T3	N0	x
42	T3	N0	M0
43	T3	N0	M0
44	T3	N0	M0
45	T3	N0	M0
46	T3	N0	x
47	T1	N0	M0
48	x	x	x
49	x	x	x

APPENDIX G

Table G.1 Primary Tumor (T), Regional Lymph Node (N), and Metastasis (M) Scores for, TCGA Cohort

Patient #	Tumor (T)	Lymph Node (N)	Metastasis (M)
TCGA-A6-2670	T3	N0	M0
TCGA-A6-2672	T3	N1	M0
TCGA-A6-2674	T3	N2	M1
TCGA-A6-2676	T4	N0	M0
TCGA-A6-2677	T3	N2	M0
TCGA-A6-2678	T3	N1	M0
TCGA-A6-2683	T4	N0	M1
TCGA-A6-3807	T3	N2	M0
TCGA-A6-3808	T3	N0	M0
TCGA-A6-3809	T4	N0	M0
TCGA-A6-3810	T3	N0	M0
TCGA-AA-3514	T2	N0	M0
TCGA-AA-3516	T3	N2	M0
TCGA-AA-3517	T3	N0	M0
TCGA-AA-3518	T3	N0	M0
TCGA-AA-3519	T3	N1	M0
TCGA-AA-3520	T3	N0	M0
TCGA-AA-3521	T3	N0	M0
TCGA-AA-3522	T3	N0	M0
TCGA-AA-3524	T3	N0	M0
TCGA-AA-3525	T3	N1	M0
TCGA-AA-3526	T2	N0	M0
TCGA-AA-3527	T3	N0	M0
TCGA-AA-3529	T3	N2	M0
TCGA-AA-3530	T2	N0	M0
TCGA-AA-3531	T3	N0	M0
TCGA-AA-3532	T3	N0	M0
TCGA-AA-3534	T3	N0	M0
TCGA-AA-3538	T2	N0	M0
TCGA-AA-3542	T3	N2	M0
TCGA-AA-3543	T2	N0	M0
TCGA-AA-3544	T2	N0	M0
TCGA-AA-3548	T3	N2	M0
TCGA-AA-3549	T2	N0	M0
TCGA-AA-3552	T3	N2	M0
TCGA-AA-3553	T2	N0	M0
TCGA-AA-3554	T3	N0	M0
TCGA-AA-3555	T3	N0	M0

Table G.1 Primary Tumor (T), Regional Lymph Node (N), and Metastasis (M) Scores for, TCGA Cohort --continued

Patient #	Tumor (T)	Lymph Node (N)	Metastasis (M)
TCGA-AA-3556	T2	N0	M0
TCGA-AA-3558	T2	N0	M0
TCGA-AA-3560	T3	N2	M0
TCGA-AA-3561	T3	N0	M0
TCGA-AA-3562	T3	N2	M0
TCGA-AA-3664	T3	N0	M0
TCGA-AA-3666	T3	N1	M0
TCGA-AA-3667	T2	N0	M0
TCGA-AA-3672	T3	N1	M0
TCGA-AA-3673	T3	N0	M0
TCGA-AA-3675	T3	N0	M0
TCGA-AA-3678	T2	N1	M0
TCGA-AA-3679	T3	N2	M1
TCGA-AA-3680	T4	N2	M1
TCGA-AA-3681	T3	N1	M0
TCGA-AA-3684	T4	N2	M1
TCGA-AA-3685	T3	N0	M0
TCGA-AA-3688	T3	N1	M1
TCGA-AA-3692	T3	N2	M1
TCGA-AA-3693	T4	N1	M1
TCGA-AA-3695	T3	N2	M1
TCGA-AA-3696	T3	N1	M1
TCGA-AA-3710	T3	N0	M0
TCGA-AA-3715	T3	N0	M0
TCGA-AA-3811	T3	N2	M0
TCGA-AA-3812	T3	N0	M0
TCGA-AA-3814	T3	N0	M0
TCGA-AA-3815	T3	N0	M0
TCGA-AA-3818	T3	N0	M0
TCGA-AA-3819	T3	N0	M0
TCGA-AA-3821	T2	N0	M0
TCGA-AA-3831	T3	N0	M0
TCGA-AA-3833	T3	N0	M0
TCGA-AA-3837	T3	N0	M0
TCGA-AA-3841	T3	N0	M0
TCGA-AA-3842	T2	N1	M0
TCGA-AA-3844	T3	N2	M0
TCGA-AA-3845	T3	N0	M0
TCGA-AA-3846	T3	N0	M0
TCGA-AA-3848	T3	N2	M0
TCGA-AA-3850	T2	N0	M0
TCGA-AA-3851	T3	N0	M0

Table G.1 Primary Tumor (T), Regional Lymph Node (N), and Metastasis (M) Scores for, TCGA Cohort --continued

Patient #	Tumor (T)	Lymph Node (N)	Metastasis (M)
TCGA-AA-3852	T3	N0	M0
TCGA-AA-3854	T2	N0	M0
TCGA-AA-3855	T2	N0	M0
TCGA-AA-3856	T3	N0	M0
TCGA-AA-3858	T2	N0	M0
TCGA-AA-3860	T3	N1	M0
TCGA-AA-3861	T3	N0	M0
TCGA-AA-3862	T3	N0	M0
TCGA-AA-3864	T3	N0	M0
TCGA-AA-3866	T2	N0	M0
TCGA-AA-3867	T3	N2	M1
TCGA-AA-3869	T4	N2	M1
TCGA-AA-3870	T3	N2	M1
TCGA-AA-3872	T4	N2	M1
TCGA-AA-3875	T1	N0	M0
TCGA-AA-3877	T1	N0	M0
TCGA-AA-3930	T3	N2	M1
TCGA-AA-3939	T3	N0	M0
TCGA-AA-3941	T4	N1b	M1a
TCGA-AA-3947	T4	N0	M0
TCGA-AA-3949	T3	N1	M0
TCGA-AA-3950	T3	N0	M0
TCGA-AA-3952	T3	N2	M0
TCGA-AA-3955	T2	N2a	M0
TCGA-AA-3956	T3	N0	M0
TCGA-AA-3966	T3	N0	M0
TCGA-AA-3968	T2	N0	M0
TCGA-AA-3970	T3	N0	M0
TCGA-AA-3971	T3	N1	M0
TCGA-AA-3972	T3	N1	M1
TCGA-AA-3973	T4	N1	M1
TCGA-AA-3975	T2	N0	M0
TCGA-AA-3976	T2	N1	M0
TCGA-AA-3977	T2	N0	[Not Available]
TCGA-AA-3979	T3	N0	M0
TCGA-AA-3980	T2	N0	M0
TCGA-AA-3982	T3	N1	M0
TCGA-AA-3984	T3	N0	M0
TCGA-AA-3986	T2	N0	M0
TCGA-AA-3989	T3	N2	M1
TCGA-AA-3994	T3	N1	M0
TCGA-AA-A004	T3	N0	M0

Table G.1 Primary Tumor (T), Regional Lymph Node (N), and Metastasis (M) Scores for, TCGA Cohort --continued

Patient #	Tumor (T)	Lymph Node (N)	Metastasis (M)
TCGA-AA-A00D	T2	N0	M0
TCGA-AA-A00E	T3	N0	M0
TCGA-AA-A00F	T3	N2	M0
TCGA-AA-A00J	T4	N1	M0
TCGA-AA-A00K	T3	N0	M0
TCGA-AA-A00L	T3	N0	M0
TCGA-AA-A00N	T4	N0	M0
TCGA-AA-A00O	T3	N2	M0
TCGA-AA-A00Q	T4	N1	M0
TCGA-AA-A00R	T2	N0	M0
TCGA-AA-A00U	T3	N1	M0
TCGA-AA-A00W	T1	N0	M0
TCGA-AA-A00Z	T3	N0	M0
TCGA-AA-A010	T4	N0	M0
TCGA-AA-A017	T3	N0	M0
TCGA-AA-A01C	T2	N1	M0
TCGA-AA-A01D	T3	N2	M0
TCGA-AA-A01F	T3	N1	M0
TCGA-AA-A01G	T3	N0	M0
TCGA-AA-A01I	T2	N0	M0
TCGA-AA-A01K	T3	N2	M0
TCGA-AA-A01Q	T3	N0	M0
TCGA-AA-A024	T3	N0	M0
TCGA-AA-A029	T3	N0	M0
TCGA-AA-A02E	T3	N1	M1
TCGA-AA-A02F	T3	N1	M1
TCGA-AA-A02H	T3	N2	M1
TCGA-AA-A02J	T3	N0	M1
TCGA-AA-A02R	T3	N0	M0
TCGA-AA-A02W	T2	N0	M0
TCGA-AF-2689	T3	N2	M1
TCGA-AF-2691	T1	N0	M0
TCGA-AF-3400	T3	N0	M0
TCGA-AF-3913	T3	N1a	M1
TCGA-AG-3574	T3	N0	M0
TCGA-AG-3575	T3	N0	M0
TCGA-AG-3578	T3	N0	M0
TCGA-AG-3580	T1	N0	M0
TCGA-AG-3581	T2	N0	M0
TCGA-AG-3582	T3	N1	M1
TCGA-AG-3583	T3	N2	M1
TCGA-AG-3584	T3	N2	M1

Table G.1 Primary Tumor (T), Regional Lymph Node (N), and Metastasis (M) Scores for, TCGA Cohort --continued

Patient #	Tumor (T)	Lymph Node (N)	Metastasis (M)
TCGA-AG-3586	T3	N2	M0
TCGA-AG-3587	T2	N0	M0
TCGA-AG-3593	T3	N0	M0
TCGA-AG-3594	T3	N0	M0
TCGA-AG-3598	T3	N0	M0
TCGA-AG-3599	T2	N0	M0
TCGA-AG-3600	T3	N2	M0
TCGA-AG-3601	T4	N1	M0
TCGA-AG-3602	T3	N2	M0
TCGA-AG-3605	T3	N1	M1
TCGA-AG-3608	T3	N0	M0
TCGA-AG-3609	T3	N2	M0
TCGA-AG-3611	T3	N0	M0
TCGA-AG-3612	T3	N1	M0
TCGA-AG-3726	T2	N0	M0
TCGA-AG-3727	T3	N1	M0
TCGA-AG-3728	T3	N1	M0
TCGA-AG-3878	T2	N0	M0
TCGA-AG-3881	T3	N0	M0
TCGA-AG-3882	T2	N0	M0
TCGA-AG-3883	T2	N0	M0
TCGA-AG-3885	T3	N1	M0
TCGA-AG-3887	T3	N0	M0
TCGA-AG-3890	T2	N0	M0
TCGA-AG-3892	T1	N0	M0
TCGA-AG-3893	T3	N1	M0
TCGA-AG-3894	T3	N0	M0
TCGA-AG-3896	T2	N0	M0
TCGA-AG-3898	T3	N0	M0
TCGA-AG-3901	T3	N1	M0
TCGA-AG-3902	T3	N0	M0
TCGA-AG-3909	T3	N1	M0
TCGA-AG-3999	T3	N2	M0
TCGA-AG-4001	T3	N0	M0
TCGA-AG-4005	T3	N2	M1
TCGA-AG-4007	T4	N2	M1
TCGA-AG-4008	T3	N0	M0
TCGA-AG-4015	T3	N0	M0
TCGA-AG-A002	T2	N0	M0
TCGA-AG-A008	T2	N0	M0
TCGA-AG-A00C	T3	N1	M0
TCGA-AG-A00H	T3	N0	M0

Table G.1 Primary Tumor (T), Regional Lymph Node (N), and Metastasis (M) Scores for, TCGA Cohort --continued

Patient #	Tumor (T)	Lymph Node (N)	Metastasis (M)
TCGA-AG-A00Y	T3	N0	M0
TCGA-AG-A011	T3	N0	M0
TCGA-AG-A014	T2	N0	M0
TCGA-AG-A015	T1	N0	M0
TCGA-AG-A016	T3	N2	M1
TCGA-AG-A01J	T3	N0	M0
TCGA-AG-A01L	T3	N1	M0
TCGA-AG-A01N	T2	N0	M1
TCGA-AG-A023	T4	N2	M1
TCGA-AG-A025	T1	N0	M0
TCGA-AG-A026	T4	N0	M0
TCGA-AG-A02G	T2	N1	M1
TCGA-AG-A02X	T2	N0	M0
TCGA-AG-A032	T3	N1	M0
TCGA-AY-4070	T3	N2	M0

APPENDIX H

Table H.1 Summary of Percentage of Marker Methylation, IRB#011-030 Cohort

Patient #	SOCS1	RUNX3	MLH1	NEUROG1	CACNAG1	CIMP?
1	NA	NA	NA	NA	NA	NA
2	2	1	2	16	13	
3	18	3	2	8	11	
4	2	2	1	22	3	
5	9	2	2	25	2	
6	2	2	1	13	3	
7	2	2	2	11	14	
8	3	2	1	18	3	
9	2	13	2	52	27	
10	NA	NA	NA	NA	NA	NA
11	12	31	1	31	37	CIMP
12	8	3	1	36	4	
13	NA	NA	NA	NA	NA	NA
14	2	2	2	23	3	
15	2	2	1	16	3	
16	4	2	4	3	4	
17	5	0	0	13	2	
18	NA	NA	NA	NA	NA	NA
19	2	1	0	29	2	
20	1	2	0	26	2	
21	1	29	1	9	27	
22	2	3	1	22	4	
23	1	25	0	0	6	
24	2	30	2	2	3	
25	2	2	1	9	2	
26	2	2	2	4	2	
27a	2	3	2	21	3	
27b	2	2	1	26	1	
28	NA	NA	NA	NA	NA	NA
29	2	5	1	6	2	
30	NA	NA	NA	NA	NA	NA
31	4	25	5	11	6	CIMP
32	6	11	1	40	4	CIMP
33	2	2	1	22	3	
34	2	3	1	29	3	
35	17	2	0	30	2	
36	2	2	1	17	3	
37	2	2	1	12	7	

Table H.1 Summary of Percentage of Marker Methylation, IRB#011-030 Cohort -- continued

Patient #	SOCS1	RUNX3	MLH1	NEUROG1	CACNAG1	CIMP?
38	2	2	1	26	3	
39	46	45	62	17	45	CIMP
40	2	2	0	41	2	
41a	2	2	0	10	12	
41b	3	3	2	40	3	
42	3	3	1	10	25	
43	2	2	0	16	2	
44	2	2	2	14	4	
45	4	4	1	40	4	
46	2	2	5	76	13	
47	11	11	2	28	2	
48	NA	NA	NA	NA	NA	NA
49	NA	NA	NA	NA	NA	NA

APPENDIX I

I In Silico Testing of Primers Using UCSC Genome Browser

CCL2

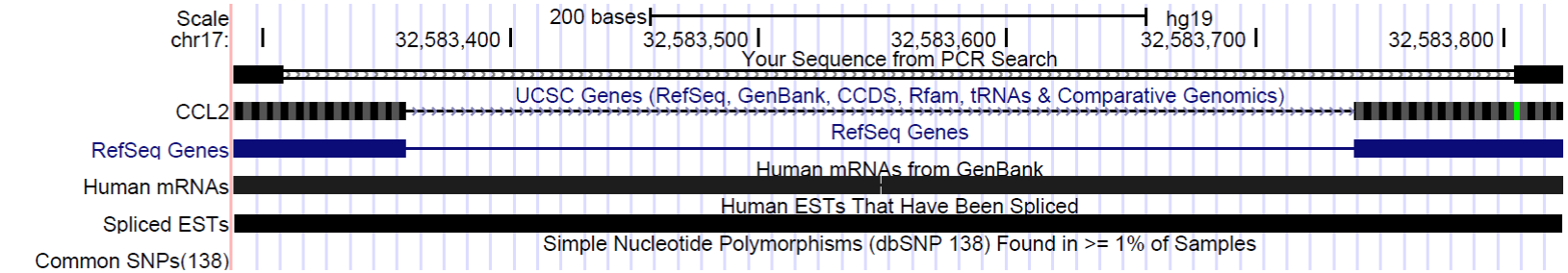

CCL5

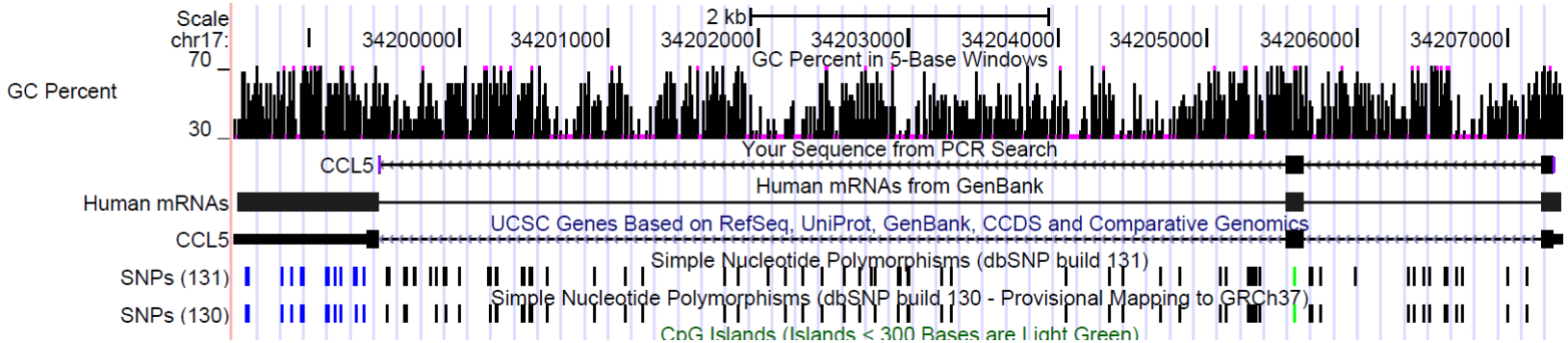

CCL11

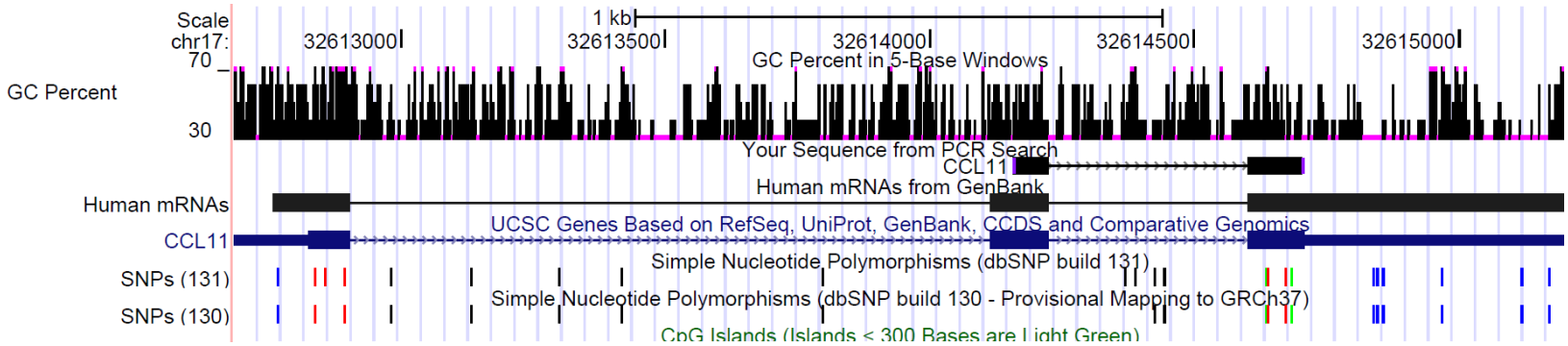
Scale
chr17:
1 kb
32613000
32613500
32614000
32614500
32615000
70
GC Percent
30
GC Percent in 5-Base Windows
Your Sequence from PCR Search
CCL11
Human mRNAs
Human mRNAs from GenBank
CCL11
UCSC Genes Based on RefSeq, UniProt, GenBank, CCDS and Comparative Genomics
SNPs (131)
Simple Nucleotide Polymorphisms (dbSNP build 131)
SNPs (130)
Simple Nucleotide Polymorphisms (dbSNP build 130 - Provisional Mapping to GRCh37)
CpG Islands (Islands < 300 Bases are Light Green)

CD8A

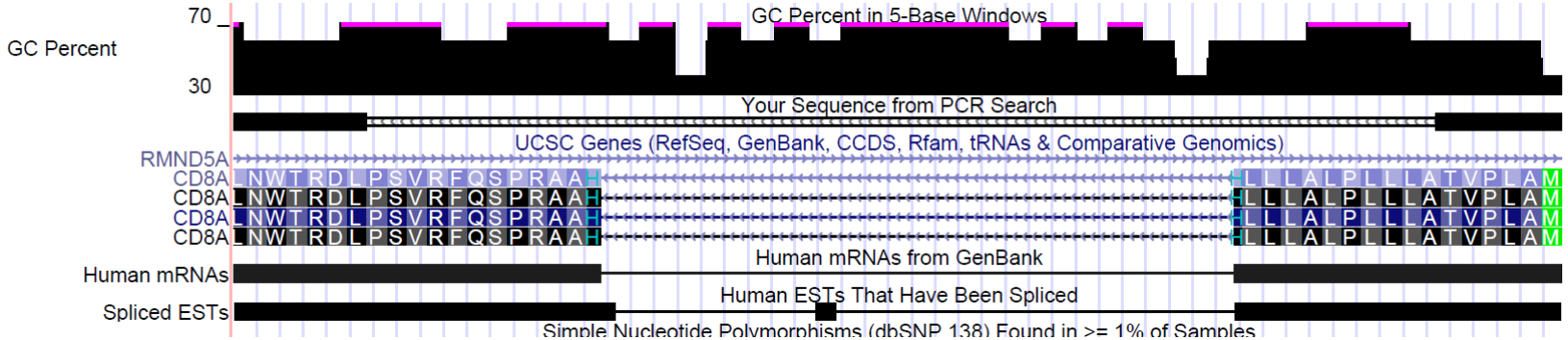
70
GC Percent
30
GC Percent in 5-Base Windows
Your Sequence from PCR Search
UCSC Genes (RefSeq, GenBank, CCDS, Rfam, tRNAs & Comparative Genomics)
RMND5A
CD8A
CD8A
CD8A
CD8A
Human mRNAs
Human mRNAs from GenBank
Spliced ESTs
Human ESTs That Have Been Spliced
Simple Nucleotide Polymorphisms (dbSNP 138) Found in >= 1% of Samples

CXCL9

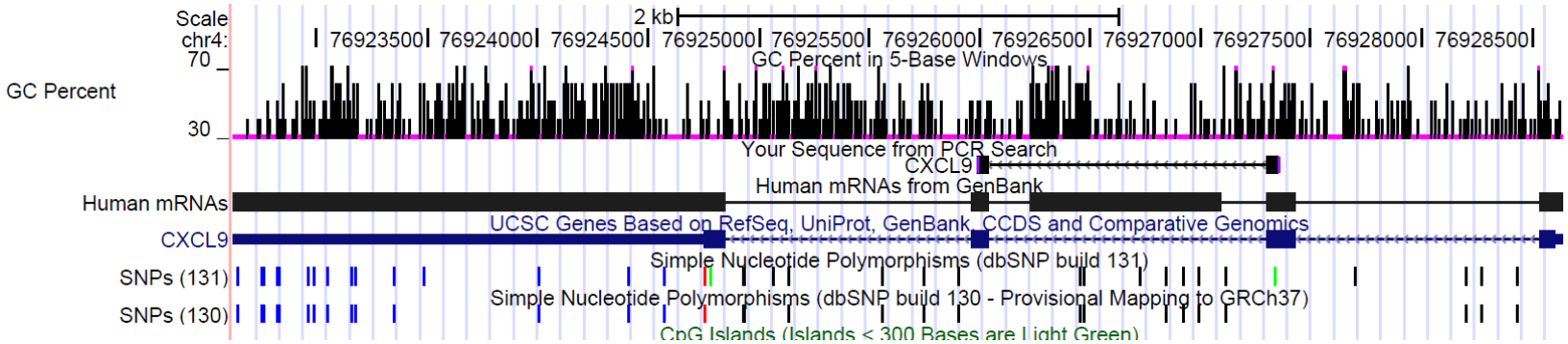

CXCL10

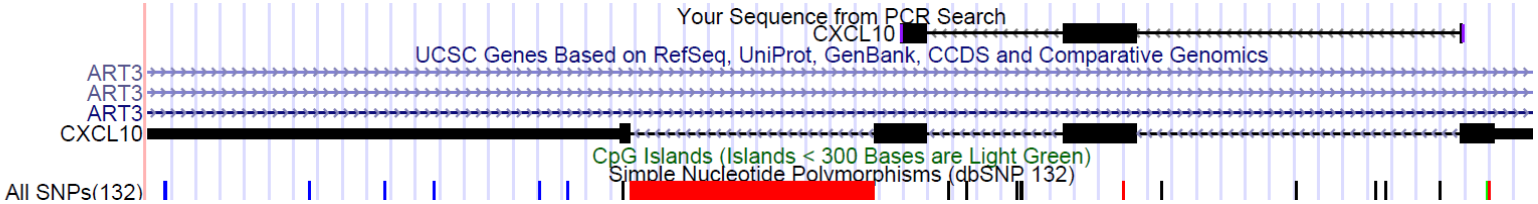

CX3CL1

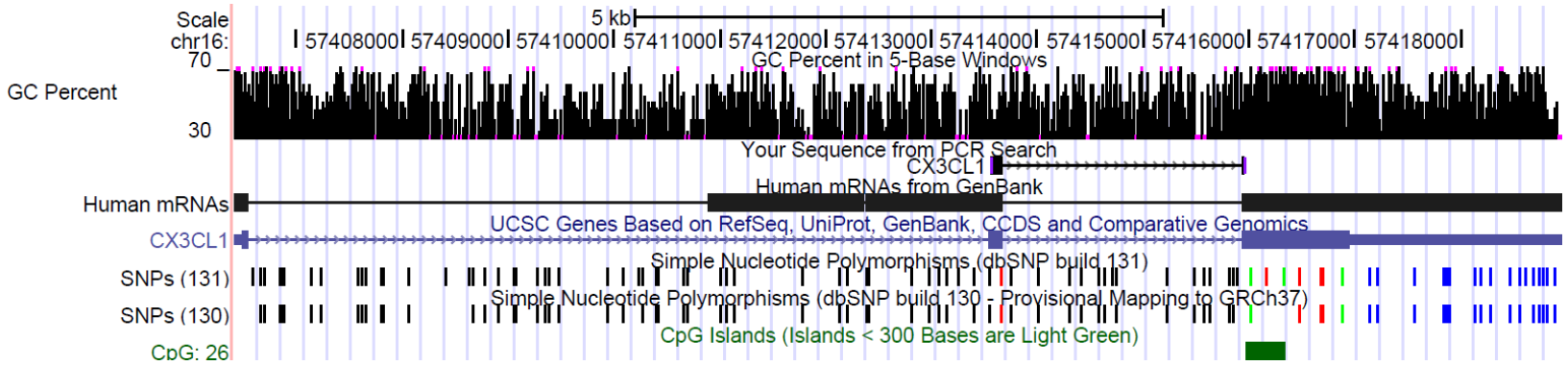

GAPDH

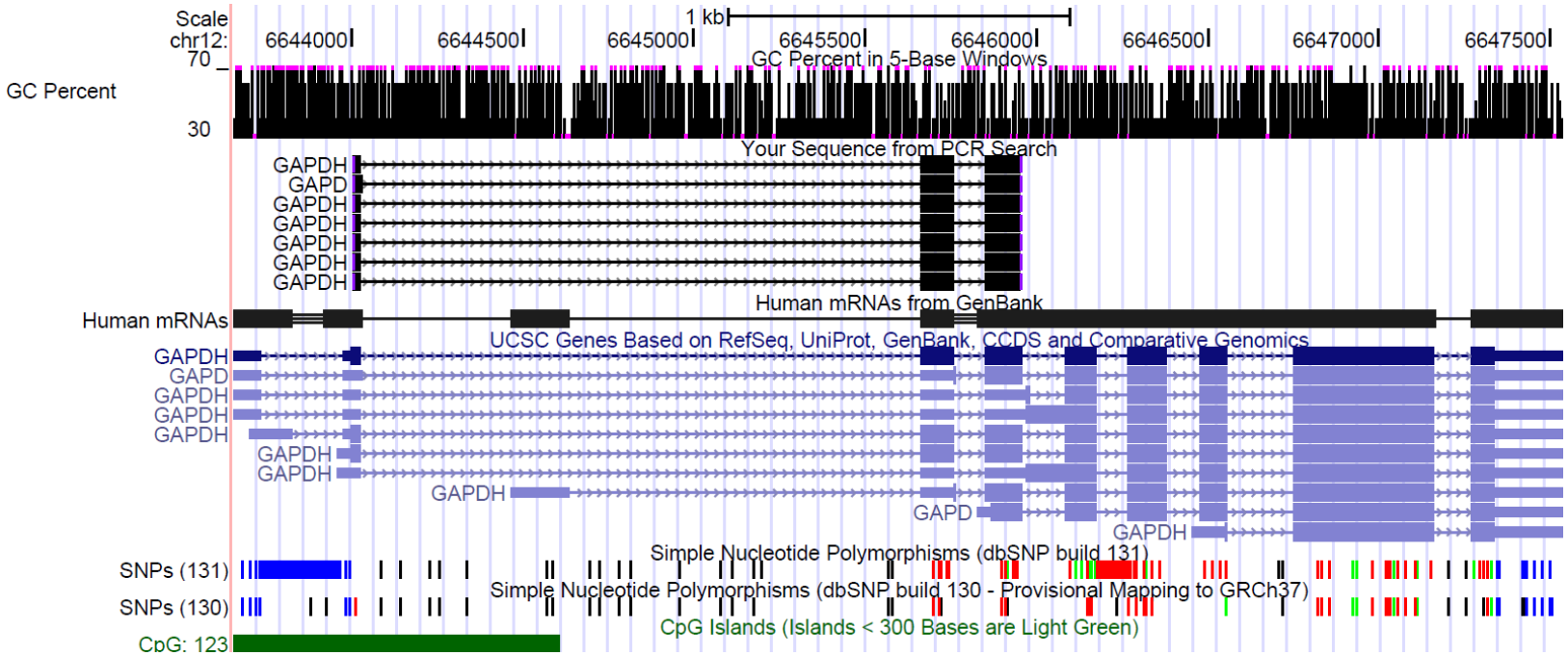
Scale
chr12:
1 kb
6644000
6644500
6645000
6645500
6646000
6646500
6647000
6647500
GC Percent in 5-Base Windows
GC Percent
70
30
Your Sequence from PCR Search
GAPDH
GAPD
Human mRNAs
Human mRNAs from GenBank
UCSC Genes Based on RefSeq, UniProt, GenBank, CCDS and Comparative Genomics
SNPs (131)
Simple Nucleotide Polymorphisms (dbSNP build 131)
SNPs (130)
Simple Nucleotide Polymorphisms (dbSNP build 130 - Provisional Mapping to GRCh37)
CpG: 123
CpG Islands (Islands < 300 Bases are Light Green)

GATA3

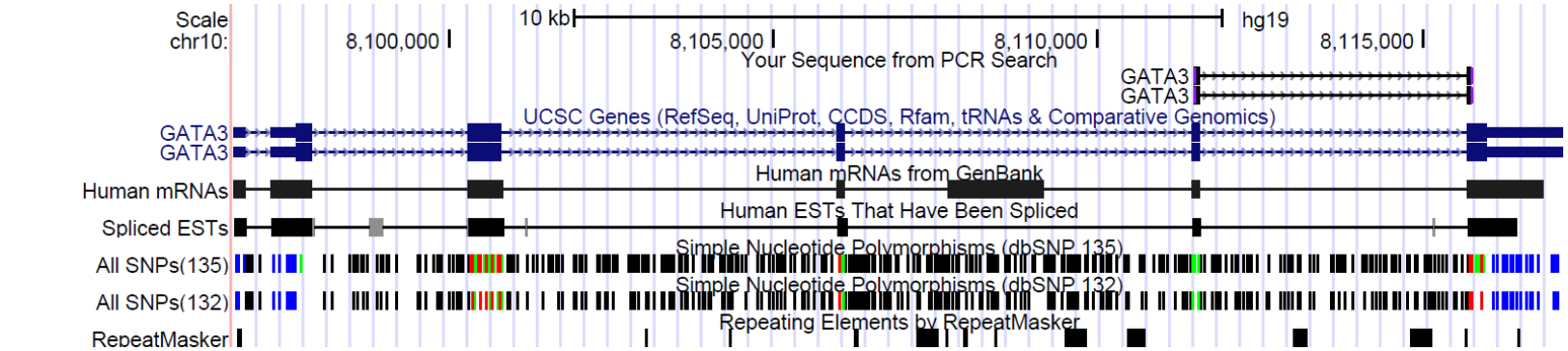
Scale
chr10:
10 kb
hg19
8,100,000
8,105,000
8,110,000
8,115,000
Your Sequence from PCR Search
GATA3
GATA3
UCSC Genes (RefSeq, UniProt, CCDS, Rfam, tRNAs & Comparative Genomics)
GATA3
GATA3
Human mRNAs from GenBank
Human mRNAs
Human ESTs That Have Been Spliced
Spliced ESTs
Simple Nucleotide Polymorphisms (dbSNP 135)
All SNPs(135)
Simple Nucleotide Polymorphisms (dbSNP 132)
All SNPs(132)
Repeating Elements by RepeatMasker
RepeatMasker

GNLY

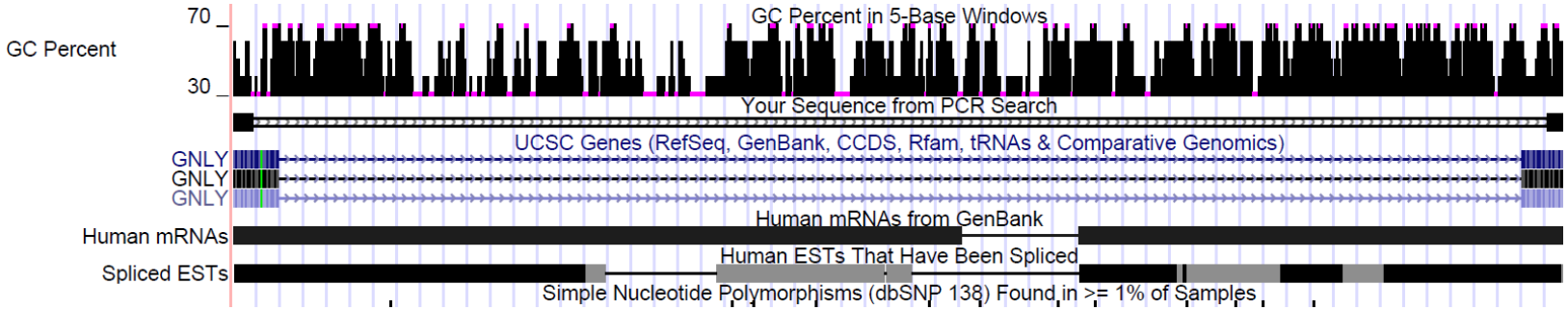
GC Percent
70
30
GC Percent in 5-Base Windows
Your Sequence from PCR Search
UCSC Genes (RefSeq, GenBank, CCDS, Rfam, tRNAs & Comparative Genomics)
GNLY
GNLY
GNLY
Human mRNAs from GenBank
Human mRNAs
Human ESTs That Have Been Spliced
Spliced ESTs
Simple Nucleotide Polymorphisms (dbSNP 138) Found in >= 1% of Samples

GZMB

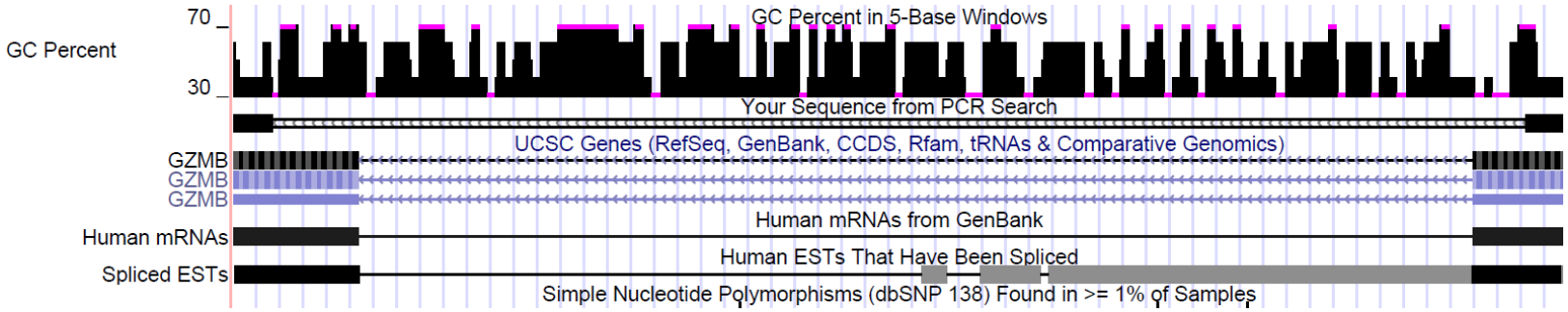
GC Percent
70
30
GC Percent in 5-Base Windows
Your Sequence from PCR Search
UCSC Genes (RefSeq, GenBank, CCDS, Rfam, tRNAs & Comparative Genomics)
GZMB
GZMB
GZMB
Human mRNAs
Human mRNAs from GenBank
Spliced ESTs
Human ESTs That Have Been Spliced
Simple Nucleotide Polymorphisms (dbSNP 138) Found in >= 1% of Samples

ICAM1

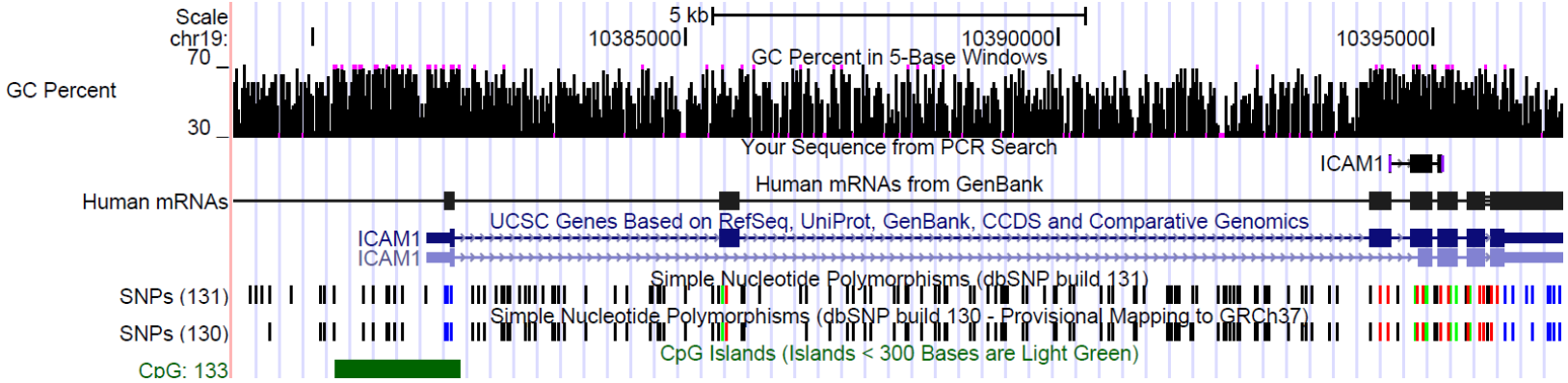
Scale
chr19:
5 kb
10385000
10390000
10395000
GC Percent
70
30
GC Percent in 5-Base Windows
Your Sequence from PCR Search
ICAM1
Human mRNAs
Human mRNAs from GenBank
UCSC Genes Based on RefSeq, UniProt, GenBank, CCDS and Comparative Genomics
ICAM1
ICAM1
Simple Nucleotide Polymorphisms (dbSNP build 131)
SNPs (131)
Simple Nucleotide Polymorphisms (dbSNP build 130 - Provisional Mapping to GRCh37)
SNPs (130)
CpG Islands (Islands < 300 Bases are Light Green)
CpG: 133

IFNG

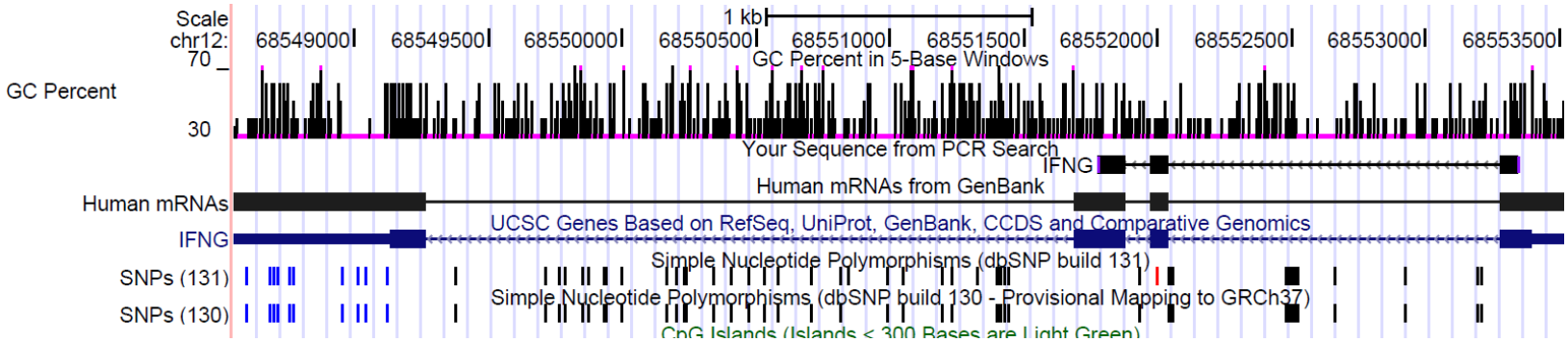

IRF1

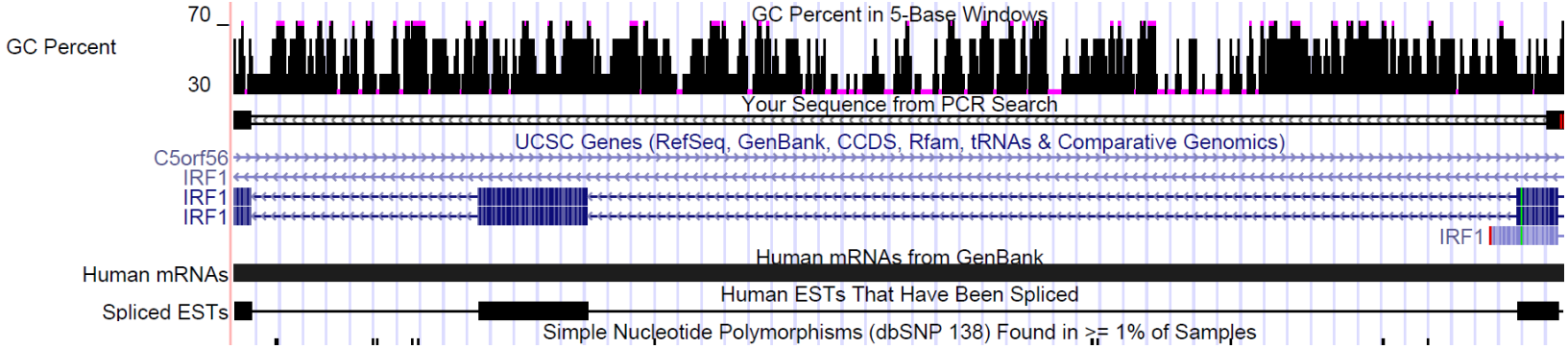

TBX21

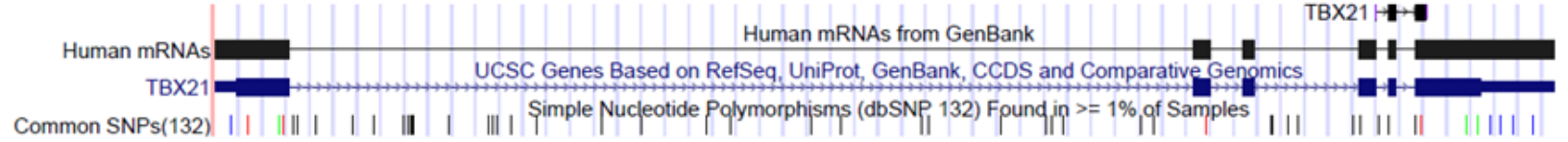

BIBLIOGRAPHY

Aaltonen, L.A., Peltomaki, P., Leach, F.S., Sistonen, P., Pylkkanen, L., Mecklin, J.P., Jarvinen, H., Powell, S.M., Jen, J., and Hamilton, S.R., (1993). Clues to the pathogenesis of familial colorectal cancer. Science *260* , 812-816.

Ajioka, Y., Allison, L.J., and Jass, J.R., (1996). Significance of MUC1 and MUC2 mucin expression in colorectal cancer. J. Clin. Pathol. *49* , 560-564.

Alberts, B., Johnson, A., Lewis, J., Raff, M., and Roberts, K., (2008). Molecular Biology of the Cell (270 Madison Avenue, New York, NY 10016.: Garland Science, Taylor & Francis Group, LLC).

Altman, D.G., Bland, J.M., (2011). How to obtain the confidence interval from a P value. BMJ *343* , d2090.

Alvarez, D.F., Helm, K., Degregori, J., Roederer, M., and Majka, S., (2010). Publishing flow cytometry data. Am. J. Physiol. Lung Cell. Mol. Physiol. *298* , L127-30.

Anitei, M.G., Zeitoun, G., Mlecnik, B., Marliot, F., Haicheur, N., Todosi, A.M., Kirilovsky, A., Lagorce, C., Bindea, G., Ferariu, D., Danciu, M., Bruneval, P., Scripcariu, V., Chevallier, J.M., Zinzindohoue, F., Berger, A., Galon, J., and Pages, F., (2014). Prognostic and predictive values of the immunoscore in patients with rectal cancer. Clin. Cancer Res. *20* , 1891-1899.

Aspord, C., Pedroza-Gonzalez, A., Gallegos, M., Tindle, S., Burton, E.C., Su, D., Marches, F., Banchereau, J., and Palucka, A.K., (2007). Breast cancer instructs dendritic cells to prime interleukin 13-secreting CD4+ T cells that facilitate tumor development. J. Exp. Med. *204* , 1037-1047.

Baier, G., Wagner, J., (2009). PKC inhibitors: potential in T cell-dependent immune diseases. Curr. Opin. Cell Biol. *21* , 262-267.

Baker, S.J., Fearon, E.R., Nigro, J.M., Hamilton, S.R., Preisinger, A.C., Jessup, J.M., vanTuinen, P., Ledbetter, D.H., Barker, D.F., Nakamura, Y., White, R., and Vogelstein, B., (1989). Chromosome 17 deletions and p53 gene mutations in colorectal carcinomas. Science *244* , 217-221.

Balkwill, F., (2004). Cancer and the chemokine network. Nat. Rev. Cancer. *4* , 540-550.

Banerjea, A., Ahmed, S., Hands, R.E., Huang, F., Han, X., Shaw, P.M., Feakins, R., Bustin, S.A., and Dorudi, S., (2004). Colorectal cancers with microsatellite instability display mRNA expression signatures characteristic of increased immunogenicity. Mol. Cancer. *3* , 21.

Banerjee, A., Schambach, F., DeJong, C.S., Hammond, S.M., and Reiner, S.L., (2010). Micro-RNA-155 inhibits IFN-gamma signaling in CD4+ T cells. Eur. J. Immunol. *40* , 225-231.

Bartel, D.P., (2009). MicroRNAs: target recognition and regulatory functions. Cell *136* , 215-233.

Bauer, K., Michel, S., Reuschenbach, M., Nelius, N., von Knebel Doeberitz, M., and Kloor, M., (2011). Dendritic cell and macrophage infiltration in microsatellite-unstable and microsatellite-stable colorectal cancer. Fam. Cancer. *10* , 557-565.

Baumjohann, D., Ansel, K.M., (2013). MicroRNA-mediated regulation of T helper cell differentiation and plasticity. Nat. Rev. Immunol. *13* , 666-678.

Beahrs, O., Henson, D., Hutter, R., and Kennedy, B. (1993). Handbook for Staging of Cancer: From the Manual for Staging of Cancer, Fourth Edition. In: Anonymous Lippincott Williams & Wilkins) .

Bell, D., Chomarat, P., Broyles, D., Netto, G., Harb, G.M., Lebecque, S., Valladeau, J., Davoust, J., Palucka, K.A., and Banchereau, J., (1999). In breast carcinoma tissue, immature dendritic cells reside within the tumor, whereas mature dendritic cells are located in peritumoral areas. J. Exp. Med. *190* , 1417-1426.

Benevolo, M., Mottolese, M., Tremante, E., Rollo, F., Diodoro, M.G., Ercolani, C., Sperduti, I., Lo Monaco, E., Cosimelli, M., and Giacomini, P., (2011). High expression of HLA-E in colorectal carcinoma is associated with a favorable prognosis. J. Transl. Med. *9* , 184-5876-9-184.

Bennecke, M., Kriegl, L., Bajbouj, M., Retzlaff, K., Robine, S., Jung, A., Arkan, M.C., Kirchner, T., and Greten, F.R., (2010). Ink4a/Arf and oncogene-induced senescence prevent tumor progression during alternative colorectal tumorigenesis. Cancer. Cell. *18* , 135-146.

Bernal, M., Garcia-Alcalde, F., Concha, A., Cano, C., Blanco, A., Garrido, F., and Ruiz-Cabello, F., (2012). Genome-wide differential genetic profiling characterizes colorectal cancers with genetic instability and specific routes to HLA class I loss and immune escape. Cancer Immunol. Immunother. *61* , 803-816.

Berry, M.P., Graham, C.M., McNab, F.W., Xu, Z., Bloch, S.A., Oni, T., Wilkinson, K.A., Banchereau, R., Skinner, J., Wilkinson, R.J., Quinn, C., Blankenship, D., Dhawan, R., Cush, J.J., Mejias, A., Ramilo, O., Kon, O.M., Pascual, V., Banchereau, J., Chaussabel, D., and O'Garra, A., (2010). An interferon-inducible neutrophil-driven blood transcriptional signature in human tuberculosis. Nature *466* , 973-977.

Bindea, G., Mlecnik, B., Tosolini, M., Kirilovsky, A., Waldner, M., Obenauf, A.C., Angell, H., Fredriksen, T., Lafontaine, L., Berger, A., Bruneval, P., Fridman, W.H., Becker, C., Pages, F., Speicher, M.R., Trajanoski, Z., and Galon, J., (2013). Spatiotemporal dynamics of intratumoral immune cells reveal the immune landscape in human cancer. Immunity *39* , 782-795.

Bird, A.P., (1986). CpG-rich islands and the function of DNA methylation. Nature *321* , 209-213.

Bodmer, W.F., Bailey, C.J., Bodmer, J., Bussey, H.J., Ellis, A., Gorman, P., Lucibello, F.C., Murday, V.A., Rider, S.H., and Scambler, P., (1987). Localization of the gene for familial adenomatous polyposis on chromosome 5. Nature *328* , 614-616.

Boland, C.R., (2005). Evolution of the nomenclature for the hereditary colorectal cancer syndromes. Fam. Cancer. *4* , 211-218.

Boland, C.R., Goel, A., (2010). Microsatellite instability in colorectal cancer. Gastroenterology *138* , 2073-2087.e3.

Boland, C.R., Shin, S.K., and Goel, A., (2009). Promoter methylation in the genesis of gastrointestinal cancer. Yonsei Med. J. *50* , 309-321.

Boland, C.R., Luciani, M.G., Gasche, C., and Goel, A., (2005). Infection, inflammation, and gastrointestinal cancer. Gut *54* , 1321-1331.

Boland, C.R., Sato, J., Appelman, H.D., Bresalier, R.S., and Feinberg, A.P., (1995). Microallelotyping defines the sequence and tempo of allelic losses at tumour suppressor gene loci during colorectal cancer progression. Nat. Med. *1* , 902-909.

Boland, C.R., Thibodeau, S.N., Hamilton, S.R., Sidransky, D., Eshleman, J.R., Burt, R.W., Meltzer, S.J., Rodriguez-Bigas, M.A., Fodde, R., Ranzani, G.N., and Srivastava, S., (1998). A National Cancer Institute Workshop on Microsatellite Instability for cancer detection and familial predisposition: development of international criteria for the determination of microsatellite instability in colorectal cancer. Cancer Res. *58* , 5248-5257.

Bonecchi, R., Bianchi, G., Bordignon, P.P., D'Ambrosio, D., Lang, R., Borsatti, A., Sozzani, S., Allavena, P., Gray, P.A., Mantovani, A., and Sinigaglia, F., (1998). Differential expression of chemokine receptors and chemotactic responsiveness of type 1 T helper cells (Th1s) and Th2s. J. Exp. Med. *187* , 129-134.

Borenstein, M., Higgins, J.P., (2013). Meta-analysis and subgroups. Prev. Sci. *14* , 134-143.

Branch, P., Hampson, R., and Karran, P., (1995). DNA mismatch binding defects, DNA damage tolerance, and mutator phenotypes in human colorectal carcinoma cell lines. Cancer Res. *55* , 2304-2309.

Branch, P., Aquilina, G., Bignami, M., and Karran, P., (1993). Defective mismatch binding and a mutator phenotype in cells tolerant to DNA damage. Nature *362* , 652-654.

Breitfeld, D., Ohl, L., Kremmer, E., Ellwart, J., Sallusto, F., Lipp, M., and Forster, R., (2000). Follicular B helper T cells express CXC chemokine receptor 5, localize to B cell follicles, and support immunoglobulin production. J. Exp. Med. *192* , 1545-1552.

Bronevetsky, Y., Villarino, A.V., Eisley, C.J., Barbeau, R., Barczak, A.J., Heinz, G.A., Kremmer, E., Heissmeyer, V., McManus, M.T., Erle, D.J., Rao, A., and Ansel, K.M., (2013). T cell activation induces proteasomal degradation of Argonaute and rapid remodeling of the microRNA repertoire. J. Exp. Med. *210* , 417-432.

Buckowitz, A., Knaebel, H.P., Benner, A., Blaker, H., Gebert, J., Kienle, P., von Knebel Doeberitz, M., and Kloor, M., (2005). Microsatellite instability in colorectal cancer is associated with local lymphocyte infiltration and low frequency of distant metastases. Br. J. Cancer *92* , 1746-1753.

Bui, J.D., Carayannopoulos, L.N., Lanier, L.L., Yokoyama, W.M., and Schreiber, R.D., (2006). IFN-dependent down-regulation of the NKG2D ligand H60 on tumors. J. Immunol. *176* , 905-913.

Burnet, M., (1957). Cancer; a biological approach. I. The processes of control. Br. Med. J. *1* , 779-786.

Cancer Genome Atlas Research Network, Weinstein, J.N., Collisson, E.A., Mills, G.B., Shaw, K.R., Ozenberger, B.A., Ellrott, K., Shmulevich, I., Sander, C., and Stuart, J.M., (2013). The Cancer Genome Atlas Pan-Cancer analysis project. Nat. Genet. *45* , 1113-1120.

Carethers, J.M., Smith, E.J., Behling, C.A., Nguyen, L., Tajima, A., Doctolero, R.T., Cabrera, B.L., Goel, A., Arnold, C.A., Miyai, K., and Boland, C.R., (2004). Use of 5-fluorouracil and survival in patients with microsatellite-unstable colorectal cancer. Gastroenterology *126* , 394-401.

Chang, E.Y., Dorsey, P.B., Frankhouse, J., Lee, R.G., Walts, D., Johnson, W., Anadiotis, G., and Johnson, N., (2009). Combination of microsatellite instability and lymphocytic infiltrate as a prognostic indicator in colon cancer. Arch. Surg. *144* , 511-515.

Chendrimada, T.P., Finn, K.J., Ji, X., Baillat, D., Gregory, R.I., Liebhaber, S.A., Pasquinelli, A.E., and Shiekhattar, R., (2007). MicroRNA silencing through RISC recruitment of eIF6. Nature *447* , 823-828.

Chiba, T., Ohtani, H., Mizoi, T., Naito, Y., Sato, E., Nagura, H., Ohuchi, A., Ohuchi, K., Shiiba, K., Kurokawa, Y., and Satomi, S., (2004). Intraepithelial CD8+ T-cell-count becomes a prognostic factor after a longer follow-up period in human colorectal carcinoma: possible association with suppression of micrometastasis. Br. J. Cancer *91* , 1711-1717.

Chou, J., Provot, S., and Werb, Z., (2010). GATA3 in development and cancer differentiation: cells GATA have it! J. Cell. Physiol. *222* , 42-49.

Clarke, S.L., Betts, G.J., Plant, A., Wright, K.L., El-Shanawany, T.M., Harrop, R., Torkington, J., Rees, B.I., Williams, G.T., Gallimore, A.M., and Godkin, A.J., (2006). CD4+CD25+FOXP3+ regulatory T cells suppress anti-tumor immune responses in patients with colorectal cancer. PLoS One *1* , e129.

Cole, K.E., Strick, C.A., Paradis, T.J., Ogborne, K.T., Loetscher, M., Gladue, R.P., Lin, W., Boyd, J.G., Moser, B., Wood, D.E., Sahagan, B.G., and Neote, K., (1998). Interferon-inducible T cell alpha chemoattractant (I-TAC): a novel non-ELR CXC chemokine with potent activity on activated T cells through selective high affinity binding to CXCR3. J. Exp. Med. *187* , 2009-2021.

Contasta, I., Berghella, A.M., Pellegrini, P., and Adorno, D., (2003). Passage from normal mucosa to adenoma and colon cancer: alteration of normal sCD30 mechanisms regulating TH1/TH2 cell functions. Cancer Biother. Radiopharm. *18* , 549-557.

Correale, P., Rotundo, M.S., Botta, C., Del Vecchio, M.T., Tassone, P., and Tagliaferri, P., (2012). Tumor infiltration by chemokine receptor 7 (CCR7)(+) T-lymphocytes is a favorable prognostic factor in metastatic colorectal cancer. Oncoimmunology *1* , 531-532.

Correale, P., Rotundo, M.S., Del Vecchio, M.T., Remondo, C., Migali, C., Ginanneschi, C., Tsang, K.Y., Licchetta, A., Mannucci, S., Loiacono, L., Tassone, P., Francini, G., and Tagliaferri, P., (2010). Regulatory (FoxP3+) T-cell tumor infiltration is a favorable prognostic factor in advanced colon cancer patients undergoing chemo or chemoimmunotherapy. J. Immunother. *33* , 435-441.

Csiszar, A., Szentes, T., Haraszti, B., Balazs, A., Petranyi, G.G., and Pocsik, E., (2004). The pattern of cytokine gene expression in human colorectal carcinoma. Pathol. Oncol. Res. *10* , 109-116.

Cui, G., Florholmen, J., (2008). Polarization of cytokine profile from Th1 into Th2 along colorectal adenoma-carcinoma sequence: implications for the biotherapeutic target? Inflamm. Allergy Drug Targets *7* , 94-97.

Cui, G., Goll, R., Olsen, T., Steigen, S.E., Husebekk, A., Vonen, B., and Florholmen, J., (2007). Reduced expression of microenvironmental Th1 cytokines accompanies adenomas-carcinomas sequence of colorectum. Cancer Immunol. Immunother. *56* , 985-995.

Dahlin, A.M., Henriksson, M.L., Van Guelpen, B., Stenling, R., Oberg, A., Rutegard, J., and Palmqvist, R., (2011). Colorectal cancer prognosis depends on T-cell infiltration and molecular characteristics of the tumor. Mod. Pathol. *24* , 671-682.

de Miranda, N.F., Goudkade, D., Jordanova, E.S., Tops, C.M., Hes, F.J., Vasen, H.F., van Wezel, T., and Morreau, H., (2012). Infiltration of Lynch colorectal cancers by activated immune cells associates with early staging of the primary tumor and absence of lymph node metastases. Clin. Cancer Res. *18* , 1237-1245.

deLeeuw, R.J., Kost, S.E., Kakal, J.A., and Nelson, B.H., (2012). The prognostic value of FoxP3+ tumor-infiltrating lymphocytes in cancer: a critical review of the literature. Clin. Cancer Res. *18* , 3022-3029.

Dolcetti, R., Viel, A., Doglioni, C., Russo, A., Guidoboni, M., Capozzi, E., Vecchiato, N., Macri, E., Fornasarig, M., and Boiocchi, M., (1999). High prevalence of activated intraepithelial cytotoxic T lymphocytes and increased neoplastic cell apoptosis in colorectal carcinomas with microsatellite instability. Am. J. Pathol. *154* , 1805-1813.

Dong, C., (2008). TH17 cells in development: an updated view of their molecular identity and genetic programming. Nat. Rev. Immunol. *8* , 337-348.

Drescher, K.M., Sharma, P., Watson, P., Gatalica, Z., Thibodeau, S.N., and Lynch, H.T., (2009). Lymphocyte recruitment into the tumor site is altered in patients with MSI-H colon cancer. Fam. Cancer. *8* , 231-239.

Dudda, J.C., Salaun, B., Ji, Y., Palmer, D.C., Monnot, G.C., Merck, E., Boudousquie, C., Utzschneider, D.T., Escobar, T.M., Perret, R., Muljo, S.A., Hebeisen, M., Rufer, N., Zehn, D., Donda, A., Restifo, N.P., Held, W., Gattinoni, L., and Romero, P., (2013). MicroRNA-155 is required for effector CD8+ T cell responses to virus infection and cancer. Immunity *38* , 742-753.

Dunn, G.P., Koebel, C.M., and Schreiber, R.D., (2006). Interferons, immunity and cancer immunoediting. Nat. Rev. Immunol. *6* , 836-848.

Dunn, G.P., Old, L.J., and Schreiber, R.D., (2004). The three Es of cancer immunoediting. Annu. Rev. Immunol. *22* , 329-360.

Dunn, G.P., Bruce, A.T., Ikeda, H., Old, L.J., and Schreiber, R.D., (2002). Cancer immunoediting: from immunosurveillance to tumor escape. Nat. Immunol. *3* , 991-998.

Dvorak, H.F., (1986). Tumors: wounds that do not heal. Similarities between tumor stroma generation and wound healing. N. Engl. J. Med. *315* , 1650-1659.

El-Bchiri, J., Guilloux, A., Dartigues, P., Loire, E., Mercier, D., Buhard, O., Sobhani, I., de la Grange, P., Auboeuf, D., Praz, F., Flejou, J.F., and Duval, A., (2008). Nonsense-mediated mRNA decay impacts MSI-driven carcinogenesis and anti-tumor immunity in colorectal cancers. PLoS One *3* , e2583.

Engelhardt, M., Drullinsky, P., Guillem, J., and Moore, M.A., (1997). Telomerase and telomere length in the development and progression of premalignant lesions to colorectal cancer. Clin. Cancer Res. *3* , 1931-1941.

Erreni, M., Bianchi, P., Laghi, L., Mirolo, M., Fabbri, M., Locati, M., Mantovani, A., and Allavena, P., (2009). Expression of chemokines and chemokine receptors in human colon cancer. Methods Enzymol. *460* , 105-121.

Esteller, M., (2008). Epigenetics in cancer. N. Engl. J. Med. *358* , 1148-1159.

Esteller, M., Sparks, A., Toyota, M., Sanchez-Cespedes, M., Capella, G., Peinado, M.A., Gonzalez, S., Tarafa, G., Sidransky, D., Meltzer, S.J., Baylin, S.B., and Herman, J.G., (2000). Analysis of adenomatous polyposis coli promoter hypermethylation in human cancer. Cancer Res. *60* , 4366-4371.

Evans, C., Morrison, I., Heriot, A.G., Bartlett, J.B., Finlayson, C., Dalgleish, A.G., and Kumar, D., (2006). The correlation between colorectal cancer rates of proliferation and apoptosis and systemic cytokine levels; plus their influence upon survival. Br. J. Cancer *94* , 1412-1419.

Fearon, E.R., Vogelstein, B., (1990). A genetic model for colorectal tumorigenesis. Cell *61* , 759-767.

Fearon, E.R., Hamilton, S.R., and Vogelstein, B., (1987). Clonal analysis of human colorectal tumors. Science *238* , 193-197.

Fishel, R., (2001). The selection for mismatch repair defects in hereditary nonpolyposis colorectal cancer: revising the mutator hypothesis. Cancer Res. *61* , 7369-7374.

Fishel, R., (1999). Signaling mismatch repair in cancer. Nat. Med. *5* , 1239-1241.

Fishel, R., Lescoe, M.K., Rao, M.R., Copeland, N.G., Jenkins, N.A., Garber, J., Kane, M., and Kolodner, R., (1993). The human mutator gene homolog MSH2 and its association with hereditary nonpolyposis colon cancer. Cell *75* , 1027-1038.

Fleming, N.I., Jorissen, R.N., Mouradov, D., Christie, M., Sakthianandeswaren, A., Palmieri, M., Day, F., Li, S., Tsui, C., Lipton, L., Desai, J., Jones, I.T., McLaughlin, S., Ward, R.L., Hawkins, N.J., Ruszkiewicz, A.R., Moore, J., Zhu, H.J., Mariadason, J.M., Burgess, A.W., Busam, D., Zhao, Q., Strausberg, R.L., Gibbs, P., and Sieber, O.M., (2013). SMAD2, SMAD3 and SMAD4 mutations in colorectal cancer. Cancer Res. *73* , 725-735.

Forster, R., Davalos-Misslitz, A.C., and Rot, A., (2008). CCR7 and its ligands: balancing immunity and tolerance. Nat. Rev. Immunol. *8* , 362-371.

Frey, D.M., Droeser, R.A., Viehl, C.T., Zlobec, I., Lugli, A., Zingg, U., Oertli, D., Kettelhack, C., Terracciano, L., and Tornillo, L., (2010). High frequency of tumor-infiltrating FOXP3(+) regulatory T cells predicts improved survival in mismatch repair-proficient colorectal cancer patients. Int. J. Cancer *126* , 2635-2643.

Fridman, W.H., Galon, J., Dieu-Nosjean, M.C., Cremer, I., Fisson, S., Damotte, D., Pages, F., Tartour, E., and Sautes-Fridman, C., (2011). Immune infiltration in human cancer: prognostic significance and disease control. Curr. Top. Microbiol. Immunol. *344* , 1-24.

Friedberg, E.C., Walker, G.C., Siede, W., Wood, R.D., Schultz, R.A., and Ellenberger, T., (2006). DNA Repair and Mutagenesis (USA.: ASM Press).

Fruci, D., Lo Monaco, E., Cifaldi, L., Locatelli, F., Tremante, E., Benevolo, M., and Giacomini, P., (2013). T and NK cells: two sides of tumor immunoevasion. J. Transl. Med. *11* , 30-5876-11-30.

Funada, Y., Noguchi, T., Kikuchi, R., Takeno, S., Uchida, Y., and Gabbert, H.E., (2003). Prognostic significance of CD8+ T cell and macrophage peritumoral infiltration in colorectal cancer. Oncol. Rep. *10* , 309-313.

Galon, J., Fridman, W.H., and Pages, F., (2007). The adaptive immunologic microenvironment in colorectal cancer: a novel perspective. Cancer Res. *67* , 1883-1886.

Galon, J., Costes, A., Sanchez-Cabo, F., Kirilovsky, A., Mlecnik, B., Lagorce-Pages, C., Tosolini, M., Camus, M., Berger, A., Wind, P., Zinzindohoue, F., Bruneval, P., Cugnenc, P.H., Trajanoski, Z., Fridman, W.H., and Pages, F., (2006). Type, density, and location of immune cells within human colorectal tumors predict clinical outcome. Science *313* , 1960-1964.

Galon, J., Mlecnik, B., Bindea, G., Angell, H.K., Berger, A., Lagorce, C., Lugli, A., Zlobec, I., Hartmann, A., Bifulco, C., Nagtegaal, I.D., Palmqvist, R., Masucci, G.V., Botti, G., Tatangelo, F., Delrio, P., Maio, M., Laghi, L., Grizzi, F., Asslaber, M., D'Arrigo, C., Vidal-Vanaclocha, F., Zavadova, E., Chouchane, L., Ohashi, P.S., Hafezi-Bakhtiari, S., Wouters, B.G., Roehrl, M., Nguyen, L., Kawakami, Y., Hazama, S., Okuno, K., Ogino, S., Gibbs, P., Waring, P., Sato, N., Torigoe, T., Itoh, K., Patel, P.S., Shukla, S.N., Wang, Y., Kopetz, S., Sinicrope, F.A., Scripcariu, V., Ascierto, P.A., Marincola, F.M., Fox, B.A., and Pages, F., (2014). Towards the introduction of the 'Immunoscore' in the classification of malignant tumours. J. Pathol. *232* , 199-209.

Gardiner-Garden, M., Frommer, M., (1987). CpG islands in vertebrate genomes. J. Mol. Biol. *196* , 261-282.

Geigl, J.B., Obenauf, A.C., Schwarzbraun, T., and Speicher, M.R., (2008). Defining 'chromosomal instability'. Trends Genet. *24* , 64-69.

Gerlach, K., Hwang, Y., Nikolaev, A., Atreya, R., Dornhoff, H., Steiner, S., Lehr, H.A., Wirtz, S., Vieth, M., Waisman, A., Rosenbauer, F., McKenzie, A.N., Weigmann, B., and Neurath, M.F., (2014). TH9 cells that express the transcription factor PU.1 drive T cell-mediated colitis via IL-9 receptor signaling in intestinal epithelial cells. Nat. Immunol. *15* , 676-686.

Goel, A., Nagasaka, T., Hamelin, R., and Boland, C.R., (2010a). An optimized pentaplex PCR for detecting DNA mismatch repair-deficient colorectal cancers. PLoS One *5* , e9393.

Goel, A., Nagasaka, T., Arnold, C.N., Inoue, T., Hamilton, C., Niedzwiecki, D., Compton, C., Mayer, R.J., Goldberg, R., Bertagnolli, M.M., and Boland, C.R., (2007). The CpG island methylator phenotype and chromosomal instability are inversely correlated in sporadic colorectal cancer. Gastroenterology *132* , 127-138.

Goel, A., Xicola, R.M., Nguyen, T.P., Doyle, B.J., Sohn, V.R., Bandipalliam, P., Rozek, L.S., Reyes, J., Cordero, C., Balaguer, F., Castells, A., Jover, R., Andreu, M., Syngal, S., Boland, C.R., and Llor, X., (2010b). Aberrant DNA methylation in hereditary nonpolyposis colorectal cancer without mismatch repair deficiency. Gastroenterology *138* , 1854-1862.

Golgher, D., Jones, E., Powrie, F., Elliott, T., and Gallimore, A., (2002). Depletion of CD25+ regulatory cells uncovers immune responses to shared murine tumor rejection antigens. Eur. J. Immunol. *32* , 3267-3275.

Gracias, D.T., Stelekati, E., Hope, J.L., Boesteanu, A.C., Doering, T.A., Norton, J., Mueller, Y.M., Fraietta, J.A., Wherry, E.J., Turner, M., and Katsikis, P.D., (2013). The microRNA miR-155 controls CD8(+) T cell responses by regulating interferon signaling. Nat. Immunol. *14* , 593-602.

Grivennikov, S.I., Karin, M., (2011). Inflammatory cytokines in cancer: tumour necrosis factor and interleukin 6 take the stage. Ann. Rheum. Dis. *70 Suppl 1* , i104-8.

Grivennikov, S.I., Greten, F.R., and Karin, M., (2010). Immunity, inflammation, and cancer. Cell *140* , 883-899.

Grivennikov, S.I., Wang, K., Mucida, D., Stewart, C.A., Schnabl, B., Jauch, D., Taniguchi, K., Yu, G.Y., Osterreicher, C.H., Hung, K.E., Datz, C., Feng, Y., Fearon, E.R., Oukka, M., Tessarollo, L., Coppola, V., Yarovinsky, F., Cheroutre, H., Eckmann, L., Trinchieri, G., and Karin, M., (2012). Adenoma-linked barrier defects and microbial products drive IL-23/IL-17-mediated tumour growth. Nature *491* , 254-258.

Groom, J.R., Luster, A.D., (2011). CXCR3 ligands: redundant, collaborative and antagonistic functions. Immunol. Cell Biol. *89* , 207-215.

Gryfe, R., Kim, H., Hsieh, E.T., Aronson, M.D., Holowaty, E.J., Bull, S.B., Redston, M., and Gallinger, S., (2000). Tumor microsatellite instability and clinical outcome in young patients with colorectal cancer. N. Engl. J. Med. *342* , 69-77.

Guarda, G., Hons, M., Soriano, S.F., Huang, A.Y., Polley, R., Martin-Fontecha, A., Stein, J.V., Germain, R.N., Lanzavecchia, A., and Sallusto, F., (2007). L-selectin-negative CCR7- effector and memory CD8+ T cells enter reactive lymph nodes and kill dendritic cells. Nat. Immunol. *8* , 743-752.

Guidoboni, M., Gafa, R., Viel, A., Doglioni, C., Russo, A., Santini, A., Del Tin, L., Macri, E., Lanza, G., Boiocchi, M., and Dolcetti, R., (2001). Microsatellite instability and high content of activated cytotoxic lymphocytes identify colon cancer patients with a favorable prognosis. Am. J. Pathol. *159* , 297-304.

Guo, H.S., Xie, Q., Fei, J.F., and Chua, N.H., (2005). MicroRNA directs mRNA cleavage of the transcription factor NAC1 to downregulate auxin signals for arabidopsis lateral root development. Plant Cell *17* , 1376-1386.

Haas, M., Dimmler, A., Hohenberger, W., Grabenbauer, G.G., Niedobitek, G., and Distel, L.V., (2009). Stromal regulatory T-cells are associated with a favourable prognosis in gastric cancer of the cardia. BMC Gastroenterol. *9* , 65-230X-9-65.

Haigis, K.M., Kendall, K.R., Wang, Y., Cheung, A., Haigis, M.C., Glickman, J.N., Niwa-Kawakita, M., Sweet-Cordero, A., Sebolt-Leopold, J., Shannon, K.M., Settleman, J., Giovannini, M., and Jacks, T., (2008). Differential effects of oncogenic K-Ras and N-Ras on proliferation, differentiation and tumor progression in the colon. Nat. Genet. *40* , 600-608.

Halama, N., Braun, M., Kahlert, C., Spille, A., Quack, C., Rahbari, N., Koch, M., Weitz, J., Kloor, M., Zoernig, I., Schirmacher, P., Brand, K., Grabe, N., and Falk, C.S., (2011a). Natural killer cells are scarce in colorectal carcinoma tissue despite high levels of chemokines and cytokines. Clin. Cancer Res. *17* , 678-689.

Halama, N., Michel, S., Kloor, M., Zoernig, I., Benner, A., Spille, A., Pommerencke, T., von Knebel, D.M., Folprecht, G., Luber, B., Feyen, N., Martens, U.M., Beckhove, P., Gnjatic, S., Schirmacher, P., Herpel, E., Weitz, J., Grabe, N., and Jaeger, D., (2011b). Localization and density of immune cells in the invasive margin of human colorectal cancer liver metastases are prognostic for response to chemotherapy. Cancer Res. *71* , 5670-5677.

Hanahan, D., Weinberg, R.A., (2011). Hallmarks of cancer: the next generation. Cell *144* , 646-674.

Hanahan, D., Weinberg, R.A., (2000). The hallmarks of cancer. Cell *100* , 57-70.

Harrington, L.E., Hatton, R.D., Mangan, P.R., Turner, H., Murphy, T.L., Murphy, K.M., and Weaver, C.T., (2005). Interleukin 17-producing CD4+ effector T cells develop via a lineage distinct from the T helper type 1 and 2 lineages. Nat. Immunol. *6* , 1123-1132.

Harris, C.C., (1996). P53 Tumor Suppressor Gene: from the Basic Research Laboratory to the Clinic--an Abridged Historical Perspective. Carcinogenesis *17* , 1187-1198.

Heusinkveld, M., van der Burg, S.H., (2011). Identification and manipulation of tumor associated macrophages in human cancers. J. Transl. Med. *9* , 216-5876-9-216.

Heusinkveld, M., de Vos van Steenwijk, P.J., Goedemans, R., Ramwadhdoebe, T.H., Gorter, A., Welters, M.J., van Hall, T., and van der Burg, S.H., (2011). M2 macrophages induced by prostaglandin E2 and IL-6 from cervical carcinoma are switched to activated M1 macrophages by CD4+ Th1 cells. J. Immunol. *187* , 1157-1165.

Higgins, J.P., Thompson, S.G., Deeks, J.J., and Altman, D.G., (2003). Measuring inconsistency in meta-analyses. BMJ *327* , 557-560.

Huffaker, T.B., Hu, R., Runtsch, M.C., Bake, E., Chen, X., Zhao, J., Round, J.L., Baltimore, D., and O'Connell, R.M., (2012). Epistasis between microRNAs 155 and 146a during T cell-mediated antitumor immunity. Cell. Rep. *2* , 1697-1709.

Ionov, Y., Peinado, M.A., Malkhosyan, S., Shibata, D., and Perucho, M., (1993). Ubiquitous somatic mutations in simple repeated sequences reveal a new mechanism for colonic carcinogenesis. Nature *363* , 558-561.

Issa, J.P., (2004). CpG island methylator phenotype in cancer. Nat. Rev. Cancer. *4* , 988-993.

Iyer, R.R., Pluciennik, A., Burdett, V., and Modrich, P.L., (2006). DNA mismatch repair: functions and mechanisms. Chem. Rev. *106* , 302-323.

Jascur, T., Boland, C.R., (2006). Structure and function of the components of the human DNA mismatch repair system. Int. J. Cancer *119* , 2030-2035.

Jass, J.R., (1986). Lymphocytic infiltration and survival in rectal cancer. J. Clin. Pathol. *39* , 585-589.

Jass, J.R., Do, K.A., Simms, L.A., Iino, H., Wynter, C., Pillay, S.P., Searle, J., Radford-Smith, G., Young, J., and Leggett, B., (1998). Morphology of sporadic colorectal cancer with DNA replication errors. Gut *42* , 673-679.

Jones, S., Chen, W.D., Parmigiani, G., Diehl, F., Beerenwinkel, N., Antal, T., Traulsen, A., Nowak, M.A., Siegel, C., Velculescu, V.E., Kinzler, K.W., Vogelstein, B., Willis, J., and Markowitz, S.D., (2008). Comparative lesion sequencing provides insights into tumor evolution. Proc. Natl. Acad. Sci. U. S. A. *105* , 4283-4288.

Kammertoens, T., Blankenstein, T., (2009). Making and circumventing tolerance to cancer. Eur. J. Immunol. *39* , 2345-2353.

Kane, M.F., Loda, M., Gaida, G.M., Lipman, J., Mishra, R., Goldman, H., Jessup, J.M., and Kolodner, R., (1997). Methylation of the hMLH1 promoter correlates with lack of expression of hMLH1 in sporadic colon tumors and mismatch repair-defective human tumor cell lines. Cancer Res. *57* , 808-811.

Kaplan, D.H., Shankaran, V., Dighe, A.S., Stockert, E., Aguet, M., Old, L.J., and Schreiber, R.D., (1998). Demonstration of an interferon gamma-dependent tumor surveillance system in immunocompetent mice. Proc. Natl. Acad. Sci. U. S. A. *95* , 7556-7561.

Karakas, B., Bachman, K.E., and Park, B.H., (2006). Mutation of the PIK3CA oncogene in human cancers. Br. J. Cancer *94* , 455-459.

Kent, W.J., Sugnet, C.W., Furey, T.S., Roskin, K.M., Pringle, T.H., Zahler, A.M., and Haussler, D., (2002). The human genome browser at UCSC. Genome Res. *12* , 996-1006.

Khong, H.T., Restifo, N.P., (2002). Natural selection of tumor variants in the generation of "tumor escape" phenotypes. Nat. Immunol. *3* , 999-1005.

Kikuchi, H., Itoh, J., and Fukuda, S., (2008). Chronic nicotine stimulation modulates the immune response of mucosal T cells to Th1-dominant pattern via nAChR by upregulation of Th1-specific transcriptional factor. Neurosci. Lett. *432* , 217-221.

Kim, C.H., Nagata, K., and Butcher, E.C., (2003). Dendritic cells support sequential reprogramming of chemoattractant receptor profiles during naive to effector T cell differentiation. J. Immunol. *171* , 152-158.

Kinzler, K.W., Vogelstein, B., (1996). Lessons from hereditary colorectal cancer. Cell *87* , 159-170.

Kloor, M., Michel, S., and von Knebel Doeberitz, M., (2010). Immune evasion of microsatellite unstable colorectal cancers. Int. J. Cancer *127* , 1001-1010.

Kloor, M., Michel, S., Buckowitz, B., Ruschoff, J., Buttner, R., Holinski-Feder, E., Dippold, W., Wagner, R., Tariverdian, M., Benner, A., Schwitalle, Y., Kuchenbuch, B., and von Knebel Doeberitz, M., (2007). Beta2-microglobulin mutations in microsatellite unstable colorectal tumors. Int. J. Cancer *121* , 454-458.

Knudson, A.G.,Jr, (1971). Mutation and cancer: statistical study of retinoblastoma. Proc. Natl. Acad. Sci. U. S. A. *68* , 820-823.

Koch, M., Beckhove, P., Op den Winkel, J., Autenrieth, D., Wagner, P., Nummer, D., Specht, S., Antolovic, D., Galindo, L., Schmitz-Winnenthal, F.H., Schirrmacher, V., Buchler, M.W., and Weitz, J., (2006). Tumor infiltrating T lymphocytes in colorectal cancer: Tumor-selective activation and cytotoxic activity in situ. Ann. Surg. *244* , 986-92; discussion 992-3.

Koelzer, V.H., Lugli, A., Dawson, H., Hadrich, M., Berger, M.D., Borner, M., Mallaev, M., Galvan, J.A., Amsler, J., Schnuriger, B., Zlobec, I., and Inderbitzin, D., (2014). CD8/CD45RO T-cell infiltration in endoscopic biopsies of colorectal cancer predicts nodal metastasis and survival. J. Transl. Med. *12* , 81-5876-12-81.

Koesters, R., Linnebacher, M., Coy, J.F., Germann, A., Schwitalle, Y., Findeisen, P., and von Knebel Doeberitz, M., (2004). WT1 is a tumor-associated antigen in colon cancer that can be recognized by in vitro stimulated cytotoxic T cells. Int. J. Cancer *109* , 385-392.

Koi, M., Umar, A., Chauhan, D.P., Cherian, S.P., Carethers, J.M., Kunkel, T.A., and Boland, C.R., (1994). Human chromosome 3 corrects mismatch repair deficiency and microsatellite instability and reduces N-methyl-N'-nitro-N-nitrosoguanidine tolerance in colon tumor cells with homozygous hMLH1 mutation. Cancer Res. *54* , 4308-4312.

Kong, D., Li, Y., Wang, Z., and Sarkar, F.H., (2011). Cancer Stem Cells and Epithelial-to-Mesenchymal Transition (EMT)-Phenotypic Cells: Are They Cousins or Twins? Cancers (Basel) *3* , 716-729.

Kordatou, Z., Kountourakis, P., and Papamichael, D., (2014). Treatment of older patients with colorectal cancer: a perspective review. Ther. Adv. Med. Oncol. *6* , 128-140.

Kryczek, I., Liu, R., Wang, G., Wu, K., Shu, X., Szeliga, W., Vatan, L., Finlayson, E., Huang, E., Simeone, D., Redman, B., Welling, T.H., Chang, A., and Zou, W., (2009). FOXP3 defines regulatory T cells in human tumor and autoimmune disease. Cancer Res. *69* , 3995-4000.

Kryczek, I., Lin, Y., Nagarsheth, N., Peng, D., Zhao, L., Zhao, E., Vatan, L., Szeliga, W., Dou, Y., Owens, S., Zgodzinski, W., Majewski, M., Wallner, G., Fang, J., Huang, E., and Zou, W., (2014). IL-22(+)CD4(+) T cells promote colorectal cancer stemness via STAT3 transcription factor activation and induction of the methyltransferase DOT1L. Immunity *40* , 772-784.

Ladoire, S., Martin, F., and Ghiringhelli, F., (2011). Prognostic role of FOXP3+ regulatory T cells infiltrating human carcinomas: the paradox of colorectal cancer. Cancer Immunol. Immunother. *60* , 909-918.

Laghi, L., Malesci, A., (2012). Microsatellite instability and therapeutic consequences in colorectal cancer. Dig. Dis. *30* , 304-309.

Langowski, J.L., Zhang, X., Wu, L., Mattson, J.D., Chen, T., Smith, K., Basham, B., McClanahan, T., Kastelein, R.A., and Oft, M., (2006). IL-23 promotes tumour incidence and growth. Nature *442* , 461-465.

Le Gouvello, S., Bastuji-Garin, S., Aloulou, N., Mansour, H., Chaumette, M.T., Berrehar, F., Seikour, A., Charachon, A., Karoui, M., Leroy, K., Farcet, J.P., and Sobhani, I., (2008). High prevalence of Foxp3 and IL17 in MMR-proficient colorectal carcinomas. Gut *57* , 772-779.

Leary, R.J., Lin, J.C., Cummins, J., Boca, S., Wood, L.D., Parsons, D.W., Jones, S., Sjoblom, T., Park, B.H., Parsons, R., Willis, J., Dawson, D., Willson, J.K., Nikolskaya, T., Nikolsky, Y., Kopelovich, L., Papadopoulos, N., Pennacchio, L.A., Wang, T.L., Markowitz, S.D., Parmigiani, G., Kinzler, K.W., Vogelstein, B., and Velculescu, V.E., (2008). Integrated analysis of homozygous deletions, focal amplifications, and sequence alterations in breast and colorectal cancers. Proc. Natl. Acad. Sci. U. S. A. *105* , 16224-16229.

Lee, S.Y., Miyai, K., Han, H.S., Hwang, D.Y., Seong, M.K., Chung, H., Jung, B.H., Devaraj, B., McGuire, K.L., and Carethers, J.M., (2012). Microsatellite instability, EMAST, and morphology associations with T cell infiltration in colorectal neoplasia. Dig. Dis. Sci. *57* , 72-78.

Lengauer, C., Kinzler, K.W., and Vogelstein, B., (1998). Genetic instabilities in human cancers. Nature *396* , 643-649.

Linnebacher, M., Gebert, J., Rudy, W., Woerner, S., Yuan, Y.P., Bork, P., and von Knebel Doeberitz, M., (2001). Frameshift peptide-derived T-cell epitopes: a source of novel tumor-specific antigens. Int. J. Cancer *93* , 6-11.

Loddenkemper, C., Schernus, M., Noutsias, M., Stein, H., Thiel, E., and Nagorsen, D., (2006). In situ analysis of FOXP3+ regulatory T cells in human colorectal cancer. J. Transl. Med. *4* , 52.

Lodoen, M.B., Lanier, L.L., (2006). Natural killer cells as an initial defense against pathogens. Curr. Opin. Immunol. *18* , 391-398.

Loeb, G.B., Khan, A.A., Canner, D., Hiatt, J.B., Shendure, J., Darnell, R.B., Leslie, C.S., and Rudensky, A.Y., (2012). Transcriptome-wide miR-155 binding map reveals widespread noncanonical microRNA targeting. Mol. Cell *48* , 760-770.

Loeb, L.A., (1991). Mutator phenotype may be required for multistage carcinogenesis. Cancer Res. *51* , 3075-3079.

Loeb, L.A., Loeb, K.R., and Anderson, J.P., (2003). Multiple mutations and cancer. Proc. Natl. Acad. Sci. U. S. A. *100* , 776-781.

Loetscher, P., Uguccioni, M., Bordoli, L., Baggiolini, M., Moser, B., Chizzolini, C., and Dayer, J.M., (1998). CCR5 is characteristic of Th1 lymphocytes. Nature *391* , 344-345.

Luchtenborg, M., Weijenberg, M.P., Roemen, G.M., de Bruine, A.P., van den Brandt, P.A., Lentjes, M.H., Brink, M., van Engeland, M., Goldbohm, R.A., and de Goeij, A.F., (2004). APC mutations in sporadic colorectal carcinomas from The Netherlands Cohort Study. Carcinogenesis *25* , 1219-1226.

Lugli, A., Karamitopoulou, E., Panayiotides, I., Karakitsos, P., Rallis, G., Peros, G., Iezzi, G., Spagnoli, G., Bihl, M., Terracciano, L., and Zlobec, I., (2009). CD8+ lymphocytes/ tumour-budding index: an independent prognostic factor representing a 'pro-/anti-tumour' approach to tumour host interaction in colorectal cancer. Br. J. Cancer *101* , 1382-1392.

Lynch, H.T., Smyrk, T.C., Watson, P., Lanspa, S.J., Lynch, J.F., Lynch, P.M., Cavalieri, R.J., and Boland, C.R., (1993). Genetics, natural history, tumor spectrum, and pathology of hereditary nonpolyposis colorectal cancer: an updated review. Gastroenterology *104* , 1535-1549.

Mantovani, A., Sica, A., (2010). Macrophages, innate immunity and cancer: balance, tolerance, and diversity. Curr. Opin. Immunol. *22* , 231-237.

Mantovani, A., Allavena, P., Sica, A., and Balkwill, F., (2008). Cancer-related inflammation. Nature *454* , 436-444.

Marcus, A., Gowen, B.G., Thompson, T.W., Iannello, A., Ardolino, M., Deng, W., Wang, L., Shifrin, N., and Raulet, D.H., (2014). Recognition of tumors by the innate immune system and natural killer cells. Adv. Immunol. *122* , 91-128.

Menon, A.G., Janssen-van Rhijn, C.M., Morreau, H., Putter, H., Tollenaar, R.A., van de Velde, C.J., Fleuren, G.J., and Kuppen, P.J., (2004). Immune system and prognosis in colorectal cancer: a detailed immunohistochemical analysis. Lab. Invest. *84* , 493-501.

Meyers, M., Wagner, M.W., Hwang, H.S., Kinsella, T.J., and Boothman, D.A., (2001). Role of the hMLH1 DNA mismatch repair protein in fluoropyrimidine-mediated cell death and cell cycle responses. Cancer Res. *61* , 5193-5201.

Michel, S., Benner, A., Tariverdian, M., Wentzensen, N., Hoefler, P., Pommerencke, T., Grabe, N., von Knebel Doeberitz, M., and Kloor, M., (2008). High density of FOXP3-positive T cells infiltrating colorectal cancers with microsatellite instability. Br. J. Cancer *99* , 1867-1873.

Mittal, D., Gubin, M.M., Schreiber, R.D., and Smyth, M.J., (2014). New insights into cancer immunoediting and its three component phases-elimination, equilibrium and escape. Curr. Opin. Immunol. *27C* , 16-25.

Miyaki, M., Iijima, T., Kimura, J., Yasuno, M., Mori, T., Hayashi, Y., Koike, M., Shitara, N., Iwama, T., and Kuroki, T., (1999a). Frequent mutation of beta-catenin and APC genes in primary colorectal tumors from patients with hereditary nonpolyposis colorectal cancer. Cancer Res. *59* , 4506-4509.

Miyaki, M., Konishi, M., Tanaka, K., Kikuchi-Yanoshita, R., Muraoka, M., Yasuno, M., Igari, T., Koike, M., Chiba, M., and Mori, T., (1997). Germline mutation of MSH6 as the cause of hereditary nonpolyposis colorectal cancer. Nat. Genet. *17* , 271-272.

Miyaki, M., Iijima, T., Konishi, M., Sakai, K., Ishii, A., Yasuno, M., Hishima, T., Koike, M., Shitara, N., Iwama, T., Utsunomiya, J., Kuroki, T., and Mori, T., (1999b). Higher frequency of Smad4 gene mutation in human colorectal cancer with distant metastasis. Oncogene *18* , 3098-3103.

Mlecnik, B., Bindea, G., Pages, F., and Galon, J., (2011a). Tumor immunosurveillance in human cancers. Cancer Metastasis Rev. *30* , 5-12.

Mlecnik, B., Tosolini, M., Kirilovsky, A., Berger, A., Bindea, G., Meatchi, T., Bruneval, P., Trajanoski, Z., Fridman, W.H., Pages, F., and Galon, J., (2011b). Histopathologic-based prognostic factors of colorectal cancers are associated with the state of the local immune reaction. J. Clin. Oncol. *29* , 610-618.

Mlecnik, B., Tosolini, M., Charoentong, P., Kirilovsky, A., Bindea, G., Berger, A., Camus, M., Gillard, M., Bruneval, P., Fridman, W.H., Pages, F., Trajanoski, Z., and Galon, J., (2010). Biomolecular network reconstruction identifies T-cell homing factors associated with survival in colorectal cancer. Gastroenterology *138* , 1429-1440.

Moser, B., Loetscher, P., (2001). Lymphocyte traffic control by chemokines. Nat. Immunol. *2* , 123-128.

Moser, B., Loetscher, M., Piali, L., and Loetscher, P., (1998). Lymphocyte responses to chemokines. Int. Rev. Immunol. *16* , 323-344.

Mosmann, T.R., Cherwinski, H., Bond, M.W., Giedlin, M.A., and Coffman, R.L., (1986). Two types of murine helper T cell clone. I. Definition according to profiles of lymphokine activities and secreted proteins. J. Immunol. *136* , 2348-2357.

Motz, G.T., Coukos, G., (2011). The parallel lives of angiogenesis and immunosuppression: cancer and other tales. Nat. Rev. Immunol. *11* , 702-711.

Murakami, M., Sakamoto, A., Bender, J., Kappler, J., and Marrack, P., (2002). CD25+CD4+ T cells contribute to the control of memory CD8+ T cells. Proc. Natl. Acad. Sci. U. S. A. *99* , 8832-8837.

Murphy, P.M., Travers, P., Walport, M., and Janeway, C., (2008). Janeway's Immunobiology (270 Madison Avenue, New york, NY 10016, US.: Garland Science, Taylor & Francis Group LLC).

Musha, H., Ohtani, H., Mizoi, T., Kinouchi, M., Nakayama, T., Shiiba, K., Miyagawa, K., Nagura, H., Yoshie, O., and Sasaki, I., (2005). Selective infiltration of CCR5(+)CXCR3(+) T lymphocytes in human colorectal carcinoma. Int. J. Cancer *116* , 949-956.

Nagorsen, D., Voigt, S., Berg, E., Stein, H., Thiel, E., and Loddenkemper, C., (2007). Tumor-infiltrating macrophages and dendritic cells in human colorectal cancer: relation to local regulatory T cells, systemic T-cell response against tumor-associated antigens and survival. J. Transl. Med. *5* , 62.

Nagtegaal, I.D., Tot, T., Jayne, D.G., McShane, P., Nihlberg, A., Marshall, H.C., Pahlman, L., Brown, J.M., Guillou, P.J., and Quirke, P., (2011). Lymph nodes, tumor deposits, and TNM: are we getting better? J. Clin. Oncol. *29* , 2487-2492.

Naito, Y., Saito, K., Shiiba, K., Ohuchi, A., Saigenji, K., Nagura, H., and Ohtani, H., (1998). CD8+ T cells infiltrated within cancer cell nests as a prognostic factor in human colorectal cancer. Cancer Res. *58* , 3491-3494.

Neyeloff, J.L., Fuchs, S.C., and Moreira, L.B., (2012). Meta-analyses and Forest plots using a microsoft excel spreadsheet: step-by-step guide focusing on descriptive data analysis. BMC Res. Notes *5* , 52-0500-5-52.

Nishihara, T., Zekri, L., Braun, J.E., and Izaurralde, E., (2013). miRISC recruits decapping factors to miRNA targets to enhance their degradation. Nucleic Acids Res. *41* , 8692-8705.

Nordling, C.O., (1953). A new theory on cancer-inducing mechanism. Br. J. Cancer *7* , 68-72.

Nosho, K., Baba, Y., Tanaka, N., Shimas, K., Hayashi, M., Meyerhardt, J.A., Giovannucci, E., Dranoff, G., Fuchs, C.S., and Ogino, S., (2010). Tumour-infiltrating T-cell subsets, molecular changes in colorectal cancer, and prognosis: cohort study and literature review. J. Pathol. *222* , 350-366.

Novellino, L., Castelli, C., and Parmiani, G., (2005). A listing of human tumor antigens recognized by T cells: March 2004 update. Cancer Immunol. Immunother. *54* , 187-207.

Nowell, P.C., (1976). The clonal evolution of tumor cell populations. Science *194* , 23-28.

O'Connell, R.M., Chaudhuri, A.A., Rao, D.S., and Baltimore, D., (2009). Inositol phosphatase SHIP1 is a primary target of miR-155. Proc. Natl. Acad. Sci. U. S. A. *106* , 7113-7118.

Ogino, S., Cantor, M., Kawasaki, T., Brahmandam, M., Kirkner, G.J., Weisenberger, D.J., Campan, M., Laird, P.W., Loda, M., and Fuchs, C.S., (2006). CpG island methylator phenotype (CIMP) of colorectal cancer is best characterised by quantitative DNA methylation analysis and prospective cohort studies. Gut *55* , 1000-1006.

O'Hagan, R.C., Chang, S., Maser, R.S., Mohan, R., Artandi, S.E., Chin, L., and DePinho, R.A., (2002). Telomere dysfunction provokes regional amplification and deletion in cancer genomes. Cancer. Cell. *2* , 149-155.

Ong, S.M., Tan, Y.C., Beretta, O., Jiang, D., Yeap, W.H., Tai, J.J., Wong, W.C., Yang, H., Schwarz, H., Lim, K.H., Koh, P.K., Ling, K.L., and Wong, S.C., (2012). Macrophages in human colorectal cancer are pro-inflammatory and prime T cells towards an anti-tumour type-1 inflammatory response. Eur. J. Immunol. *42* , 89-100.

Pages, F., Galon, J., and Fridman, W.H., (2008). The essential role of the in situ immune reaction in human colorectal cancer. J. Leukoc. Biol. *84* , 981-987.

Pages, F., Galon, J., Dieu-Nosjean, M.C., Tartour, E., Sautes-Fridman, C., and Fridman, W.H., (2010). Immune infiltration in human tumors: a prognostic factor that should not be ignored. Oncogene *29* , 1093-1102.

Pages, F., Kirilovsky, A., Mlecnik, B., Asslaber, M., Tosolini, M., Bindea, G., Lagorce, C., Wind, P., Marliot, F., Bruneval, P., Zatloukal, K., Trajanoski, Z., Berger, A., Fridman, W.H., and Galon, J., (2009). In situ cytotoxic and memory T cells predict outcome in patients with early-stage colorectal cancer. J. Clin. Oncol. *27* , 5944-5951.

Pages, F., Berger, A., Camus, M., Sanchez-Cabo, F., Costes, A., Molidor, R., Mlecnik, B., Kirilovsky, A., Nilsson, M., Damotte, D., Meatchi, T., Bruneval, P., Cugnenc, P.H., Trajanoski, Z., Fridman, W.H., and Galon, J., (2005). Effector memory T cells, early metastasis, and survival in colorectal cancer. N. Engl. J. Med. *353* , 2654-2666.

Palucka, A.K., Ueno, H., Fay, J.W., and Banchereau, J., (2007). Taming cancer by inducing immunity via dendritic cells. Immunol. Rev. *220* , 129-150.

Palucka, K., Banchereau, J., (2012). Cancer immunotherapy via dendritic cells. Nat. Rev. Cancer. *12* , 265-277.

Pankla, R., Buddhisa, S., Berry, M., Blankenship, D.M., Bancroft, G.J., Banchereau, J., Lertmemongkolchai, G., and Chaussabel, D., (2009). Genomic transcriptional profiling identifies a candidate blood biomarker signature for the diagnosis of septicemic melioidosis. Genome Biol. *10* , R127-2009-10-11-r127. Epub 2009 Nov 10.

Parmar, M.K., Torri, V., and Stewart, L., (1998). Extracting summary statistics to perform meta-analyses of the published literature for survival endpoints. Stat. Med. *17* , 2815-2834.

Pattyn, F., Speleman, F., De Paepe, A., and Vandesompele, J., (2003). RTPrimerDB: the real-time PCR primer and probe database. Nucleic Acids Res. *31* , 122-123.

Pattyn, F., Robbrecht, P., De Paepe, A., Speleman, F., and Vandesompele, J., (2006). RTPrimerDB: the real-time PCR primer and probe database, major update 2006. Nucleic Acids Res. *34* , D684-8.

Pedroza-Gonzalez, A., Xu, K., Wu, T.C., Aspord, C., Tindle, S., Marches, F., Gallegos, M., Burton, E.C., Savino, D., Hori, T., Tanaka, Y., Zurawski, S., Zurawski, G., Bover, L., Liu, Y.J., Banchereau, J., and Palucka, A.K., (2011). Thymic stromal lymphopoietin fosters human breast tumor growth by promoting type 2 inflammation. J. Exp. Med. *208* , 479-490.

Peltomaki, P., Aaltonen, L.A., Sistonen, P., Pylkkanen, L., Mecklin, J.P., Jarvinen, H., Green, J.S., Jass, J.R., Weber, J.L., and Leach, F.S., (1993). Genetic mapping of a locus predisposing to human colorectal cancer. Science *260* , 810-812.

Perucho, M., (1999). Correspondence re: C.R. Boland et al., A National Cancer Institute workshop on microsatellite instability for cancer detection and familial predisposition: development of international criteria for the determination of microsatellite instability in colorectal cancer. Cancer Res., 58: 5248-5257, 1998. Cancer Res. *59* , 249-256.

Peterson, J.E., Zurakowski, D., Italiano, J.E.,Jr, Michel, L.V., Connors, S., Oenick, M., D'Amato, R.J., Klement, G.L., and Folkman, J., (2012). VEGF, PF4 and PDGF are elevated in platelets of colorectal cancer patients. Angiogenesis *15* , 265-273.

Phillips, S.M., Banerjea, A., Feakins, R., Li, S.R., Bustin, S.A., and Dorudi, S., (2004). Tumour-infiltrating lymphocytes in colorectal cancer with microsatellite instability are activated and cytotoxic. Br. J. Surg. *91* , 469-475.

Piancatelli, D., Romano, P., Sebastiani, P., Adorno, D., and Casciani, C.U., (1999). Local expression of cytokines in human colorectal carcinoma: evidence of specific interleukin-6 gene expression. J. Immunother. *22* , 25-32.

Pietra, G., Manzini, C., Rivara, S., Vitale, M., Cantoni, C., Petretto, A., Balsamo, M., Conte, R., Benelli, R., Minghelli, S., Solari, N., Gualco, M., Queirolo, P., Moretta, L., and Mingari, M.C., (2012). Melanoma cells inhibit natural killer cell function by modulating the expression of activating receptors and cytolytic activity. Cancer Res. *72* , 1407-1415.

Pino, M.S., Chung, D.C., (2010). The chromosomal instability pathway in colon cancer. Gastroenterology *138* , 2059-2072.

Pitti, R.M., Marsters, S.A., Lawrence, D.A., Roy, M., Kischkel, F.C., Dowd, P., Huang, A., Donahue, C.J., Sherwood, S.W., Baldwin, D.T., Godowski, P.J., Wood, W.I., Gurney, A.L., Hillan, K.J., Cohen, R.L., Goddard, A.D., Botstein, D., and Ashkenazi, A., (1998). Genomic amplification of a decoy receptor for Fas ligand in lung and colon cancer. Nature *396* , 699-703.

Popat, S., Hubner, R., and Houlston, R.S., (2005). Systematic review of microsatellite instability and colorectal cancer prognosis. J. Clin. Oncol. *23* , 609-618.

Prall, F., Duhrkop, T., Weirich, V., Ostwald, C., Lenz, P., Nizze, H., and Barten, M., (2004). Prognostic role of CD8+ tumor-infiltrating lymphocytes in stage III colorectal cancer with and without microsatellite instability. Hum. Pathol. *35* , 808-816.

Pugh, S.A., Harrison, R.J., Primrose, J.N., and Khakoo, S.I., (2014). T cells but not NK cells are associated with a favourable outcome for resected colorectal liver metastases. BMC Cancer *14* , 180-2407-14-180.

Qian, B.Z., Pollard, J.W., (2010). Macrophage diversity enhances tumor progression and metastasis. Cell *141* , 39-51.

Quail, D.F., Joyce, J.A., (2013). Microenvironmental regulation of tumor progression and metastasis. Nat. Med. *19* , 1423-1437.

Rehwinkel, J., Behm-Ansmant, I., Gatfield, D., and Izaurralde, E., (2005). A crucial role for GW182 and the DCP1:DCP2 decapping complex in miRNA-mediated gene silencing. RNA *11* , 1640-1647.

Reuschenbach, M., Kloor, M., Morak, M., Wentzensen, N., Germann, A., Garbe, Y., Tariverdian, M., Findeisen, P., Neumaier, M., Holinski-Feder, E., and von Knebel Doeberitz, M., (2010). Serum antibodies against frameshift peptides in microsatellite unstable colorectal cancer patients with Lynch syndrome. Fam. Cancer. *9* , 173-179.

Ribic, C.M., Sargent, D.J., Moore, M.J., Thibodeau, S.N., French, A.J., Goldberg, R.M., Hamilton, S.R., Laurent-Puig, P., Gryfe, R., Shepherd, L.E., Tu, D., Redston, M., and Gallinger, S., (2003). Tumor microsatellite-instability status as a predictor of benefit from fluorouracil-based adjuvant chemotherapy for colon cancer. N. Engl. J. Med. *349* , 247-257.

Ripberger, E., Linnebacher, M., Schwitalle, Y., Gebert, J., and von Knebel Doeberitz, M., (2003). Identification of an HLA-A0201-restricted CTL epitope generated by a tumor-specific frameshift mutation in a coding microsatellite of the OGT gene. J. Clin. Immunol. *23* , 415-423.

Rissland, O.S., Hong, S.J., and Bartel, D.P., (2011). MicroRNA destabilization enables dynamic regulation of the miR-16 family in response to cell-cycle changes. Mol. Cell *43* , 993-1004.

Roger, L., Jones, R.E., Heppel, N.H., Williams, G.T., Sampson, J.R., and Baird, D.M., (2013). Extensive telomere erosion in the initiation of colorectal adenomas and its association with chromosomal instability. J. Natl. Cancer Inst. *105* , 1202-1211.

Rosenblum, J.M., Shimoda, N., Schenk, A.D., Zhang, H., Kish, D.D., Keslar, K., Farber, J.M., and Fairchild, R.L., (2010). CXC chemokine ligand (CXCL) 9 and CXCL10 are antagonistic costimulation molecules during the priming of alloreactive T cell effectors. J. Immunol. *184* , 3450-3460.

Rousalova, I., Krepela, E., (2010). Granzyme B-induced apoptosis in cancer cells and its regulation (review). Int. J. Oncol. *37* , 1361-1378.

Sadanandam, A., Lyssiotis, C.A., Homicsko, K., Collisson, E.A., Gibb, W.J., Wullschleger, S., Ostos, L.C., Lannon, W.A., Grotzinger, C., Del Rio, M., Lhermitte, B., Olshen, A.B., Wiedenmann, B., Cantley, L.C., Gray, J.W., and Hanahan, D., (2013). A colorectal cancer classification system that associates cellular phenotype and responses to therapy. Nat. Med. *19* , 619-625.

Salama, P., Phillips, M., Grieu, F., Morris, M., Zeps, N., Joseph, D., Platell, C., and Iacopetta, B., (2009). Tumor-infiltrating FOXP3+ T regulatory cells show strong prognostic significance in colorectal cancer. J. Clin. Oncol. *27* , 186-192.

Sallusto, F., Lenig, D., Mackay, C.R., and Lanzavecchia, A., (1998). Flexible programs of chemokine receptor expression on human polarized T helper 1 and 2 lymphocytes. J. Exp. Med. *187* , 875-883.

Samson, M., Labbe, O., Mollereau, C., Vassart, G., and Parmentier, M., (1996). Molecular cloning and functional expression of a new human CC-chemokine receptor gene. Biochemistry *35* , 3362-3367.

Samuels, Y., Ericson, K., (2006). Oncogenic PI3K and its role in cancer. Curr. Opin. Oncol. *18* , 77-82.

Sandel, M.H., Dadabayev, A.R., Menon, A.G., Morreau, H., Melief, C.J., Offringa, R., van der Burg, S.H., Janssen-van Rhijn, C.M., Ensink, N.G., Tollenaar, R.A., van de Velde, C.J., and Kuppen, P.J., (2005). Prognostic value of tumor-infiltrating dendritic cells in colorectal cancer: role of maturation status and intratumoral localization. Clin. Cancer Res. *11* , 2576-2582.

Sankila, R., Aaltonen, L.A., Jarvinen, H.J., and Mecklin, J.P., (1996). Better survival rates in patients with MLH1-associated hereditary colorectal cancer. Gastroenterology *110* , 682-687.

Schoenborn, J.R., Wilson, C.B., (2007). Regulation of interferon-gamma during innate and adaptive immune responses. Adv. Immunol. *96* , 41-101.

Schreiber, R.D., Old, L.J., and Smyth, M.J., (2011). Cancer immunoediting: integrating immunity's roles in cancer suppression and promotion. Science *331* , 1565-1570.

Schutte, M., Hruban, R.H., Hedrick, L., Cho, K.R., Nadasdy, G.M., Weinstein, C.L., Bova, G.S., Isaacs, W.B., Cairns, P., Nawroz, H., Sidransky, D., Casero, R.A.,Jr, Meltzer, P.S., Hahn, S.A., and Kern, S.E., (1996). DPC4 gene in various tumor types. Cancer Res. *56* , 2527-2530.

Schwitalle, Y., Linnebacher, M., Ripberger, E., Gebert, J., and von Knebel Doeberitz, M., (2004). Immunogenic peptides generated by frameshift mutations in DNA mismatch repair-deficient cancer cells. Cancer. Immun. *4* , 14.

Schwitalle, Y., Kloor, M., Eiermann, S., Linnebacher, M., Kienle, P., Knaebel, H.P., Tariverdian, M., Benner, A., and von Knebel Doeberitz, M., (2008). Immune response against frameshift-induced neopeptides in HNPCC patients and healthy HNPCC mutation carriers. Gastroenterology *134* , 988-997.

Sconocchia, G., Arriga, R., Tornillo, L., Terracciano, L., Ferrone, S., and Spagnoli, G.C., (2012). Melanoma cells inhibit NK cell functions. Cancer Res. *72* , 5428-9; author reply 5430.

Sconocchia, G., Zlobec, I., Lugli, A., Calabrese, D., Iezzi, G., Karamitopoulou, E., Patsouris, E.S., Peros, G., Horcic, M., Tornillo, L., Zuber, M., Droeser, R., Muraro, M.G., Mengus, C., Oertli, D., Ferrone, S., Terracciano, L., and Spagnoli, G.C., (2011). Tumor infiltration by FcgammaRIII (CD16)+ myeloid cells is associated with improved survival in patients with colorectal carcinoma. Int. J. Cancer *128* , 2663-2672.

Shay, J.W., (2013). Determining if telomeres matter in colon cancer initiation or progression. J. Natl. Cancer Inst. *105* , 1166-1168.

Shields, J.D., Kourtis, I.C., Tomei, A.A., Roberts, J.M., and Swartz, M.A., (2010). Induction of lymphoidlike stroma and immune escape by tumors that express the chemokine CCL21. Science *328* , 749-752.

Shinto, E., Hase, K., Hashiguchi, Y., Sekizawa, A., Ueno, H., Shikina, A., Kajiwara, Y., Kobayashi, H., Ishiguro, M., and Yamamoto, J., (2014). CD8+ and FOXP3+ Tumor-Infiltrating T Cells Before and After Chemoradiotherapy for Rectal Cancer. Ann. Surg. Oncol. .

Simpson, J.A., Al-Attar, A., Watson, N.F., Scholefield, J.H., Ilyas, M., and Durrant, L.G., (2010). Intratumoral T cell infiltration, MHC class I and STAT1 as biomarkers of good prognosis in colorectal cancer. Gut *59* , 926-933.

Smith, G., Carey, F.A., Beattie, J., Wilkie, M.J., Lightfoot, T.J., Coxhead, J., Garner, R.C., Steele, R.J., and Wolf, C.R., (2002). Mutations in APC, Kirsten-ras, and p53--alternative genetic pathways to colorectal cancer. Proc. Natl. Acad. Sci. U. S. A. *99* , 9433-9438.

Smyrk, T.C., Watson, P., Kaul, K., and Lynch, H.T., (2001). Tumor-infiltrating lymphocytes are a marker for microsatellite instability in colorectal carcinoma. Cancer *91* , 2417-2422.

Spandidos, A., Wang, X., Wang, H., and Seed, B., (2010). PrimerBank: a resource of human and mouse PCR primer pairs for gene expression detection and quantification. Nucleic Acids Res. *38* , D792-9.

Spandidos, A., Wang, X., Wang, H., Dragnev, S., Thurber, T., and Seed, B., (2008). A comprehensive collection of experimentally validated primers for Polymerase Chain Reaction quantitation of murine transcript abundance. BMC Genomics *9* , 633-2164-9-633.

Steinman, R.M., Cohn, Z.A., (1973). Identification of a novel cell type in peripheral lymphoid organs of mice. I. Morphology, quantitation, tissue distribution. J. Exp. Med. *137* , 1142-1162.

Straus, D.S., (2013). TNFalpha and IL-17 cooperatively stimulate glucose metabolism and growth factor production in human colorectal cancer cells. Mol. Cancer. *12* , 78-4598-12-78.

Strauss, B.S., (1999). Frameshift mutation, microsatellites and mismatch repair. Mutat. Res. *437* , 195-203.

Street, N.E., Mosmann, T.R., (1991). Functional diversity of T lymphocytes due to secretion of different cytokine patterns. FASEB J. *5* , 171-177.

Street, S.E., Cretney, E., and Smyth, M.J., (2001). Perforin and interferon-gamma activities independently control tumor initiation, growth, and metastasis. Blood *97* , 192-197.

Suzuki, H., Chikazawa, N., Tasaka, T., Wada, J., Yamasaki, A., Kitaura, Y., Sozaki, M., Tanaka, M., Onishi, H., Morisaki, T., and Katano, M., (2010). Intratumoral CD8(+) T/FOXP3 (+) cell ratio is a predictive marker for survival in patients with colorectal cancer. Cancer Immunol. Immunother. *59* , 653-661.

Szabo, S.J., Sullivan, B.M., Peng, S.L., and Glimcher, L.H., (2003). Molecular mechanisms regulating Th1 immune responses. Annu. Rev. Immunol. *21* , 713-758.

Takayama, T., Miyanishi, K., Hayashi, T., Kukitsu, T., Takanashi, K., Ishiwatari, H., Kogawa, T., Abe, T., and Niitsu, Y., (2005). Aberrant crypt foci: detection, gene abnormalities, and clinical usefulness. Clin. Gastroenterol. Hepatol. *3* , S42-5.

Thai, T.H., Calado, D.P., Casola, S., Ansel, K.M., Xiao, C., Xue, Y., Murphy, A., Frendewey, D., Valenzuela, D., Kutok, J.L., Schmidt-Supprian, M., Rajewsky, N., Yancopoulos, G., Rao, A., and Rajewsky, K., (2007). Regulation of the germinal center response by microRNA-155. Science *316* , 604-608.

Thibodeau, S.N., Bren, G., and Schaid, D., (1993). Microsatellite instability in cancer of the proximal colon. Science *260* , 816-819.

Toiyama, Y., Takahashi, M., Hur, K., Nagasaka, T., Tanaka, K., Inoue, Y., Kusunoki, M., Boland, C.R., and Goel, A., (2013). Serum miR-21 as a diagnostic and prognostic biomarker in colorectal cancer. J. Natl. Cancer Inst. *105* , 849-859.

Tosolini, M., Kirilovsky, A., Mlecnik, B., Fredriksen, T., Mauger, S., Bindea, G., Berger, A., Bruneval, P., Fridman, W.H., Pages, F., and Galon, J., (2011). Clinical impact of different classes of infiltrating T cytotoxic and helper cells (Th1, th2, treg, th17) in patients with colorectal cancer. Cancer Res. *71* , 1263-1271.

Tougeron, D., Maby, P., Elie, N., Fauquembergue, E., Le Pessot, F., Cornic, M., Sabourin, J.C., Michel, P., Frebourg, T., and Latouche, J.B., (2013). Regulatory T lymphocytes are associated with less aggressive histologic features in microsatellite-unstable colorectal cancers. PLoS One *8* , e61001.

Toyota, M., Ahuja, N., Ohe-Toyota, M., Herman, J.G., Baylin, S.B., and Issa, J.P., (1999). CpG island methylator phenotype in colorectal cancer. Proc. Natl. Acad. Sci. U. S. A. *96* , 8681-8686.

Umar, A., Boland, C.R., Terdiman, J.P., Syngal, S., de la Chapelle, A., Ruschoff, J., Fishel, R., Lindor, N.M., Burgart, L.J., Hamelin, R., Hamilton, S.R., Hiatt, R.A., Jass, J., Lindblom, A., Lynch, H.T., Peltomaki, P., Ramsey, S.D., Rodriguez-Bigas, M.A., Vasen, H.F., Hawk, E.T., Barrett, J.C., Freedman, A.N., and Srivastava, S., (2004). Revised Bethesda Guidelines for hereditary nonpolyposis colorectal cancer (Lynch syndrome) and microsatellite instability. J. Natl. Cancer Inst. *96* , 261-268.

van der Bruggen, P., Traversari, C., Chomez, P., Lurquin, C., De Plaen, E., Van den Eynde, B., Knuth, A., and Boon, T., (1991). A gene encoding an antigen recognized by cytolytic T lymphocytes on a human melanoma. Science *254* , 1643-1647.

van Dijk, E., Cougot, N., Meyer, S., Babajko, S., Wahle, E., and Seraphin, B., (2002). Human Dcp2: a catalytically active mRNA decapping enzyme located in specific cytoplasmic structures. EMBO J. *21* , 6915-6924.

van Rooij, E., Olson, E.N., (2012). MicroRNA therapeutics for cardiovascular disease: opportunities and obstacles. Nat. Rev. Drug Discov. *11* , 860-872.

Vesely, M.D., Schreiber, R.D., (2013). Cancer immunoediting: antigens, mechanisms, and implications to cancer immunotherapy. Ann. N. Y. Acad. Sci. *1284* , 1-5.

Vittal, R., Fan, L., Greenspan, D.S., Mickler, E.A., Gopalakrishnan, B., Gu, H., Benson, H.L., Zhang, C., Burlingham, W., Cummings, O.W., and Wilkes, D.S., (2013). IL-17 induces type V collagen overexpression and EMT via TGF-beta-dependent pathways in obliterative bronchiolitis. Am. J. Physiol. Lung Cell. Mol. Physiol. *304* , L401-14.

Vogelstein, B., Kinzler, K.W., (2004). Cancer genes and the pathways they control. Nat. Med. *10* , 789-799.

Vogelstein, B., Papadopoulos, N., Velculescu, V.E., Zhou, S., Diaz, L.A.,Jr, and Kinzler, K.W., (2013). Cancer genome landscapes. Science *339* , 1546-1558.

Vogelstein, B., Fearon, E.R., Hamilton, S.R., Kern, S.E., Preisinger, A.C., Leppert, M., Nakamura, Y., White, R., Smits, A.M., and Bos, J.L., (1988). Genetic alterations during colorectal-tumor development. N. Engl. J. Med. *319* , 525-532.

von Knebel Doeberitz, M., Kloor, M., (2013). Towards a vaccine to prevent cancer in Lynch syndrome patients. Fam. Cancer. *12* , 307-312.

Wang, X., Seed, B., (2003). A PCR primer bank for quantitative gene expression analysis. Nucleic Acids Res. *31* , e154.

Weisenberger, D.J., Siegmund, K.D., Campan, M., Young, J., Long, T.I., Faasse, M.A., Kang, G.H., Widschwendter, M., Weener, D., Buchanan, D., Koh, H., Simms, L., Barker, M., Leggett, B., Levine, J., Kim, M., French, A.J., Thibodeau, S.N., Jass, J., Haile, R., and Laird, P.W., (2006). CpG island methylator phenotype underlies sporadic microsatellite instability and is tightly associated with BRAF mutation in colorectal cancer. Nat. Genet. *38* , 787-793.

Williams, D.S., Bird, M.J., Jorissen, R.N., Yu, Y.L., Walker, F., Zhang, H.H., Nice, E.C., and Burgess, A.W., (2010). Nonsense mediated decay resistant mutations are a source of expressed mutant proteins in colon cancer cell lines with microsatellite instability. PLoS One *5* , e16012.

Wood, L.D., Parsons, D.W., Jones, S., Lin, J., Sjoblom, T., Leary, R.J., Shen, D., Boca, S.M., Barber, T., Ptak, J., Silliman, N., Szabo, S., Dezso, Z., Ustyanksky, V., Nikolskaya, T., Nikolsky, Y., Karchin, R., Wilson, P.A., Kaminker, J.S., Zhang, Z., Croshaw, R., Willis, J., Dawson, D., Shipitsin, M., Willson, J.K., Sukumar, S., Polyak, K., Park, B.H., Pethiyagoda, C.L., Pant, P.V., Ballinger, D.G., Sparks, A.B., Hartigan, J., Smith, D.R., Suh, E., Papadopoulos, N., Buckhaults, P., Markowitz, S.D., Parmigiani, G., Kinzler, K.W., Velculescu, V.E., and Vogelstein, B., (2007). The genomic landscapes of human breast and colorectal cancers. Science *318* , 1108-1113.

Wu, L., Fan, J., and Belasco, J.G., (2006). MicroRNAs direct rapid deadenylation of mRNA. Proc. Natl. Acad. Sci. U. S. A. *103* , 4034-4039.

Yoon, H.H., Orrock, J.M., Foster, N.R., Sargent, D.J., Smyrk, T.C., and Sinicrope, F.A., (2012). Prognostic impact of FoxP3+ regulatory T cells in relation to CD8+ T lymphocyte density in human colon carcinomas. PLoS One *7* , e42274.

Yuan, A., Steigen, S.E., Goll, R., Vonen, B., Husbekk, A., Cui, G., and Florholmen, J., (2008). Dendritic cell infiltration pattern along the colorectal adenoma-carcinoma sequence. APMIS *116* , 445-456.

Zhou, Q., Peng, R.Q., Wu, X.J., Xia, Q., Hou, J.H., Ding, Y., Zhou, Q.M., Zhang, X., Pang, Z.Z., Wan, D.S., Zeng, Y.X., and Zhang, X.S., (2010). The density of macrophages in the invasive front is inversely correlated to liver metastasis in colon cancer. J. Transl. Med. *8* , 13-5876-8-13.

Zimmermann, T., Moehler, M., Gockel, I., Sgourakis, G.G., Biesterfeld, S., Muller, M., Berger, M.R., Lang, H., Galle, P.R., and Schimanski, C.C., (2010). Low expression of chemokine receptor CCR5 in human colorectal cancer correlates with lymphatic dissemination and reduced CD8+ T-cell infiltration. Int. J. Colorectal Dis. *25* , 417-424.

Zitvogel, L., Tesniere, A., and Kroemer, G., (2006). Cancer despite immunosurveillance: immunoselection and immunosubversion. Nat. Rev. Immunol. *6* , 715-727.

Zlobec, I., Bihl, M., Foerster, A., Rufle, A., and Lugli, A., (2011). Comprehensive analysis of CpG island methylator phenotype (CIMP)-high, -low, and -negative colorectal cancers based on protein marker expression and molecular features. J. Pathol. *225* , 336-343.

Zlobec, I., Karamitopoulou, E., Terracciano, L., Piscuoglio, S., Iezzi, G., Muraro, M.G., Spagnoli, G., Baker, K., Tzankov, A., and Lugli, A., (2010). TIA-1 cytotoxic granule-associated RNA binding protein improves the prognostic performance of CD8 in mismatch repair-proficient colorectal cancer. PLoS One *5* , e14282.